Characterization and activity profiling of candidate drugs against PFD0975w from *Plasmodium falciparum.*

A thesis submitted
in partial fulfillment of the requirements for the degree of

DOCTOR OF PHILOSOPHY.

By

Mr. Arnish Chakraborty

Department of Biosciences & Bioengineering,
Indian Institute of Technology, Guwahati.
Guwahati- 781039, Assam, India.
March 2015

Dedicated to my parents,

Who have stood beside me, with patience and faith in all my journeys and ventures towards success…

-Arnish

Indian Institute of Technology,

Department of Biosciences & Bioengineering.

Statement

I hereby declare that the matter embodied in this thesis entitled "**Characterization and activity profiling of candidate drugs against PFD0975w from *Plasmodium falciparum.*"** is a cumulative account of the results of investigations carried out in the Department of Biosciences and Bioengineering, Indian Institute of Technology, Guwahati, India, under the joint supervision of **Dr. Vishal Trivedi** & **Dr. Vibin Ramakrishnan**.

In keeping with the general practice of reporting scientific observations, due acknowledgements have been made wherever the work of other investigators are referred.

Arnish Chakraborty

March 2015

Roll no: 11610601

Indian Institute of Technology,

Department of Biosciences & Bioengineering.

Certificate

It is certified that the work described in this thesis entitled, "**Characterization and activity profiling of candidate drugs against PFD0975w from *Plasmodium falciparum.*",** by **Mr. Arnish Chakraborty** (Roll no: 11610601), submitted to Indian Institute of Technology, Guwahati, India, for the award of the degree of Doctor of Philosophy, is an authentic record of results obtained from the research work carried out under our joint supervision at the Department of Biosciences & Bioengineering, Indian Institute of Technology, Guwahati, Assam, India. This work has not been submitted elsewhere for a degree.

Dr. Vishal Trivedi **Dr. Vibin Ramakrishnan**

Acknowledgements

It is a matter of great pleasure to express my love and gratitude to those people who have helped me immensely in the successful and timely completion of my doctoral thesis. I would like to thank:

- My thesis supervisors, Dr. Vishal Trivedi and Dr. Vibin Ramakrishnan, who have constantly supported and supervised my project. I am thankful to them for lending out their support, cooperation and valuable expertise and insights to guide me during my research endeavor.
- My doctoral committee members, Dr. Nitin Chaudhary, Dr. Sanjukta Patra and Dr. Suresh Kartha, for the periodic evaluation of my research work and valuable suggestions from time to time.
- Scientists and staff from CSIR-CDRI Lucknow, Dr. Kumkum Srivastava, Dr. Amogh.A. Sahasrabuddhe, Mr. Ahsan Manhas, Ms Pooja Agarwal and Mr. Kuldeep Chaudhary, who have helped me with the part of my research work conducted at CSIR-CDRI, Lucknow.
- Dr. Pillai (ICMR-NIMR, New Delhi) for training me in the cultivation of malaria parasite.
- Past and present members of Malaria Research Group, Department of Biosciences & Bioengineering, IIT Guwahati.
- Research scholars from Department of Biosciences & Bioengineering, belonging to Dr. V.K Dubey's lab, Dr. A. Goyal's lab and Dr. B.Anand's lab, who have helped me with my research.
- Department of Biosciences & Bioengineering, IIT Guwahati for research infrastructure and a cooperative environment for my work.
- Indian Institute of Technology, Guwahati, for research fellowship.

-Arnish

Table of contents

List of figures

List of tables

List of abbreviations used

ATP	**Adenosine triphosphate**
cAMP	**Cyclic adenosine monophosphate**
CDPK	**Cyclin dependent protein kinase**
cGMP	**Cyclic guanosine monophosphate**
CLK	**CDC like kinase**
CQ	**Chloroquine**
DAPI	**4',6-diamidino-2-phenylindole**
DDT	**dichlorodiphenyltrichloroethane**
DHFR	**Dihydrofolate Reductase**
ePK	**Eukaryotic protein kinase**
FITC	**Fluorescein isothiocyanate**
GSH	**Reduced glutathione**
GSK	**Glycogen synthase kinase**
IFNγ	**Interferon Gamma**
IL	**Interleukin**
MQ	**Mefloquine**
NADH	**Nicotinamide adenine dinucleotide**
PK	**Protein Kinase**
PKC	**Protein kinase C**
PVDF	**Polyvinylidene fluoride**
RBC	**Red blood cell**
RIO	**Right open reading frame**
rRNA	**Ribosomal ribonucleic acid**
S-P	**Sulfadoxine- pyrimethamine**
TNF	**Tumor necrosis factor**

List of units used

Å	Angstrom
mM	Milli Mole
µM	Micro Mole
nM	Nano Mole
µg	Microgram
mg	Milligram
°C	Degree Celsius
ml	Milliliter
Hrs.	Hours
Mins.	Minutes

Chapter I

Malaria: An overview of disease biology and drug targets.

1.1 Introduction

Malaria is an infectious parasitic disease that affects humans and other animals. The causative agents are parasitic, apicomplexan protozoans of the *Plasmodium* species, the most virulent of them being *Plasmodium falciparum*. The disease is transmitted when an infected female *Anopheles* mosquito, bites a healthy individual releasing *Plasmodium*sporozoites into the bloodstream. The clinical manifestations typically begin 8-25 days after infection and include recurrent fever with chills, fatigue, vomiting, nauseaand headaches. One of the classic symptoms of the malaria fever (also known as paroxysm) isthe cyclic recurrence chill and fever after every 36-48 hours.A severe manifestation of the disease is cerebral malaria in which the patient exhibits critical neurological symptoms, due to obstruction of blood flow to the brain. The disease is typically diagnosed by preparing a thin smear from the blood of a suspected individual and the detection of *Plasmodium* parasites within the RBC confirms an infection.

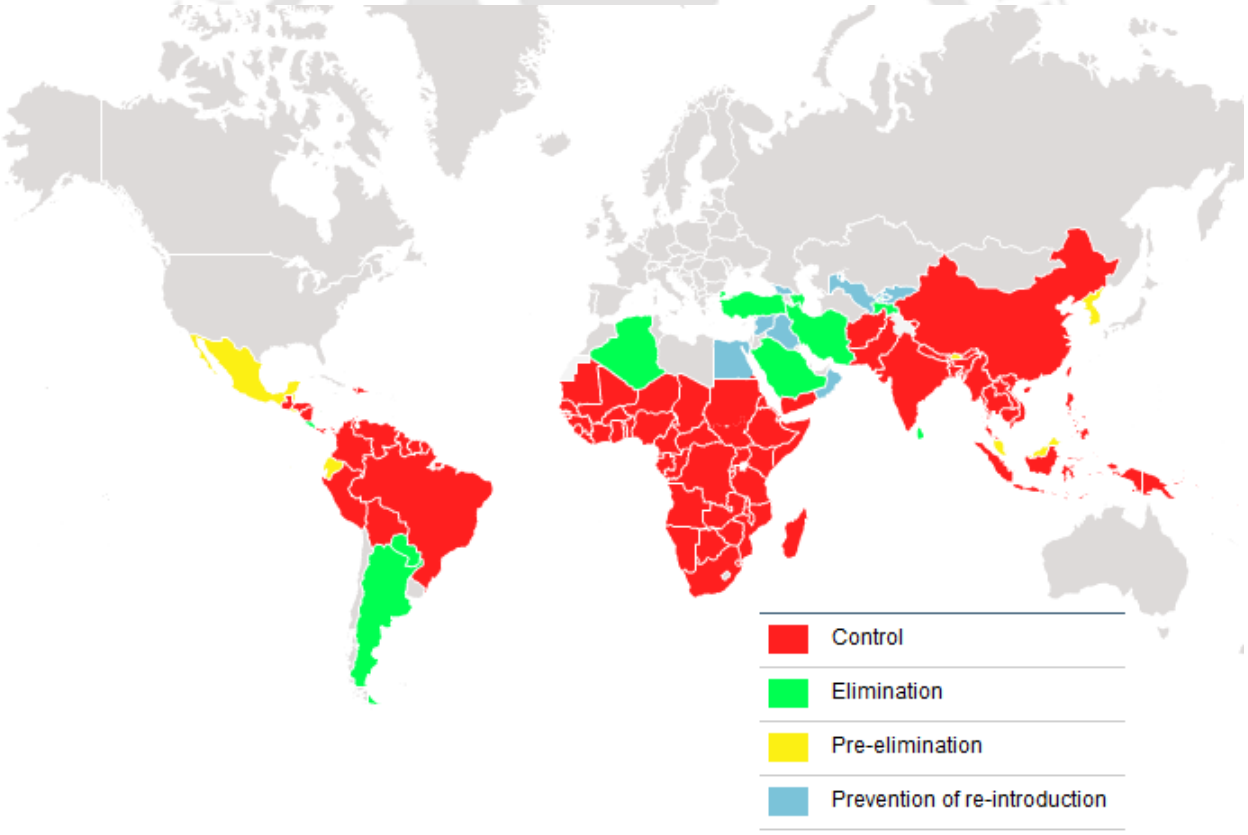

Figure 1.1: Distribution of malaria endemic regions of the world (as on December 2014). Data reproduced from World health organization, Global Malaria Mapper (http://worldmalariareport.org/).

The disease is prevalent in the tropical and sub-tropical regions of the world (Figure 1.1). Sub-Saharan Africa, South-east Asia and Latin America are highly endemic regions with a high rate

of infection and disease transmission.The prevalence of the malaria parasite in these sub-tropical regions could be attributed to the climatic, geographic as well as the poor medical and publichealth-care infrastructure of these less developed countries. According to the 2014 report of the World Health Organization, more than 207 million cases of malaria infection were registered that year. In these endemic areas, malaria has taken its toll on approximately 789,000 lives; most of the victims were African children below the age of 10 years (Figure 1.2). Malaria is thus not only a major threat to human life and welfare, but also a burden on economic development. The fight against malaria has been a long journey with little success.

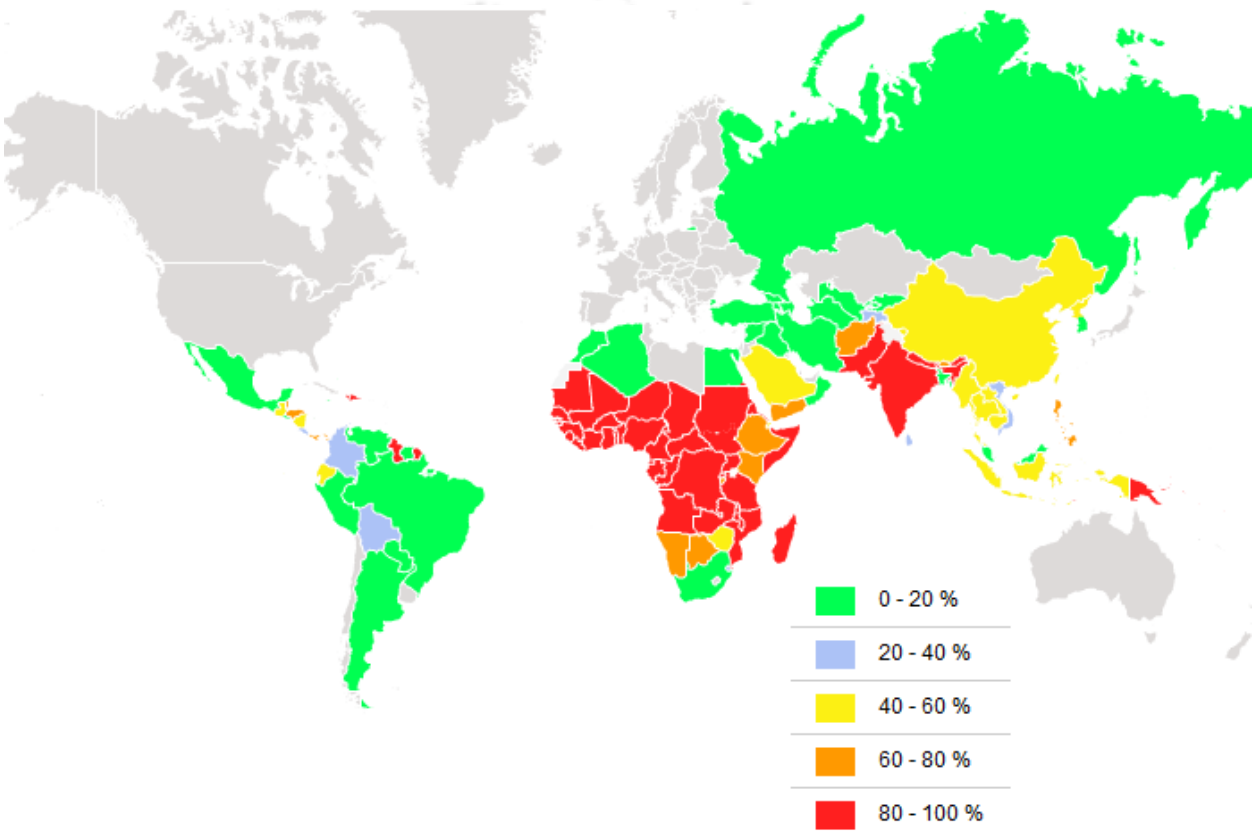

Figure 1.2: Geographic distribution of population living at risk of malaria infection and transmission (as on December 2014). Data reproduced from World health organization, Global Malaria Mapper (http://worldmalariareport.org/)

The primary strategy was to eliminate the mosquito population using insecticides such as DDT. It was soon realized that vector control strategies were inadequate and expensive both in terms of money and ecological stability. Antimalarial medications such as chloroquine, mefloquine and doxycycline had been the chief weapons to combat the disease but their success was short lived due to the evolution of drug resistant parasites. Many more antimalarial drugs such as amodiaquine, lumefantrineand sulfadoxine/pyrimethaminecombinations came to the market but the resistance to these newer drugs evolved in short time complicating the treatment of malaria

more than ever before. In the 21st century this disease continues to wreak havoc with an ever increasing number of infected individuals. There is no vaccine to this disease with an operational impact and the ever increasing dependence on chemotherapy has given birth to various multi-drug resistant strains of *Plasmodium falciparum*. Various private and public funded laboratories the world over have thus taken up the task of understanding the biology of this complex parasite and device strategies to fight against it.

1.2 Systemic manifestations of malarial fever.

Infections with the malaria parasite are characterized by recurrent occurrences of fever also known as paroxysms which develop in three distinct stages. The first stage of the fever attacks manifests as chills. Severe shaking may occur during chills and it may also be accompanied with headache, fatigue, pain in the muscles, diarrhea, vomiting andnausea. The second stage is characterized by fevers causing the patient's skin to become hot and dry. With the lowering of fever and body temperature, the typical symptoms of the third stage are seen: sweating occurs causing extreme fatigue and weakness in the limbs. The classic malaria symptoms generally begin to appear within 10 to 16 days after the an infectious mosquito bite and the systemic manifestations described above are caused due to a myriad of internal changes due to host-pathogen interactions and the body's immune reaction to the invading pathogen.

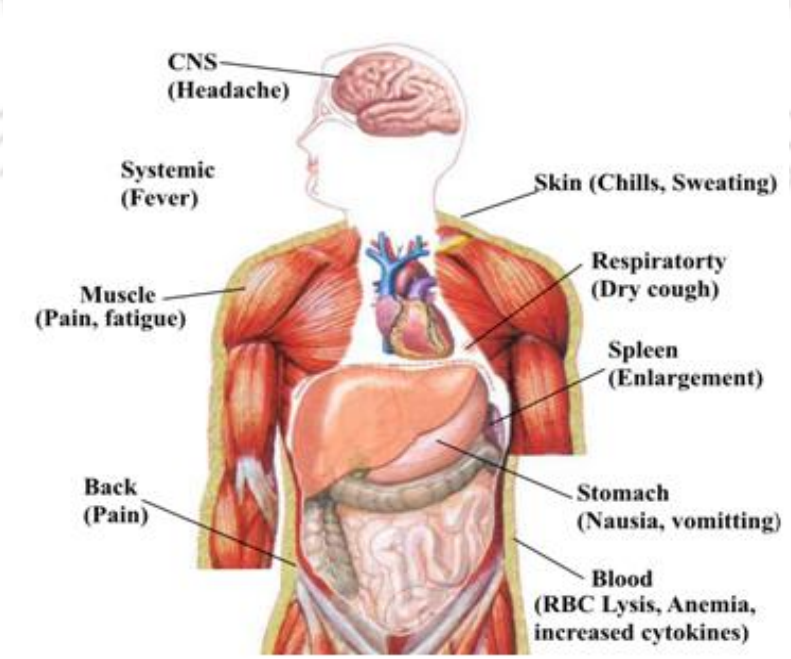

Figure 1.3: Common symptoms in human during the course of malaria.

The course of molecular changes occurring within the body varies slightly between populations. This may be attributed to the minor differences in host factors between populations as well as the strain of *Plasmodium* parasite that infected the host. An immune adult, native to an endemic region, might not exhibit fever or typical chills with increase in blood parasitemia. In contrast, for a non-immune individual, an infectious bite may be rapidly fatal. Jaundice is a common occurrence in malaria and can be due to a variety of reasons. The most common causes are the intravascular haemolysis of infected RBCs and a liver damage due to sporozoites. Hepatic dysfunction often causes bilirubinaemia in patients. The major symptoms of malaria are summarized in figure 1.3.

Anaemia is anothertypical feature of acute malarialinfection. The person may develop anemia rapidly, with a heavy loss of hemoglobin as the parasitemia increases. Increase in blood parasitemia is also involved in deranged renal functions, like a sharp rise in blood ureaand creatinine levels and often results in dehydration.

During the asexual blood stages of parasite life cycle of*Plasmodium falciparum* infection, there is an increase in the levels of pro-inflammatory cytokines in blood such as Interleukin-1,6 and 12. There is also an increase in TNF-α and INFγ in the blood. The blood levels of IL-10 and TGF-β lowers simultaneously, resulting in classic malaria symptoms such as fever and anemia. Although the major damage in the patient's system is caused because of the lysis of infected red cells, the process of removal of RBC debris by the spleen,and occlusion of RBCs in blood vessels, yetpro-inflammatory cytokines, speciallyIL-1 and TNF-α, also plays crucial additive role in malaria pathogenesis by causing mitochondrial damageand an increase in the expression of endothelial cell adhesion molecules.

1.3 Life cycle of the malaria parasite.

The life cycle of *Plasmodium falciparum* is completed in two phases: The asexual phase of the life cycle occurs within human RBC and the sexual phase of the cycle occurs inside the mosquito (Figure 1.4).The process of infection initiates when sporozoites; the infectious form of the parasite, is injected into a healthy person through the saliva of an infected mosquito on a blood feed.Upon entry, the sporozoites migrate to the liver and invade the liver cells, where they undergo asexual division inside the hepatocytes. The resulting merozoitesare released into the bloodstream. Merozoites invade RBCs and this stage is referred to as ring stage due to its appearance under the microscope.

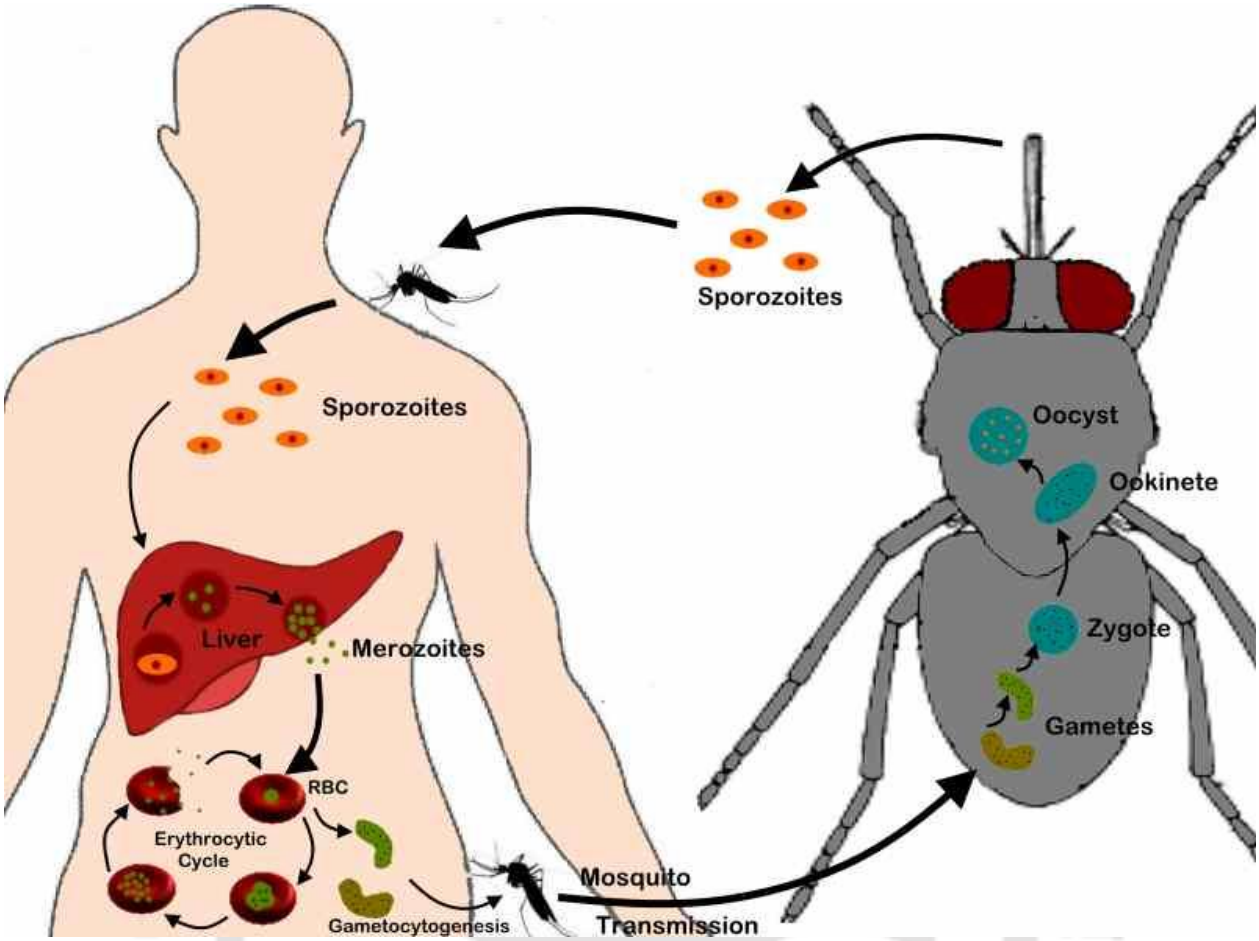

Figure 1.4: Life Cycle of the malaria parasite.

The malaria parasite then undergoes a feeding and growing phase, where it enlarges and consumes more of the space within the RBC. This growing, feeding stage of the parasite is called trophozoite.During this stage the parasite undergoes active cellular metabolism including the digestion ofhaemoglobin from host RBC. At the end of the growthperiod, the parasite undergoes several rounds of nuclear division without any cytokinesis. This multi-nucleate form is called theschizont.

Schizonts burst as RBC membrane becomes fragile, releasing daughter merozoites, which in turn invade new RBCs as the asexual cycle follows. With the increase in the number of asexual cycles the blood parasitemia (percentage of infected RBCs) increase. In *Plasmodium falciparum* one complete asexual cycle from the ring to the schizont takes approximately 36 hours (Figure 1.5).The parasite can switch over to the sexual phase of the life cycle by differentiating into sexual forms of the parasite, known as gametocytes.During a blood meal, the mosquito might ingest one of these gametocytes, triggering the gametogenesis process.

Factors such as a temperature drop increase in CO_2 level or the presence of metabolites from mosquito can trigger the gametogenesis process

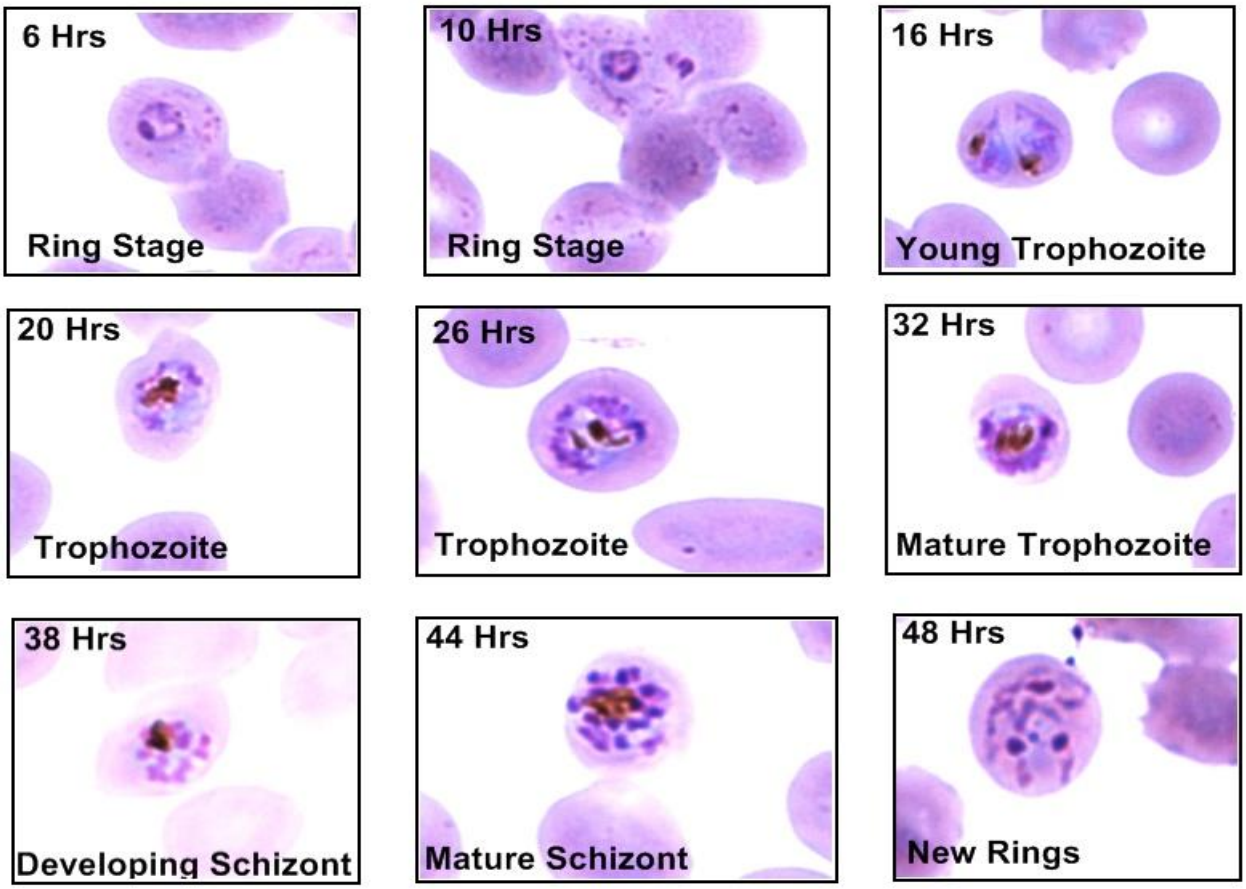

Figure 1.5: Microscopic images of a typical time line of asexual blood stages of the malaria parasite

During a blood meal, the mosquito might ingest one of these gametocytes, triggering the gametogenesis process. Factors such as a temperature drop increase in CO_2 level or the presence of metabolites from mosquito can trigger the gametogenesis process.Gametocytes differentiate into male and female microgametes. Fusion of male and female microgamete leads to the formation of the zygote.

The zygote matures into the motile ookineteform which penetrates the epithelial cells of the mosquitomid-gut andgerminates into oocyst. The oocyst divides by multiple rounds of asexual divisions and ruptures inside the mosquito haemocoel,leading to the development of sporozoites. These sporozoites then invade the mosquito salivary glands, thus starting the infection process again.

1.4 Drug resistance in malaria.

Drug resistance in malaria has grown to be a great challenge inthe control and eradication of the disease. The malaria parasite is reported to have developed resistance to all known antimalarials till date except the latest artemisinin and its derivative drugs. Table 1.1 summarizes the geographic distribution of drug resistant malaria infections in different regions of the world.

Chloroquine resistance in*P. falciparum was* first reported in Thai-Cambodian border of Southeast Asia and Colombia of South Americain late 1950s.Ever since chloroquine resistancehas become a serious concern and has spread to other endemic parts of the world. Soonchloroquine resistance spread to most of African subcontinent by 1978 and Asia and Oceania by 1989. In India the first instance of chloroquine resistance was reported in 1973 in Assam (Karbi-Anglong & Nowgong district).

Table 1.1: Distribution of drug resistance across the globe

Region	**Resistance Reported**		
	CQ	**S-P**	**MQ**
Central America (Mexico, Belize, Guatemala, Honduras, El Salvador, Nicaragua, Costa Rica, NW Panama)	No	No	No
Caribbean (Haiti & Dominican Republic)	No	No	No
South America (SE Panama, Columbia, Peru, Brazil, Venezuela, Ecuador, Bolivia	Yes	Yes	Yes
Western Africa	Yes	Yes	Yes
Southern Africa	Yes	Yes	No
Eastern Africa	Yes	Yes	No
Indian Subcontinent	Yes	No	No
South-East Asia & Oceania	Yes	Yes	Yes
East Asia (China)	Yes	Yes	Yes

The distribution of drug resistant parasite and resistant malaria infections reported across the globe. South America and the African subcontinent are the most deadly endemic areas with resistance reported to more than just CQ, S-P and MQ. (CQ= Chloroquine, S-P= Sulphadoxine-pyrimethamine combinations and MQ= Mefloquine.Source: WHO, 2013. (http://www.who.int/malaria/areas/drug_resistance/en/)

The risingchloroquine resistance had shifted the first line of drug choice to sulphadoxine-pyrimethamine combination. Sooner resistance to SP was also reported along the Thai-

Cambodian border in 1960s. Similarly the first report of resistanceto quinine was reported fromthe same place in mid 1960s. Resistance to another popular drug, mefloquine was first reported in late 1980snear the borders of Thailand-Cambodia. Figure 1.6 summarizes the reports of various drug resistant infections around the world.

Plasmodium falciparum is an extremely complex organism as they can easilyadapt themselves between changes in microenvironments, different hosts, metabolicchanges and drug pressure. The general idea is that, drug resistance results due to a series of spontaneous mutations that confer the parasite with a reduced sensitivity to that particular drug. Also drug resistance appears to develop faster in regions where a largepopulation of parasites are exposed to a specific drug pressure. Natural selection takes care that sensitive parasites are destroyed, while resistant ones would survive.Resistance to several popular antimalarials have been reported over the decade (Figure 1.7). Molecular causes of resistance to different antimalarials have been probed by scientific community. For examplechloroquine resistanceof *P. falciparum*is attributedto the enhanced capacity of the resistant parasite toexpel chloroquine at a rate that does not allow chloroquineto accumulate in levels required for inhibition of heme polymerization.

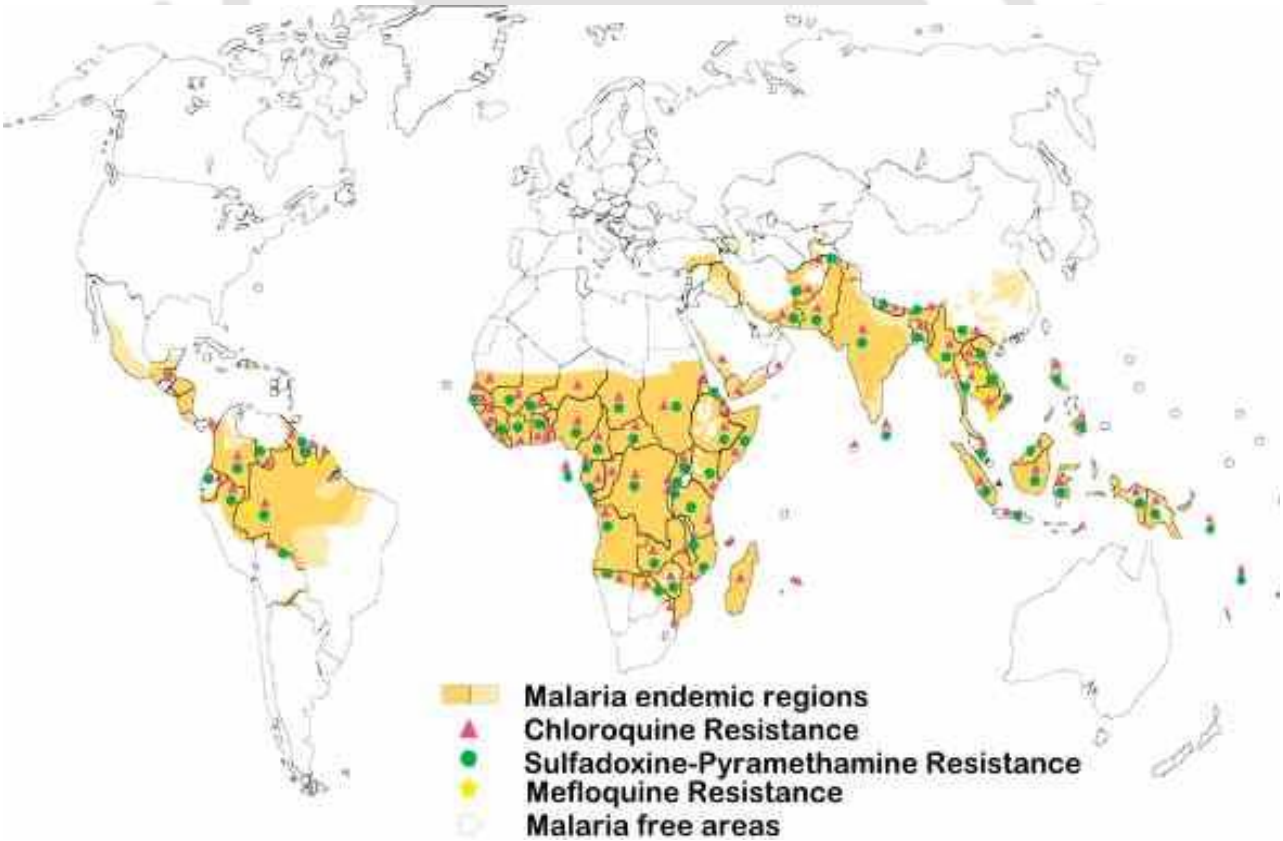

Figure 1.6: Geographical distribution of drug resistance across the world. Courtesy:World health organization, 2012).

Recent studies have identified genes *pfmdr*-1 & 2 and *pfcrt*, that play crucial role in the resistance to quinolone based drugs such as chloroquine and quinine. Similarly folate inhibitors like sulphadoxine-pyrimethamine inhibit the *Plasmodium* dihydrofolate reductase(DHFR) while sulphones and sulphonamide compoundsinhibit the action of dihydropteroate synthase of the parasite. Mutations in these crucial proteins in resistant strains leads to 400–800 fold less binding of the drug to its target. Drug resistance has raised the morbidity and made the treatment of malaria very difficult. Newer approaches to tackle drug resistance (such as the use of combination therapies) have already been resorted to. Alternatively newer drug targets must be identified in *Plasmodium* that would give rise to new antimalarials to tackle the grave situation from a different perspective.

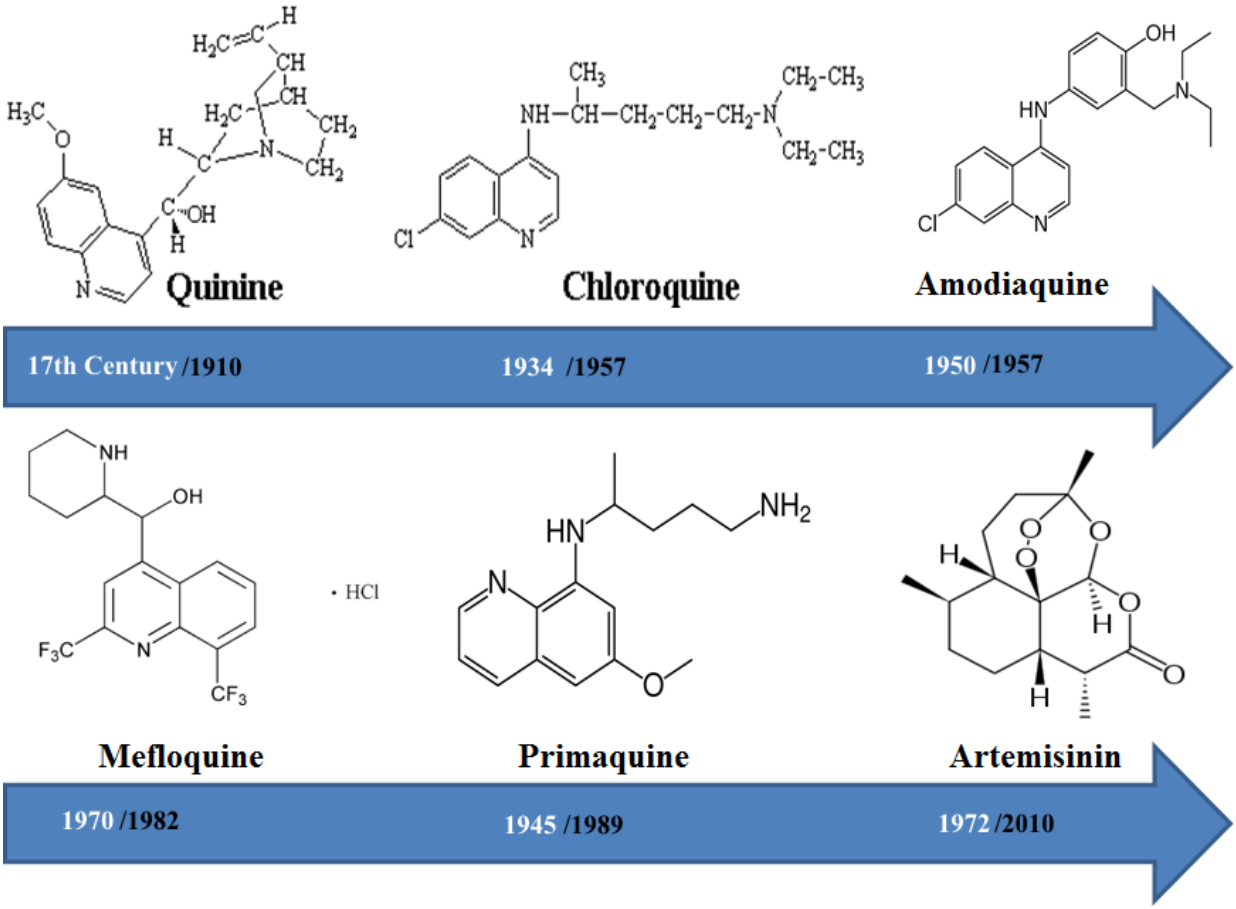

Figure 1.7: Chemical structures of popular antimalarial drugs. The year indicated in white text denotes the year in which the drug was discovered. The year indicated in black text denotes the year in which the first report of resistance against that drug was published.

1.5 Potential drug targets in *Plasmodium falciparum*.

The sequencing of the *Plasmodium falciparum* genome in 2002 has been a milestone development in malaria research. Since then the identification of key parasite genes and metabolic pathways has been a research priority. Gene expression and proteomic profiles of different stages of the malaria parasite have helped in identifying proteins playing key roles in specific life cycle stages. High throughput proteomics has revealed 43% of the identified genes being expressed in the sporozoite stage; 35% being expressed during merozoite stage; 42% being expressed in trophozoite and schizont stage and 47% of the identified genes being expressed in gametocyte stage (Florens et al., 2002). Laboratories working on this disease model have since then identified many plausible drug targets in the parasite. These targets include identified proteases, dehydrogenases and kinases from the *Plasmodium* genome. The cited literature (Tables 1.2 and 1.3) describes the identification, cloning, expression, biochemical characterization, the design and synthesis of inhibitors against key drug targets and the subsequent validation of anti-plasmodial inhibition.

1.6 The kinome of the malaria parasite.

Protein kinases are defined as enzymes that chemically modify other proteins by adding a phosphate moiety to them; thus modifying the function of the target protein. The phosphorylation of target proteins usually results in a change in its function, cellular localization of rate of enzyme activity.

The importance of protein kinases in driving the cellular signaling system can be well understood from the fact that the human genome contains 518 protein kinases, which make up an approximate 2% of the genome (Manning, Whyte et al. 2002).

Table 1.2: Drug targets in the malaria parasite belonging to oxido-reductase and hydrolase groups of enzyme classification.

Drug target in *Plasmodium* species	**References**
1. Dihydroorotate oxidase	(Krungkrai, Krungkrai et al. 1992, McRobert and McConkey 2002, Baldwin, Michnoff et al. 2005, Boa, Canavan et al. 2005, Heikkila, Thirumalairajan et al. 2006)
2. Succinate dehydrogenase	(Suraveratum, Krungkrai et al. 2000)

3. Dihydrofolate reductase	(Fidock, Nomura et al. 1998, Le Bras and Durand 2003, Dar, Khan et al. 2008)
4. NADH dehydrogenase	(Krungkrai, Kanchanarithisak et al. 2002)
5. Glutathione reductase	(Zhang, Hempelmann et al. 1988, Biot, Bauer et al. 2004)
6. Thioredoxin reductase.	(Luersen, Walter et al. 2000, Krnajski, Gilberger et al. 2002)
7. Cytochrome c reductase.	(Fieser, Berliner et al. 1948)
8. Ribonucleoside-diphosphate reductase.	(Chakrabarti, Schuster et al. 1993, Lytton, Mester et al. 1994, Barker, Metelev et al. 1996)
9. HMB-PP reductase	(Rohrich, Englert et al. 2005, Vinayak and Sharma 2007)
10. S-adenosyl-l-homocysteine hydrolase	(Messika, Golenser et al. 1990, Kitade, Kozaki et al. 1999, Shuto, Minakawa et al. 2002, Bujnicki, Prigge et al. 2003)
11. Leucine aminopeptidase	(Nankya-Kitaka, Curley et al. 1998)
12. Dipeptidyl aminopeptidase 1	(Klemba, Gluzman et al. 2004)
13. Plasmepsins (aspartic acid proteases)	(Noteberg, Hamelink et al. 2003, Romeo, Dell'Agli et al. 2004)

A comprehensive list of *Plasmodium* drug targets, belonging to oxido-reductase and hydrolase group of enzymes, which have been studied.

Similarly the genome sequence of *Plasmodium falciparum* has revealed the presence of 65 eukaryotic protein kinases which approximately amounts to 1.6% of the transcriptionally active genes (Ward, Equinet et al. 2004, Anamika, Srinivasan et al. 2005). Upto 30% of the *Plasmodium* proteins exist in their phosphorylated state during any instance along the asexual blood stages of the parasite.

Table 1.3: Drug targets in the malaria parasite belonging to transferase group of enzyme classification.

Drug target in *Plasmodium* species	**References**
1. RNA methyltransferase	(Riguet, Desire et al. 2005, Leber, Skippen et al. 2009)
2. G3P acyltransferase	(Santiago, Zufferey et al. 2004, Wydysh, Medghalchi et al. 2009)
3. CDPK7	(Kumar, Tripathi et al. 2014, Morlon-Guyot, Berry et al. 2014)
4. CDPK6	(Coppi, Tewari et al. 2007, Ejigiri and Sinnis 2009, Koyama, Chakrabarti et al. 2009, Tewari, Straschil et al.

	2010)
5. PI-4-P-5-kinase	(Santiago, Zufferey et al. 2004)
6. TKL3	(Abdi, Eschenlauer et al. 2010)
7. PEP carboxykinase	(Hayward 2000)
8. Sphingosine-N-acyltransferase	(Gerold and Schwarz 2001)
9. Serine-palmitoyltransferase	(Gerold and Schwarz 2001)
10. Purine-nucleoside phosphorylase	(Kicska, Tyler et al. 2002)
11. Hypoxanthine phosphoribosyltransferase	(Dawson, Cochran et al. 1993, Sarma and Kumar 1998, Li, Tyler et al. 1999)
12. Glutathione transferase	(Harwaldt, Rahlfs et al. 2002, Liebau, Bergmann et al. 2002, Fritz-Wolf, Becker et al. 2003, Perbandt, Burmeister et al. 2004)
13. Farnesyl-diphosphate farnesyltransferase	(Chakrabarti, Da Silva et al. 2002)
14. Choline kinase	(Choubey, Maity et al. 2007)
15. Guanylate kinase	(Tarun, Peng et al. 2008)

A comprehensive list of *Plasmodium* drug targets, belonging to transferase group of enzymes that have been studied.

Protein kinases have always been considered as an important group of drug-targets (Cohen 2002) for many reasons. The primary reason is that the chemical kinetics of a phosphorylation reaction and the overall structural features of most PKs are basically conserved which means an array of small molecules can bind to their catalytic site, displacing the natural substrate ATP (Gray, Detivaud et al. 1999). Secondly, the reversible protein phosphorylation mechanism is a recurring theme in the regulation of cellular homeostasis, growth, proliferation and differentiation in all forms of life ranging from archaea to human. As a result pharmaceutical companies first aim at identifying novel kinases as drug targets in their drug discovery programs against diabetes, neuropathic diseases, cancer, inflammation and autoimmune disorders. Thus many protein kinase inhibitors (for various disease models) are either available in the market or are undergoing late clinical studies(Giamas, Stebbing et al. 2007).

Significant differences in the structure and signaling mechanisms of the human and *Plasmodium* protein kinases suggest that selective inhibition of the parasite PKs are possible (Holton, Merckx

et al. 2003). Many recombinant kinases from the *Plasmodium* genome have displayed *in vitro* kinase activity which increases the success of high throughput screening strategies. Taking advantages of 3D- modeling or solved protein kinase structures medicinal chemistry has rapidly expanded. The search for active molecules that could inhibit key parasite kinases is now a fast process due to the advent of structure–activity relationship (SAR)-based approaches.

The 65 ePK sequences can be broadly classified into the following classes:

1.6.1 The Caesin kinase 1 group: Most eukaryotic organisms possess multiple kinases of the CK1 group. The *Plasmodium* kinome on the other hand has a single member of the CK1 group (Barik, Taylor et al. 1997).Although the role of this kinase in the parasite life cycle has not been elucidated clearly, the recombinant CK1enzyme shows phosphorylation activity in vitro and phosphorylates many proteins from *Plasmodium* extracts.

1.6.2 The CMGC group: This group derives its name from the included members (a) The Cyclin dependent kinases (CDKs), which are key modulators of cell-cycle progression. (b) Mitogen activated protein kinases (MAPK), which are known to relay extra-cellular of intra-cellular signals to effector molecules such as proteins which control cell-cycle progression or act as transcription factors. (c) Glycogen synthase kinase 3 (GSK 3) family, which also play important roles in cell proliferation and (d) Cyclin dependent kinase like kinases (CLKs), which regulate the cellular RNA metabolism.

A total of 18 *Plasmodium* kinases fall under this category, making the CMGC group, the most prominent one in the *Plasmodium* kinome. The abundance of CMGC kinases in the *Plasmodium* kinome correlates with the number of successive proliferative and non-proliferative phases which makes up the life cycle of *P. falciparum*.

1.6.2.1 Cyclindependent kinases: Many CDKs have been found to be present in the *Plasmodium*kinome(Doerig, Endicott et al. 2002, Ward, Equinet et al. 2004).Two CDKs, PfPK5 and Pfmrk, have shown to be regulated by the cyclin binding events. The activity of malaria CDKs have been shown to be highly regulated, the target residues are mostly conserved (Doerig, Endicott et al. 2002) and most of them exhibit auto-phosphorylation activity *in vitro*. Cyclin dependent kinase inhibitors are small conserved protein molecules which inhibit cyclin dependent kinases in response to DNA damage and stress. Figure 1.7 shows the crystal structure of PfCDPK4 from *Plasmodium falciparum* (Wernimont, Walker et al. 2014).

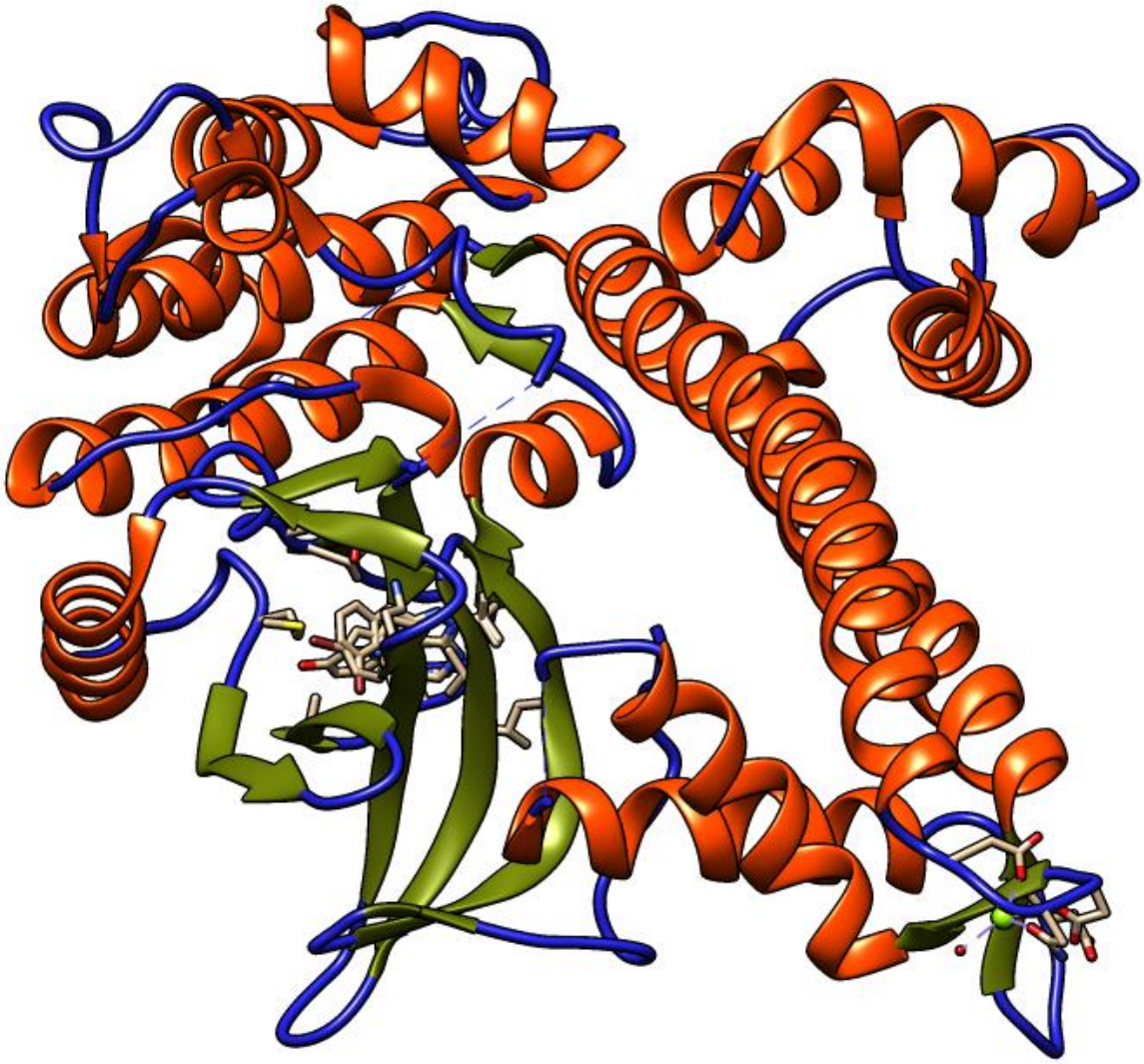

Figure 1.8: Crystal structure of CDPK4(PDB code: 4QOX) from *Plasmodium falciparum* 3D7 (Wernimont, Walker et al. 2014). Structure was re-drawn from the original pdb file using UCSF Chimera 1.10.

CDK inhibitor proteins have not yet been found to be coded by the *Plasmodium*genome; nevertheless, *Plasmodium* CDKs have been shown to be inhibited by mammalian cyclindependent kinase inhibitors *in vitro*. This implies that the key structural aspects required for CDK inhibition are conserved in both the mammalian and *Plasmodium* CDKs(Li, Le Roch et al. 2001). PfPK5 (Figure 1.8)and PfCDPK4 (Figure 1.7) are the cyclindependent kinases for which a published crystal structure is available.

Information revealed from this structure along with future structural biology studies on PfPK5 might disclose unique ways in which PfCDKs regulate cellular proliferation(Holton, Merckx et al. 2003). Considering the unusual mechanism of *Plasmodium*schizogony, in which then genome replicates multiple times in the absence of cytokinesis, PfCDKs might play critical

regulatory roles. The particular roles played by these kinases in *Plasmodium* cell cycle control and coordination remains to be elucidated and chemical CDK inhibitors might come handy in unraveling the cellular functions of CDKs(Graeser, Wernli et al. 1996)

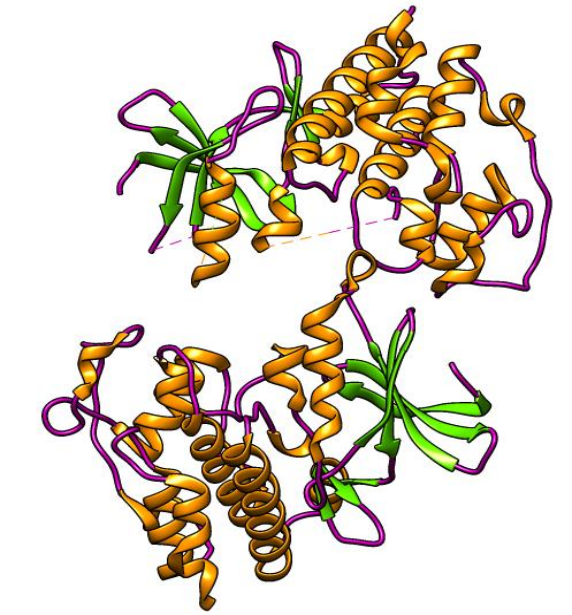

Figure 1.9: Crystal structure of PfPK5 from *Plasmodium falciparum* (PDB code: 1OB3)(Holton, Merckx et al. 2003). Structure was re-drawn from the original pdb file using UCSF Chimera 1.10.

.

1.6.2.2 Mitogen activated protein kinases (MAPKs): MAPKs are known to regulate cell cycle proliferation and cellular differentiation in eukaryotes in response to a wide variety of internal or external stimuli(Owens and Keyse 2007). *Plasmodium falciparum*kinome contains 2 atypical MAPKinase homologues, Pfmap-1 and Pfmap-2. Studies have shown that Pfmap-1 and Pfmap-2 might act in a supplementary fashion i.e., inactivation of *pfmap-1* does not hinder detectable parasite growth in vitro but the over-expression of Pfmap-2 in the *pfmap-1*¯mutant parasites clearly indicates that Pfmap-1 serves an important function in the parasites and this function must be taken over or supplemented by the other MAPK (Pfmap-2) in the absence of Pfmap-1.

The function of Pfmap-2 appears to be essential for the parasite to complete the erythrocytic asexual cycle(Dorin-Semblat, Quashie et al. 2007). Classical MAPK kinase (MAPKK) orthologsseem to be absent in different strains of the malaria parasite (Dorin-Semblat, Quashie et al. 2007). The regulatory mechanisms of PfMAPKs remain to be elucidated although some studies (Dorin, Le Roch et al. 2001, Lye, Chan et al. 2006) suggest that *Plasmodium* NIMA kinases might act as atypical regulators of Pfmap-2. Figure 1.9 shows the crystal structure of the MAPK, PF11_0147 from *Plasmodium falciparum.*

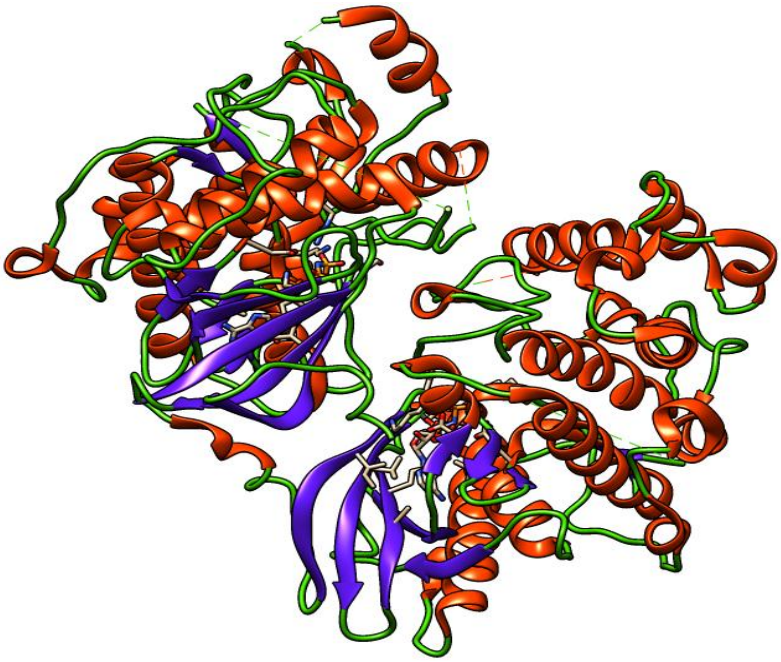

Figure 1.10: Crystal structure of a MAPK(PF11_0147) from *Plasmodium falciparum* (PDB code: 3NIE), (Wernimont, Walker et al. 2010). Structure was re-drawn from the original pdb file using UCSF Chimera 1.10.

.

***1.6.2.3 GSK3 and CLKs*:** Three *P. falciparum* sequences fall under the GSK3 subfamily. One of them has been extensively characterized: PfGSK3. PfGSK3 has been found to co-localize with Maurer's clefts, and is believed to be exported to host RBCs (Droucheau, Primot et al. 2004). Only a single published report of *Plasmodium* CLK; preliminary characterization of a LAMMER-like kinase is available(Li, Le Roch et al. 2001).

1.6.3 The CAMK group: Thirteen *Plasmodium*ePKs have been classified under this group (Ward, Equinet et al. 2004). Among them, the CDPKs have been studies extensively. Five *Plasmodium* CDPKs are structurally similar to plant CDPKs in domain organization, while CDPK6 is structurally different, containing an incomplete C-terminal calmodulin-like domain an N-terminal kinase domain, with an extra EF hand (Coppi, Tewari et al. 2007). Knockout of CDPK genes in *P. berghei* has revealed that CDPKs areindispensible for parasite ookinete motility(Ishino, Orito et al. 2006, Siden-Kiamos, Ecker et al. 2006), formation of microgametes(Billker, Dechamps et al. 2004)and the invasion of hepatocytes by the sporozoites(Coppi, Tewari et al. 2007). Calcium ions regulate the activity of CDPKs by acting as a second messenger and the sub-cellular localization of some CDPKs is known to be governed

by the protein's N-terminal acylation (Moskes, Burghaus et al. 2004). N-terminal acylationalong with the stage-specific expression profiles of the genes, contribute to the CDPK signaling specificity in response secondary messenger. A recent study has demonstrated PfCDPK1 to be essential for the parasite to complete the erythrocytic cycle(Kato, Sakata et al. 2008). This study also reports that treatment of asexual stage parasites with CDPK1 inhibitor preventsmerozoite egression. The study strongly relates CDPK1 to parasite motility and the observation that CDPK1 phosphorylates a glideosome component, MTIP, *in vitro*, further validates the above findings.

1.6.4 The AGC group: Recent reports have unraveled the importance of cAMP and cGMP dependent kinase signaling pathways during different stages of the *Plasmodium* life-cycle. Three*P. falciparum* protein kinases that has been classified and extensively characterized under the AGC group are: PfPKA, PfPKG and PfPKB.

PfPKA is the only parasite cAMP effector kinase. Inhibition of this kinase blocksparasite growth *in vitro*(Syin, Parzy et al. 2001), but their mechanism of action is unclear. One hypothesis proposes PKA as a cAMPdependent modulator of anion channel conductance of the host RBC(Merckx, Le Roch et al. 2003). Experiments on *P. falciparum* blood stages indicate that cAMPdependent PKA signaling regulates the level of cytosolic calcium thereby keeping a tight control over the parasite cell division*in vitro*(Beraldo, Almeida et al. 2005). cAMP and calcium-dependent signaling has been shown to regulate the exocytosis of microneme from parasite cytosol in *P. berghei* and hence is an essential step in the invasion of hepatocytes(Ono, Cabrita-Santos et al. 2008).

PfPKG of parasite is found to be selectively inhibited over its human counterpart by trisubstitutedpyrrole based compounds (Gurnett, Liberator et al. 2002). It has also been demonstrated in *T. gondii*, that a single amino acid substitution in the ATP-binding site, makes the PKG kinase resistant to inhibition by the above compounds (Donald, Allocco et al. 2002). Further studies have revealed the role of *T. gondii* PKG ingliding motility, secretion of micronemes, attachment to host RBC and invasion(Wiersma, Galuska et al. 2004). The above trisubstitutedpyrrole based compounds failed to block the rounding up of gametocytes *in vitro* in malaria parasites expressing a resistant version of the PKG gene. This demonstrates a key role of PKG in gametocyte activation(Diaz, Allocco et al. 2006).

PfPKB is the third characterized kinase in this group. Regulation of mammalian PKB is governed by phosphoinositides which interact with the PH domain of PKB (Marte and Downward 1997). PKB from *Plasmodium* lacks a PH domain. It is activated when calcium-boundcalmodulinbinds to thecalmodulin-binding domain (CBD) at the N-terminal region of the kinase (Kumar, Vaid et al. 2004, Vaid and Sharma 2006). This type of novel calmodulin based signaling pathway, involving activation of PKB was recently discovered in *P. falciparum*. Phospholipase C is involved in calcium secretion and hence could be a regulator of this kinase signaling pathway(Vaid, Thomas et al. 2008). Experimental evidences that PfPKBphosphorylates aglideosome-associated protein, raises expectation that in the near future the functions of many more *Plasmodium* kinases would be unraveled.

1.6.5 The TKL group: Five kinases from *Plasmodium* are homologous to human TKLs, but there are no published reports on them yet.

1.6.6 The NIMA-related kinase (Nek) Group: Four *P. falciparum* kinases cluster under this family.NIMA-related kinases are thought to play key roles in the cell division process, particularly taking part in centrosome replication(Fry, O'Regan et al. 2012). Data from microarray studies demonstratethe expression of Pfnek-1 in both the asexual and sexual stages. Other 3 Neksfrom *Plasmodium*are found to be expressed particularly in gametocyte stage (Le Roch, Zhou et al. 2003). Interestingly it has been shown that Pfnek-1 phosphorylates MAPK Pfmap-2 *in vitro*, but does not phosphorylate Pfmap-1 or any other mammalian MAPKs(Dorin, Le Roch et al. 2001). The orthologue of Pfnek-1 from *P. berghei* is found to be expressed in the male gametocytes but not in the female ones (Khan, Franke-Fayard et al. 2005), hence it is believed that Pfnek-1 plays a possible role in male gametogenesis. Soon after another Pfnek enzyme (Pfnek-3) was found to phosphorylate Pfmap-2(Lye, Chan et al. 2006). The only report that reveals the role of any plasmodial Nek in the parasite life cycle is that of Pbnek-4 which has been shown to be essential in ookinete maturation in the rodent malaria model.

1.6.7 Orphan kinases: The *Plasmodium falciparum* kinome contains several kinases that do not resemble structurally to any of the established ePK groups, and hence are classified under orphan kinases. PfPK7 is one of these orphan kinases which have been well studied (Figure 1.10). C-terminal lobe of PfPK7 shows highest homology to MAPKKs, while its N-terminal domain is homologous to fungal PKAs (Dorin, Semblat et al. 2005).Parasites in which PfPK7 is deleted shows slower growth rate, produces lesser number of daughter merozoites, as well as

demonstrate impairment in oocyst formation (Dorin-Semblat, Sicard et al. 2008).Another well studied orphan kinase from *Plasmodium* is PfPK9 (Philip and Haystead 2007) , which demonstrates the ability to auto-phosphorylate itself as well as phosphorylate exogenous substrates *in vitro*. Auto-phosphorylation specifically occurs on 3 residues. When any of the critical residues are mutated, enzyme activity is abolished, which suggests a potentially complex mechanism of regulation of this kinase *in vivo*. Recombinant PfPK9 displays selective phosphorylation of an E2 ubiquitin-conjugating enzyme from parasite extract, thereby down-regulating its ubiquitin-conjugating activity (Philip and Haystead 2007). These findings suggest the pivotal role played by PfPK9 in proteasome regulation of *Plasmodium*.A distinct cluster of twenty one orphan *kinases in* the malaria parasite belong to the FIKKs. These kinases appear to be solely present in apicomplexans, with a maximum of one enzyme in most species.

These kinases possess a *Plasmodium* export element (PEXEL) motif (Schneider and Mercereau-Puijalon 2005), and one of the FIKKs have been shown to localize in the host RBC (Nunes, Goldring et al. 2007).

1.6.8 Atypical Protein Kinases (aPKs): Atypical protein kinases are grouped into a separate class due to their lack of sequence similarity to established ePK domains, but have been demonstrated experimentally to possess protein kinase activity. All aPK families are invariably small; many families have just a single member in vertebrates, and none in lower organisms. Other aPK families might be discovered in the near future using biochemical methods, but since all of the discovered aPK families are small, it can be understood their distribution in the genome is rare. Atypical protein kinases can be further classified into the following families.

1.6.8.1 Alpha Kinases:The earliest discovered kinase of this family is the heavy chains of myosin kinases from the amoeba *Dictyostelium discoideum*. Although these kinases are evolutionarily restricted, they are homologous to the commonly found eF2 kinases. Several other kinases from mammalian origin have been shown to be homologous to alpha kinases. The channel kinases Chak1 and Chak2, known to be multi-purpose trans-membrane proteins, which act as kinases as well as ion channels are also found to be homologous to alpha kinases. Study of the 3D structure of CHAK1 gene has (Yamaguchi, Matsushita et al. 2001)revealed a clear structural similarity to the ePK domain. Kinase activity has been demonstrated in several members of this aPK family

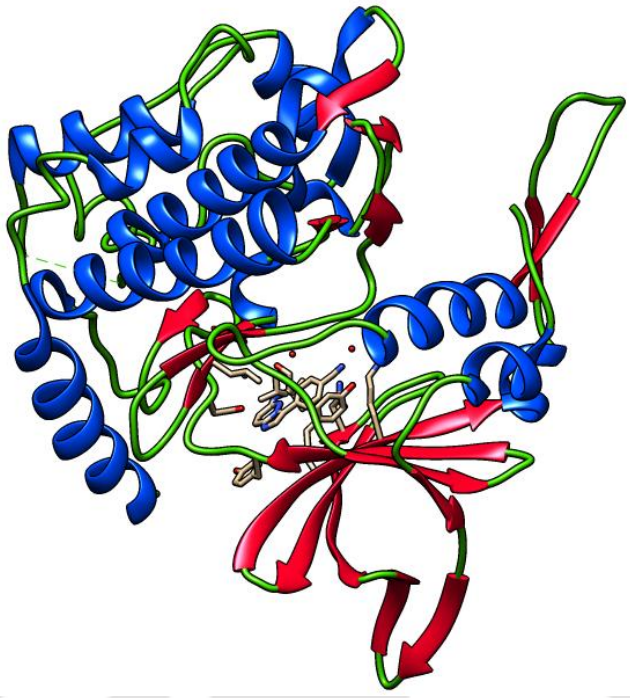

Figure 1.11: Crystal structure of orphan kinase PfPK7 from *Plasmodium falciparum* (PDB code: 2PML)(Merckx, Echalier et al. 2008). Structure was re-drawn from the original pdb file using UCSF Chimera 1.10.

1.6.8.2Phosphatidyl inositol 3' kinase-related kinase family (PIKK):This family of aPK contains either a phosphatidyl inositol 3 or phosphatidyl inositol 4 kinase , flankedby a FAT domain at the N-terminal and a FATC domain at its C-terminal (Bosotti, Isacchi et al. 2000). Human genome contains 6 members of this family and 5 of them have been shown to have distinct protein kinase activity. Multiple sequence alignment demonstrates that PI34K domains belong to a distinct domain subfamily. The PI34K domain is homologous to ePK domain; with a strong similarity in structures and conservation of critical catalytic residues. This includes the catalytic asp residue, the DFG and the HRD motifs (Walker, Perisic et al. 1999).

1.6.8.3The A6 kinase family:The A6 family consists of the related human A6r and A6 genes, along with its close homologs in *Drosophila*, *C. elegans* and yeast. The first report in which an A6 kinase was first cloned and expressed was in 1994. This study demonstrated tyrosine kinase activity of A6 in bacterial expression system (Beeler, LaRochelle et al. 1994). A6r was soon discovered. Both the kinases were found to bind ATP but could not yield kinase activity *in vitro*(Rohwer, Kittstein et al. 1999).

1.6.8.4 ABC1/ADCK family:This conserved family of aPKs was discovered as putative kinases by computational methods such as Protein-Blast and HMMs. ABC1/ADCK domains are weakly homologous to the ePK domain, but most conserved catalytic motifs are highly conserved (Leonard, Aravind et al. 1998). Although these kinases lack an overall sequence similarity with the ePK domain, yet these kinases contain motifs which are exclusive toprotein kinases. These include the kinase catalytic VAIK motif, the DFG motif, and a QTD motif.

1.6.8.5 Pyruvate Dehydrogenase Kinase family (PDK):This family of kinases is found in the mitochondria and contains a domain homologous to the prokaryotic histidine kinases. Biochemical experiments have revealed that PDKs phosphorylate serine rather thanhistidine. Published crystal structures (Machius, Chuang et al. 2001, Steussy, Popov et al. 2001) confirm that the PDK domain is homologous to that of histidine kinases, and is not related to the typical ePK domain.

1.6.8.6Bromodomain Kinase family (BRDs):This family of kinases consists of the BRD2 kinase and its near homologs in human and other model organisms. Dennis and Green (1996) BRD2 was first identified as an auto-phosphorylating protein specifically active in nuclear extracts of Hela cells (Denis and Green 1996). Studies in which recombinant BRD2 was expressed in *E. coli*, the recombinant protein showed kinase activity *in vitro*. Mutation of putative catalytic K578 resulted in abolished kinase activity. In another study recombinant BRD2 purified from COS cells also demonstrated *in vitro* kinase activity.

1.6.8.7 TAF – TATA binding factor associated factors:TAF1 gene is known to be a component of the basal transcriptional machinery in all eukaryotes. It has no close homologs. It was reported that TAF1 is a protein kinase and contains two lobes which are independent of each other and can phosphorylate another basal transcription factor RAP74 (Dikstein, Ruppert et al. 1996). Immune-purified TFIID from Hela cells as well as cloned TAF1in insect cells and*E. Coli* showed *in vitro* kinase activities despite significant sequence similarity to other protein kinases. Later studies have confirmed similar findings (O'Brien and Tjian 1998, Solow, Salunek et al. 2001). It was revealed that TAF1L, a retro-transposed copy of TAF1is present in human and other primates. This kinase was expressed during spermatogenesis and is a substitute for TAF1 (Wang and Page 2002).

1.6.8.8 BCR:This gene isbest known as the fusion partner of Abl kinase in leukemia. TheBCR gene also shows auto- and trans-phosphorylation activities due to conserved cysteines and tyrosines(Maru and Witte 1991). The human isoform as well as the Drosophila counterpartis ~70% and ~ 36% identical to ePK respectively but both lack the N-terminal putative kinase domain.

1.6.8.9 FASTK:The human Fas-activated kinase was characterized by as a novel kinase that was de-phosphorylated and activated during apoptosis (Tian, Taupin et al. 1995). Differential expression of FASTK during apoptosis signaling pathways has been reported (Brutsche, Brutsche et al. 2001). A close orthologue of this gene is reported in mouse but a low (~27%) identity between these genesit is not sufficient to confidently assign a kinase function to the mouse orthologue.

1.6.8.10 G11 kinase:This family contains a single gene called G11/STK19, which has been shown to bind ATP, and have serine/threonine kinase activity against alpha casein as substrate with a putative catalytic lysine shown as a requirement for enzyme function (Gomez-Escobar, Chou et al. 1998). Homologs of this kinase are found in rat and mouse (~85% identity), and adivergent putative homolog has also been identified in zebrafish (45% identity) with no other homolog seen in any other model organism.

1.6.8.11 Transcriptional Intermediary Factor 1 family:Three Transcriptional Intermediary Factor 1 genes have been grouped in this family, out of which only this kinase has been demonstrated to have kinase activity, *in vitro*(Fraser at al, 1998). The other two genes are nearly similar and are also likely to be kinases. Drosophila and mosquito genomes also contain a single copy of this gene. Auto-phosphorylation was detected in immune-purified proteins and is believed to be involved in the transcriptional machinery by phosphorylating several other TATA-associated factors. Like TAFs and BRD kinases, the TIFs also contain bromodomains.

1.6.8.12 H11 kinases:*The* H11 kinase is homologous to the ICP10 gene of Herpes simplex virus, both having distinct kinase activity (Nelson, Zhu et al. 1996, Smith, Yu et al. 2000). Kinase activity of H11was demonstrated in proteins purified from both bacterial and eukaryoticexpression systems. Mutation of a putative catalytic lysine destroyed the kinase activity.

1.6.8.13 RIO family of kinases:The RIO family has 3 distinct subfamilies, with at least a single member of each subfamily in *Drosophila*, Human and *C.elegans*. *S. cerevisiae* has two members, one of each of RIO1 and RIO2 kinases and the fungi *Aspergillusnidulans*has a single member among the third subfamily, RIO3. Structural homologs of RIO kinases are also present in many archeal genomes. The first biochemically characterized, Yeast RIO1, was reported to have ser kinase activity (Angermayr, Roidl et al. 2002). Their sequences do not align to a great extent with known eukaryotic protein kinases.Nevertheless,several critical catalytic residues required for kinase activity are conserved in the RIO family too.

1.7 RIO family of atypical kinases

The protein kinases of the RIO family were characterized only recently, based on the studies conducted on the right open reading frame gene or RIO-1 of *S. cerevisiae*(Angermayr and Bandlow 1997). Subsequently, detailed analysis of sequence databases resulted in the discovery of many more genes that were homologous to the kinase-like domain of yeast RIO-1(Leonard, Aravind et al. 1998, Manning, Whyte et al. 2002). Later on a distinct RIO-2 kinase was isolated and characterized in yeast(Geerlings, Faber et al. 2003). Even though, the RIO domain contains a kinase signature motif, it hardly shows any similarity in sequence data with eukaryotic protein kinases (ePKs)(Angermayr, Roidl et al. 2002).As a result, it had to be classified as an atypical protein kinase(Manning, Whyte et al. 2002). Bioinformatics analysis confirms that representatives of the RIO domain are well conserved in organisms ranging from archaea to humans.

1.7.1 Structural features of RIO kinases: When the crystal structures of RIO-2 and RIO-1 were determined from an archaea, *A. fulgidus*, detailed structural characterization and subtle differentiation between RIO-1 and RIO-2 subfamilies were possible(LaRonde-LeBlanc and Wlodawer 2004, Laronde-Leblanc, Guszczynski et al. 2005). The overall fold of these two enzymes is quite similar. The RIO domain consists of an N-lobe made up of a twisted β –sheet (β1–β6) and a long α helix (αC) which packs the ATP-binding pocket, a hinge region, and a C-lobe, creating the niche for the catalytic loop and the metal-binding loop.The dissimilarity of the RIO kinase domain with PkC lies in the fact that it contains only three of the canonical ePK-helices (α helices E, F, and I) in the C terminal-lobe. The structures of both RIO-1 and RIO-2

contains an additional α helix (α helix R) located N-terminal to the canonical N-lobe β-sheet that extends the RIO domain (Fig. 1.7). One distinguishing feature is that, all RIO domains contain a stretch of 18–27 amino acid residues between α helix C and β sheet 3. That region was termed as the "flexible loop" as it appeared disordered in the crystal structures.

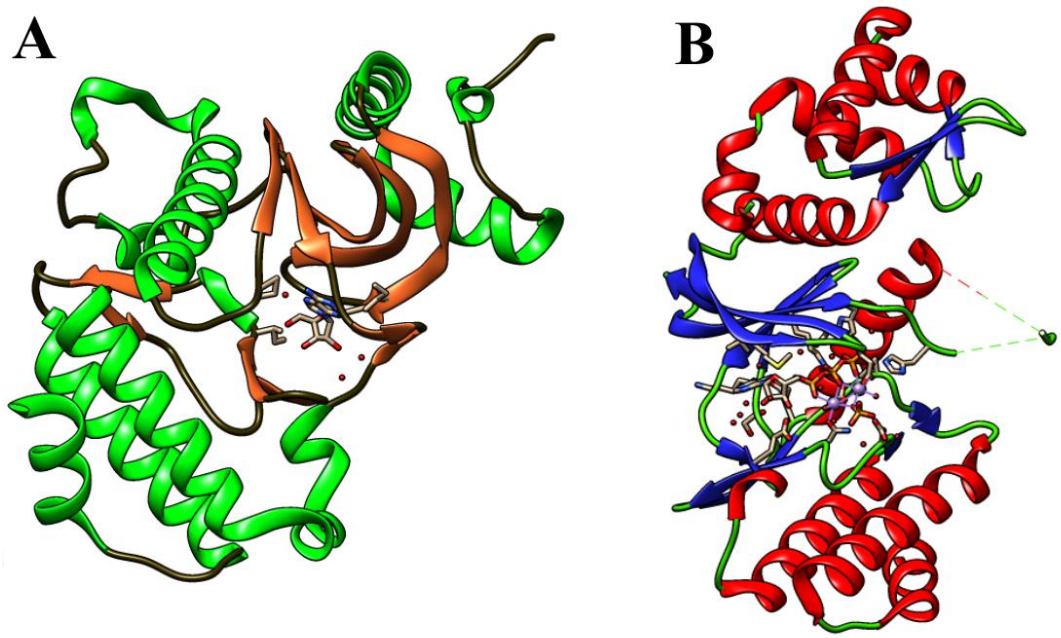

Figure 1.12: Crystal structures (A) RIO-1 kinase (PDB code: 1ZTF)(Laronde-Leblanc, Guszczynski et al. 2005)and (B) RIO-2 kinase from *Archeoglobusfulgidus* (PDB code: 1ZAO)(LaRonde-LeBlanc and Wlodawer 2004, Laronde-Leblanc, Guszczynski et al. 2005). Structure was re-drawn from the original pdb files using UCSF Chimera 1.10.

The dissimilarity of the RIO kinase domain with PkC lies in the fact that it contains only three of the canonical ePK-helices (α helices E, F, and I) in the C terminal-lobe. The structures of both RIO-1 and RIO-2 contains an additional α helix (α helix R) located N-terminal to the canonical N-lobe β-sheet that extends the RIO domain (Fig. 1.11). One distinguishing feature is that, all RIO domains contain a stretch of 18–27 amino acid residues between α helix C and β sheet 3. That region was termed as the "flexible loop" as it appeared disordered in the crystal structures.

1.7.2 RIO kinases and ribosome biogenesis: RIO-1 kinase, has been demonstrated to be an essential gene in *S. cerevisiae*, and is required for the correct cell cycle progression and maintenance of chromosome integrity(Angermayr, Roidl et al. 2002). When yeast cells are

deprived of RIO-1, cell cycle appears to be arrested at G1or mitosis, which suggests that RIO-1 activity is absolutely essential for cells to enter into S phase and exit from mitosis(Angermayr, Roidl et al. 2002). Also, both yeast RIO-1 and RIO-2 were recognized as non-ribosomal factors which are required for the processing of late 18 S rRNA(Angermayr, Roidl et al. 2002, Geerlings, Faber et al. 2003). In RIO-1 or RIO-2 knockouts, cellular growth rate is affected and results in an accumulation of 20 S rRNA(Geerlings, Faber et al. 2003). RIO 1 deletion results in cell cycle arrest. Deleting either RIO-1 or RIO-2 is lethal for the cells, which clearly indicates that both the proteins perform distinct functions. It has been further shown that the yeast RIO kinases have serine phosphorylation activity *in vitro*, and the presence of conserved kinase catalytic residues is required for their in vivo function (Vanrobays, Gleizes et al. 2001).

1.7.3 Structural features of *Archaeoglobusfulgidus* RIO-2 kinase :The first RIO-2 kinase was systematically studied in the archaea *Archeoglobusfulgidus*(LaRonde-LeBlanc and Wlodawer 2004). When the crystal structure of afRIO-2 was analyzed, the structure clearly revealed the presence of two domains (Figure 1.12). The N-terminal domain was structurally very different from the members of RIO-1 proteins but was conserved in members of the RIO-2 family only.

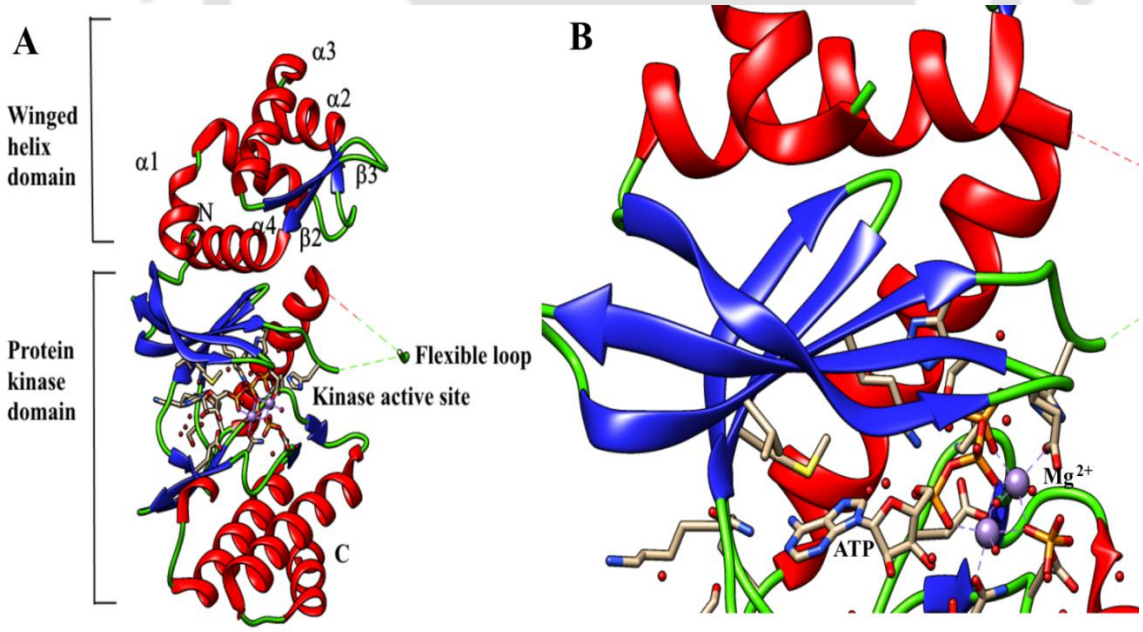

Figure 1.13: (A) Structural annotation of the crystal structure of RIO-2 kinase from *Archeoglobusfulgidus*.(PDB code: 1ZAO) (B) ATP binding pocket of AfRIO-2 kinase (LaRonde-LeBlanc and Wlodawer 2004). Structure was re-drawn from the original pdb file using UCSF Chimera 1.10.

This domain is homologous to the 'winged helix' domain (Fig 6) which has been previously reported to be a part of DNA binding proteins. The structure reveals that this domain is made up of 4 α helices followed by 2 β strands and a 5th helix. A strand which joins the 2nd and 3rd helices combines with the other 2 β strands to give a β sheet. The loop between the 2nd and 3rdβ strands takes up the appearance of a "wing", from which the name 'winged helix' came into existence(LaRonde-LeBlanc and Wlodawer 2004). The sequence of the C-terminal domain of AfRIO-2 is conserved in both RIO-1 and RIO-2 proteins. This domain bears a great deal of structural homology to the existing protein kinase domains. It is a dual lobe structure (an N terminal and C terminal lobe) with a twisted five-stranded β sheet and only a single long α helix in the N-terminal lobe while the C-terminal lobe is made up of four β strands and three α helices. A combination of a winged helix domain and a protein kinase domain has never been previously reported.

1.7.4 RIO-2 kinase from *Chaetomiumthermophilum:* Structurally ctRIO-2 is almost entirely similar to the afRIO-2 structure which was previously solved. The presence of the winged helix domain and protein kinase domain connected by a flexible hinge region is also seen in ctRIO-2 (Figure 1.13)(Ferreira-Cerca, Sagar et al. 2012). .

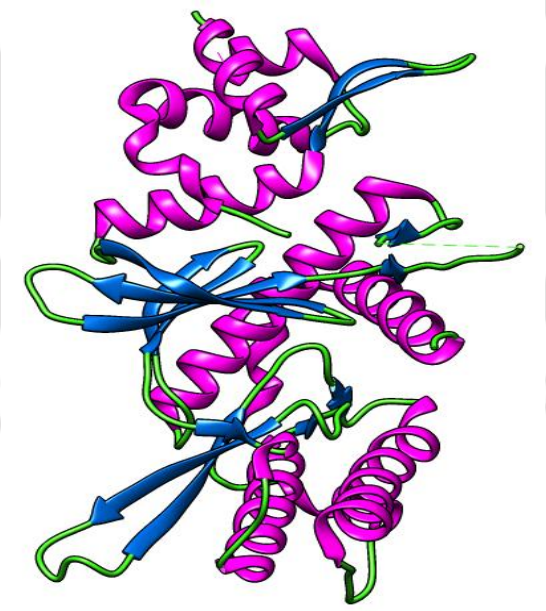

Figure 1.13: Crystal structure of RIO-2 kinase from *Chaetomiumthermophilum*(PBD code: 4GYG)(Ferreira-Cerca, Sagar et al. 2012). Structure was re-drawn from the original pdb file using UCSF Chimera 1.10.

Unlike afRIO-2, the ctRIO-2–ATP complex is a bit unusual in the sense that the β-γ phosphate bond of ATP is broken into ADP-Mg2+ and an auto-phosphorylated phosphor-aspartate residue which resulted from transfer of the γ-phosphate to Asp257 (which in the case of yeast RIO-2 is

Asp253), This phosphorylated aspartate is absent in the apo-ctRIO-2 structure(Ferreira-Cerca, Sagar et al. 2012). The phosphorylation activity was assayed in purified ctRIO-2 using [γ-32P] phosphate-labeled ATP, and concentration of released radioactive γ-phosphate was recorded. Wild-type ctRIO-2 demonstrated an *in vitro* ATP hydrolysis activity, in a protein concentration–dependent manner, with the disappearance of ATP and the simultaneous increase in [γ-32P] phosphate.*In silico* docking of ctRIO-2 with yeast pre-40S particle was performed and the best fit showed that the protein's active site faces the 40 S rRNA, which occludes outside substrate to access the proteins active site.

1.8RIO kinases are serine/threonine kinases

Protein kinases, as described above, play a pivotal role in signal transduction events by catalyzing reversible phosphorylation of proteins. When an organism senses external stimuli, protein kinases undergo auto-phosphorylation or proceed to phosphorylate their specific substrate proteins. Phosphorylation typically occurs on specific amino acid residues of a protein, most commonly serine, threonine, tyrosine, histidine, and aspartate residues. These phosphorylation events in turn modulate the activity levels of the target proteins. The modulation of activity can be direct such as inducing conformational changes within the active site, or indirect, such as the regulation of protein-protein interactions.

Protein phosphorylation on Ser and Thr residues were extensively studied in eukaryotic models (De Verdier 1952, Sutherland and Wosilait 1955). After initial studies, the functional importance of these phosphorylation events were realized, and soon it became clear that protein phosphorylation is one of the key mechanisms that regulate the activity of proteins andsubsequently, control cellular functions. Eukaryotic Ser/Thr kinases are classified in the eukaryotic protein kinase super-family based on sequence homology between their kinase domains(Hanks and Hunter 1995). The domains are usually arranged into 12 sub-domains that fold in a typicaltwo-lobed catalytic core, with the kinase active site positioned in a deep creviceformed between the two lobes (Hanks and Hunter 1995, Kornev and Taylor 2010). The N-terminal domain is smaller and primarily involves the binding and orientation of the phosphate donor ATP molecule. The C-terminal lobe is larger, binds the kinase substrate and is responsible for the initiation of phosphate transfer. The conservation of these structural features of the

catalytic domain of different kinases is remarkable and this conservation is observed across kingdoms.

1.8.1 Mechanism of phosphorylation by Ser/Thr kinases: The activation loop of any kinase is one of most vital regulatory element of kinase action. The activation segment of a typical ser/thr kinase includesconserved DFG and APE motifs(Nolen, Taylor et al. 2004), a Mg^{2+}binding loop, an activation loop, and the P+1 loop. Substrate specificity of a kinase is governed by the activation loop and hence its sequence varies between kinases. Many Ser/Thrkinases are activated by addition of phosphate from ATP on at least one Ser or Thr residue within the activation loop. This phosphate addition could be either by auto-phosphorylation or by trans-phosphorylation by another upstream kinase. Phosphorylation event follows several interactions that stabilize the activation loop in a conformation that facilitates binding of substrate and subsequent catalysis(Huse and Kuriyan 2002, Nolen, Taylor et al. 2004). The (P+1) loop brings the phosphate donor and its substrate closer to make such a transfer possible. The P+1 loop is thus a majorfactor that distinguishes the substrate specificity between Ser/Thr and Tyr kinases. In case of Ser/Thr kinases, this loop includes a highly conserved Ser or Thr residue that makes interactions with the catalytic loop. The P loop is also important since it contains a glycine-rich consensus motif which covers the β- and γ-phosphates and plays a pivotal role both in the phosphoryl transfer event as wellas the ATP/ADP exchange during catalysis. Upon binding of ATP, all of theabove mentioned conformational changes occur which facilitates the ATP γ-phosphate, substrate phosphate acceptorSer/Thr residue and the kinase catalytic (Asp) residue together in 3D space, facilitating the smooth transfer of the γ-phosphate from the ATP to the phosphate acceptor Ser or Thr residue in the substrate protein.

1.9 Aim and Significance of the study

1.9.1 Significance: Malaria is a parasitic disease which adds to the economic burden of the developing nations. The fight against malaria has been a long and futile one, with the malaria parasite, coming out victorious every single time. Drug resistance has made the treatment difficult in high risk zones of the world. There hasn't been a malaria vaccine licensed for use yet, leaving anti-malarial drugs as the last choice. The identification of new drug targets is essential for the design, synthesis and identification of novel therapeutic molecules. This work entails the characterization of a previously annotated putative protein kinase (PFD0975w), which is believed to be a ser/thr kinase, with the aim to understand the role of the kinase in malaria

biology and to identify and develop new chemotherapeutic molecules to inhibit PFD0975w. We believe that PFD0975w might be an essential cellular gene in *Plasmodium* and its inhibition could kill parasites. The characterization of this new drug target could enable us not only to gain an insight into the disease biology but also to design and identify novel molecules to fight the disease.

1.9.2 Aims of the current study:

- To understand whether PFD0975w could serve as a good drug target for anti-malarial drug development.
- To clone, over-express and purify PFD0975w in bacterial system.
- To characterize the substrate binding activity of recombinant PFD0975w.
- To study the localization pattern of PFD0975w in *Plasmodium falciparum* during RBC stages.
- To study the localization pattern of PFD0975w in *Plasmodium falciparum* during exogenous and endogenous stress conditions.
- To design and identify novel inhibitors against PFD0975w.
- To identify candidate drugs against PFD0975w.

1.10 References

- Abdi, A., S. Eschenlauer, L. Reininger and C. Doerig (2010). "SAM domain-dependent activity of PfTKL3, an essential tyrosine kinase-like kinase of the human malaria parasite Plasmodium falciparum." Cell Mol Life Sci**67**(19): 3355-3369.

- Anamika, N. Srinivasan and A. Krupa (2005). "A genomic perspective of protein kinases in Plasmodium falciparum." Proteins**58**(1): 180-189.

- Angermayr, M. and W. Bandlow (1997). "The type of basal promoter determines the regulated or constitutive mode of transcription in the common control region of the yeast gene pair GCY1/RIO1." J Biol Chem**272**(50): 31630-31635.

- Angermayr, M., A. Roidl and W. Bandlow (2002). "Yeast Rio1p is the founding member of a novel subfamily of protein serine kinases involved in the control of cell cycle progression." Mol Microbiol**44**(2): 309-324.

- Baldwin, J., C. H. Michnoff, N. A. Malmquist, J. White, M. G. Roth, P. K. Rathod and M. A. Phillips (2005). "High-throughput screening for potent and selective inhibitors of Plasmodium falciparum dihydroorotate dehydrogenase." J Biol Chem**280**(23): 21847-21853.

- Barker, R. H., Jr., V. Metelev, E. Rapaport and P. Zamecnik (1996). "Inhibition of Plasmodium falciparum malaria using antisense oligodeoxynucleotides." Proc Natl Acad Sci U S A**93**(1): 514-518.

- Beeler, J. F., W. J. LaRochelle, M. Chedid, S. R. Tronick and S. A. Aaronson (1994). "Prokaryotic expression cloning of a novel human tyrosine kinase." Mol Cell Biol**14**(2): 982-988.

- Beraldo, F. H., F. M. Almeida, A. M. da Silva and C. R. Garcia (2005). "Cyclic AMP and calcium interplay as second messengers in melatonin-dependent regulation of Plasmodium falciparum cell cycle." J Cell Biol**170**(4): 551-557.

- Billker, O., S. Dechamps, R. Tewari, G. Wenig, B. Franke-Fayard and V. Brinkmann (2004). "Calcium and a calcium-dependent protein kinase regulate gamete formation and mosquito transmission in a malaria parasite." Cell**117**(4): 503-514.

- Biot, C., H. Bauer, R. H. Schirmer and E. Davioud-Charvet (2004). "5-substituted tetrazoles as bioisosteres of carboxylic acids. Bioisosterism and mechanistic studies on glutathione reductase inhibitors as antimalarials." J Med Chem**47**(24): 5972-5983.

- Boa, A. N., S. P. Canavan, P. R. Hirst, C. Ramsey, A. M. Stead and G. A. McConkey (2005). "Synthesis of brequinar analogue inhibitors of malaria parasite dihydroorotate dehydrogenase." Bioorg Med Chem**13**(6): 1945-1967.

- Bosotti, R., A. Isacchi and E. L. Sonnhammer (2000). "FAT: a novel domain in PIK-related kinases." Trends Biochem Sci**25**(5): 225-227.

- Brutsche, M. H., I. C. Brutsche, P. Wood, A. Brass, N. Morrison, M. Rattay, N. Mogulkoc, N. Simler, M. Craven, A. Custovic, J. J. Egan and A. Woodcock (2001). "Apoptosis signals in atopy and asthma measured with cDNA arrays." Clin Exp Immunol**123**(2): 181-187.

- Bujnicki, J. M., S. T. Prigge, D. Caridha and P. K. Chiang (2003). "Structure, evolution, and inhibitor interaction of S-adenosyl-L-homocysteine hydrolase from Plasmodium falciparum." Proteins**52**(4): 624-632.

- Chakrabarti, D., T. Da Silva, J. Barger, S. Paquette, H. Patel, S. Patterson and C. M. Allen (2002). "Protein farnesyltransferase and protein prenylation in Plasmodium falciparum." J Biol Chem**277**(44): 42066-42073.

- Chakrabarti, D., S. M. Schuster and R. Chakrabarti (1993). "Cloning and characterization of subunit genes of ribonucleotide reductase, a cell-cycle-regulated enzyme, from Plasmodium falciparum." Proc Natl Acad Sci U S A**90**(24): 12020-12024.

- Choubey, V., P. Maity, M. Guha, S. Kumar, K. Srivastava, S. K. Puri and U. Bandyopadhyay (2007). "Inhibition of Plasmodium falciparum choline kinase by hexadecyltrimethylammonium bromide: a possible antimalarial mechanism." Antimicrob Agents Chemother**51**(2): 696-706.

- Cohen, P. (2002). "Protein kinases--the major drug targets of the twenty-first century?" Nat Rev Drug Discov**1**(4): 309-315.

- Coppi, A., R. Tewari, J. R. Bishop, B. L. Bennett, R. Lawrence, J. D. Esko, O. Billker and P. Sinnis (2007). "Heparan sulfate proteoglycans provide a signal to Plasmodium sporozoites to stop migrating and productively invade host cells." Cell Host Microbe**2**(5): 316-327.

- Dar, O., M. S. Khan and I. Adagu (2008). "The potential use of methotrexate in the treatment of falciparum malaria: in vitro assays against sensitive and multidrug-resistant falciparum strains." Jpn J Infect Dis**61**(3): 210-211.

- Dawson, P. A., D. A. Cochran, B. T. Emmerson and R. B. Gordon (1993). "Inhibition of Plasmodium falciparum hypoxanthine-guanine phosphoribosyltransferase mRNA by antisense oligodeoxynucleotide sequence." Mol Biochem Parasitol**60**(1): 153-156.

- De Verdier, C. H. (1952). "Isolation of phosphothreonine from bovine casein." Nature**170**(4332): 804-805.

- Denis, G. V. and M. R. Green (1996). "A novel, mitogen-activated nuclear kinase is related to a Drosophila developmental regulator." Genes Dev**10**(3): 261-271.

- Diaz, C. A., J. Allocco, M. A. Powles, L. Yeung, R. G. Donald, J. W. Anderson and P. A. Liberator (2006). "Characterization of Plasmodium falciparum cGMP-dependent protein kinase (PfPKG): antiparasitic activity of a PKG inhibitor." Mol Biochem Parasitol**146**(1): 78-88.

- Dikstein, R., S. Ruppert and R. Tjian (1996). "TAFII250 is a bipartite protein kinase that phosphorylates the base transcription factor RAP74." Cell**84**(5): 781-790.

- Doerig, C., J. Endicott and D. Chakrabarti (2002). "Cyclin-dependent kinase homologues of Plasmodium falciparum." Int J Parasitol**32**(13): 1575-1585.

- Donald, R. G., J. Allocco, S. B. Singh, B. Nare, S. P. Salowe, J. Wiltsie and P. A. Liberator (2002). "Toxoplasma gondii cyclic GMP-dependent kinase: chemotherapeutic targeting of an essential parasite protein kinase." Eukaryot Cell**1**(3): 317-328.

- Dorin-Semblat, D., N. Quashie, J. Halbert, A. Sicard, C. Doerig, E. Peat, L. Ranford-Cartwright and C. Doerig (2007). "Functional characterization of both MAP kinases of the human malaria parasite Plasmodium falciparum by reverse genetics." Mol Microbiol**65**(5): 1170-1180.

- Dorin-Semblat, D., A. Sicard, C. Doerig, L. Ranford-Cartwright and C. Doerig (2008). "Disruption of the PfPK7 gene impairs schizogony and sporogony in the human malaria parasite Plasmodium falciparum." Eukaryot Cell**7**(2): 279-285.

- Dorin, D., K. Le Roch, P. Sallicandro, P. Alano, D. Parzy, P. Poullet, L. Meijer and C. Doerig (2001). "Pfnek-1, a NIMA-related kinase from the human malaria parasite Plasmodium falciparum Biochemical properties and possible involvement in MAPK regulation." Eur J Biochem**268**(9): 2600-2608.

- Dorin, D., J. P. Semblat, P. Poullet, P. Alano, J. P. Goldring, C. Whittle, S. Patterson, D. Chakrabarti and C. Doerig (2005). "PfPK7, an atypical MEK-related protein kinase, reflects the absence of classical three-component MAPK pathways in the human malaria parasite Plasmodium falciparum." Mol Microbiol**55**(1): 184-196.

- Droucheau, E., A. Primot, V. Thomas, D. Mattei, M. Knockaert, C. Richardson, P. Sallicandro, P. Alano, A. Jafarshad, B. Baratte, C. Kunick, D. Parzy, L. Pearl, C. Doerig and L. Meijer (2004). "Plasmodium falciparum glycogen synthase kinase-3: molecular model, expression, intracellular localisation and selective inhibitors." Biochim Biophys Acta**1697**(1-2): 181-196.

- Ejigiri, I. and P. Sinnis (2009). "Plasmodium sporozoite-host interactions from the dermis to the hepatocyte." Curr Opin Microbiol**12**(4): 401-407.

- Ferreira-Cerca, S., V. Sagar, T. Schafer, M. Diop, A. M. Wesseling, H. Lu, E. Chai, E. Hurt and N. LaRonde-LeBlanc (2012). "ATPase-dependent role of the atypical kinase Rio2 on the evolving pre-40S ribosomal subunit." Nat Struct Mol Biol**19**(12): 1316-1323.

- Fidock, D. A., T. Nomura and T. E. Wellems (1998). "Cycloguanil and its parent compound proguanil demonstrate distinct activities against Plasmodium falciparum malaria parasites transformed with human dihydrofolate reductase." Mol Pharmacol**54**(6): 1140-1147.

- Fieser, L. F., E. Berliner and et al. (1948). "Naphthoquinone antimalarials; general survey." J Am Chem Soc**70**(10): 3151-3155.

- Fritz-Wolf, K., A. Becker, S. Rahlfs, P. Harwaldt, R. H. Schirmer, W. Kabsch and K. Becker (2003). "X-ray structure of glutathione S-transferase from the malarial parasite Plasmodium falciparum." Proc Natl Acad Sci U S A**100**(24): 13821-13826.

- Fry, A. M., L. O'Regan, S. R. Sabir and R. Bayliss (2012). "Cell cycle regulation by the NEK family of protein kinases." J Cell Sci**125**(Pt 19): 4423-4433.

- Geerlings, T. H., A. W. Faber, M. D. Bister, J. C. Vos and H. A. Raue (2003). "Rio2p, an evolutionarily conserved, low abundant protein kinase essential for processing of 20 S Pre-rRNA in Saccharomyces cerevisiae." J Biol Chem**278**(25): 22537-22545.

- Gerold, P. and R. T. Schwarz (2001). "Biosynthesis of glycosphingolipids de-novo by the human malaria parasite Plasmodium falciparum." Mol Biochem Parasitol**112**(1): 29-37.

- Giamas, G., J. Stebbing, C. E. Vorgias and U. Knippschild (2007). "Protein kinases as targets for cancer treatment." Pharmacogenomics**8**(8): 1005-1016.

- Gomez-Escobar, N., C. F. Chou, W. W. Lin, S. L. Hsieh and R. D. Campbell (1998). "The G11 gene located in the major histocompatibility complex encodes a novel nuclear serine/threonine protein kinase." J Biol Chem**273**(47): 30954-30960.

- Graeser, R., B. Wernli, R. M. Franklin and B. Kappes (1996). "Plasmodium falciparum protein kinase 5 and the malarial nuclear division cycles." Mol Biochem Parasitol**82**(1): 37-49.

- Gray, N., L. Detivaud, C. Doerig and L. Meijer (1999). "ATP-site directed inhibitors of cyclin-dependent kinases." Curr Med Chem**6**(9): 859-875.

- Gurnett, A. M., P. A. Liberator, P. M. Dulski, S. P. Salowe, R. G. Donald, J. W. Anderson, J. Wiltsie, C. A. Diaz, G. Harris, B. Chang, S. J. Darkin-Rattray, B. Nare, T. Crumley, P. S. Blum, A. S. Misura, T. Tamas, M. K. Sardana, J. Yuan, T. Biftu and D. M. Schmatz (2002). "Purification and molecular characterization of cGMP-dependent protein kinase from Apicomplexan parasites. A novel chemotherapeutic target." J Biol Chem**277**(18): 15913-15922.

- Hanks, S. K. and T. Hunter (1995). "Protein kinases 6. The eukaryotic protein kinase superfamily: kinase (catalytic) domain structure and classification." FASEB J**9**(8): 576-596.

- Harwaldt, P., S. Rahlfs and K. Becker (2002). "Glutathione S-transferase of the malarial parasite Plasmodium falciparum: characterization of a potential drug target." Biol Chem**383**(5): 821-830.

- Hayward, R. E. (2000). "Plasmodium falciparum phosphoenolpyruvate carboxykinase is developmentally regulated in gametocytes." Mol Biochem Parasitol**107**(2): 227-240.

- Heikkila, T., S. Thirumalairajan, M. Davies, M. R. Parsons, A. G. McConkey, C. W. Fishwick and A. P. Johnson (2006). "The first de novo designed inhibitors of Plasmodium falciparum dihydroorotate dehydrogenase." Bioorg Med Chem Lett**16**(1): 88-92.

- Holton, S., A. Merckx, D. Burgess, C. Doerig, M. Noble and J. Endicott (2003). "Structures of P. falciparum PfPK5 test the CDK regulation paradigm and suggest mechanisms of small molecule inhibition." Structure**11**(11): 1329-1337.

- Huse, M. and J. Kuriyan (2002). "The conformational plasticity of protein kinases." Cell**109**(3): 275-282.

- Ishino, T., Y. Orito, Y. Chinzei and M. Yuda (2006). "A calcium-dependent protein kinase regulates Plasmodium ookinete access to the midgut epithelial cell." Mol Microbiol**59**(4): 1175-1184.

- Kato, N., T. Sakata, G. Breton, K. G. Le Roch, A. Nagle, C. Andersen, B. Bursulaya, K. Henson, J. Johnson, K. A. Kumar, F. Marr, D. Mason, C. McNamara, D. Plouffe, V. Ramachandran, M. Spooner, T. Tuntland, Y. Zhou, E. C. Peters, A. Chatterjee, P. G. Schultz, G. E. Ward, N. Gray, J. Harper and E. A. Winzeler (2008). "Gene expression signatures and small-molecule compounds link a protein kinase to Plasmodium falciparum motility." Nat Chem Biol**4**(6): 347-356.

- Khan, S. M., B. Franke-Fayard, G. R. Mair, E. Lasonder, C. J. Janse, M. Mann and A. P. Waters (2005). "Proteome analysis of separated male and female gametocytes reveals novel sex-specific Plasmodium biology." Cell**121**(5): 675-687.

- Kicska, G. A., P. C. Tyler, G. B. Evans, R. H. Furneaux, V. L. Schramm and K. Kim (2002). "Purine-less death in Plasmodium falciparum induced by immucillin-H, a transition state analogue of purine nucleoside phosphorylase." J Biol Chem**277**(5): 3226-3231.

- Kitade, Y., A. Kozaki, T. Gotoh, T. Miwa, M. Nakanishi and C. Yatome (1999). "Synthesis of S-adenosyl-L-homocysteine hydrolase inhibitors and their biological activities." Nucleic Acids Symp Ser(42): 25-26.

- Klemba, M., I. Gluzman and D. E. Goldberg (2004). "A Plasmodium falciparum dipeptidyl aminopeptidase I participates in vacuolar hemoglobin degradation." J Biol Chem**279**(41): 43000-43007.

- Kornev, A. P. and S. S. Taylor (2010). "Defining the conserved internal architecture of a protein kinase." Biochim Biophys Acta**1804**(3): 440-444.

- Koyama, F. C., D. Chakrabarti and C. R. Garcia (2009). "Molecular machinery of signal transduction and cell cycle regulation in Plasmodium." Mol Biochem Parasitol**165**(1): 1-7.

- Krnajski, Z., T. W. Gilberger, R. D. Walter, A. F. Cowman and S. Muller (2002). "Thioredoxin reductase is essential for the survival of Plasmodium falciparum erythrocytic stages." J Biol Chem**277**(29): 25970-25975.

- Krungkrai, J., R. Kanchanarithisak, S. R. Krungkrai and S. Rochanakij (2002). "Mitochondrial NADH dehydrogenase from Plasmodium falciparum and Plasmodium berghei." Exp Parasitol**100**(1): 54-61.

- Krungkrai, J., S. R. Krungkrai and K. Phakanont (1992). "Antimalarial activity of orotate analogs that inhibit dihydroorotase and dihydroorotate dehydrogenase." Biochem Pharmacol**43**(6): 1295-1301.

- Kumar, A., A. Vaid, C. Syin and P. Sharma (2004). "PfPKB, a novel protein kinase B-like enzyme from Plasmodium falciparum: I. Identification, characterization, and possible role in parasite development." J Biol Chem**279**(23): 24255-24264.

- Kumar, P., A. Tripathi, R. Ranjan, J. Halbert, T. Gilberger, C. Doerig and P. Sharma (2014). "Regulation of Plasmodium falciparum development by calcium-dependent protein kinase 7 (PfCDPK7)." J Biol Chem**289**(29): 20386-20395.

- Laronde-Leblanc, N., T. Guszczynski, T. Copeland and A. Wlodawer (2005). "Structure and activity of the atypical serine kinase Rio1." FEBS J**272**(14): 3698-3713.

- LaRonde-LeBlanc, N. and A. Wlodawer (2004). "Crystal structure of A. fulgidus Rio2 defines a new family of serine protein kinases." Structure**12**(9): 1585-1594.

- Le Bras, J. and R. Durand (2003). "The mechanisms of resistance to antimalarial drugs in Plasmodium falciparum." Fundam Clin Pharmacol**17**(2): 147-153.

- Le Roch, K. G., Y. Zhou, P. L. Blair, M. Grainger, J. K. Moch, J. D. Haynes, P. De La Vega, A. A. Holder, S. Batalov, D. J. Carucci and E. A. Winzeler (2003). "Discovery of gene function by expression profiling of the malaria parasite life cycle." Science**301**(5639): 1503-1508.

- Leber, W., A. Skippen, Q. L. Fivelman, P. W. Bowyer, S. Cockcroft and D. A. Baker (2009). "A unique phosphatidylinositol 4-phosphate 5-kinase is activated by ADP-ribosylation factor in Plasmodium falciparum." Int J Parasitol**39**(6): 645-653.

- Leonard, C. J., L. Aravind and E. V. Koonin (1998). "Novel families of putative protein kinases in bacteria and archaea: evolution of the "eukaryotic" protein kinase superfamily." Genome Res**8**(10): 1038-1047.

- Li, C. M., P. C. Tyler, R. H. Furneaux, G. Kicska, Y. Xu, C. Grubmeyer, M. E. Girvin and V. L. Schramm (1999). "Transition-state analogs as inhibitors of human and malarial hypoxanthine-guanine phosphoribosyltransferases." Nat Struct Biol**6**(6): 582-587.

- Li, Z., K. Le Roch, J. A. Geyer, C. L. Woodard, S. T. Prigge, J. Koh, C. Doerig and N. C. Waters (2001). "Influence of human p16(INK4) and p21(CIP1) on the in vitro activity of recombinant Plasmodium falciparum cyclin-dependent protein kinases." Biochem Biophys Res Commun**288**(5): 1207-1211.

- Liebau, E., B. Bergmann, A. M. Campbell, P. Teesdale-Spittle, P. M. Brophy, K. Luersen and R. D. Walter (2002). "The glutathione S-transferase from Plasmodium falciparum." Mol Biochem Parasitol**124**(1-2): 85-90.

- Luersen, K., R. D. Walter and S. Muller (2000). "Plasmodium falciparum-infected red blood cells depend on a functional glutathione de novo synthesis attributable to an enhanced loss of glutathione." Biochem J**346 Pt 2**: 545-552.

- Lye, Y. M., M. Chan and T. S. Sim (2006). "Pfnek3: an atypical activator of a MAP kinase in Plasmodium falciparum." FEBS Lett**580**(26): 6083-6092.

- Lytton, S. D., B. Mester, J. Libman, A. Shanzer and Z. I. Cabantchik (1994). "Mode of action of iron (III) chelators as antimalarials: II. Evidence for differential effects on parasite iron-dependent nucleic acid synthesis." Blood**84**(3): 910-915.

- Machius, M., J. L. Chuang, R. M. Wynn, D. R. Tomchick and D. T. Chuang (2001). "Structure of rat BCKD kinase: nucleotide-induced domain communication in a mitochondrial protein kinase." Proc Natl Acad Sci U S A**98**(20): 11218-11223.

- Manning, G., D. B. Whyte, R. Martinez, T. Hunter and S. Sudarsanam (2002). "The protein kinase complement of the human genome." Science**298**(5600): 1912-1934.

- Marte, B. M. and J. Downward (1997). "PKB/Akt: connecting phosphoinositide 3-kinase to cell survival and beyond." Trends Biochem Sci**22**(9): 355-358.

- Maru, Y. and O. N. Witte (1991). "The BCR gene encodes a novel serine/threonine kinase activity within a single exon." Cell**67**(3): 459-468.

- McRobert, L. and G. A. McConkey (2002). "RNA interference (RNAi) inhibits growth of Plasmodium falciparum." Mol Biochem Parasitol**119**(2): 273-278.

- Merckx, A., A. Echalier, K. Langford, A. Sicard, G. Langsley, J. Joore, C. Doerig, M. Noble and J. Endicott (2008). "Structures of P. falciparum protein kinase 7 identify an activation motif and leads for inhibitor design." Structure**16**(2): 228-238.

- Merckx, A., K. Le Roch, M. P. Nivez, D. Dorin, P. Alano, G. J. Gutierrez, A. R. Nebreda, D. Goldring, C. Whittle, S. Patterson, D. Chakrabarti and C. Doerig (2003). "Identification and initial characterization of three novel cyclin-related proteins of the human malaria parasite Plasmodium falciparum." J Biol Chem**278**(41): 39839-39850.

- Messika, E., J. Golenser, L. Abu-Elheiga, M. Robert-Gero, E. Lederer and U. Bachrach (1990). "Effect of sinefungin on macromolecular biosynthesis and cell cycle of Plasmodium falciparum." Trop Med Parasitol**41**(3): 273-278.

- Morlon-Guyot, J., L. Berry, C. T. Chen, M. J. Gubbels, M. Lebrun and W. Daher (2014). "The Toxoplasma gondii calcium-dependent protein kinase 7 is involved in early steps of parasite division and is crucial for parasite survival." Cell Microbiol**16**(1): 95-114.

- Moskes, C., P. A. Burghaus, B. Wernli, U. Sauder, M. Durrenberger and B. Kappes (2004). "Export of Plasmodium falciparum calcium-dependent protein kinase 1 to the parasitophorous vacuole is dependent on three N-terminal membrane anchor motifs." Mol Microbiol**54**(3): 676-691.

- Nankya-Kitaka, M. F., G. P. Curley, C. S. Gavigan, A. Bell and J. P. Dalton (1998). "Plasmodium chabaudi chabaudi and P. falciparum: inhibition of aminopeptidase and parasite growth by bestatin and nitrobestatin." Parasitol Res**84**(7): 552-558.

- Nelson, J. W., J. Zhu, C. C. Smith, M. Kulka and L. Aurelian (1996). "ATP and SH3 binding sites in the protein kinase of the large subunit of herpes simplex virus type 2 of ribonucleotide reductase (ICP10)." J Biol Chem**271**(29): 17021-17027.

- Nolen, B., S. Taylor and G. Ghosh (2004). "Regulation of protein kinases; controlling activity through activation segment conformation." Mol Cell**15**(5): 661-675.

- Noteberg, D., E. Hamelink, J. Hulten, M. Wahlgren, L. Vrang, B. Samuelsson and A. Hallberg (2003). "Design and synthesis of plasmepsin I and plasmepsin II inhibitors with activity in Plasmodium falciparum-infected cultured human erythrocytes." J Med Chem**46**(5): 734-746.

- Nunes, M. C., J. P. Goldring, C. Doerig and A. Scherf (2007). "A novel protein kinase family in Plasmodium falciparum is differentially transcribed and secreted to various cellular compartments of the host cell." Mol Microbiol**63**(2): 391-403.

- O'Brien, T. and R. Tjian (1998). "Functional analysis of the human TAFII250 N-terminal kinase domain." Mol Cell**1**(6): 905-911.

- Ono, T., L. Cabrita-Santos, R. Leitao, E. Bettiol, L. A. Purcell, O. Diaz-Pulido, L. B. Andrews, T. Tadakuma, P. Bhanot, M. M. Mota and A. Rodriguez (2008). "Adenylyl cyclase alpha and cAMP signaling mediate Plasmodium sporozoite apical regulated exocytosis and hepatocyte infection." PLoS Pathog**4**(2): e1000008.

- Owens, D. M. and S. M. Keyse (2007). "Differential regulation of MAP kinase signalling by dual-specificity protein phosphatases." Oncogene**26**(22): 3203-3213.

- Perbandt, M., C. Burmeister, R. D. Walter, C. Betzel and E. Liebau (2004). "Native and inhibited structure of a Mu class-related glutathione S-transferase from Plasmodium falciparum." J Biol Chem**279**(2): 1336-1342.

- Philip, N. and T. A. Haystead (2007). "Characterization of a UBC13 kinase in Plasmodium falciparum." Proc Natl Acad Sci U S A**104**(19): 7845-7850.

- Riguet, E., J. Desire, O. Boden, V. Ludwig, M. Gobel, C. Bailly and J. L. Decout (2005). "Neamine dimers targeting the HIV-1 TAR RNA." Bioorg Med Chem Lett**15**(21): 4651-4655.

- Rohrich, R. C., N. Englert, K. Troschke, A. Reichenberg, M. Hintz, F. Seeber, E. Balconi, A. Aliverti, G. Zanetti, U. Kohler, M. Pfeiffer, E. Beck, H. Jomaa and J. Wiesner (2005). "Reconstitution of an apicoplast-localised electron transfer pathway involved in the isoprenoid biosynthesis of Plasmodium falciparum." FEBS Lett**579**(28): 6433-6438.

- Rohwer, A., W. Kittstein, F. Marks and M. Gschwendt (1999). "Cloning, expression and characterization of an A6-related protein." Eur J Biochem**263**(2): 518-525.

- Romeo, S., M. Dell'Agli, S. Parapini, L. Rizzi, G. Galli, M. Mondani, A. Sparatore, D. Taramelli and E. Bosisio (2004). "Plasmepsin II inhibition and antiplasmodial activity of Primaquine-Statine 'double-drugs'." Bioorg Med Chem Lett**14**(11): 2931-2934.

- Santiago, T. C., R. Zufferey, R. S. Mehra, R. A. Coleman and C. B. Mamoun (2004). "The Plasmodium falciparum PfGatp is an endoplasmic reticulum membrane protein important for the initial step of malarial glycerolipid synthesis." J Biol Chem**279**(10): 9222-9232.

- Sarma, P. S. and R. S. Kumar (1998). "Abdominal pain in a patient with falciparum malaria." Postgrad Med J**74**(873): 425-427.

- Schneider, A. G. and O. Mercereau-Puijalon (2005). "A new Apicomplexa-specific protein kinase family: multiple members in Plasmodium falciparum, all with an export signature." BMC Genomics**6**: 30.

- Shuto, S., N. Minakawa, S. Niizuma, H. S. Kim, Y. Wataya and A. Matsuda (2002). "New neplanocin analogues. 12. Alternative synthesis and antimalarial effect of (6'R)-6'-C-methylneplanocin A, a potent AdoHcy hydrolase inhibitor." J Med Chem**45**(3): 748-751.

- Siden-Kiamos, I., A. Ecker, S. Nyback, C. Louis, R. E. Sinden and O. Billker (2006). "Plasmodium berghei calcium-dependent protein kinase 3 is required for ookinete gliding motility and mosquito midgut invasion." Mol Microbiol**60**(6): 1355-1363.

- Smith, C. C., Y. X. Yu, M. Kulka and L. Aurelian (2000). "A novel human gene similar to the protein kinase (PK) coding domain of the large subunit of herpes simplex virus type 2 ribonucleotide reductase (ICP10) codes for a serine-threonine PK and is expressed in melanoma cells." J Biol Chem**275**(33): 25690-25699.

- Solow, S., M. Salunek, R. Ryan and P. M. Lieberman (2001). "Taf(II) 250 phosphorylates human transcription factor IIA on serine residues important for TBP binding and transcription activity." J Biol Chem**276**(19): 15886-15892.

- Steussy, C. N., K. M. Popov, M. M. Bowker-Kinley, R. B. Sloan, Jr., R. A. Harris and J. A. Hamilton (2001). "Structure of pyruvate dehydrogenase kinase. Novel folding pattern for a serine protein kinase." J Biol Chem**276**(40): 37443-37450.

- Suraveratum, N., S. R. Krungkrai, P. Leangaramgul, P. Prapunwattana and J. Krungkrai (2000). "Purification and characterization of Plasmodium falciparum succinate dehydrogenase." Mol Biochem Parasitol**105**(2): 215-222.

- Sutherland, E. W., Jr. and W. D. Wosilait (1955). "Inactivation and activation of liver phosphorylase." Nature**175**(4447): 169-170.

- Syin, C., D. Parzy, F. Traincard, I. Boccaccio, M. B. Joshi, D. T. Lin, X. M. Yang, K. Assemat, C. Doerig and G. Langsley (2001). "The H89 cAMP-dependent protein kinase inhibitor blocks Plasmodium falciparum development in infected erythrocytes." Eur J Biochem**268**(18): 4842-4849.

- Tarun, A. S., X. Peng, R. F. Dumpit, Y. Ogata, H. Silva-Rivera, N. Camargo, T. M. Daly, L. W. Bergman and S. H. Kappe (2008). "A combined transcriptome and proteome survey of malaria parasite liver stages." Proc Natl Acad Sci U S A**105**(1): 305-310.

- Tewari, R., U. Straschil, A. Bateman, U. Bohme, I. Cherevach, P. Gong, A. Pain and O. Billker (2010). "The systematic functional analysis of Plasmodium protein kinases identifies essential regulators of mosquito transmission." Cell Host Microbe**8**(4): 377-387.

- Tian, Q., J. Taupin, S. Elledge, M. Robertson and P. Anderson (1995). "Fas-activated serine/threonine kinase (FAST) phosphorylates TIA-1 during Fas-mediated apoptosis." J Exp Med**182**(3): 865-874.

- Vaid, A. and P. Sharma (2006). "PfPKB, a protein kinase B-like enzyme from Plasmodium falciparum: II. Identification of calcium/calmodulin as its upstream activator and dissection of a novel signaling pathway." J Biol Chem**281**(37): 27126-27133.

- Vaid, A., D. C. Thomas and P. Sharma (2008). "Role of Ca2+/calmodulin-PfPKB signaling pathway in erythrocyte invasion by Plasmodium falciparum." J Biol Chem**283**(9): 5589-5597.

- Vanrobays, E., P. E. Gleizes, C. Bousquet-Antonelli, J. Noaillac-Depeyre, M. Caizergues-Ferrer and J. P. Gelugne (2001). "Processing of 20S pre-rRNA to 18S ribosomal RNA in yeast requires Rrp10p, an essential non-ribosomal cytoplasmic protein." EMBO J**20**(15): 4204-4213.

- Vinayak, S. and Y. D. Sharma (2007). "Inhibition of Plasmodium falciparum ispH (lytB) gene expression by hammerhead ribozyme." Oligonucleotides**17**(2): 189-200.

- Walker, E. H., O. Perisic, C. Ried, L. Stephens and R. L. Williams (1999). "Structural insights into phosphoinositide 3-kinase catalysis and signalling." Nature**402**(6759): 313-320.

- Wang, P. J. and D. C. Page (2002). "Functional substitution for TAF(II)250 by a retroposed homolog that is expressed in human spermatogenesis." Hum Mol Genet**11**(19): 2341-2346.

- Ward, P., L. Equinet, J. Packer and C. Doerig (2004). "Protein kinases of the human malaria parasite Plasmodium falciparum: the kinome of a divergent eukaryote." BMC Genomics**5**: 79.

- Wiersma, H. I., S. E. Galuska, F. M. Tomley, L. D. Sibley, P. A. Liberator and R. G. Donald (2004). "A role for coccidian cGMP-dependent protein kinase in motility and invasion." Int J Parasitol**34**(3): 369-380.

- Wydysh, E. A., S. M. Medghalchi, A. Vadlamudi and C. A. Townsend (2009). "Design and synthesis of small molecule glycerol 3-phosphate acyltransferase inhibitors." J Med Chem**52**(10): 3317-3327.

- Yamaguchi, H., M. Matsushita, A. C. Nairn and J. Kuriyan (2001). "Crystal structure of the atypical protein kinase domain of a TRP channel with phosphotransferase activity." Mol Cell**7**(5): 1047-1057.

- Zhang, Y. A., E. Hempelmann and R. H. Schirmer (1988). "Glutathione reductase inhibitors as potential antimalarial drugs. Effects of nitrosoureas on Plasmodium falciparum in vitro." Biochem Pharmacol**37**(5): 855-860.

Chapter II

Cloning, over-expression, purification and preliminary immunolocalization studies of PFD0975w.

2.1 Introduction

Protein kinases are crucial players in cellular signaling cascades. Thus they are excellent drug targets and have been exploited to design novel inhibitors to target various diseases. As already discussed, the kinome of the malaria parasite offers an avalanche of attractive drug targets, of which many kinases are yet to be biochemically or functionally characterized. PFD0975w is chosen for study because of a multitude of reasons. PFD0975w is a putative ser/thr kinase in the plasmodium falciparum 3D7 genome. BLAST analysis revealed that PFD0975w contains a signature kinase like domain fused to an N- terminal DNA binding domain, typical of an RIO kinase domain. PFD0975w is a putative kinase containing a signature kinase like domain fused to an N- terminal DNA binding domain, suggesting dual function of this enzyme. The enzyme is small in size (~35 KDa) and is believed to be easy to clone and characterize. Lastly, crystal structure of close homolog from other species is available, which makes it easier to explore the relevance of this enzyme in *Plasmodium falciparum* from different perspectives.

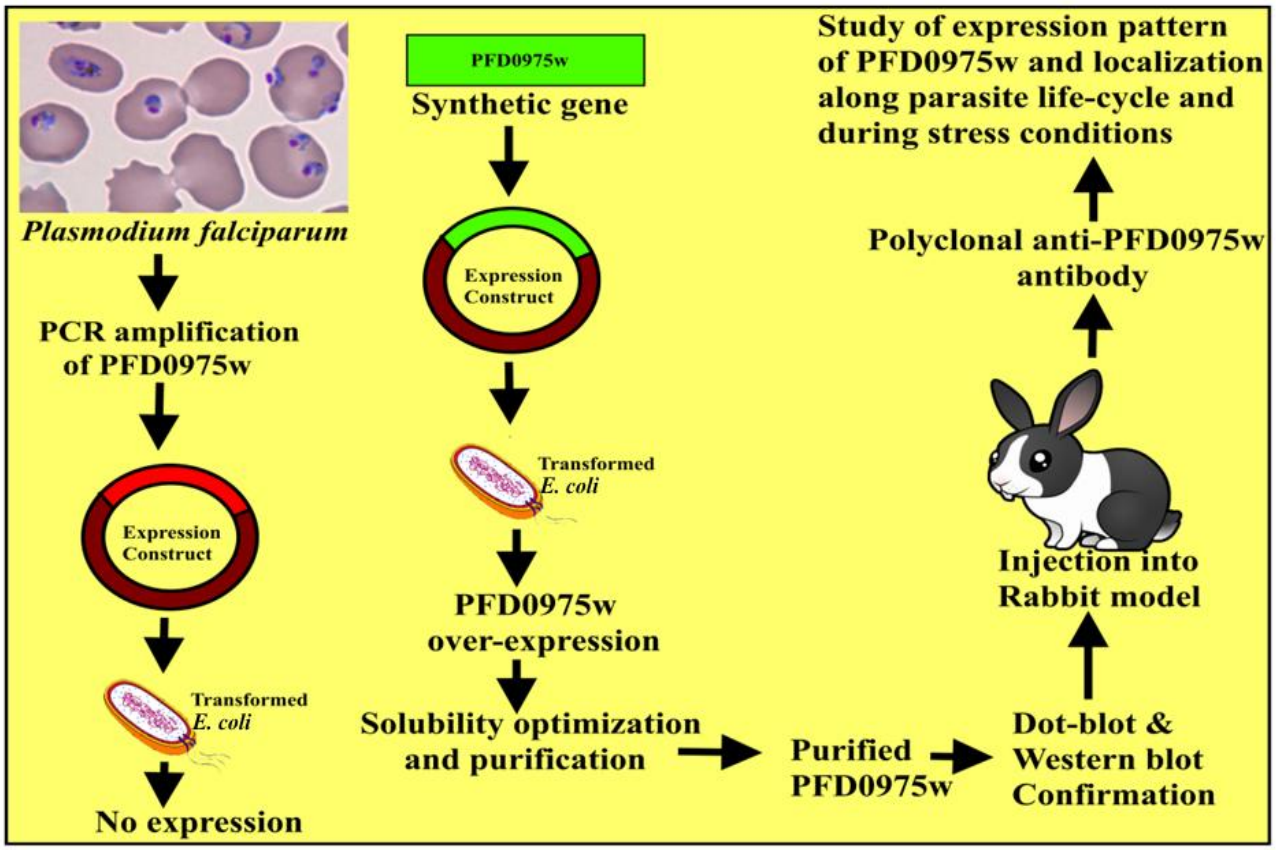

Figure 2.1: Schematic representation of the work discussed in chapter II

Cloning, over-expression, purification and localization of this putative atypical kinase sheds light on the importance of this enzyme in the parasite's life cycle and also paves way for further biochemical characterization. The current chapter highlights the cloning of the atypical protein kinase PFD0975w from malaria kinome (Figure 2.1). Native PFD0975w from *Plasmodium falciparum* did not express well in the bacterial system, and hence a codon optimized truncated version of the gene was synthesized. It was cloned and over-expressed in *E. coli*. This chapter also describes the optimization and fine tuning of bacterial strains, IPTG concentration, induction temp, and growth medium for obtaining soluble expression of PFD0975w. It also describes the generation of antibodies against PFD0975w in rabbit which were used to study the changes in expression pattern of PFD0975w during the parasite's asexual stages in the presence and absence of exogenous cellular stress.

2.2 Experimental Procedure

2.2.1 Cloning of PFD0975w from *Plasmodium falciparum* genomic DNA: Genomic DNA was isolated from a 1 ml culture of 10% parasitemia using saponin lysis method. PFD0975w gene (1.74Kb) was amplified from the genomic DNA using site-specific forward primer 5′-TAA**GGATCC**ATGAAGTTGGATATTTCGTG-3′ and reverse primer 5′-ATTC**AAGCTT**TAAGTAATTTTTTATTTT-3′ containing BamHI and HindIII restriction sites respectively. The PCR cycles were as follows: 15 cycles of denaturation at 94°C for 1 minute, annealing at 32°C for 1:30 minutes and an extension at 65°C for 4:00 minutes. It was followed by another 25 cycles of denaturation at 94°C for 1 minute, annealing at 45°C for 1:30 minutes and extension at 72°C for 3:00 minutes. The 1.74 Kb DNA fragment was excised and purified from agarose gel using Himedia gel extraction kit. The DNA fragment was cloned into vector PTZ7R provided with InsTAclone^{TM} PCR Cloning kit. Plasmid isolated from the clones were double digested with BamHI and HindIII and ligated to expression vector pET23a. Ligation mixture was transformed into *E. coli* DH5α. Clones were screened using colony PCR and expression construct from positive colony was isolated and transformed into BL21 (DE3) for over-expression.

2.2.2 Cloning of codon optimized synthetic PFD0975w: A codon-optimized, truncated version (~300 amino acids) of PFD0975w was custom synthesized from Integrated DNA technologies, Coralville, USA within a self-replicating plasmid bounded by BamHI and HindIII restriction sites. The resulting synthetic version of the gene is termed as PFD0975ws.The plasmid was double

digested with BamHI/HindIII and ~900 bp DNA fragment was purified from agarose gel and cloned into expression vector pET23a. The resulting expression clone is termed as PFD0975ws_pET23a.

2.2.3 Over-expression of PFD0975ws in transformed *E. coli*: PFD0975ws_pET23a construct was transformed into BL21 (DE3) using heat shock method (Chung, Niemela et al. 1989, Trivedi, Chand et al. 2005). A single transformed colony was inoculated into 5 ml LB media containing ampicillin (100µg/ml) and allowed to grow until O.D~0.6 at 37°C in an incubator shaker. The bacterial culture was induced using 0.5mM IPTG for 3 hrs. Cells were harvested by centrifugation at 7000 RPM for 10 minutes and re-suspended in buffer A (50 mM Sodium phosphate pH 8.0, 500 mM NaCl, 1 mM PMSF). Cells were lysed by sonication in ice for 10 minute with a duty cycle of 35% (5 seconds on and 5 seconds off).The sonicated lysate was centrifuged at 14,000 RPM for 30 minutes at 4°C. The supernatant and pellet fractions were isolated and analyzed on 12% SDS-PAGE gel. Similar experimental protocol followed for checking the over-expression of PFD0975ws in other *E.coli* strains.

2.2.4 Purification of PFD0975ws from the soluble fraction: Rosetta-gami™ cells are used to produce the protein in the soluble fraction to purify the PFD0975ws in the native conditions. Bacterial cells transformed as described previously and grown overnight at 20°C in 5 ml LB media supplemented with ampicillin (100µg/ml) and chloramphenicol (35µg/ml). Following day, the culture was scaled up to 1 liter with an inoculum of 1:500 from overnight grown culture. Cells were grown at 37°C till O.D~0.6 and induced with 0.5mM IPTG at 37°C for 3 hrs. Cells were harvested by centrifugation at 7000 RPM for 10 minutes and re-suspended in 20 ml ice-cold buffer B (50 mM sodium phosphate pH 8.0, 500 mM NaCl, 20 mM imidazole, 1 mM PMSF). Cells lysed by sonication in ice for 10 minute with a duty cycle of 35% (5 seconds on and 5 seconds off). Bacterial culture lysate was centrifuged at 14,000 RPM for 30 minutes and clarified supernatant containing soluble PFD0975w was loaded onto a pre-packed 1 ml Ni-NTA column. Column was washed with 6 column volumes of buffer C (50 mM sodium phosphate pH 8.0, 700 mM NaCl, 70 mM imidazole) and presence of protein was monitored from the column eluate using Bradford reagent. Column bound PFD0975w was eluted with buffer A containing imidazole linear gradient (0.1-1 M). All the fractions were preserved, and degree of purification was analyzed on 12% SDS-PAGE gel. All buffers used were chilled to 4°C, and a constant flow rate of 1.5 ml/min was maintained using a peristaltic pump.

2.2.5 Determination of subunit molecular weight of PFD0975ws: The gel images opened in Gel Analyzer 2010 (www.gelanalyzer.com). The lane corresponding to the molecular weight marker bands was defined. The measurement of distances run by the individual protein band was used to calculate the relative mobilities (R_f) of each protein band using the following formula;

$$Rf = \frac{\text{Distance travelled by Protein (D1)}}{\text{Distance travelled by dye front (D2)}} \quad \text{……..(eq 2.1)}$$

A correlation curve between Log (molecular weight) vs. relative mobility (R_f) was plotted. Following a similar procedure, R_f value for PFD0975ws was calculated and used to determine the subunit molecular weight of the protein.

2.2.6 Development of polyclonal antibody against PFD0975w in rabbit: Lyophilized purified PFD0975w is dissolved in sterile water at 0.5 mg/ml. An emulsion (total volume 0.8ml) was prepared by mixing the antigen solution with Freund's complete adjuvant in 1:1 ratio. A healthy rabbit was immunized with this mixture through subcutaneous injections at different regions with along its ventral trunk. A second booster dose of the antigen mixed with Freund's incomplete adjuvant was administered to the animal on the 32nd day after the first injection. On the 43rd day, the blood was withdrawn from the ear vein. Antibody titer of the serum was determined using in-direct ELISA. Dot blot analysis of the generated antibody against purified PFD0975ws was performed to check the presence of protein-specific antibody.

2.2.7 Dot blot confirmation of soluble expression of PFD0975ws: Pellet, supernatant, purified fraction and primary anti-rabbit PFD0975w (positive control) were blotted on two small strips of nitrocellulose membrane using a blow dryer. Membranes were blocked with 3% skim milk in PBS followed by washing three times with wash buffer (PBS containing 0.5% Tween-20). Membranes were incubated with anti-PFD0975w (1:500) for 4 hrs at 37°C and washed three times with wash buffer. Membranes were incubated with 1:2000 dilution of HRP conjugated anti-rabbit secondary antibody for 2 hrs at 37°C. Membranes were washed three times with wash buffer and developed with DAB substrate (DAB 1 mg/ ml in PBS and 0.05% H_2O_2).

2.2.8 Western blotting of PFD0975ws from the soluble fraction: Purified PFD0975w was resolved on a 12% SDS-PAGE at 120 volts, and it was transferred to PVDF membrane at 100 volts for 4 hrs.

at 4°C. Membrane was blocked with 3% skim milk in PBS followed by washing three times with wash buffer (PBS containing 0.5% Tween-20). Membrane was incubated with anti-PFD0975w (1:500) for 4 hrs at 37°C and washed three times with wash buffer. Membrane was incubated with 1:2000 dilution of HRP conjugated anti-rabbit secondary antibody for 2 hrs at 37°C. Membrane was washed three times with wash buffer and developed with DAB substrate (DAB 1 mg/ ml in PBS and 0.05% H_2O_2).

2.2.9 Immunolocalization studies: *Plasmodium falciparum* 3D7 culture at high parasitemia (~8%) is used to prepare thin blood smears on glass cover slips. Smears were air dried and fixed in a 1:1 mixture of methanol and acetone at -20°C. Smears were permeabilized with 0.05% Triton-X 100 in PBS for 10 minutes at 37°C and washed three times with PBS. Smears were blocked with 5% BSA for 30 minutes at room temperature with intermittent mixing on a gel rocker. Smears were washed three times with PBS and incubated with anti-PFD0975w antibody (1:500) at 4°C overnight. Smears were washed three times with PBS and incubated with FITC conjugated anti-rabbit IgG (1: 2000) for 4 hrs at 4°C with intermittent mixing on a gel rocker. Finally, smears were washed three times with PBS and mounted on clean glass slides with mounting media containing DAPI. Cells were observed under 100X objective (oil emersion) attached to fluorescence microscope Nikon 80i and images were captured from 5-10 random fields.

For starvation experiment, parasites culture was spun down gently at 1000 RPM and re-suspended in RPMI media (no glucose) containing Albumax II and antibiotics for 90 minutes. Post incubation, a thin blood smear was prepared on glass coverslips. Similarly for the chloroquine experiment, parasite culture was spun down gently at 1000 RPM and re-suspended in complete media containing 0.5 µg/ml chloroquine for 90 minutes before making thin blood smears on glass coverslips.

2.3 Results

2.3.1 Cloning of PFD0975w from *Plasmodium falciparum*: The full-length PFD0975w was PCR amplified from the genomic DNA of *Plasmodium falciparum* using site-specific primers. The PCR product showed a ~1.6 Kb DNA fragment (Figure 2.2A) which is a close match to the full-length PFD0975w gene of 1.74 Kb. The full-length clone in expression vector pET23a was transformed in *E. coli* BL21 (DE3) and its expression was induced by IPTG. The full-length PFD0975w clone failed to express in the bacterial system. It didn't give detectable amount of protein even with the

optimization of several parameters such as expression in different host strains, induction at different temperatures or IPTG concentrations. The most probable reason for this could be attributed to the inefficiency of *E. coli* RNA Polymerase to transcribe the AT-rich DNA stretches (Baca and Hol 2000). Another factor could be the codon biasness due to which bacterial expression system fails to recognize eukaryotic codon (Gustafsson, Govindarajan et al. 2004).

Considering these factors, a codon-optimized version of PFD0975w gene was designed to solve the expression problem in the bacterial system. The structural and molecular modeling studies on PFD0975w suggested that amino acid residues 1-280 were sufficient to obtain fully functional RIO-2 kinase (Trivedi and Nag 2012). As a result, 912 bp synthetic PFD0975w gene covering structurally conserved winged helix domain, the catalytic kinase domain, and the unstructured loop present in PFD0975w with a total amino acid length of 1-300 was synthesized. The codon-optimized DNA sequence of PFD0975ws and its corresponding amino acid sequence is given in appendix (Appendix III).

PFD0975ws cloned into expression vector pET23a. The clones selected over the ampicillin (100µg/ml) and double digestion of plasmids with BamHI/HindIII has released insert of ~900bp (Figure 2.2B). It matches well with the actual size of PFD0975ws (912 bp) and confirm the presence of PFD0975ws.

2.3.2 Over-expression of PFD0975ws: PFD0975ws expression construct transformed into BL21 (DE3) strain of *E. coli* and its over-expression was checked. A thick band of ~35 KDa weight was observed on SDS-PAGE (Figure 2.2C). The molecular weight of the over-expressed band matched with the theoretical molecular weight of the PFD0975ws protein (35.54 KDa). The protein was almost exclusively being produced as insoluble inclusion bodies in BL21 (DE3). Since our objective is to get native fully functional protein produced in *E. coli*, it was preferred to avoid the urea mediated refolding strategies.

2.3.3 Optimization of soluble expression of PFD0975w: Efforts were given to optimizing several parameters to obtain soluble expression of PFD0975ws in *E. coli*. Different *E.coli* K-12 expression strains are available to address different expression related problems and each strain has its unique advantage. PFD0975ws_pET23a expression construct transformed into *E. coli* expression strains

such as BL21 (DE3), Codon + RP, C41 (DE3) and Rosetta-Gami™. The expression and the fraction of protein in the soluble part were analyzed on SDS-PAGE (Figure 2.3A).

Among the different strains tested, the highest percentage of soluble PFD0975ws (25.39%) was found in Rosetta-Gami™ (Figure 2.3A).

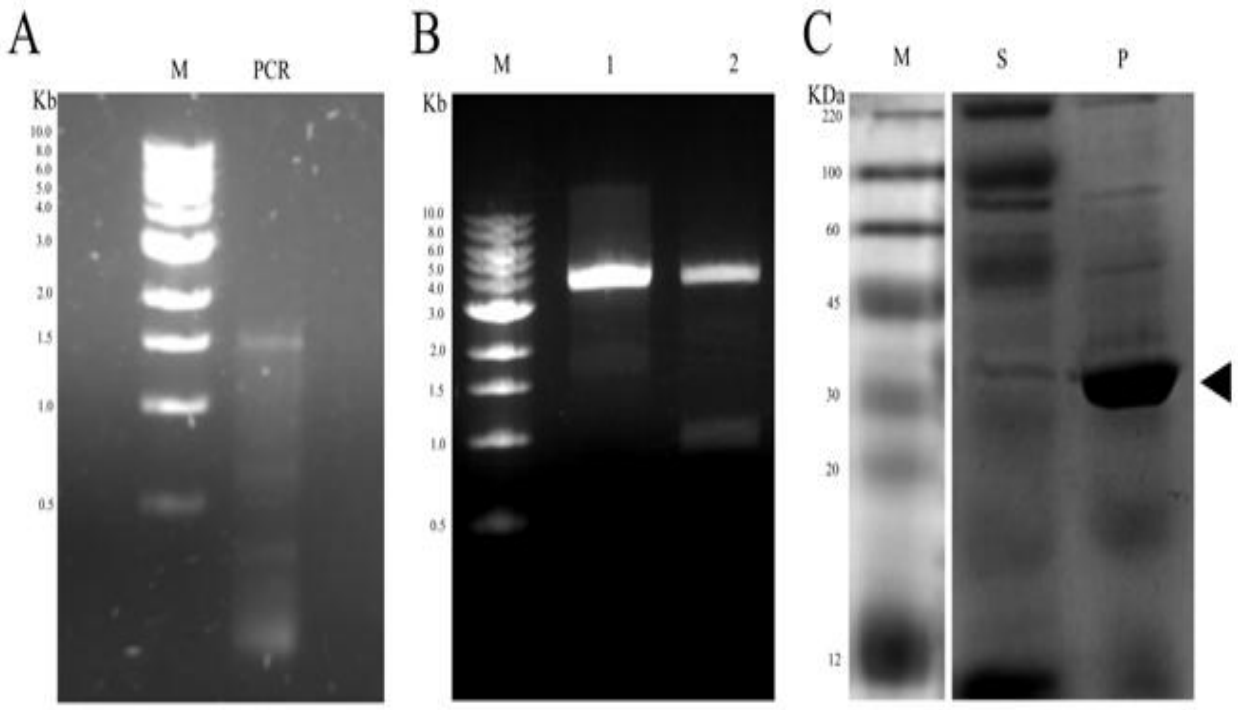

Figure 2.2: Cloning and over-expression of PFD0975w from *Plasmodium falciparum*. (A) PCR from genomic DNA. (B) Cloning of synthetic gene. M=Marker Lane 1=Undigested clone in pET23a Lane 2=Clone digested with BamHI & HindIII. (C) Over-expression of cloned construct in BL21 (DE3). M= Marker, S=Soluble fraction, P=Insoluble fraction. Triangle mark in (C) represents the position of overexpressed PFD0975ws on 12% SDS PAGE Gel.

The concentration of IPTG to induce the recombinant protein production plays a critical factor governing protein production and soluble expression (Kopetzki, Schumacher et al. 1989, Sorensen and Mortensen 2005). Among the different concentrations tested, the optimal IPTG concentration was determined to be 0.5 mM (Figure 2.3B). Induction temperature plays a crucial role in the soluble expression of recombinant protein in bacterial expression system (Sorensen and Mortensen 2005). Induction temperatures of 37°C and 18°C were tested for optimal soluble expression. It was found that there was an overall 7.3 fold increase in protein production at 37°C than 18°C, although induction

at 18°C could fairly increase the percentage of soluble PFD0975w (Figure 2.3C).Incorporation of high concentration of osmolyte in the culture media is known to enhance the soluble expression of recombinant protein in *E. coli* expression system (de Marco, Vigh et al. 2005, Oganesyan, Ankoudinova et al. 2007). The precise mechanism is not clear but it is believed that high concentration of osmolytes such as NaCl or D-sorbitol could act as molecular chaperones to prevent aggregation in the presence of compatible solute such as glycinebetaine (Oganesyan, Ankoudinova et al. 2007). To explore such a possibility, we examined the soluble expression of PFD0975w at varying concentrations of NaCl (0-2 M) in the presence of fixed concentration of glycinebetaine (20 mM). Almost 10.25% of PFD0975ws appeared in the soluble fraction when bacterial cells were cultured at 2M NaCl (Figure 2.3D).

Similarly, we tested the soluble expression of PFD0975w at varying concentrations of D-sorbitol (0-2 M) in the presence of fixed concentration of glycinebetaine (20mM). The percentage of soluble PFD0975w increased up to 28.95% when bacteria were osmotically stressed at 2 M sorbitol (Figure 2.3E). It realized that the strategies involving the modification of the culture media did not always yield a reproducible amount of protein in the soluble fraction and moreover culture scale-up using such techniques was a difficult issue. Protein solubility present in solution majorly governed by the pH of the solution and the solubility is minimal at the isoelectric point (pI). The bacterial pellets were re-suspended in buffers of varying pH (6.0-9.0), and cells were disrupted using sonication. The soluble expression of PFD0975ws was analyzed on SDS-PAGE. Among the buffers tested, there was no remarkable increase in PFD0975w solubility (Figure 2.3F). Testing different factors allowed to come up with the optimized conditions; PFD0975ws_pET23a construct was expressed in Rosetta-Gami™ host strain. Cells were grown at 37°C to an OD of ~0.6 following which the culture was induced with 0.5mM IPTG for four hr. at 37°C.

2.3.4 Purification of PFD0975w from transformed Rosetta-Gami™ cells: The protein production was scaled up to 1 liter and recombinant PFD0975w containing a C-terminal hexa-histidine tag was purified from the soluble fraction using Ni-NTA affinity chromatography. PFD0975ws binds well to the column matrix, and no detectable protein was seen in the flow-through and wash fractions. The column bound PFD0975ws was eluted using an imidazole gradient from 100mM to 1M and the single band of PFD0975ws was present in the eluted fractions (350mM to 500mM imidazole) without any detectable contaminating protein (Figure 2.4A).

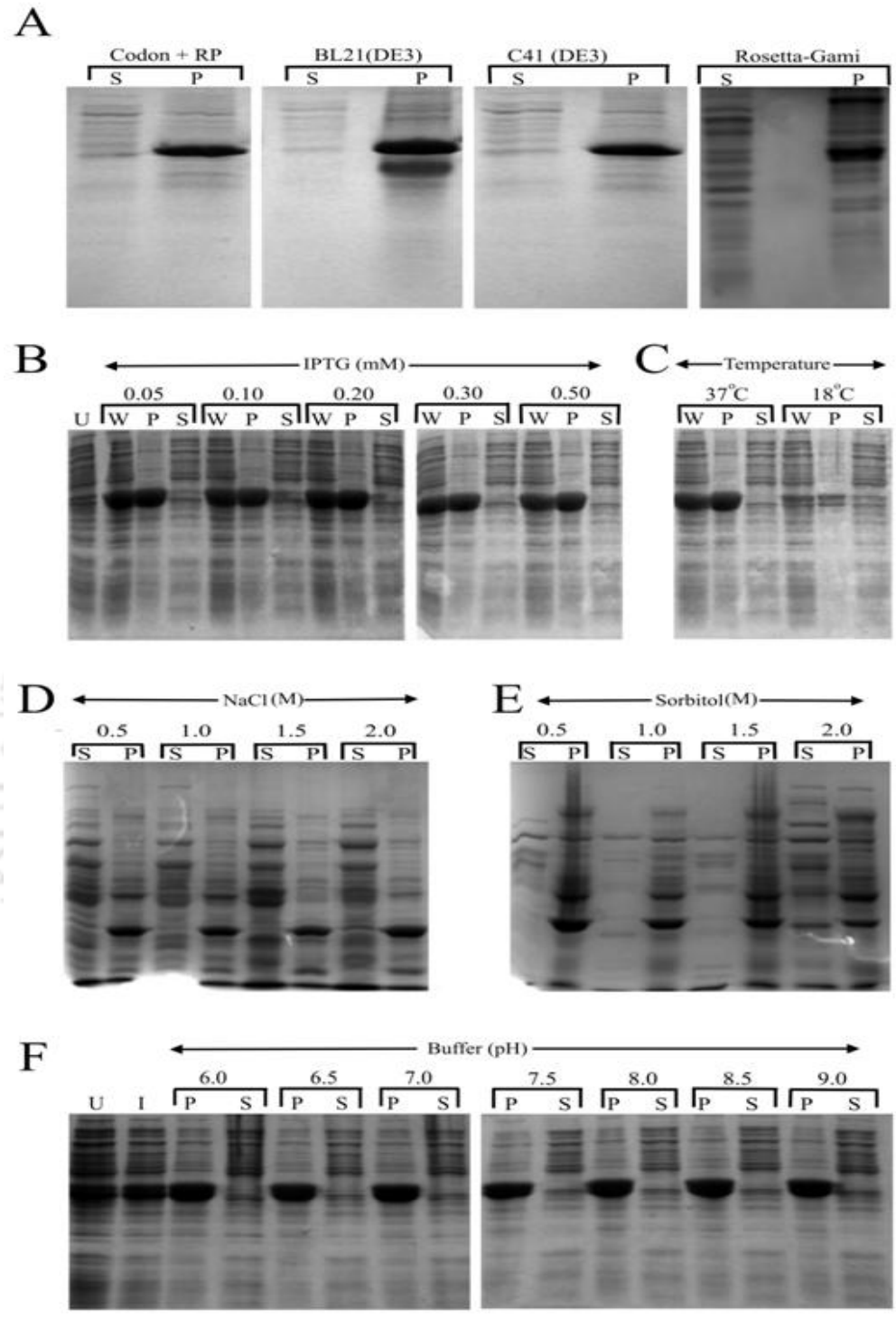

Figure 2.3: Optimization of soluble expression of PFD0975w in bacterial system. Over-expression of PFD0975w (A) in different *E.coli* expression hosts, (B) at different IPTG concentrations, (C) at different induction temperatures, (D) in the presence of different concentrations of osmolyte NaCl and Glycine betaine (20 mM) and (E) Sorbitol and Glycine betaine (20mM). (F) Solubility profile of pFD0975w extracted in lysis buffers at different pH. U=Uninduced, I=Induced, W=Whole cell SDS, S=Soluble fraction, P=Insoluble fraction.

The relative mobility (R_f) of each protein band present in molecular weight marker is determined (Figure 2.3B). Using calibration curve between Log (Molecular weight) vs Relative mobility (Rf), the purified protein was found to be molecular weight 36.3±1.2 KDa (Figure 2.4C), matched well to the theoretical molecular weight of truncated PFD0975w product (35.4 KDa).

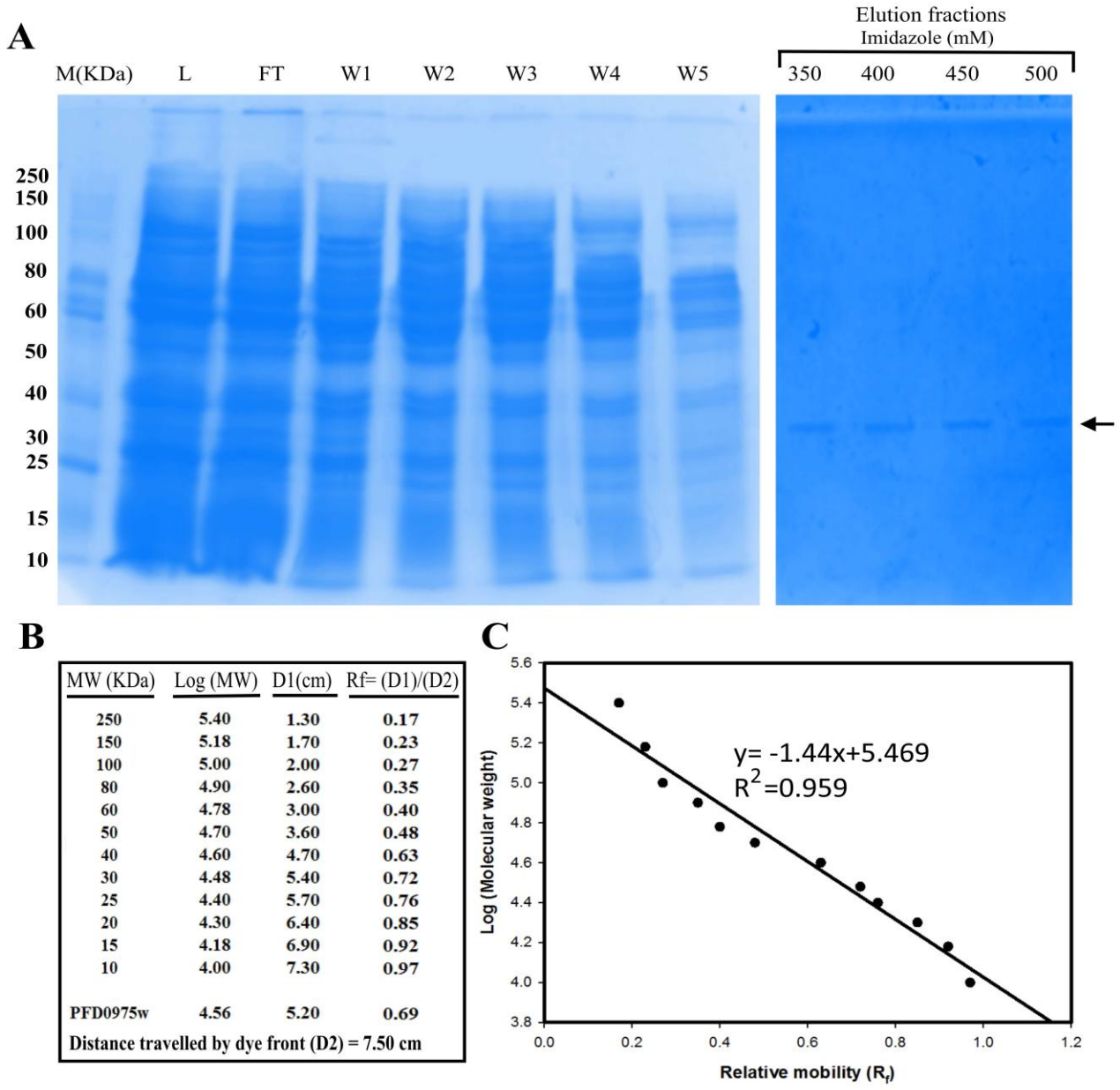

MW (KDa)	Log (MW)	D1(cm)	Rf= (D1)/(D2)
250	5.40	1.30	0.17
150	5.18	1.70	0.23
100	5.00	2.00	0.27
80	4.90	2.60	0.35
60	4.78	3.00	0.40
50	4.70	3.60	0.48
40	4.60	4.70	0.63
30	4.48	5.40	0.72
25	4.40	5.70	0.76
20	4.30	6.40	0.85
15	4.18	6.90	0.92
10	4.00	7.30	0.97
PFD0975w	4.56	5.20	0.69

Distance travelled by dye front (D2) = 7.50 cm

Figure 2.4: Purification and estimation of molecular weight of PFD0975w. (A) Purification of PFD0975w from soluble fraction. M (Marker) L (Load) FT (Flow through) W1-W6 (Wash fractions) 350-500 (Elution fractions in imidazole gradient). (B) Determination of relative mobilities (R_f) of different molecular weight marker bands (250 KDa-10 KDa) and purified pFD0975w band on SDS-PAGE. (C) Plot of Log (Molecular weight) vs Relative mobility (R_f).

2.3.5 Polyclonal antibody generation against PFD0975w in rabbit: Antibodies against this recombinant PFD0975w were raised in rabbit as described in "experimental procedure section." Western blot of the purified recombinant protein showed specific antigen-antibody recognition when the membrane was developed with anti-PFD0975w antibody and probed with an HRP labeled secondary antibody (Figure 2.5A). PFD0975w is detected in the soluble fraction and purified fraction using dot blot (Figure 2.5 B) with two sets of antibodies; the anti-PFD0975w antibody as well as the 6x-anti his antibody.

2.3.6 PFD0975w is changing its localization during different stages of the parasite's life cycle: Since the recombinant PFD0975w is similar in amino acid composition to the native PfRIO-2 kinase, this antibody is cross-reactive to the native PDF0975w within the malaria parasite. Using the antibodies, immunolocalization studies were performed to qualitatively determine the expression level and pattern of PFD0975w within the RBC stages of malaria parasite.

At ring stage, the expression is moderate whereas it is highest at the trophozoite and then decreases in the schizont stage. In addition, it gradually tapers off as the schizont divides to release its merozoites (Figure 2.5C). PFD0975w is constitutively expressed within RBC stages with the level of expression changing from the ring to schizont. The observed expression pattern is correlating with the microarray expression profile of PFD0975w (as re-annotated id as PF3D7_0420100) during different asexual RBC stages of *Plasmodium falciparum* 3D7 (Figure 2.6) (Bozdech, Llinas et al. 2003).

During the ring stage, PFD0975w appears to be majorly localized to the parasite's cytosol with little or no signal outside the parasite membrane. As the parasite matures into trophozoite and takes up more space within the RBC, the PFD0975w signal was found throughout the infected RBC, even outside the parasite membrane. During the schizont stage, the expression pattern scatters as the parasite membrane become fragile (Figure 2.5C). Our observations match with the microarray expression data of DeRisi Lab (UCSF) who performed a whole genome transcriptomics of three *Plasmodium falciparum* strains (Llinás, Bozdech et al. 2006).

2.3.7 PFD0975w localization within RBC is changing in response to exogenous stresses: Oxidative stress increases within the parasite as it proceeds from the ring to the schizont stage within RBC.

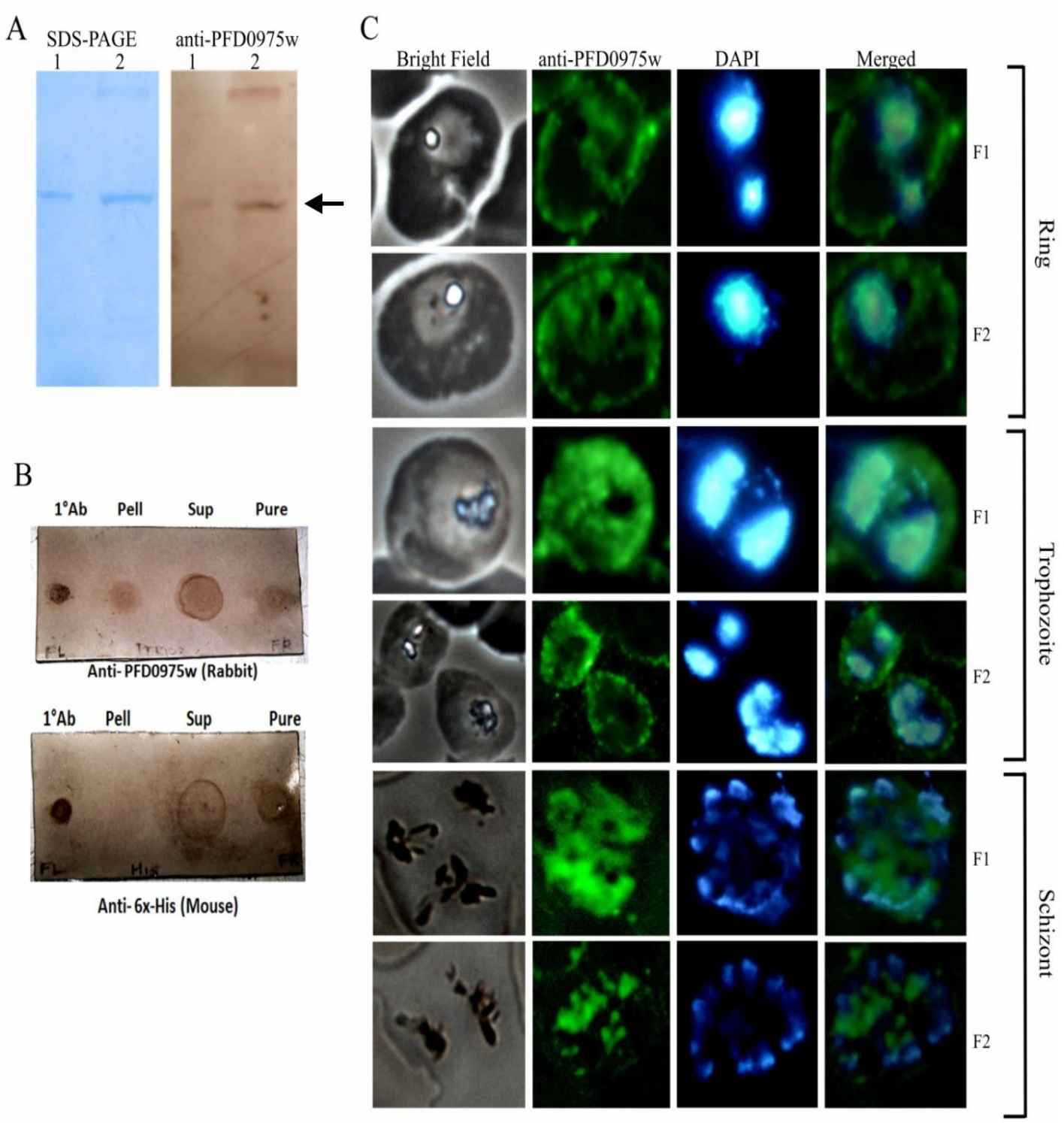

Figure 2.5: Western blot, Dot blot and Immunolocalization of PFD0975w in *Plasmodium falciparum* infected erythrocytes using anti-PFD0975w antibody generated in rabbit. (A) SDS-PAGE and western blot of purified PFD0975w in (1) 350 mM and (2) 400 mM imidazole elution fractions. (B) Immunolocalization of PFD0975w in *Plasmodium falciparum* infected RBCs during different stages of the parasite's asexual life cycle.

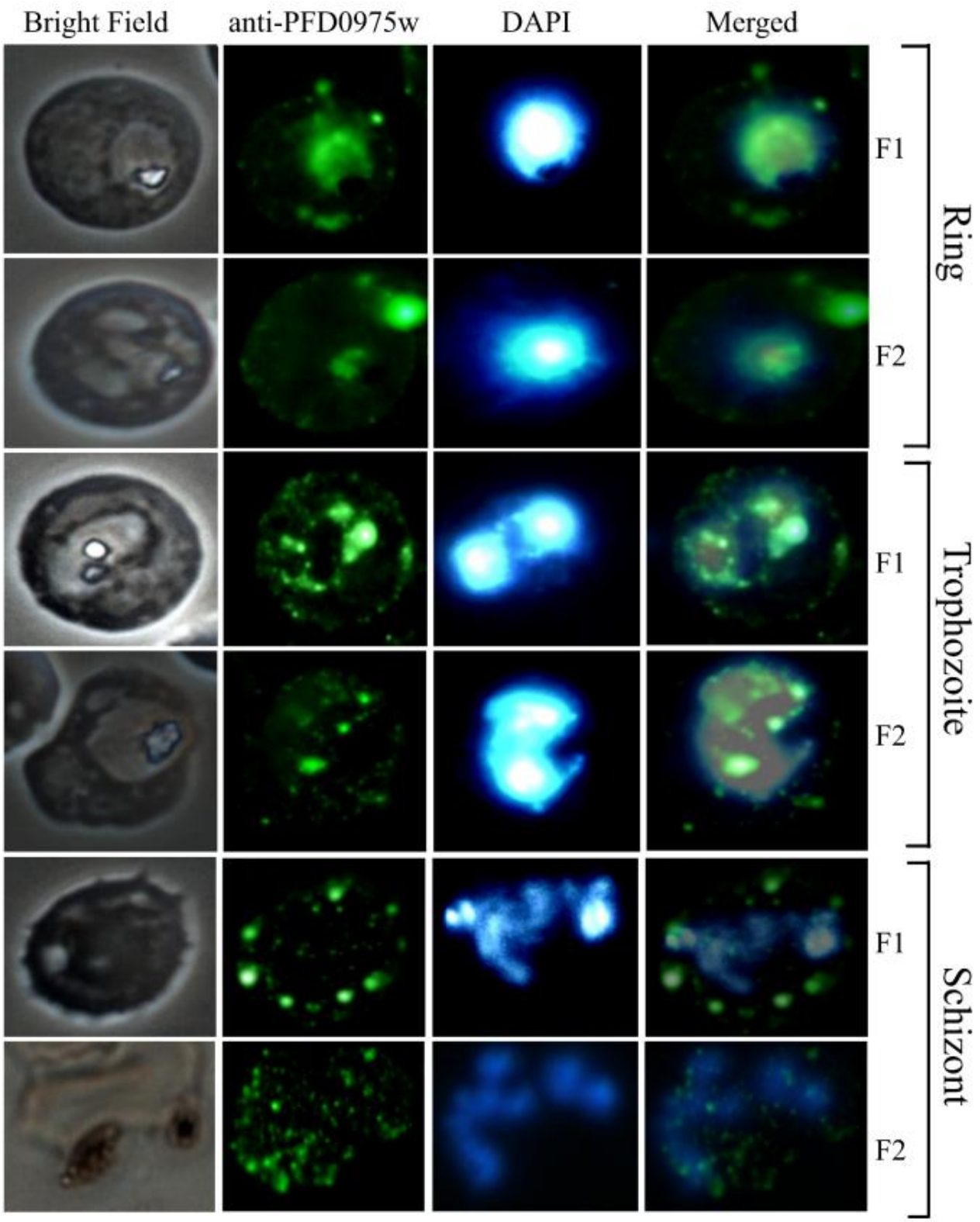

Figure 2.6: Immunolocalization pattern of PFD0975w in *Plasmodium falciparum* exposed to endogenous stress: Glucose starvation for 90 minutes.

To counteract this increase in stress; parasite has to produce anti-oxidant enzymes or increase the expression of membrane channels to import anti-oxidant molecules (such as GSH from RBC) from the RBC cytosol. RIO-2 kinases are known to participate in ribosome maturation and proposed to have an indirect role in protein production, required to manage the oxidative stress (LaRonde-LeBlanc and Wlodawer 2005). To test the relevance of PFD0975w in the parasite biology during exogenous stress, we have challenged the parasites with two different kinds of stress: (1) starvation, such as depletion of glucose from culture medium, and (2) anti-malarial drug pressure. The pattern of PFD0975w signal changes in glucose starved parasite (Figure 2.6).

The localization pattern of PFD0975w during the ring stage of treated parasite gives uniform level of expression throughout the parasite cytosol. It is similar to that of the ring stage of untreated parasite (Figure 2.5C).

In the mature stages of the parasite such as trophozoite and schizont, the protein appears to be expressed in a punctuate fashion with condensed spots of PFD0975w signal within cytoplasm. Glucose starvation thus shifts the uniformity of PFD0975w expression into localized cellular spots. The probable explanation for the observed pattern is that the ring stage parasites are rich in nutrients and hence better ability to manage stress caused by glucose starvation. As a result, PFD0975w expression pattern is least responsive to exogenous stress during the ring stage. Transition of ring stage into trophozoite and schizont, nutrients deplete within the infected cell with lesser resources to manage stress. The marked change in the localization pattern of PFD0975w in trophozoite and schizont could be a means to overcome stress due to starvation. Parasite treated with 0.5 µg/ml chloroquine; exhibit a marked overall down-regulation of PFD0975w expression during the RBC stages (Figure 2.7). The observed pattern reflects oxidative stress generated within the parasite as a result of anti-malarial drug pressure.

2.4 Discussion

Protein kinases are involved in the regulation of vital cellular processes. They phosphorylate themselves or downstream signaling molecules in a cascade, enabling a cell to respond to external or internal stimuli. RIO-2 kinases have been found to be crucial in the assembly of ribosome units for protein production within the cell and have been demonstrated to be essential in yeast. The primary

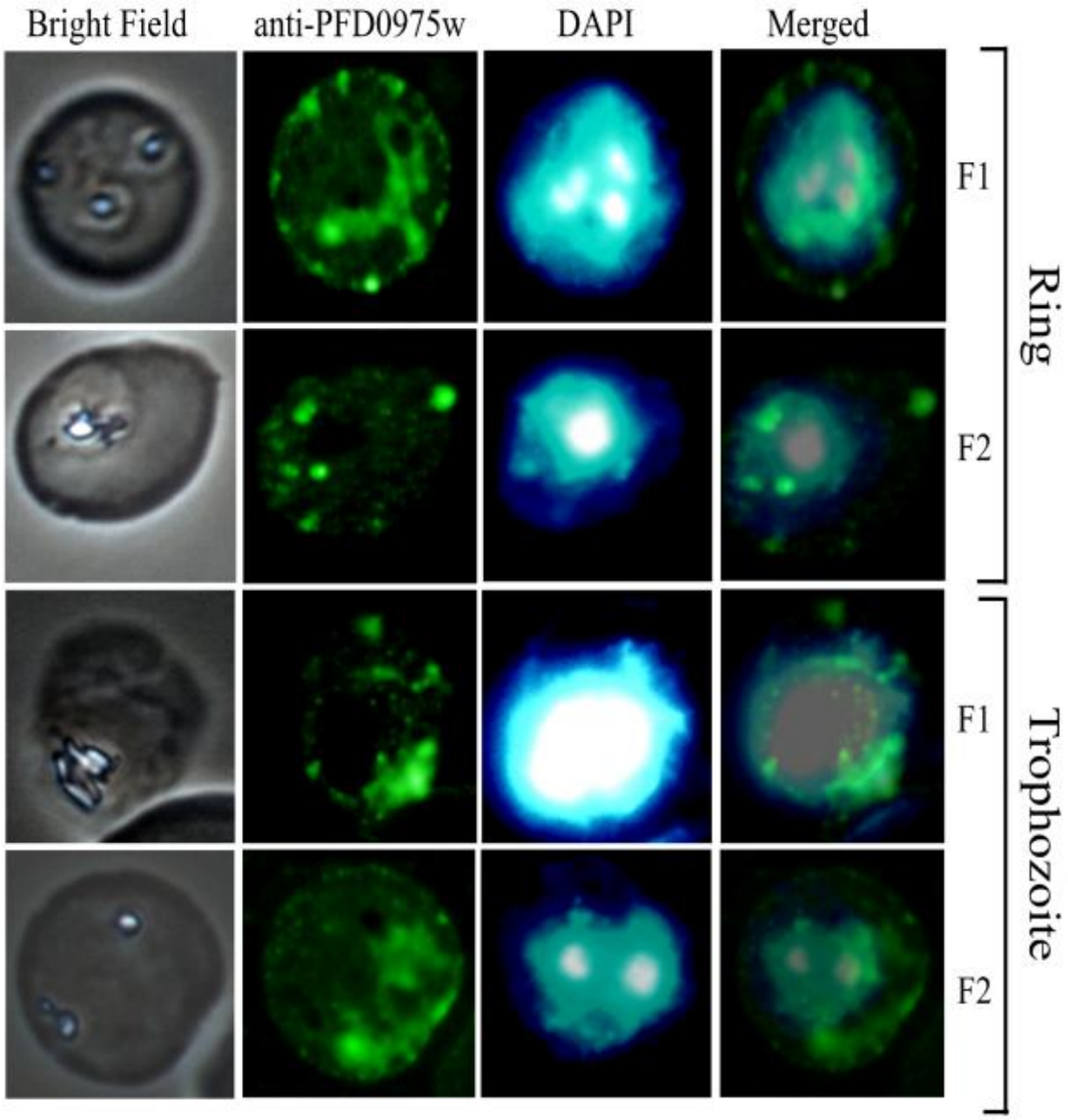

Figure 2.7: Immunolocalization of PFD0975w in *Plasmodium falciparum* exposed to exogenous stress: Exposure to 0.5 µg/ml (IC_{50}) of antimalarial agent chloroquine.

intent of cloning and over expression of the RIO-2 kinase from the malaria parasite is due to the belief that this kinase might play an essential role in the parasite's life cycle too. Bacterial expression system is chosen because of its simplicity, abundance of over-expressed protein within the bacterial cell, cost-effectiveness and yield of the purification process. The initial attempt was to clone the native PfRIO-2 kinase gene from *Plasmodium falciparum* using PCR amplification. The native gene failed to express in bacterial system due to codon bias between prokaryotic and eukaryotic protein

synthesis machinery. To circumvent the expression problem, a codon optimized synthetic version of PfRIO2- kinase was commercially synthesized. This synthetic version (PFD0975ws) of the gene was designed for high level expression in the bacterial system and consisted of the winged helix domain (residues 1-88) and the protein kinase domain (residues 89-270) of the native protein.

The next major challenge was the appearance of the protein in insoluble fraction. Solubility optimization experiments were conducted to see the effect of different host bacterial strains, media supplementation, buffer pH, inducer concentration, induction time and temperature on the yield of soluble PFD0975ws. The results revealed that the highest yield of soluble protein was obtained when Rosetta-gami™ host strains were used to express the protein. Rosetta-gami™ host cells, from Novagen are derivatives of Origami™, that combine the enhanced disulfide bond formation resulting from *trxB/gor* mutations with enhanced expression of eukaryotic protein that contain codons rarely used in *E. coli*. This strain supplies tRNAs for AGG, AGA, AUA, CUA, CCC, and GGA on a compatible chloramphenicol-resistant plasmid. The hexa-histidine tagged recombinant PfRIO-2 kinase was purified using immobilized metal affinity chromatography and its native molecular weight is estimated to be ~ 35 KDa using gel image analyses. Antibodies were generated against PFD0975w in rabbit model and the purified polyclonal antibody was used to study the changes in expression pattern of PFD0975w during the parasite's asexual stages in the presence and absence of exogenous cellular stress. Studies on *Saccharomyces cerevisiae* and cancer cell lines have shown that exogenous cellular stress like glucose starvation results in increased phosphorylation of specific protein kinases along with the production of ROS (Graham, Tahmasian et al. 2012, Braun, Vaga et al. 2014). Studies have also correlated the cellular stress in *Plasmodium falciparum* with the increased phosphorylation of eIF2α kinases like PK4 (Zhang, Mishra et al. 2012). The shift in the observed expression of PFD0975w during glucose starvation and in the presence of antimalarial chloroquine indicates a correlation between PFD0975w and parasite stress response. The results of our current work juxtaposed with our previous findings (Nag, Prasad et al. 2012, Trivedi and Nag 2012, Nag, Chouhan et al. 2013), strongly suggests PFD0975w as a key player in the cellular signal transduction events during growth as well as under stress conditions. The expression pattern of this protein kinase is strongly governed by the stage of growth as well as the microenvironment and stress factors involved which surround the parasite. The results indicate that PFD0975w might be an essential cellular gene in *Plasmodium falciparum* and can be an attractive drug target, opening new avenues for antimalarial chemotherapy.

2.5 References

- Baca, A. M. and W. G. Hol (2000). "Overcoming codon bias: a method for high-level overexpression of Plasmodium and other AT-rich parasite genes in Escherichia coli." Int J Parasitol **30**(2): 113-118.

- Bozdech, Z., M. Llinas, B. L. Pulliam, E. D. Wong, J. Zhu and J. L. DeRisi (2003). "The transcriptome of the intraerythrocytic developmental cycle of Plasmodium falciparum." PLoS Biol **1**(1): E5.

- Braun, K. A., S. Vaga, K. M. Dombek, F. Fang, S. Palmisano, R. Aebersold and E. T. Young (2014). "Phosphoproteomic analysis identifies proteins involved in transcription-coupled mRNA decay as targets of Snf1 signaling." Sci Signal **7**(333): ra64.

- Chung, C. T., S. L. Niemela and R. H. Miller (1989). "One-step preparation of competent Escherichia coli: transformation and storage of bacterial cells in the same solution." Proc Natl Acad Sci U S A **86**(7): 2172-2175.

- de Marco, A., L. Vigh, S. Diamant and P. Goloubinoff (2005). "Native folding of aggregation-prone recombinant proteins in Escherichia coli by osmolytes, plasmid- or benzyl alcohol-overexpressed molecular chaperones." Cell Stress Chaperones **10**(4): 329-339.

- Engebrecht, J., R. Brent and M. A. Kaderbhai (2001). "Minipreps of plasmid DNA." Curr Protoc Mol Biol **Chapter 1**: Unit1.6.

- Graham, N. A., M. Tahmasian, B. Kohli, E. Komisopoulou, M. Zhu, I. Vivanco, M. A. Teitell, H. Wu, A. Ribas, R. S. Lo, I. K. Mellinghoff, P. S. Mischel and T. G. Graeber (2012). "Glucose deprivation activates a metabolic and signaling amplification loop leading to cell death." Mol Syst Biol **8**: 589.

- Gustafsson, C., S. Govindarajan and J. Minshull (2004). "Codon bias and heterologous protein expression." Trends Biotechnol **22**(7): 346-353.

- Kopetzki, E., G. Schumacher and P. Buckel (1989). "Control of formation of active soluble or inactive insoluble baker's yeast alpha-glucosidase PI in Escherichia coli by induction and growth conditions." Mol Gen Genet **216**(1): 149-155.

- LaRonde-LeBlanc, N. and A. Wlodawer (2005). "The RIO kinases: an atypical protein kinase family required for ribosome biogenesis and cell cycle progression." Biochim Biophys Acta **1754**(1-2): 14-24.

- Llinás, M., Z. Bozdech, E. D. Wong, A. T. Adai and J. L. DeRisi (2006). "Comparative whole genome transcriptome analysis of three Plasmodium falciparum strains." Nucleic Acids Res **34**(4): 1166-1173.

- Nag, S., D. Chouhan, S. N. Balaji, A. Chakraborty, K. Lhouvum, C. Bal, A. Sharon and V. Trivedi (2013). "Comprehensive screening of heterocyclic compound libraries to identify novel inhibitors for PfRIO-2 kinase through docking and substrate competition studies." Medicinal Chemistry Research **22**(10): 4737-4744.

- Nag, S., K. Prasad and V. Trivedi (2012). "Identification and screening of antimalarial phytochemical reservoir from northeastern Indian plants to develop PfRIO-2 kinase inhibitor." European Food Research and Technology **234**(5): 905-911.

- Oganesyan, N., I. Ankoudinova, S. H. Kim and R. Kim (2007). "Effect of osmotic stress and heat shock in recombinant protein overexpression and crystallization." Protein Expr Purif **52**(2): 280-285.

- Seidman, C. E., K. Struhl, J. Sheen and T. Jessen (2001). "Introduction of plasmid DNA into cells." Curr Protoc Mol Biol **Chapter 1**: Unit1.8.

- Sorensen, H. P. and K. K. Mortensen (2005). "Soluble expression of recombinant proteins in the cytoplasm of Escherichia coli." Microb Cell Fact **4**(1): 1.

- Trivedi, V., P. Chand, K. Srivastava, S. K. Puri, P. R. Maulik and U. Bandyopadhyay (2005). "Clotrimazole inhibits hemoperoxidase of Plasmodium falciparum and induces oxidative stress. Proposed antimalarial mechanism of clotrimazole." J Biol Chem **280**(50): 41129-41136.

- Trivedi, V. and S. Nag (2012). "In silico characterization of atypical kinase PFD0975w from Plasmodium kinome: a suitable target for drug discovery." Chem Biol Drug Des **79**(4): 600-609.

- Trivedi, V. and S. Nag (2012). "In Silico Characterization of Atypical Kinase PFD0975w from Plasmodium Kinome: A Suitable Target For Drug Discovery." Chemical Biology & Drug Design **79**(4): 600-609.

- Zhang, M., S. Mishra, R. Sakthivel, M. Rojas, R. Ranjan, W. J. Sullivan, Jr., B. M. Fontoura, R. Menard, T. E. Dever and V. Nussenzweig (2012). "PK4, a eukaryotic initiation factor 2alpha(eIF2alpha) kinase, is essential for the development of the erythrocytic cycle of Plasmodium." Proc Natl Acad Sci U S A **109**(10): 3956-3961.

2.6 Appendix-I

2.6.1 Materials: Primers were purchased from Integrated DNA technologies, Coralville, USA, vectors were purchased from MBI Fermentas and Novagen. Restriction enzymes were from New England Biolabs. LB media, gel extraction silica kit, OPD etc were purchased from Himedia. Agarose, IPTG, Nitrocellulose membrane, PVDF membranes, chemiluminiscent peroxidase substrate-1, DAB, antibodies, imidazole, Freund's complete and incomplete adjuvants were purchased from Sigma, St. Louis, MO. Nickel affinity matrix, column and low molecular weight (LMW) Calibration Kit for gel filtration were purchased from GE Healthcare. FITC and DAPI were purchased from BD Biosciences. Other chemicals and reagents were of analytical and molecular biology grade. InsTAclone^{TM} PCR Cloning kit was procured from MBI Fermentas, PA, USA. HisTrap crude FF was procured from BioRad, PA, USA.

2.6.2 Competent cells preparation: The competent cells of *E. coli* strains were prepared using PEG-DMSO method as described in(Chung, Niemela et al. 1989). *E.coli* bacterial strains DH5α, BL21 (DE3), Codon Plus, C41(DE3) and Rosetta were grown in LB media at 37°C. When OD of the culture reached 0.5, cells were harvested. The cells were re-suspended gently on ice with one-tenth volume of Transformation storage solution (TSS buffer). The re-suspended cells were incubated on ice for 15mins and dispensed as 100µl aliquot in 1.5ml centrifuge tubes.

Recipe for preparation of TSS buffer	
Components	**Amount**
LB broth	85% v/v
Polyethelene glycol	10% w/v
Dimethylsulfoxide	5% v/v
$MgCl_2$	50mM

2.6.3 Isolation of plasmids: Plasmid isolation was performed using LiCl method as described (Engebrecht, Brent et al. 2001). The bacterial culture was taken and pelleted down at 10000 rpm for 30secs.Then 100µl of TELT solution was added to the pellet and re-suspended by vortexing. Then 100µl of 1:1 PCI was added and vortexed for 5secs and let it stand for ≤ 15mins.The sample was centrifuged at 15000x g for 1min.The upper aqueous layer which contains DNA was transferred carefully in clean micro-centrifuge tube. Then two volume of chilled 100% ethanol was added for washing the plasmid DNA. The DNA was then precipitated and pelleted down at 15000x g for

5mins.The DNA pellet was air dried to removes traces of ethanol. The pellet was dissolved in 30µl sterile water and heated at 60°C for 10mins and given a short spin. The plasmid was ready to be used.

TELT solution		
Components	**Stock**	**Working soln (10ml)**
Tris base	1M pH 8	0.5ml
EDTA	0.1M pH 8	6.25ml
Triton X100		0.4ml
LiCl2	10M	2.5ml

2.6.4 Transformation of competent cells: The protocol of transformation was followed as described in(Seidman, Struhl et al. 2001). Standard plasmid of known concentration was taken and added in the competent cells aliquot to count transformation efficiency. The mixture was kept in ice for 30mins.Then heat shock was given at 42ºC for 45secs and immediately kept in ice for 2mins. Known volume of plain LB was then added to the cell mixture and incubated at 37ºC for about 1hr.Then 200µl of the cell mixture was taken and plated on LB agar ampicillin plate (100µg/ml) and incubated overnight at 37ºC.The number of colonies grown on the plate was counted and transformation efficiency was determined per µg plasmid.

2.6.5 Extraction of DNA from agarose gel: Extraction of DNA was performed by following Gel extraction kit (Himedia). The DNA band in agarose gel was excised by using scalpel blade under UV light. The gel slice was weighed and accordingly 3 volume of chaotropic salt solution was added per gel slice. The solution was incubated at 55°C for 5-10mins with intermittent mixing every 2-3mins until the agarose gel dissolved completely. Glass powder suspension (GPS) beads of about 10-20µl was added to the solution, mixed well and incubated for 10mins at RT with occasional mixing. The mixture was centrifuged at 1000rpm for 3mins and the pellet was then rinsed with 500µl of sterile water solution by re-suspending it by pipetting. The mixture was centrifuged at 10000rpm for 1min and supernatant was discarded. The washing was repeated two times. The supernatant was removed completely after last wash and the pellet was air dried for 5mins. The beads were re-suspended in 15-50µl of TE buffer or sterile water and incubated at 55°C for 10mins with intermittent mixing. The mixture was centrifuged at 10000rpm for 1min and the supernatant containing DNA was carefully transferred into a new tube.

Composition of Sterile water solution	9:1:10 ratio of water, concentrated wash solution (SWS) and 100% ethanol

2.6.6 PCR amplification recipe

Components	Final concentration	For 25 µl reaction volume	For 50 µl reaction volume
DNA	50ng	1.5µl	3µl
Forward primer	1µM	0.5µl	1µl
Reverse primer	1µM	0.5µl	1µl
2xDreamTaq Green PCR master mix	1x	12.5 µl	25 µl
Water	-	10µl	20µl
Total reaction volume	-	25µl	50µl

2.6.7 Ligation and restriction digestion recipes

Components for ligation	Final concentration	Components for Restriction Digestion	Final concentration
DNA	75ng	Vector DNA	300ng
Vector	165ng	NEB buffer 3	1x
Ligation buffer	1x	BSA	5µg
T4 DNA Ligase	5U	XhoI & BamHI	10U each
Total volume with water	30µl	Total volume with water	50µl

2.7 Appendix-II

2.7.1 Luria Bertani media and agar (LB broth and LB agar): LB broth was used for growing bacterial culture. It is composed of peptone (1%), yeast extract (0.5%), and sodium chloride (0.5%). Components were dissolved in distilled water and autoclaved for 20mins at 121°C and 15lb pressure. For LB agar solid media, agar was added in media to a final concentration of 1.5%.

2.7.2. Lysis and binding buffer: 100mM of tris buffer pH 8.8 containing 250mM NaCl.

2.7.3. Western blot wash buffer: 1x PBS containing 0.05 % tween 20.

2.7.4. Diamino-benzidine (DAB) substrate: 1x PBS containing 1mg/ml of DAB and 0.05% H_2O_2

2.7.5. Chemiluminescentperoxidisesubstrate-1: Add equal volume (1:1) of chemiluminescent substrate-1 and buffer supplied in the kit. Dissolve the solution well in dark and keep for 30mins prior to use.

2.7.6. Western blotting transfer buffer: Dissolve 5.63gm of glycine and 1.21gm of tris base in 400ml of distilled water. Add 20% of methanol (100ml) to the solution and mix well.

2.7.7. O-Phenylenediamine (OPD) substrate: Dissolve 1mg/ml of OPD using citrate buffer pH 5.6 containing 0.03% hydrogen peroxide.

2.7.8. Antigen preparation for injection into animal model: Using a syringe, mix 0.5ml of sterile PFI1625c antigen (400µg/ml) and 0.5ml of Freund's complete adjuvant until formation of micelles. Similarly prepare for Freund's incomplete adjuvant.

2.7.9. Phosphate buffer saline (PBS) and Tris acetate EDTA (TAE) buffer

PBS buffer composition	
Components	**For 10x (gm)**
NaCl	80gm
KCl	2gm
Na_2HPO_4	14.4gm
KH_2PO_4	2.4gm
Adjust pH& volume	7.4 and 1L

TAE buffer composition	
Components	**For 50x (Molar)**
Tris base	2M
Glacial acetic acid	1M
EDTA	100ml of 0.5M
Adjust pH	8.4
Final volume	1L

2.7.10. SDS-PAGE: Electrophoretic analysis of protein was carried out using sodium dodecyl sulfate polyacrylamide gel electrophoresis (SDS PAGE).The components of SDS-PAGE from preparation of the gel to de-staining of the gel are described from Table 2.2 through Table 2.7.

Table 2.1: Ingredients and preparation of stock reagents for SDS-PAGE

Stock reagent	**Preparation**
Acrylamide solution (30%)	1gm of N'N'-methylene-bis acrylamide was dissolved in 50ml ultrapure deionized water collected at 18 MΩcm (Millipore, Milli-Q water purification system) in amber coloredbottle. On complete dissolving, 29gm acrylamide was added to it and stirred on a magnetic stirrer till a clear solution was formed. The final volume was adjusted to 100ml. The solution was filtered (Whatman No. 1) and stored at 4°C in dark.
TrisHCl (1.5 M, pH 8.8)	54.45gm Tris base was dissolved in 150ml deionized water. The pH of solution was adjusted to 8.8 using HCl and volume made to 300 ml. It was stored at 4°C.
TrisHCl (1M, pH 6.8)	Tris base 6gm was dissolved in 60ml deionized water. The pH of solution was adjusted to 6.8 using HCl and volume made to 100 ml. It was stored at 4°C.
SDS (10%, w/v)	10gm sodium dodecyl sulfate (SDS) was dissolved in 60 ml deionized water. The volume made to 100 ml.
APS (10%,w/v)	100mg ammonium per sulfate (APS) was dissolved in 1ml water.

Table 2.4: Recipe for the preparation of 5x running buffer and loading buffer	
Solution	**Preparation**
5x Running Buffer	15gm Tris base, 5gm SDS and 72gm glycine were dissolved in 800ml of deionized water. The pH was adjusted to 8.3 and volume was adjusted to 1000ml. The solution was filtered (Whatman, Filter No. 1) and stored at 4°C. The buffer (5x) was diluted to 1x and pre-warmed at 37°C before use.
5x Loading Buffer	10ml 0.5M Tris (pH 6.8), 1.6ml SDS 10%, 10 ml glycerol, 0.4ml β-mercaptoethanol and 0.4ml 0.5%(w/v) bromophenol blue were dissolved in 3ml deionized water and pH was adjusted to 6.8. The final concentration of buffer was 1x by mixing 1 volume of 5x sample loading buffer to 4 volumes of sample (protein) before loading in gel.

Table 2.5: Recipe for the preparation of staining and de-staining solution		
Components	**De-staining solution**	**Staining solution**
Methanol	40ml	40ml
Acetic acid	10ml	10ml
Distilled water	50ml	50ml
Coomassie Brilliant Blue R250	-	0.25gm

Table 2.6: Recipe for preparation of 10x loading dye for SDS-PAGE		
Components	Proportion	Requirement (5ml)
Glycerol	50%	2.5ml
Bromophenol blue	0.2%	10mg
β-mercaptoethanol	10%	0.5ml
SDS	1%	0.5ml of 10% stock
Tris	250mM	1.25ml of 1M stock

Agarose gel electrophoresis: Electrophoretic analysis of DNA was carried out using agarose gel. Agarose gel was prepared by dissolving appropriate amount of agarose in 1x TAE buffer. Dissolution was achieved by heating the solution in microwave oven for several minutes (2 minutes onwards) with intermittent shaking. For plasmid DNA detection, 0.8-1% agarose was used whereas for genomic DNA detection, 0.5% agarose was used.

2.8 Appendix-III

2.8.1 Sequence of PFD0975ws gene

ATGAAGTTGGATATCTCGTGTTTCAGCTTCCTGAGCCGCAATGAATATCGTGTGCTGACG
GCGATTGAGATGGGCATGCGCAACCATGAATATCTGAGCGTATCCCTGATTAGCTCCAT
TGCCAACTTGCGTAAGGAGGGTATTGTAAGTGTTCTGAAGAAGCTGCTGAAGAACAAGC
TGATCTCGCACCAGAACAAGAAGTACGATGGCTACAAGTTGACCTACTTAGGCTATGAC

TTCCTGGCGCTGCGTACGTTCTTGAAGCGCGGCATTTTGAAGAGTATTGGCAACCAGATT
GGCGTAGGCAAGGAGTCTGATATCTATATCTGCAAGGATGTCGATGATAATCTGCTGTG
TTTAAAGATTCATCGTCTGGGCCGTATTAGCTTCCGTACCATTAAGAACAATCGTGATTA
CTATGGCAAGAAGTGCTTCCGCAATTGGTTATATCTGTCACGCATCGCGGCAACCAAGG
AGTATGCCTACTTAAAGGTCTTATATGAAAATAACTTCCCTGTGCCGAAGCCTCATGATA
TTAACCGCCACATGATTATCATGAGCTATATTAAGGGTTATCCACTGTCCCACGTTAAGC
TGAACAATCCATATAAGATTATCGATACCCTGTTCAACATCCTGGTGAAGTTCGCGAAG
GCGGACATTATTCATGGAGACTACAACGAATTCAATATCCTGGTCGATGATGATGAGAA
CGTCACAATTATTGACTTCCCACAGATTGTTAGCCTGCGTCATGTGAACGCAAAGATGTA
CTTCGAACGCGATATCAACTGCGTGATTAACCACTTCTTCAAGAAGTACAAGATTAAGA
TTCAGGAATATCCGCTGTATGAAGATGTGGTGCTGCTGAACAAGGATAAGCTGAACATT
GATGAGAAT

2.8.2 Sequence of PFD0975ws protein

M K L D I S C F S F L S R N E Y R V L T A I E M G M R N H E Y L S V S L I S S I A N L R K E
G I V S V L K K L L K N K L I S H Q N K K Y D G Y K L T Y L G Y D F L A L R T F L K R G I
L K S I G N Q I G V G K E S D I Y I C K D V D D N L L C L K I H R L G R I S F R T I K N N R
D Y Y G K K C F R N W L Y L S R I A A T K E Y A Y L K V L Y E N N F P V P K P H D I N R
H M I I M S Y I K G Y P L S H V K L N N P Y K I I D T L F N I L V K F A K A D I I H G D Y N
E F N I L V D D D E N V T I I D F P Q I V S L R H V N A K M Y F E R D I N C V I N H F F K K
Y K I K I Q E Y P L Y E D V V L L N K D K L N I D E N

Chapter III

Structural characterization of PFD0975w model; DNA and ATP binding studies.

3.1 Introduction

The reversible phosphorylation of proteins by protein kinases regulate cellular physiology and in turn are responsible for the structure, function and cellular localization of other proteins. More than one third of the typical 10,000 or more proteins on a mammalian cell are found to be in their phosphorylated state at any given point of time. Recent studies on RIO kinases in yeast and C*haetomium thermophilum* have revealed their involvement in the ribosome maturation process. The elucidation of the crystal structure of AfRIO-2 kinase was a milestone study (LaRonde-LeBlanc and Wlodawer 2004) which has shed light to the structural arrangement of the different domains of RIO-2 kinase. Protein kinases belonging to the atypical kinase family, exhibit kinase activity despite any similarity to known kinases at the sequence level. Atypical serine/threonine kinases have been reported to regulate a vast number of biological phenomenons within the cell and can be excellent drug targets (Manning, Plowman et al. 2002, Campbell, Boag et al. 2011). The typical structural features of RIO kinases include an N-terminal domain with a different function and a C-terminal kinase domain. The domains are connected to each other by a linker region. All studied RIO-2 kinases have been shown to contain a characteristic N-terminal winged helix (wHTH) domain. The winged helix domain is primarily found in proteins which have DNA binding activity such as histone H5 and transcription factors (LaRonde-LeBlanc and Wlodawer 2004). The kinase domain in RIO kinase is shorter than that of other eukaryotic protein kinase domains. This is due to the absence of the activation loop or subdomain VIII, subdomain X, and XI, which have previously been reported to be important in providing substrate specificity in typical eukaryotic protein kinases (Angermayr, Roidl et al. 2002). The variations in the ATP binding cavity between RIO-1, RIO-2, and other eukaryotic Protein kinases are quite distinct, especially with respect to charge distribution and the conformation of nucleotide binding. Both RIO-1 and RIO-2 kinase subfamilies share some biochemical and structural conservations to a considerable extent, apart from the unique characteristics of their own subfamily. The structural differences between the two RIO kinase families as well as the differences between host and parasite RIO-2 kinases are good enough for rational and selective design of drugs which will bring about the specific inhibition of parasite RIO-2 kinase.

This chapter elaborates the 3D homology modeling of PFD0975w based on sequence homology to the published crystal structure of AfRIO-2 kinase (LaRonde-LeBlanc and Wlodawer 2004). The 3D model of PFD0975w has been thoroughly described here and has been compared to the structure of

Human RIO-2 kinase and the essential differences have been charted out. The active sites of both the human and the *Plasmodium* RIO-2 kinases have been mapped and the mode in which both interact with ATP has been studied. The sequence of PFD0975w was obtained from PlasmoDB and was compared with NCBI (nr) sequence databases to obtain homologs sequences using BLASTp. PFD0975w is found to be an RIO-2 kinase from *P. falciparum* with conserved RIO-domain. The 3D model of PfRIO-2 kinase consists of an N-terminal winged helix turn helix domain (Residues 1-84), a short linker region (residues 85-147) and a C-terminal kinase domain (residues 148-275). The 3D model of PFD0975w thus developed has been used for virtual screening against known compound libraries such as ZINC, PubChem, and ChemBank etc to identify novel hits. The structures of top hits were used to scan DrugBank to identify approved drug molecules which are at least 60% or more similar to the hits and might inhibit PFD0975w. Figure 3.1 highlights the key contents of this chapter

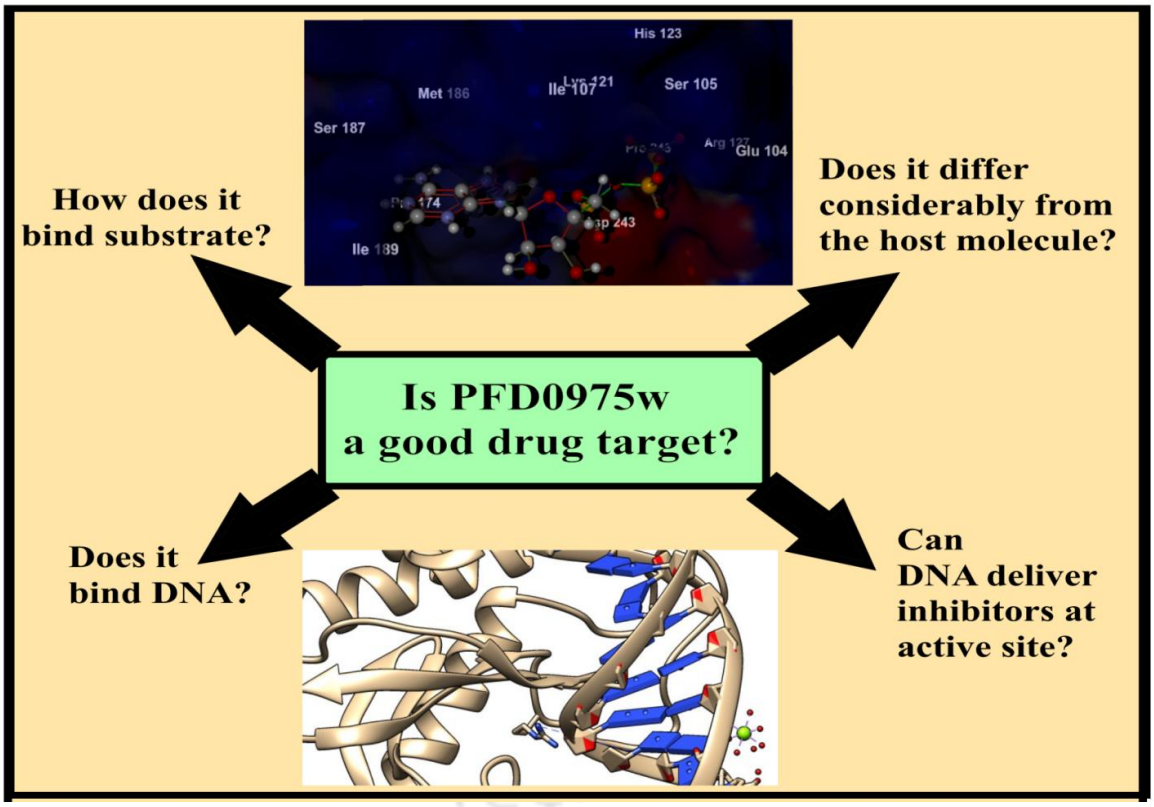

Figure 3.1: Schematic representation of the work discussed in chapter III

3.2 Experimental Procedures

3.2.1 Structural analysis of PFD0975w 3D model: The protein sequence of PFD0975w was obtained from http://www.plasmodb.org. The most suitable template to build the homology model was

determined by performing a protein BLAST of PFD0975w protein sequence against RSCB Protein databank of available crystal structures using PSI-blast. It was found out that the crystal structure of *A. fulgidus* RIO -2 kinase (PDB code 1TQI) was about 83.39% similar to PFD0975w sequence over a stretch of 265 amino acid residues (LaRonde-LeBlanc and Wlodawer 2004). The remaining 316 residues of PFD0975w, for which no sufficient homology was available, was left out and was not considered for building the homology model. The 3D model of PFD0975w was generated and has reported elsewhere (Trivedi and Nag 2012). RMSD difference between the Af-RIO2 kinase template and our developed model was structure was 0.58 Å over all Cα.

3.2.2 *In silico* DNA binding studies: The winged helix domain is known to bind DNA, hence we wanted to model the wHTH-DNA interaction of PFD0975w. 3D NMR structures of 30 AT rich DNA sequences, 30 GC rich DNA sequences and 30 mixed type DNA sequences were downloaded from nucleic acid database (Berman, Olson et al. 1992). These DNA molecules were chosen to be between 7 and 12 nucleotides long and double stranded. The DNA molecules were docked with both the ATP bound and non-bound model of PFD0975w (Trivedi and Nag 2012) using PatchDock server which was used to generate PFD0975w-DNA complexes based on surface complementarity (Schneidman-Duhovny, Inbar et al. 2005). The generated PFD0975w-DNA models were screened based on the ACE value of the complexes, the number of interacting residues of protein-DNA and the bound surface area between protein and DNA. Based on the above criteria, 9 AT rich DNA: PFD0975w complexes and 5 GC rich DNA: PFD0975w complexes were shortlisted for further study.

3.2.3 Mapping of critical DNA binding residues: To understand the mechanism of DNA binding by the winged helix domain we needed to find out which of the proteins residues make frequent interactions with DNA in our generated complexes. For this, two dimensional interaction map of the shortlisted complexes has been plotted with LigPlot server (Wallace, Laskowski et al. 1995). Residues making interactions with DNA in 3 or more complexes were considered to be critical in DNA binding.

3.2.3 *In vitro* ATP binding studies: To confirm whether the recombinant PFD0975w expressed in bacteria could bind ATP, the following strategy was employed: PFD0975ws was purified from cloned Rosetta-gami cells as described in the experimental procedures of chapter II. Purified protein was dialyzed against 100mM Tris buffer, pH 7.4. The concentration of purified protein was calculated using Beer-Lambert's law in a dual beam spectrophotometer. 1 ml reactions were set up in micro-

centrifuge tubes containing 200 nM of ATP analog mant-AMPPNP (95% similar to ATP) and varying concentrations of purified protein (from 0 µM to 50 µM) in 100 mM Tris buffer, pH 7.4. Reaction mixtures were incubated in 37°C water-bath for 1 hr and fluorescence spectra of each mixture were recorded over 300-600 nm range using an excitation of 360 nm in a spectrofluorimeter (Fluoromax 4). The shift in fluorescence emission at 488 nm was compared for all the mixtures to understand binding of ATP analog.

3.3 Results

3.3.1 Structural features of PFD0975w 3D model: Structural features observed in PFD0975w are comparable to the crystal structure of AfRIO-2 kinase with similar conformation of secondary

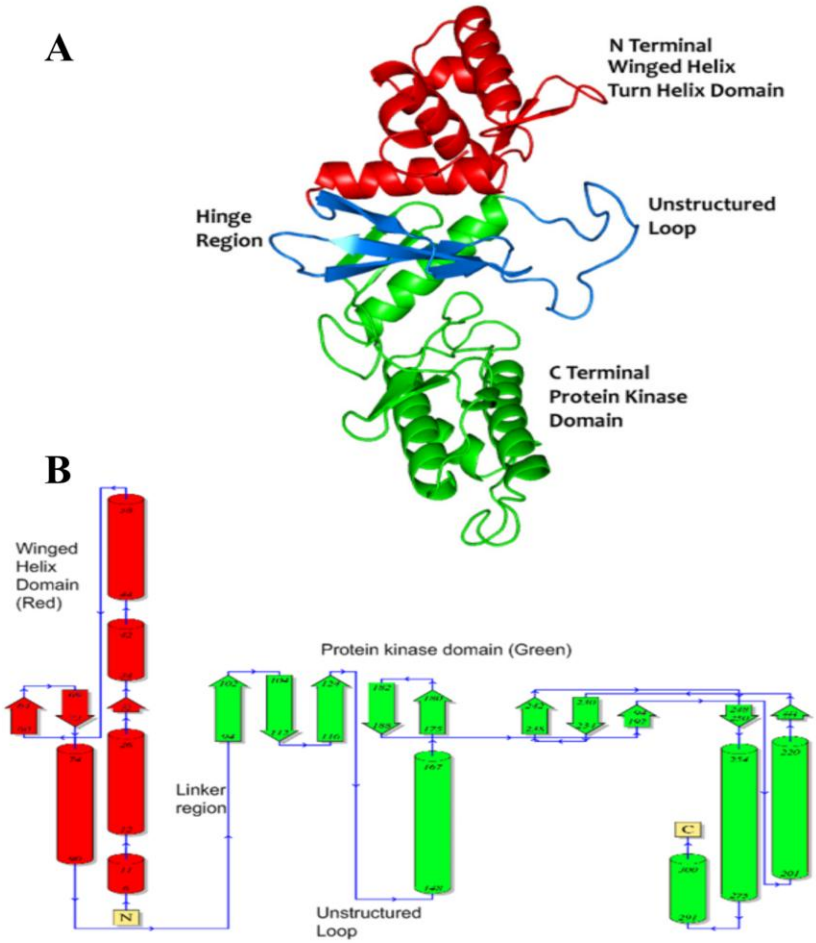

Figure 3.2: The overall folds and structural architecture of PFD0975w 3D model. (A) 3D model of PFD0975w showing the different domains in different colours (B) Topology diagram of the 3D model of PFD0975w depicting the two important domains: The winged helix domain (Red) and the protein kinase domain (green). Numbers at the beginning and end of each secondary structure indicates the residue number.

structural elements (Figure 3.2 A). The N-terminal wHTH domain comprised of three α helices followed by β-sheet and a fourth α helix. This is followed by a linker region connected to the C-terminal kinase domain. The kinase domain is almost similar in both RIO-1 and RIO-2 kinases and are structurally different from other protein kinases. The topology diagram of PFD0975w (Figure 3.2 B) depicts the organization of structural units and the way in which the two domains are connected via the linker region. The residues of the flexible loop (residues 123–149) are not structured in PFD0975w model since its corresponding region in the structure of AfRIO-2 (which was used as a template) had very weak electron density in that region and this clearly indicates that the loop region of AfRIO-2 and hence the similar region in the PFD0975w model is highly flexible and may play crucial role in the kinase activity of both the RIO-2 kinases. The flexible loop in PFD0975w might play some role in substrate recognition, or in the opening of the active site cavity to facilitate catalysis. Thorough structure–function analysis is necessary to clearly understand the importance of the unstructured loop of PFD0975w in catalysis.

The winged helix domain: The winged helix-turn-helix DNA-binding motif is a common structural domain which is mostly found in DNA binding proteins (Figure 3.3). The 'wing', or the loop, is a structure comprising of two anti-parallel beta-sheets. The winged helix domain, in most proteins, consists of 2 wing like loops (W1,W2), 3 alpha helices (α1, α2, α3) and 3 beta-sheets (β1, β2, β3) arranged in the following order: α1-β1-α2-α3-β2-W1-β3-W2 (Gajiwala and Burley 2000).

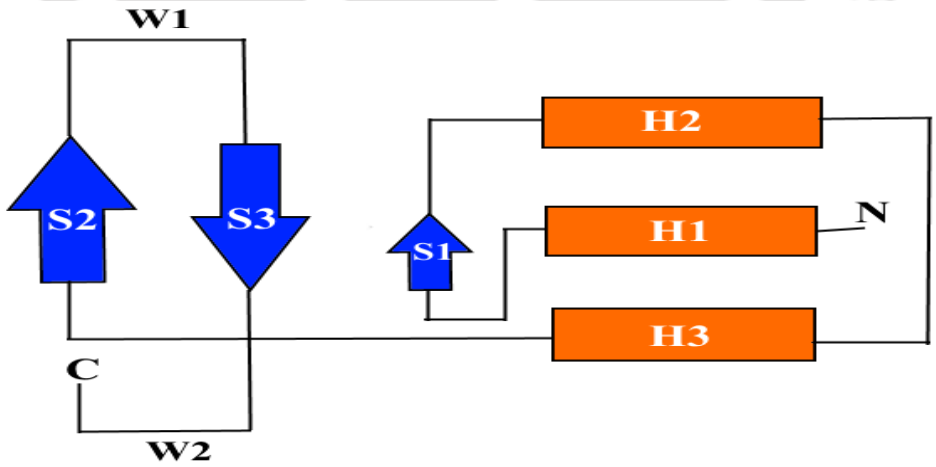

Figure 3.3: The topology of the winged helix architecture. H indicates the helices 1, 2 and 3. S indicates the β sheets 1, 2, and 3. W1 and W2 represent the two turns or wings.

This DNA-binding helix recognizes DNA and makes sequence-specific contacts with DNA backbone at the major groove while the interaction of DNA with the wings is often at the minor groove or the

DNA backbone. Numerous proteins with varying biological functions may contain a winged helix domain (Figure 3.4). This includes transcriptional repressors such as the LexA repressor, biotin repressor and the arginine repressor (Wilson, Shewchuk et al. 1992). Transcription factors often contain this DNA binding domain such as the transcription factors TFIIF and TFIIE, hepatocyte nuclear factor-3 proteins which regulate cell differentiation (Lai, Clark et al. 1993), The helicase proteins such as RuvB (Yamada, Miyata et al. 2002), the heat-shock transcription factor (Cicero, Hubl et al. 2001) and the CDC6 protein (Liu, Smith et al. 2000).

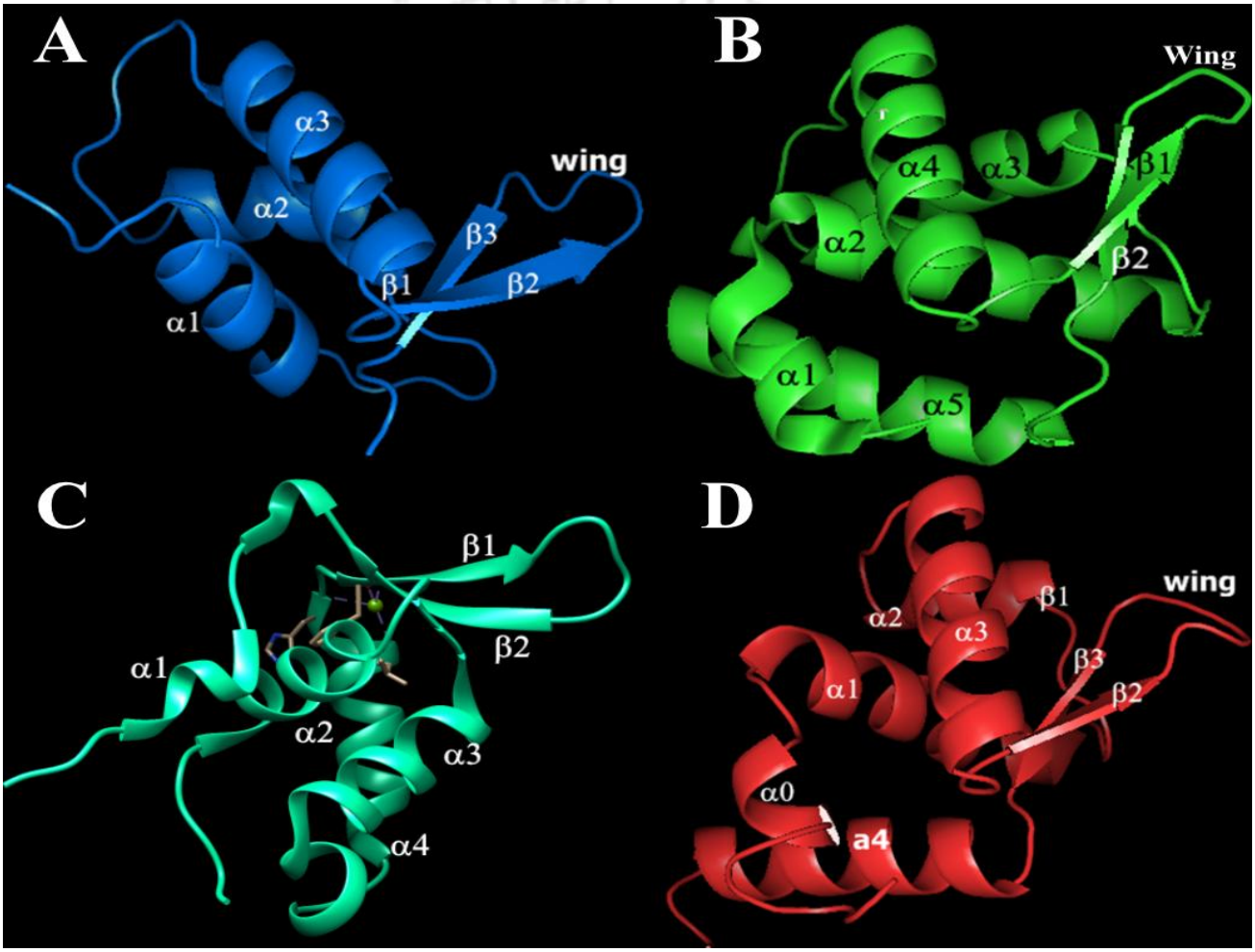

Figure 3.4: The underlying structural conservation of the winged helix domain of different proteins. (A) Winged helix domain architecture of Histone H5 (B) winged helix domain architecture of Cell division control protein 6 (Cdc6) from *Pyrobaculum aerophilum* (C) winged helix domain architecture of FoxM1 family of transcription factors (Littler, Alvarez-Fernandez et al. 2010) (D) winged helix domain architecture of PFD0975w model. (Trivedi and Nag 2012)

Some of the other winged helix proteins include the histones, restriction endonucleases like TnsA and FokI (Wah, Hirsch et al. 1997) and the Mu transposase (Clubb, Mizuuchi et al. 1996). The exact role of the winged helix domain in RIO-2 kinases have not been elucidated so far but the high level of conservation of amino acid residues observed across the winged helix domains of different DNA binding proteins clearly suggest that RIO-2 kinases could regulate gene expression by binding to DNA upon some phosphorylation signal.

The protein kinase domain: The overall folds of different kinase domains vary as per the group it belongs to. As known from the published crystal structures of the consensus RIO kinase domain, it is made up of an N- terminal lobe comprising of a twisted β –sheet structure (β1–β6) along with a long α-helix (α helix C). This N-lobe largely houses ATP-binding pocket of the enzymes with hinge region that connects it to the C-terminal lobe. The C-terminal lobe forms the basis for the metal-binding and catalytic loops of the kinase.

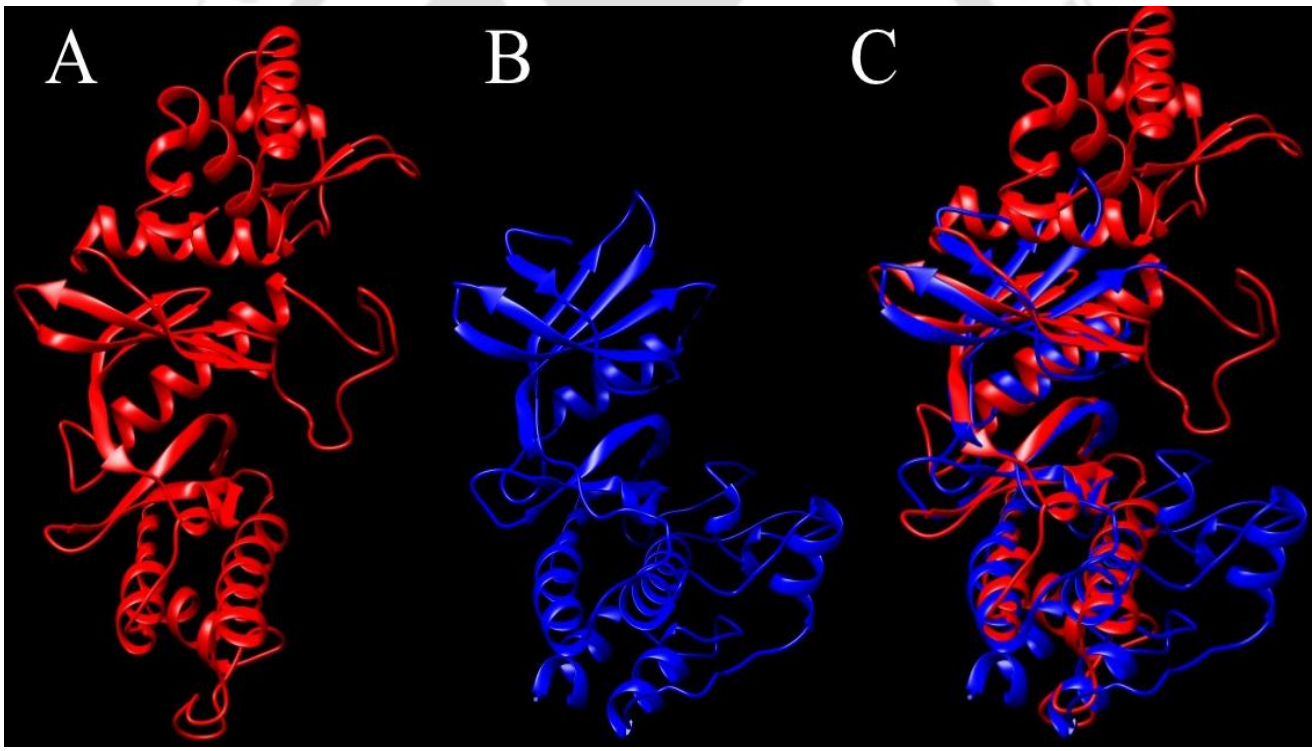

Figure 3.5: Structural differences between the protein kinase domain of PFD0975w and ePK Caesin kinase-I like kinase from *Oryza sativa*. (A) PFD0975w 3D model in red (B) ePK Caesin kinase-I like kinase from *Oryza sativa* (Park, Do et al. 2012). (C) Structural alignment of the kinase domains of PFD0975w (Red) and CK-1 like kinase demonstrating the conserved and non-conserved regions between the two kinases.

The distinguishing feature of both RIO1 and RIO2 kinase domains is that it contains only three of the typically occurring ePK helices in the C-terminal lobe. These have been named as αE, αF, and αI.

(LaRonde-LeBlanc and Wlodawer 2004). The structures of both RIO1 and RIO2 kinases contain an additional α-helix (α helix R) which is located upstream to the canonical N-terminal lobe β-sheet. Another difference from known ePKs is that all RIO domains have been shown to contain an additional insertion of 18–27 amino acids residues between α helix C and β sheet 3, called the flexible loop due to its disordered appearance in the structure of RIO2 kinase. Corresponding region in our PFD0975w 3D model also contains a disordered loop.

The DALI server identified casein kinase domain (CK1) as the nearest ePK homolog to the RIO kinase domain having a root mean square deviation of 2.8 Å. The RIO-2 kinase domain is truncated, compact and shorter than the typical kinase domains (Figure 3.5). RIO-2 domain contains two of the five α helices at the proteins C-terminal lobe. RIO-2 kinases lack subdomains VIa, IX and the activation loop (subdomain VIII) typically seen in ePKs and has been known to create a surface for substrate binding by inducing conformational flexibility (Knighton, Zheng et al. 1991, Zheng, Knighton et al. 1993, Cox, Radzio-Andzelm et al. 1994, Engh and Bossemeyer 2002).

Nucleotide binding in PFD0975w model: The crystal structure of AfRIO-2 kinase provides an insight into the ATP binding pocket of the RIO domain (LaRonde-LeBlanc and Wlodawer 2004). The similarly (Figure 3.6). In both the active site pockets the ATP molecule binds in a bent boomerang shape in which the adenosine moiety of ATP fits tightly into a deeper pocket and the ɣ-phosphate rests in a smaller pocket located at the other end of the active site. The ATP molecule in both the models appears to be bent around the β and ɣ phosphate bonds as a result of a ridge between the deeper and smaller sub-pockets. This arrangement of ATP within the RIO kinase active site domain might explain the mechanism of catalysis of ATP to ATP by breakage of the β-ɣ phosphate bond.

3.3.2 Structural differences between *Plasmodium* and Human RIO-2 kinases: For any drug development strategy to work out in vivo, the drug or inhibitors must specifically inhibit the target protein leaving the host protein undisturbed. Detailed structural analysis has revealed the important differences between *Plasmodium* and human RIO-2 kinases which could be exploited in the drug development process. Phylogenetic analysis has enabled us to chart out the evolutionary distance between *Plasmodium* and the host kinase.

The two kinases although have similar overall arrangement of folds, yet have structural differences in their active site, surface charge composition as well as mode of ATP binding.

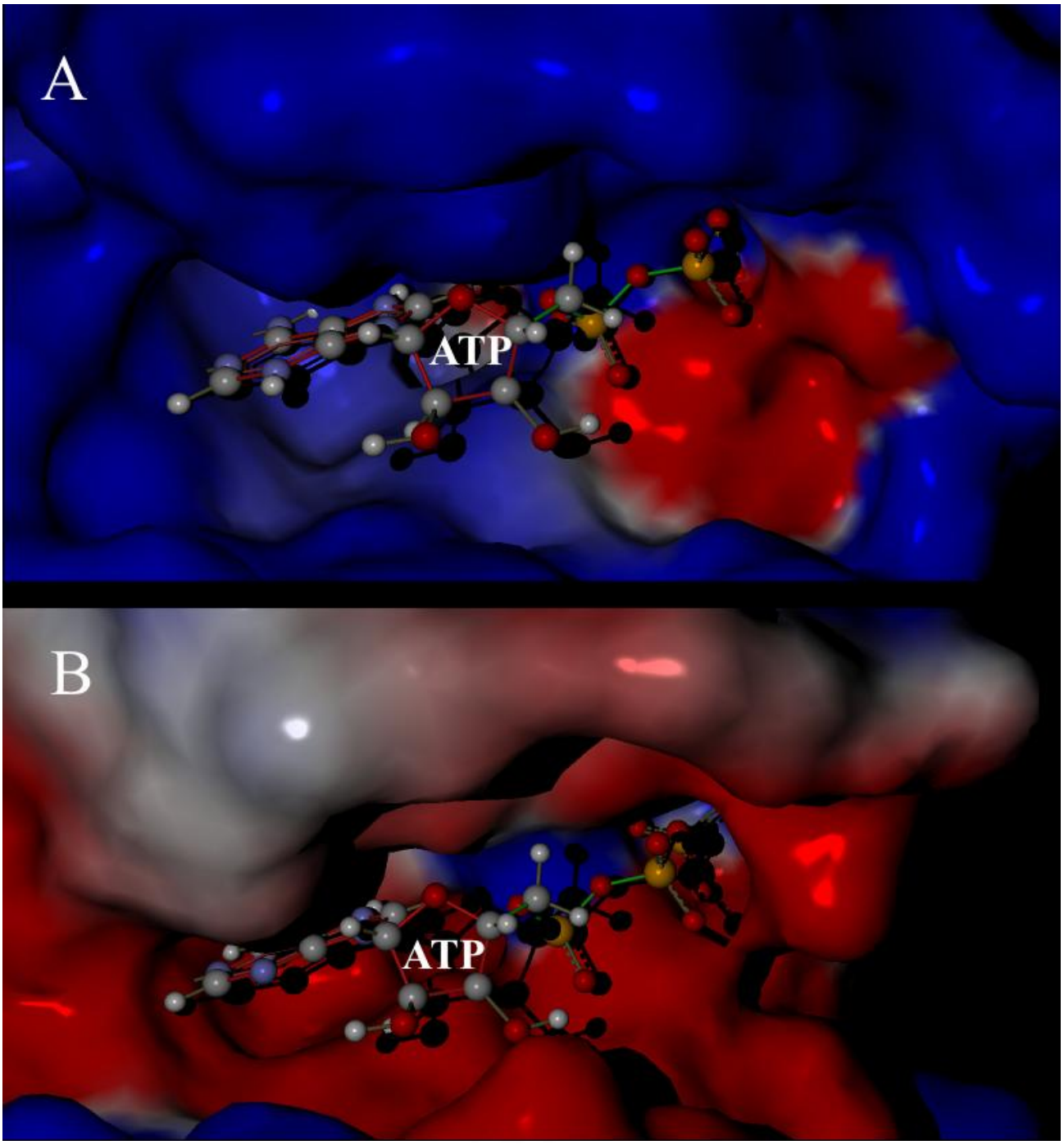

Figure 3.6: Similarities in the mode of ATP binding within the active site pocket of (A) PFD0975w 3D model and (B) The crystal structure of AfRIO-2 kinase. The ATP is bound in both the models in a conformation in which the adenine moiety lies flat within a large grove and the γ phosphate is secluded in a small groove. A septum at the β-γ phosphate bond bends the molecule in a cresant shape and might be responsible for catalysis of phosphorylation.

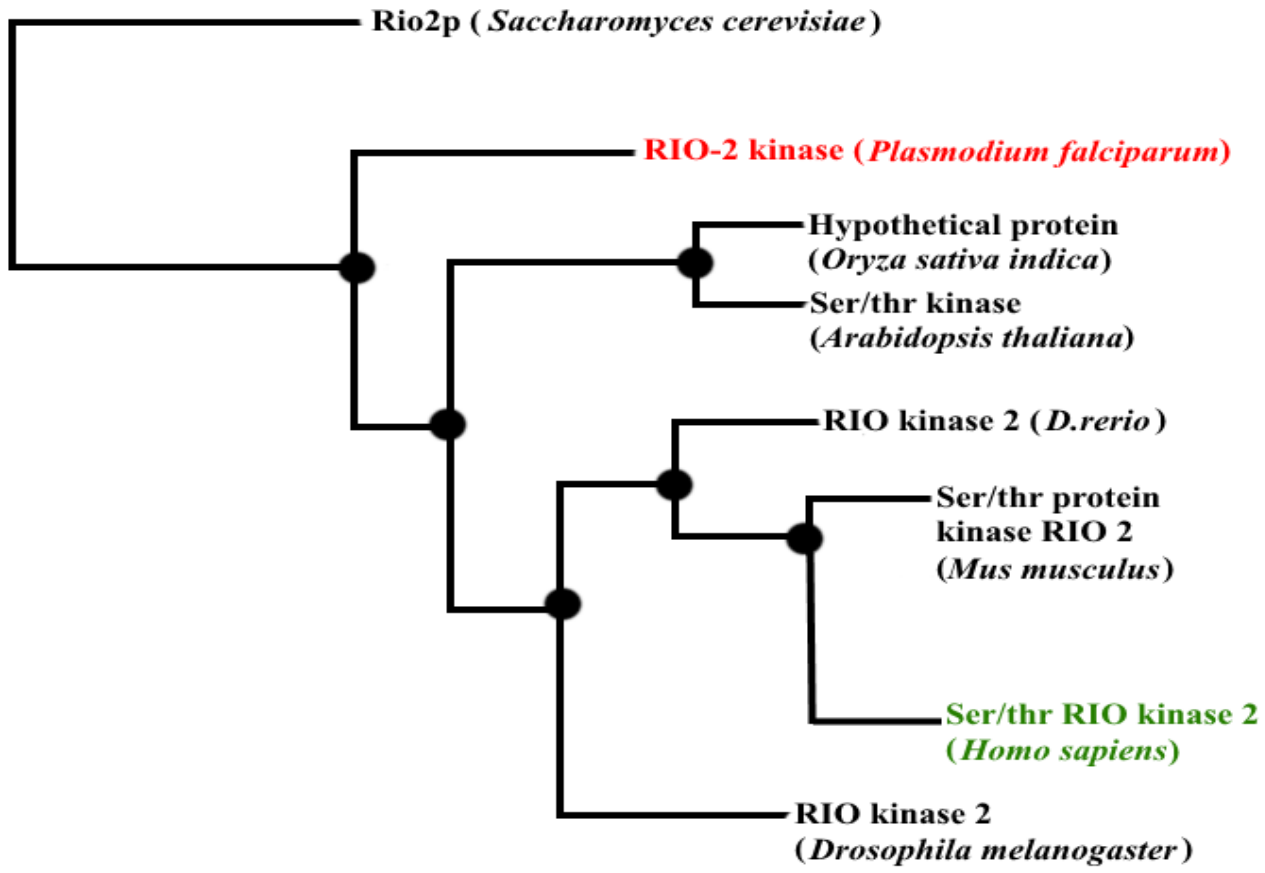

Figure 3.7: Phylogenetic tree depicting the evolutionary distance between Human and *Plasmodium* RIO-2 kinase sequences.

Phylogenetic differences: RIO-2 kinase protein sequence was scanned against similar proteins in other model organisms including human. The phylogenetic tree hence obtained (Figure 3.7) demonstrates the evolutionary distance between the Human and *Plasmodium* RIO-2 kinases. Two proteins which are evolutionarily distant from one another implies that they have structural divergences which in this case would be beneficial for the development of inhibitors specific to the *Plasmodium falciparum* RIO-2 kinase which would not cross react with the host kinase.

Overall Structural differences: Although the overall structural arrangement of both the models is similar but a closer inspection reveals subtle but important differences between the parasite and the host RIO-2 kinase (Figure 3.8). The major difference between the *Plasmodium* and Human RIO-2 kinase lies in the length, 3D orientation as well as amino acid composition of the flexible loop. The flexible loop of the human kinase is longer and contains more basic residues than the parasite kinase. Some of the minor differences include the spatial orientation of α helix3 of the winged helix domain

and the amino acid composition of the β sheet region. The overall positive charge distribution of PFD0975w is more than HuRIO-2 kinase. The winged helix domain contains more positively

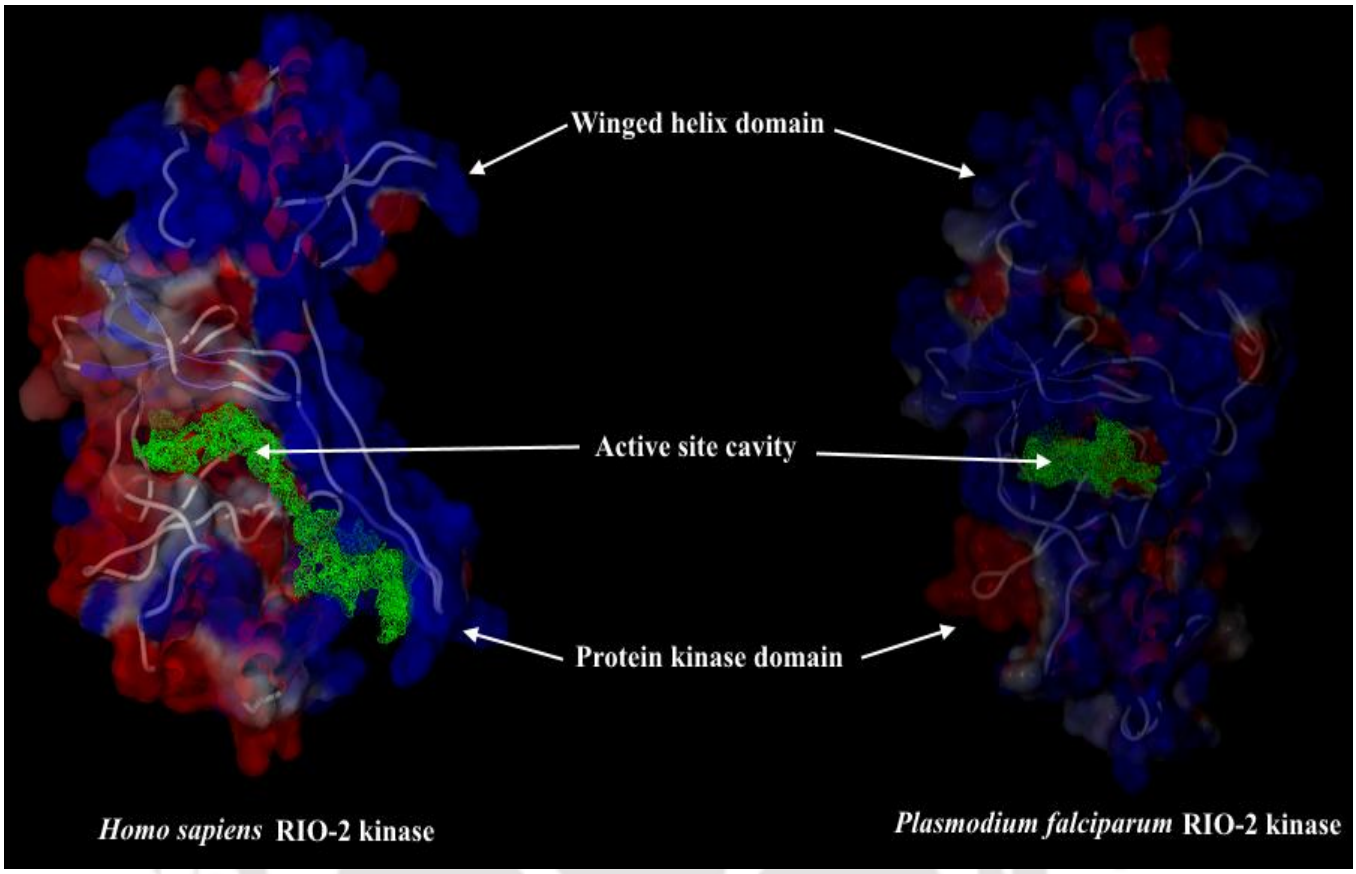

Figure 3.8: Overall structural differences in the 3D models of HuRIO-2 kinase (left) and PFD0975w (Right). Each model is an overlay of secondary structural elements and the surface potentials of that particular protein. The positively charged surfaces are shown in blue, negatively charged surfaces in red and neutral surfaces in off white. The volume of the active site cavities of both the models have been shaded in green.

charged residues in case of PfRIO2 kinase than the human enzyme. The most striking difference is that the ATP binding site and the catalytic domain (β sheet region) of PFD0975w is highly positive whereas it is mostly negatively charged or neutral in case of the human isoform (Figure 3.6). Another important difference between the two kinases is the volume and composition of the active site pocket. The PFD0975w active site pocket is small and compact with a volume of approximately 211.456 $Å^3$ whereas the active site pocket is long and more open in case of the human RIO-2 kinase with a volume of 462.336 $Å^3$. As a result the way in which both the enzymes bind ATP and the critical residues which interact with ATP are different for both the enzymes. The difference in ATP binding is advantageous to design or identify inhibitors which would be specific for the parasite RIO-2 kinase.

Composition of active sites and mode of ATP binding: Both the active sites of HuRIO-2 kinase and PFD0975w have a high affinity for its natural substrate ATP. Nevertheless the most energetically favorable conformation for ATP to bind at these cavities is largely different (Figure 3.9). HuRIO-2 kinase active site binds ATP tightly at one end of the cavity, whereas in PFD0975w the ATP molecule is more extended along the cavity with the adenosine moiety and the ɣ phosphate at different sub-pockets (Figure 3.9). The differences in ATP binding by the two enzymes could be attributed to the difference in cavity volumes and the composition of charged amino acid residues of the cavities. The active site pocket of HuRIO-2 kinase is mostly negatively charged whereas the PFD0975w pocket has distinct zones of positively and negatively charged residues. The critical residues which hold the bound ATP in the pocket are different for the two kinases (Figure 3.9).

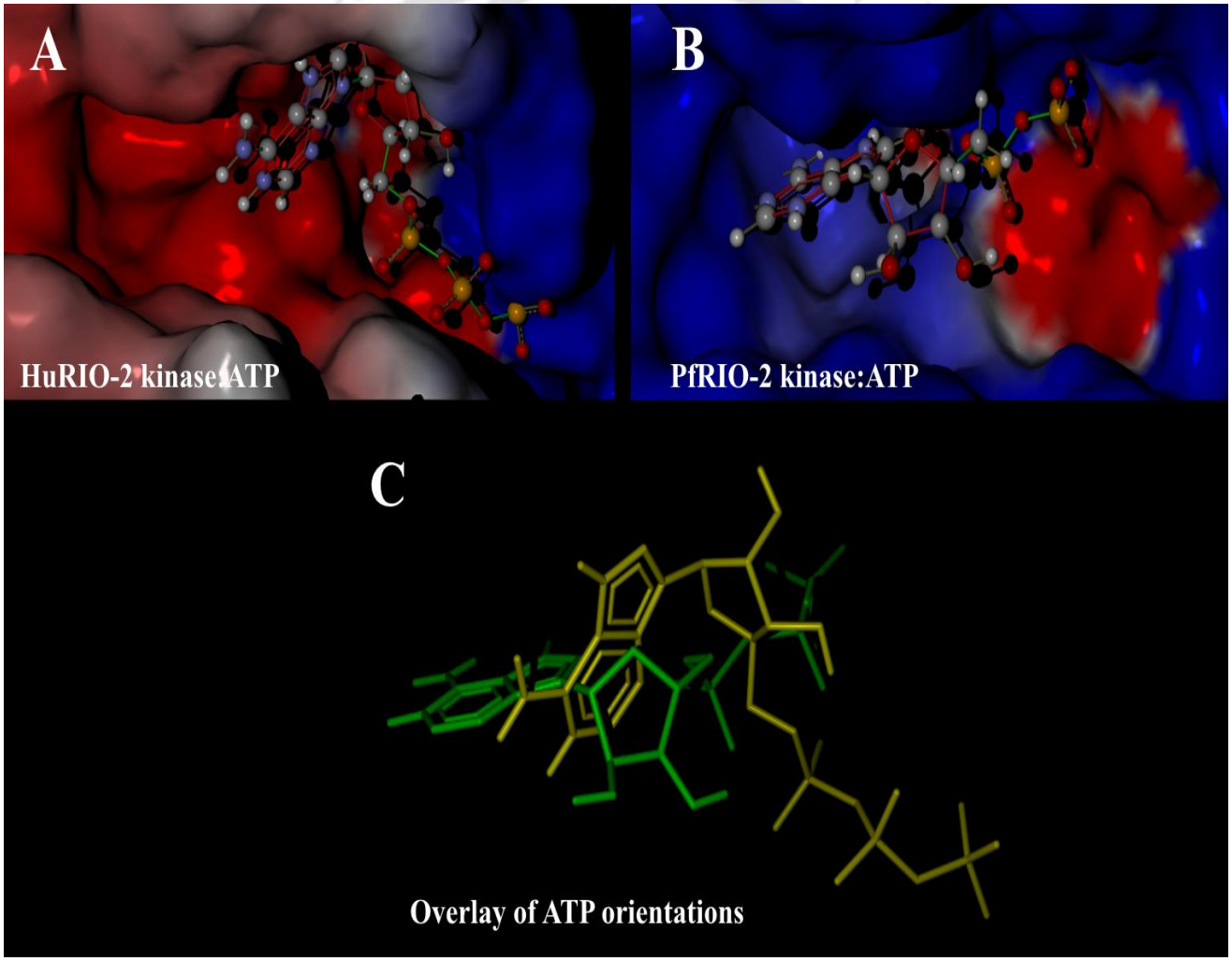

Figure 3.9: The composition of active site residues and hence the mode of ATP binding is different for (A) HuRIO-2 kinase and (B) PFD0975w. (C) Overlay of the bound ATP in HuRIO-2 kinase (yellow) and PFD0975w (green) depicting the differences in the mode of ATP binding by the two enzymes.

Within HuRIO-2 kinase pocket, the ATP molecule makes strong electrostatic interactions with Lys123, His125, Asp 240, Gln 106 and Gln 249 whereas within the PFD0975w pocket the ATP makes electrostatic interactions with Lys 121, Asp 243, His 123, Arg 127 and Glu104 (Figure 3.10).

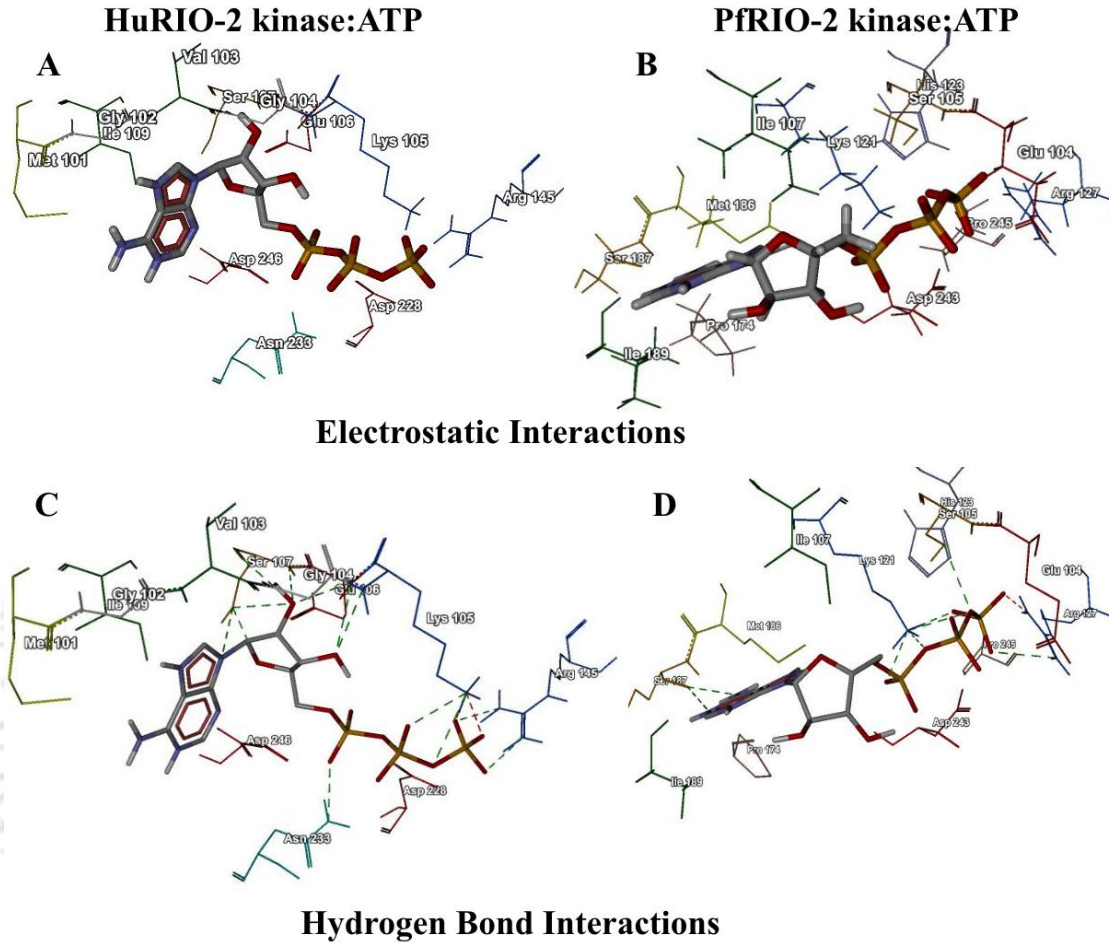

Figure 3.10: Critical residues interacting with the bound ATP are different for HuRIO-2 kinase (left) and PfRIO-2 kinase (right). (A) Electrostatic interactions of ATP with active site residues of HuRIO-2 kinase (B) Electrostatic interactions of ATP with active site residues of PfRIO-2 kinase (C) Hydrogen bond interactions of ATP with HuRIO-2 kinase and (D) Hydrogen bond interactions of ATP with PfRIO-2 kinase. Each pair of H-bond between a donor and acceptor is illustrated as green dotted lines.

Due to conformational strain on ATP within the active site of HuRIO-2 kinase, there are several key differences in the interacting residues between the host and parasite enzymes. For instance, Gln 249 and Phe 232 in HuRIO-2 kinase participates in electrostatic and hydrophobic interactions respectively. These residues do not appear to bind ATP in PfRIO-2 kinase. Similarly, due to the extended conformation of ATP within PfRIO-2 kinase pocket, hydrogen bond interactions with Ser 105 and Ser 187 are unique to PfRIO-2 kinase and is absent in ATP binding by host enzyme.

In HuRIO-2 kinase pocket three H-bonds with Asp246, His125 and Glu106 stabilize the ATP whereas the ATP is strongly held by 8 H-bonds through Ser187, Ser105 and Lys 121. These differences in the mode of ATP binding by the host and parasite RIO-2 kinases are likely to provide the necessary specificity for PFD0975w while possible inhibitor design.

3.3.3 PFD0975w prefers AT rich DNA: Docking experiment data for 30 AT rich DNA, 30 GC rich DNA and 30 mixed type DNA with PFD0975w 3D model were screened down to 14 protein: DNA complexes, based on the following criteria. Only those complexes were considered for analysis in which (i) the bound surface area between protein and DNA is greater than or equal to 2000 $Å^2$.

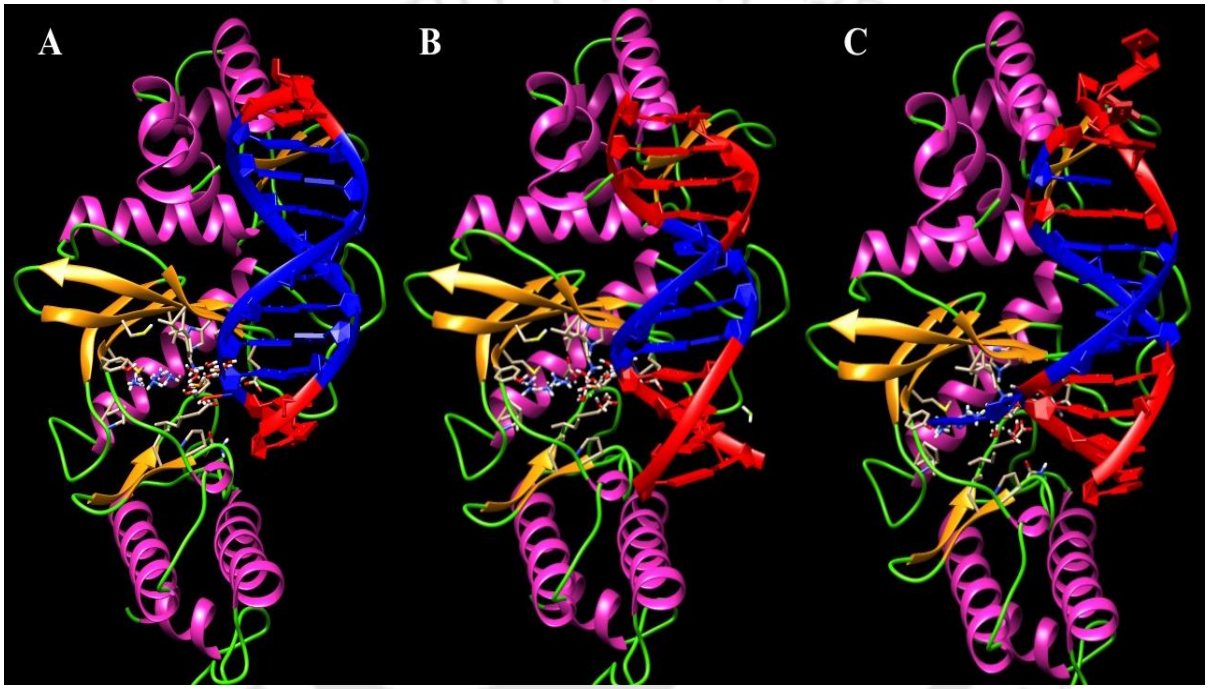

Figure 3.11: PFD0975w complexed with (A) Best fit AT rich DNA, (B) Best fit GC rich DNA and (C) Best fit mixed DNA. The winged helix domain binds DNA which extends down into the ATP binding pocket of the kinase. Helices are shown in pink, strands in yellow, coils in green. For DNA, A-T pairs are shown in blue and G-C pairs in red.

(ii) The docking score/PatchDock score for the complex is greater than or equal to 13,000. (iii) More than 2 residues of the winged helix domain participates in the DNA binding (iv) the complexes having a negative ACE value. (v) The DNA makes contact with the ATP binding pocket of the enzyme. The above set of criteria is just a hypothetical cut-off chosen to select the strong DNA-protein complexes from the weak ones and is not based on any previous findings. Based on the above criteria 30x20=600 complexes were manually screened down to 14 best complexes. It was evident from this kind of analysis that most of the complexes which passed the

above filter were the ones complexed with AT rich DNA (Table 3.1). This suggests the proteins intrinsic preference for AT rich DNA which can be correlated well since the *Plasmodium* genome is highly rich in AT bases.

Table 3.1: Shortlisted complexes for protein: DNA interaction analysis

Complex No	NDB id of DNA	DNA type	Number of bases	Complex Score	Bound Area (Å^2)	ACE Value
1	2KO0	GC Rich	16	13552	2637.4	-97.19
2	BD0041	GC Rich	12	13098	2180.6	-315.47
3	BDL018	GC Rich	12	14056	2005.2	-39.02
4	NA0856	GC Rich	19	13870	2038.9	-21.26
5	UMD010	GC Rich	13	12942	2188.1	-197.71
6	1RVH	AT Rich	12	13384	2296.7	-90.83
7	1RVH	AT Rich	12	12658	2409.8	-166.44
8	1TQR	AT Rich	17	13962	2097.1	-29.24
9	1TQR	AT Rich	17	13452	2057.3	-94.46
10	1TQR	AT Rich	17	12830	2095.8	-122.12
11	2LEV	AT Rich	15	10864	2110.5	-210.1
12	2Z33	AT Rich	16	12552	2611.6	-52.99
13	2Z33	AT Rich	16	12362	2363.8	-107.27
14	BD0011	AT Rich	12	14096	2064.3	-15.74

A total of 90 DNA molecules of length between 12-20 bases were docked with the 3D model of PFD0975w using molecular surface complementarity (PatchDock). The generated complexes were filtered through the criteria (refer text) to obtain top 14 complexes in which protein: DNA interaction is maximum. The above complexes were chosen to study wHTH domain: DNA interactions

The 14 complexes shown in table 3.1 fulfill all the five criteria and were used to study the critical residues needed for DNA binding. The complexes were energy minimized using Swiss PDB viewer and the energy minimized complexes were uploaded on LigPlot server. The 2D interaction chart obtained from LigPlot server for all the 14 complexes were analyzed manually and the critical residues of the winged helix domain responsible for different types of interactions were charted out separately for AT rich (Table 3.3) and GC rich complexes (Table 3.2)

Table 3.2: Protein residues of the wHTH domain interacting with GC rich DNA				
DNA ID	**Electrostatic**	**Hydrophobic**	**Hydrogen Bond**	**Area (Å^2)**
2KO0_16	Met(1), Lys(2),	Asp(4), Leu(3), Ser(9), Asn(58),Phe(10), Lys (59), Ile(5), Ser(6), Lys(57), Ser(9)	Nil	2637.4
BD0041_12	Met(1), Lys(2), Leu(76),	Ser(6), Cys(7),Thr(74),Asn(58),	Lys(59),Tyr(75),	2180.6
BDL018_12	Met(1), Lys(2), Leu(76),Lys(59)	Met(1),Leu(3), Ser(6),Lys(57),Asn(58), Tyr(75)	Asp(4),Leu(76),	2005.2
NA0856_19	Lys(2),	Met(1), Phe(10),Lys(57), Lys(59), Leu(76)	Asn(58), Leu(3),	2038.9
UMD010_13	Met(1),Leu(56), Lys(57),Leu(76)	Thr(74)	Leu(56),Lys(53), Tyr(75)	2188.1

The data obtained from LigPlot server was studied and the interacting residues of the protein's winged helix domain, participating in GC-rich DNA binding were categorized above as residues involved in electrostatic, hydrophobic and hydrogen bond interactions

By manual inspection of residues which occur more than thrice for a particular kind of interaction was finally selected and charted as below (Table 3.4). The more number of times a specific residue is reported to interact with DNA in different PFD0975w: DNA models, the greater is the probability of that residue to make specific interactions with DNA.

3.3.4 Purified PFD0975w binds ATP analog mant-AMPPNP: Fluorescent ATP analog, 3'-O-(N-Methyl-anthraniloyl)-adenosine-5'-[(β,ɣ)-imido]triphosphate,triethylammonium salt, also known as Mant-AMPPNP, is a fluorescent, non-hydrolysable ATP analog. This analog is >90% similar to ATP, and has been used extensively, to characterize ATP binding in protein kinases (Bujalowski and Jezewska 2000, Vineyard, Zhang et al. 2006, Bodey, Kikkawa et al. 2009).

To test whether our purified, recombinant PFD0975w protein is active or not, we chose mant-AMPPNP binding as a strategy. This fluorescent nucleotide has an emission maximum E_{max} at 448 nm. Fluorescence intensity of free nucleotide is lesser than the bound form. Thus, an increase of fluorescence at 448 nm is indicative of mant-AMPPNP binding. We tested the nucleotide binding at protein concentrations from 0 µM to 50 µM. ATP analog binding increases with the increase in protein concentration. Maximum binding occurs at 200 nM mant-AMPPNP and 50 µM protein concentration.

Table 3.3: Protein residues of the wHTH domain interacting with AT rich DNA

DNA ID	Electrostatic	Hydrophobic	Hydrogen Bond	Area (Å^2)
1RVH_12	Met(1), Lys(59)	Lys(2), Lys(57), Asn(58), Leu(60), Thr(74), Tyr(75),Leu(76)	NIL	2296.7
1TQR_17	Leu(76),Lys(59)	Leu(3),Thr(74),Tyr(75),	NIL	2097.1
1TQR_17	Met(1), Lys(59),Leu(76),	Lys(2), Tyr(75).	Met(1),Lys(59), Thr(74),	2057.3
1TQR_17	Met(1),Lys(2), Leu(76)	Met(1), Lys(57), Asn(58),Tyr(75),	NIL	2095.8
2LEV_15	Glu(30),Lys(53), Tyr(68), Asp(69),	Leu(56),Ser(62),Gln(64), Asn(65), Thr(74)	Gln(64), Leu(73),Lys(72), Tyr (75)	2110.5
2Z33_16	Met(1),Leu(3)	Met(1), Lys(57), Lys(59), Thr(74), Tyr(75)	Asp(4),	2611.6
2Z33_16	Lys(2),Leu(76),	Met(1),Leu(3), Tyr(75),	Met(1),Lys(2), Asp(79),	2363.8
BD0011_12	Met(1), Lys(59)	Lys(2), Tyr(75),	Lys(59),	2064.3

The data obtained from LigPlot server was studied and the interacting residues of the protein's winged helix domain, participating in AT-rich DNA binding were categorized above as residues involved in electrostatic, hydrophobic and hydrogen bond interactions.

Table 3.4: Residues responsible for different interactions which appears more than thrice.

Critical residues for Electrostatic interactions	Critical residues for Hydrophobic interactions	Critical residues for Hydrogen bonds
Met(1), Lys(2), Leu(76), Lys(59)	Ser(6), Lys(57), Thr(74),Tyr(75), Thr(74)	Asp(4), Tyr (75)

The critical residues involved in binding GC-rich (Table 3.2) and AT-rich sequences (Table 3.3) were scanned manually to look for specific residues occurring more than thrice in each category were selected.

We observed a consistent, detectable increase in fluorescence intensity at 50 µM of purified protein (Figure 3.10). The observed difference in fluorescence intensity is around ~40,000 units between the bound and unbound form of mant-AMPPNP and suggests that our purified recombinant PFD0975w is in native conformation, with the active site capable of binding ATP. This indirectly indicates the active state of the enzyme. Since *in silico* studies have pointed towards two other cavities apart from the active site, present in PfRIO-2 kinase, it cannot be confirmed that mant-AMPPNP binds only within the active site.

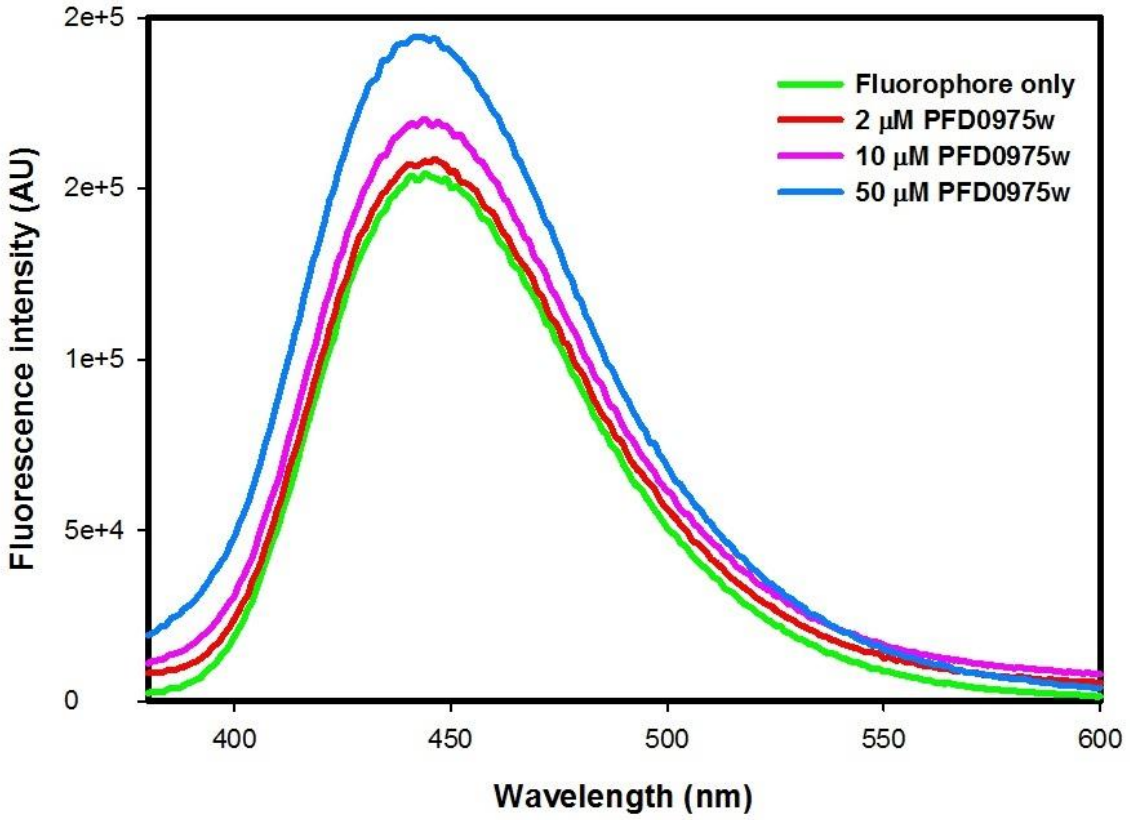

Figure 3.12: Spectrofluorometric analysis of ATP binding into the active site pocket of recombinant PFD0975w. 1 ml reaction mixtures were setup containing fixed amount of fluorophore (200 nM) and varying concentrations of purified PFD0975w in 100 mM Tris, pH 7.4. Spectra of blank (buffer only) were subtracted from the spectra of each reaction mixture before plotting.

3.4 Discussion.

The structural features of a protein are important for the development of inhibitors that can potentially bind to it. Many a times this is difficult due to the lack of crystal structure of the target protein. Approaches like homology modeling serves well at such times. PFD0975w is hypothesized to play

important role in the malaria parasite and hence its inhibition is an attractive goal. The crystal structure of AfRIO-2 kinase from *Archeoglobus fulgidus* is approximately 86% similar to PFD0975w in amino acid composition and could be used as a reliable template for the homology modeling. The PFD0975w 3D model is structurally similar to other RIO-2 kinases. It contains an N-terminal DNA binding domain coupled with a C-terminal truncated protein kinase domain via a linker region. The protein kinase domain of PFD0975w in shorter and more compact than canonical ePK domains. One of the reasons for selecting PFD0975w as a drug target is because of the unique combination of a protein kinase and a DNA binding domain, which is rare. It could imply that such proteins may have the ability to control gene expression upon auto-phosphorylation or some other kind of activation.

Closer analysis of the 3D model of PFD0975w reveals that it binds ATP molecule in its active site cavity in a similar orientation to AfRIO-2 kinase. The ATP molecule binds in a bent cresant shape in which the adenosine moiety of ATP fits tightly into a deeper pocket and the ɣ-phosphate rests in a smaller pocket located at the other end of the active site. The ATP molecule in both the models appears to be bent around the β and ɣ phosphate bonds as a result of a ridge between the deeper and smaller sub-pockets. This orientation could explain the catalytic mechanism of this kinase and the breakage of the bond between the β and ɣ phosphates during phosphorylation.

An important issue that has to be kept in mind during choosing a drug target is that the target should be structurally different enough from the host molecule so as to achieve a specific inhibition. A thorough comparative analysis of the structural models of PFD0975w and Hu-RIO-2 kinase reveals that the host and parasite kinases are evolutionarily and hence structurally divergent. The major differences between the two structures lies in (i) the volume, shape and composition of the active site pocket, (ii) the length of the unstructured loop and (iii) the surface charge distribution of the two proteins. As a result of the above structural differences, the most energetically favoured orientation of ATP is different for the host and parasite RIO-2 kinases. The active site residues holding the ATP molecule in the pocket are also different for the two enzymes. These basic differences from the host molecule would ensure that identified inhibitors against PFD0975w would be specific with little or no cross-reactivity to the human isoform. In order to confirm whether the protein could really bind ATP in the way predicted by bioinformatics analysis, ATP binding experiments with fluorescent ATP analog (mant-AMPPNP) was conducted. The recombinant PFD0975w expressed in *E. coli* was shown to be in its native form and could bind ATP analog at 50 μM protein concentration. Whether the ATP analog binds only within the putative active site is uncertain.

The DNA binding domain of PFD0975w is also of major interest since the proteins intrinsic affinity for DNA could be exploited to design drug-DNA conjugates which would bind to the protein at both the winged helix and kinase domains, inducing an irreversible structural shift and thereby very specific inhibition. Molecular recognition tool (PatchDock) was used to screen DNA molecules that would bind strongly to the proteins winged helix domain as well as reach down the active site. Stringent analysis of the complexes revealed the proteins preference to bind to AT rich DNA. This finding correlates to the AT richness of the *Plasmodium* genome. Our findings suggest that PFD0975w is a good candidate for anti-malarial drug development.

3.5 References.

- Angermayr, M., A. Roidl and W. Bandlow (2002). "Yeast Rio1p is the founding member of a novel subfamily of protein serine kinases involved in the control of cell cycle progression." Mol Microbiol **44**(2): 309-324.

- Berman, H. M., W. K. Olson, D. L. Beveridge, J. Westbrook, A. Gelbin, T. Demeny, S. H. Hsieh, A. R. Srinivasan and B. Schneider (1992). "The nucleic acid database. A comprehensive relational database of three-dimensional structures of nucleic acids." Biophys J **63**(3): 751-759.

- Campbell, B. E., P. R. Boag, A. Hofmann, C. Cantacessi, C. K. Wang, P. Taylor, M. Hu, Z. U. Sindhu, A. Loukas, P. W. Sternberg and R. B. Gasser (2011). "Atypical (RIO) protein kinases from Haemonchus contortus--promise as new targets for nematocidal drugs." Biotechnol Adv **29**(3): 338-350.

- Cicero, M. P., S. T. Hubl, C. J. Harrison, O. Littlefield, J. A. Hardy and H. C. Nelson (2001). "The wing in yeast heat shock transcription factor (HSF) DNA-binding domain is required for full activity." Nucleic Acids Res **29**(8): 1715-1723.

- Clubb, R. T., M. Mizuuchi, J. R. Huth, J. G. Omichinski, H. Savilahti, K. Mizuuchi, G. M. Clore and A. M. Gronenborn (1996). "The wing of the enhancer-binding domain of Mu phage transposase is flexible and is essential for efficient transposition." Proc Natl Acad Sci U S A **93**(3): 1146-1150.

- Cox, S., E. Radzio-Andzelm and S. S. Taylor (1994). "Domain movements in protein kinases." Curr Opin Struct Biol **4**(6): 893-901.

- Engh, R. A. and D. Bossemeyer (2002). "Structural aspects of protein kinase control-role of conformational flexibility." Pharmacol Ther **93**(2-3): 99-111.

- Gajiwala, K. S. and S. K. Burley (2000). "Winged helix proteins." Curr Opin Struct Biol **10**(1): 110-116.

- Knighton, D. R., J. H. Zheng, L. F. Ten Eyck, N. H. Xuong, S. S. Taylor and J. M. Sowadski (1991). "Structure of a peptide inhibitor bound to the catalytic subunit of cyclic adenosine monophosphate-dependent protein kinase." Science **253**(5018): 414-420.

- Lai, E., K. L. Clark, S. K. Burley and J. E. Darnell, Jr. (1993). "Hepatocyte nuclear factor 3/fork head or "winged helix" proteins: a family of transcription factors of diverse biologic function." Proc Natl Acad Sci U S A **90**(22): 10421-10423.

- LaRonde-LeBlanc, N. and A. Wlodawer (2004). "Crystal structure of A. fulgidus Rio2 defines a new family of serine protein kinases." Structure **12**(9): 1585-1594.

- Littler, D. R., M. Alvarez-Fernandez, A. Stein, R. G. Hibbert, T. Heidebrecht, P. Aloy, R. H. Medema and A. Perrakis (2010). "Structure of the FoxM1 DNA-recognition domain bound to a promoter sequence." Nucleic Acids Res **38**(13): 4527-4538.

- Liu, J., C. L. Smith, D. DeRyckere, K. DeAngelis, G. S. Martin and J. M. Berger (2000). "Structure and function of Cdc6/Cdc18: implications for origin recognition and checkpoint control." Mol Cell **6**(3): 637-648.

- Manning, G., G. D. Plowman, T. Hunter and S. Sudarsanam (2002). "Evolution of protein kinase signaling from yeast to man." Trends Biochem Sci **27**(10): 514-520.

- Park, Y. I., K. H. Do, I. S. Kim and H. H. Park (2012). "Structural and functional studies of casein kinase I-like protein from rice." Plant Cell Physiol **53**(2): 304-311.

- Schneidman-Duhovny, D., Y. Inbar, R. Nussinov and H. J. Wolfson (2005). "PatchDock and SymmDock: servers for rigid and symmetric docking." Nucleic Acids Res **33**(Web Server issue): W363-367.

- Trivedi, V. and S. Nag (2012). "In silico characterization of atypical kinase PFD0975w from Plasmodium kinome: a suitable target for drug discovery." Chem Biol Drug Des **79**(4): 600-609.

- Wah, D. A., J. A. Hirsch, L. F. Dorner, I. Schildkraut and A. K. Aggarwal (1997). "Structure of the multimodular endonuclease FokI bound to DNA." Nature **388**(6637): 97-100.

- Wallace, A. C., R. A. Laskowski and J. M. Thornton (1995). "LIGPLOT: a program to generate schematic diagrams of protein-ligand interactions." Protein Eng **8**(2): 127-134.

- Wilson, K. P., L. M. Shewchuk, R. G. Brennan, A. J. Otsuka and B. W. Matthews (1992). "Escherichia coli biotin holoenzyme synthetase/bio repressor crystal structure delineates the biotin- and DNA-binding domains." Proc Natl Acad Sci U S A **89**(19): 9257-9261.

- Yamada, K., T. Miyata, D. Tsuchiya, T. Oyama, Y. Fujiwara, T. Ohnishi, H. Iwasaki, H. Shinagawa, M. Ariyoshi, K. Mayanagi and K. Morikawa (2002). "Crystal structure of the RuvA-RuvB complex: a structural basis for the Holliday junction migrating motor machinery." Mol Cell **10**(3): 671-681.

- Zheng, J., D. R. Knighton, L. F. ten Eyck, R. Karlsson, N. Xuong, S. S. Taylor and J. M. Sowadski (1993). "Crystal structure of the catalytic subunit of cAMP-dependent protein kinase complexed with MgATP and peptide inhibitor." Biochemistry **32**(9): 2154-2161.

Chapter IV

Antimalarial activity of designed heterocyclic molecules against PFD0975w.

4.1 Introduction

Structural characterization of a drug target is perhaps the first step for a successful structure based drug development process. Structural characterization of the atypical protein kinase PFD0975w (PfRIO-2 kinase) (Trivedi and Nag 2012) indicates an N-terminal DNA binding winged helix domain (1–84), a linker region (85–147) and C-terminal kinase domain (148–275). It has a well-defined ATP binding pocket and is significantly different than the ATP binding pocket of human RIO-2 kinase (Trivedi and Nag 2012). Further, the absence of activation loop and distinguished structural features of PfRIO-2 kinase provides an opportunity to explore it as a new drug target (Trivedi and Nag 2012). Recently, naturally occurring bioactive molecules and selected heterocyclic molecules were screened against PfRIO-2 kinase, which allow us to delineate pharmacological points required for inhibitor development against PfRIO-2 kinase (Nag, Chouhan et al. 2013).

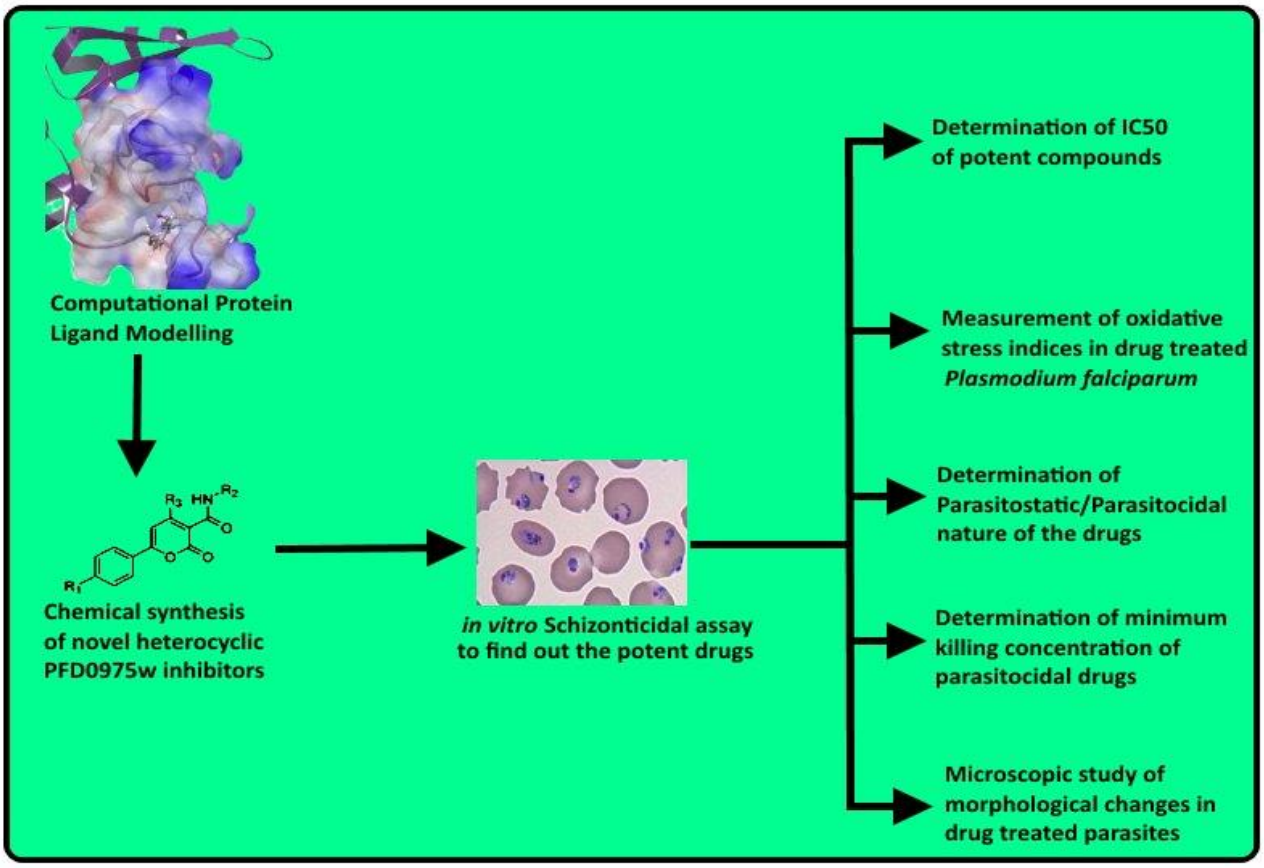

Figure 4.1: Schematic diagram of the work discussed in chapter IV.

Febrifugine (Figure 4.2), a natural product with high anti-malarial activity (Koepfli, Mead et al. 1947) was isolated in 1947 from the roots of a Chinese shrub, *Chang Shan*. The 4-quinazolinone moiety, 1′-amino and C-2′ as well as C-3″O-functionalities are crucial for the anti-malarial activity of febrifugine (Jiang, Zeng et al. 2005). Argentilactone, isolated from the roots and the leaves of *Raimondia cf. monoica* was found to have IC_{50} of 0.1 µg/mL against *Plasmodium falciparum* (Carmona, Saez et al. 2003). It was the first report of heterocyclic moleculesderivative having anti-malarial activity.

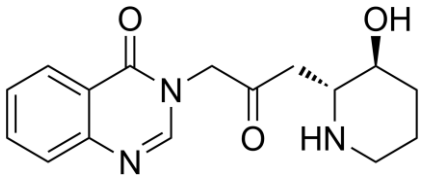

Figure 4.2: Structure of Febrifugine

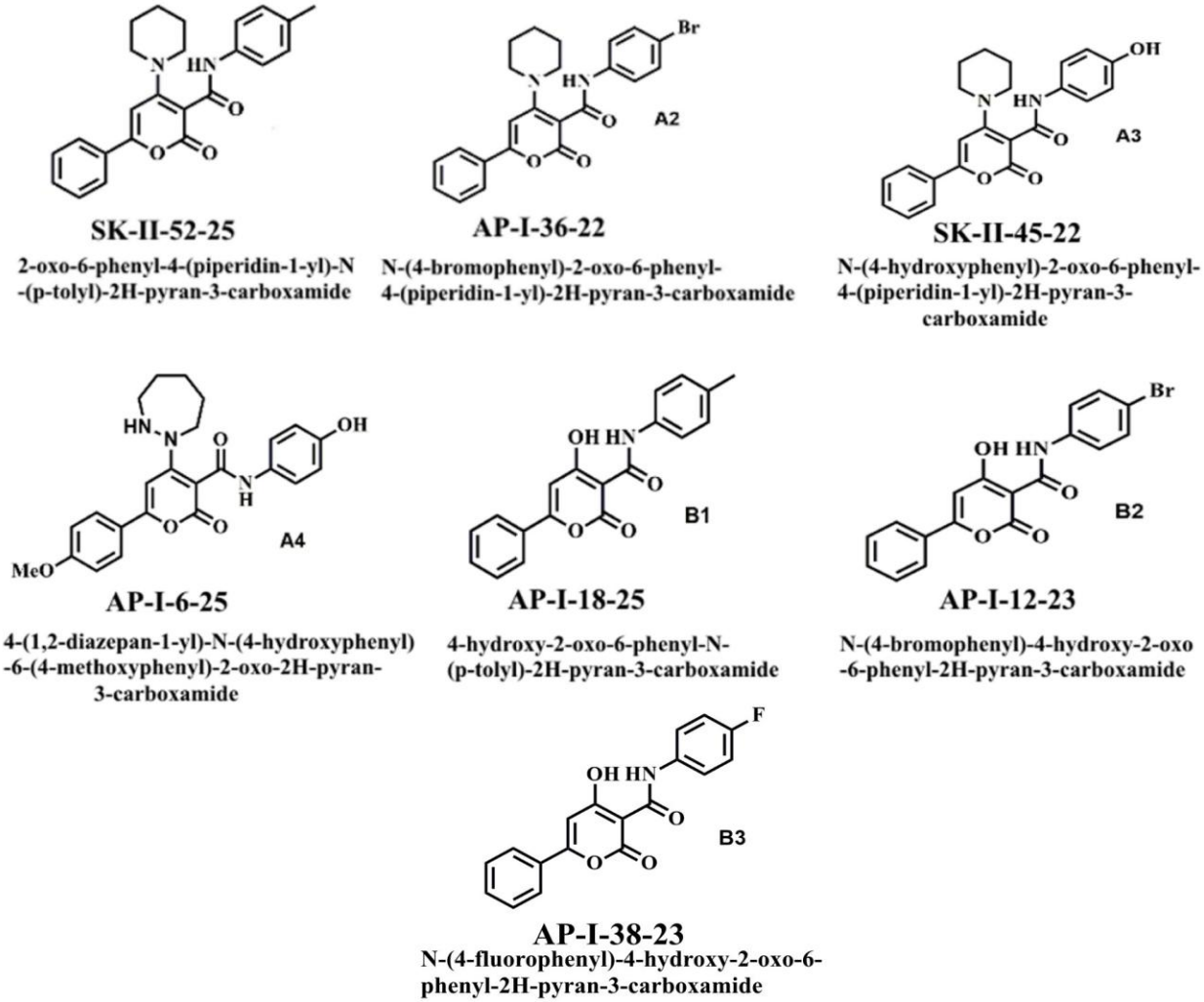

Figure 4.3: Structure and IUPAC nomenclature of synthetic heterocyclic compounds designed against PFD0975w.

However, due to toxicity (Carmona, Saez et al. 2003) and (Chien and Cheng 1970) both these molecules couldn't develop as a clinical drug. Recently, 4(1*H*)-quinolone ester derivatives with two close keto groups have been considered as promising anti-malarials needing further SAR and optimization (Zhang, Clark et al. 2012). In this chapter, we have characterized the antimalarial activity of some novel heterocyclic molecules, synthesized at a collaborating laboratory at BIT Mesra, Ranchi, India (Figure 4.1). The design of these novel inhibitors were such that the basic heterocyclic molecule skeleton as well as the identified pharmacophores were kept preserved, generating a series of analogs which exhibited good antimalarial activity *in vitro* against *Plasmodium falciparum.* Parasite death occurs as a result of inhibition of PFD0975w. Further qualitative and quantitative investigations on cultures treated with IC_{50} values of these inhibitors; reveal the accumulation of ROS within treated cultures. Moreover upon compound treatment, parasites exhibit marked morphological changes.

4.2 Experimental Procedure

4.2.1 Chemical synthesis of molecules: The molecules were synthesized chemically using a ligand based pharmacophoric approach. The molecules were synthesized in a collaborating laboratory in the Department of Applied Chemistry, Birla Institute of Technology, Mesra, Ranchi 835215, India. The synthesized molecules were verified using NMR, IR and UV/Vis spectroscopy.

4.2.2 *In vitro* cultivation of *Plasmodium falciparum* 3D7: *Plasmodium falciparum* 3D7 was cultured *in vitro* using the standard methods. In brief, Parasite culture was maintained in A^+ human erythrocytes in RPMI-1640 media containing glucose, 10% lipid-rich bovine serum albumin (Albumax II) and hypoxanthine. Cells were incubated at 37°C and 5% CO_2. Media changed after every 24 hrs and parasite growth was monitored by Giemsa staining.

4.2.3 *In-vitro* schizonticidal assay: The *in vitro* antimalarial assay was carried out in 96-well microtitre plates. In brief, test compounds were incubated with ring stage synchronized *P. falciparum* (3D7) parasitized cells at a range of drug concentrations from 0 µg/ml (Control) to 50 µg/ml. After 42 hrs. of incubation, blood smears from each well were prepared to record maturation of ring stage parasites into trophozoites and schizonts. MS-Excel Sheet based HN-

NonLin program (available from www.malaria.farch.net) was used to calculate IC_{50} of all the compounds based on their schizont inhibition profile using regression analysis.

4.2.4 Determination of the parasitostatic/parasitocidal nature of heterocyclic compounds: Test compounds were incubated with ring stage synchronized *P. falciparum* (3D7) parasitized cells at a range of drug concentrations from 0 µg/ml (Control) to 50 µg/ml. After 42 hrs of incubation, the compounds were removed and the cultures were washed 3 times with albumax II free RPMI-prepared and number of RBCs containing viable parasite was counted. The active compounds were thus categorized as parasitostatic or parasitocidal depending on the increase in parasitemia or microscopic observation of viable parasites 3 days after drug removal. The minimum concentration of compounds giving no viable parasite was used to calculate minimum killing concentration (MKC) of compounds with parasitocidal activity.

4.2.5 Microscopic imaging of parasite morphology: Giemsa stained thin smears of control as well as drug treated parasitized RBC were visualized under 100X objective in oil emersion and images were captured at using Nikon camera attached to the microscopy system.

4.2.6 Estimation of intra-cellular ROS in compound treated parasites: *Plasmodium falciparum* culture was treated with IC_{50} value of test compound in triplicates and incubated for 48 hrs at 37°C and 5% CO_2. From a 1 µM stock, 10 µL of DCF-DA was added and incubated at above conditions for 1 hr. Parasites were isolated from iRBC using saponin lysis method as follows. Cultures were centrifuged at 3000 RPM for 2 minutes and the media was aspirated. RBC pellet was re-suspended in 1 ml of 0.15% saponin solution and incubated for 5 mins. on ice and vortexed at fixed intervals. Parasites were collected by centrifugation at 6000 RPM for 3 mins at 4°C. Parasite pellet was washed 2-3 times with 1 ml of PBS and wash was discarded by spinning at 6000 RPM for 3 minutes. The weight of parasite pellet for control and treated samples (in mg) were noted down. Parasite pellets were re-dissolved in 600 µL of PBS and sonicated on ice for 1 min (5 sec on and 5 sec off). Samples were transferred in triplicates on a 96 well plate. Fluorescence was measured at excitation wavelength of 502 nm and emission wavelength of 523 nm. Results were expressed as fluorescence intensity per milligram of parasite.

4.2.7 Lipid peroxidation assay: Parasites are isolated from drug treated iRBC as described above. Isolated parasites are re-suspended in 300 µL PBS and sonicated for 1 min in ice bath (5 sec on and 5 sec off) followed by centrifugation at 10,000 RPM for 20 mins. A 200 µL aliquot of supernatant is reserved for protein estimation (described below). Remaining 100 µL supernatant is transferred into fresh centrifuge tubes and 200 µL of ice cold 10% TCA is added to precipitate proteins. Mixtures are incubated for 15 minutes in -20°C. TBA (300 µL) is added to samples and standard, subsequently heated in a dry bath at 95°C for 15 minutes. Samples and standards are cooled to room temperature and 200 µL sample and standards are transferred to a 96 well dish. Absorbance is read using a plate reader (Molecular devices) at 532 nm in triplicates. Absorbance units per mg of parasite material are calculated and are converted into folds.

4.2.8 GSH assay (Ellman's method): Parasites are isolated from drug treated iRBC as described above. Isolated parasites are resuspended in 300 µL Tris-EDTA buffer (See Appendix I) and sonicated in ice for 1 min (5 sec on and 5 sec off). This is followed by centrifugation at 10,000 RPM for 30 mins to get clear lysate. A 200 µL aliquot of supernatant is reserved for protein estimation (described below). Remaining 100 µL supernatant is transferred into fresh centrifuge tubes and 200 µL of ice cold 10% TCA is added to precipitate proteins. Mixtures are incubated for 15 minutes in -20°C followed by spinning at 13,000 RPM for 20 mins to get clear supernatant. On a 96- well dish reactions are set up by adding the following components in each well: 50 µL of sample/standard, 25 µL DTNB (See Appendix) and 100 µL of Tris-Cl pH 8.90. Absorbance is read using a plate reader (Molecular devices) at 412 nm. Absorbance units per mg of parasite material are calculated and are converted into folds.

4.2.9 Protein estimation by Folin-Lowry's method: BSA stock of 100µg/ml is prepared and a standard set of BSA concentrations were prepared by dilution. Aliquots of 200 µL of supernatant/standard is added to 280 µL of Lowry solution and incubated in dark for 20 mins. Freshly prepared Folin's solution (40 µL) is added to each sample/standard (See Appendix) and incubated in the dark for another 30 mins. Aliquots of 200 µL sample/standard are transferred per well into a 96-well dish. Absorbance is read using a plate reader (Molecular devices) at 750 nm. Standard calibration curve is plotted between absorbance and concentration of BSA. From the curve concentrations of unknown samples are calculated.

4.3 Results

4.3.1 Novel heterocyclic molecules exhibit antimalarial activity *in vitro*: The synthetic compounds retained the pharmacophoric points of antimalarial parent compound febrifugine. All of the tested novel heterocyclic molecules which were designed and synthesized at a collaborating laboratory show potent antimalarials activity *in vitro*. All of the compounds were found effective in inhibiting the growth of blood stage malaria parasites. Heterocyclic molecules AP-I-36-22, SK-II-52-25 and SK-II-45-22 was found to be the most effective compounds with inhibitory IC_{50} values of 0. 195µg/ml, 0.200 µg/ml and 0.238 µg/ml respectively (Table 4.1).

Table 4.1: Schizonticidal activity and correlation factors for novel heterocyclic compounds.

Heterocyclic compound	Polynome	IC_{50}	IC_{90}	IC_{95}	IC_{99}	R^2
AP-I-31-21	3	0.381	2.328	2.785	3.046	0.9891
AP-I-18-25	3	0.457	9.643	11.007	11.944	0.9225
SK-II-53-24	3	0.400	1.541	5.471	6.009	0.9785
SK-II-52-25	3	0.200	0.455	0.523	0.607	0.7990
SK-II-45-22	3	0.238	0.651	2.907	3.057	0.8546
SK-II-49-25	3	0.326	1.202	11.296	11.920	0.8560
AP-I-6-25	3	0.683	5.731	5.990	6.189	0.9702
AP-I-12-23	3	0.293	5.240	5.717	6.044	0.8135
AP-I-36-22	3	0.195	0.406	0.456	0.508	0.7705
AP-I-38-23	3	0.263	0.990	5.655	6.013	0.7578
AP-I-14-24	3	0.287	0.777	1.158	3.042	0.9675

Compounds were dissolved in DMSO to obtain primary stock (5 mg/ml). Primary stock was diluted in complete media to obtained secondary stock (100 µg/ml). Synchronized ring stage parasites were incubated with compounds at a concentration range of 0 (control) to 50 µg/ml and schizont inhibition was monitored. IC values were calculated using regression analysis.

Anti-malarial activities of these heterocyclic molecules suggest the inhibition of PFD0975w, due to disruption of the protein's ability to bind its natural substrate ATP. Previously shown shift in localization of PFD0975w due to CQ treatment, as well as parasite clearance on treatment with these novel PFD0975w directed molecules suggests the importance of PFD097w in parasite life-cycle and validates PFD0975w as a good drug target. The pharmacophoric attachment points of febrifugine skeleton had been kept constant during our design process of these novel ligands. This is responsible for the potent antimalarial activity of most of these molecules. Most of the molecules proved inhibitory to parasite growth, causing developmental arrest and delay in schizont maturation. It also needs to be mentioned here that compound treated schizonts bear lesser number of daughter merozoites than untreated schizonts.

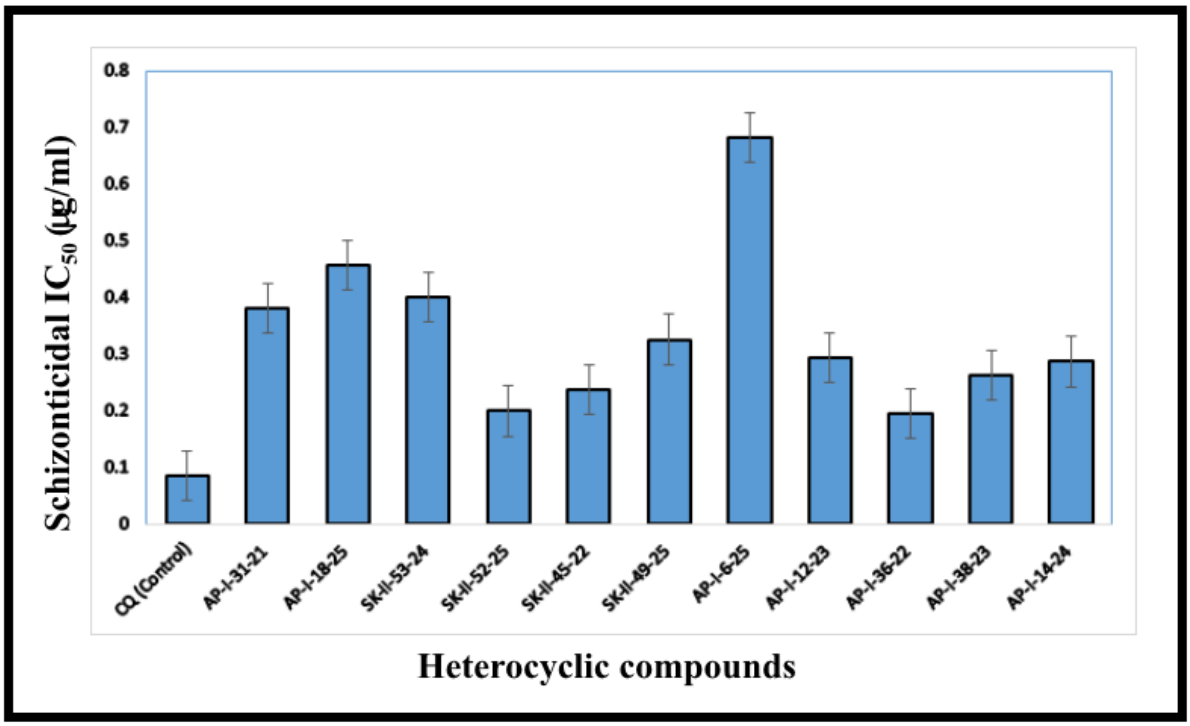

Figure 4.4: Comparison of the IC_{50}s of tested heterocyclic molecules.

4.3.2 Most of the studied heterocyclic molecules were parasitocidal in nature: Inhibition of atypical protein kinase PFD0975w by these novel heterocyclic molecules results in death of parasites *in vitro*. Out of the above compounds; only one compound appeared to be parasitostatic in nature; which means parasites could revive after the drug was removed from the system in standard assay conditions described above. Parasites treated with a minimum killing

concentration (MKC) of the parasitocidal compounds failed to revive even after 3 days of drug removal, implying a strong binding at the PFD0975w active site pocket.

4.3.3 Treatment with novel heterocyclic molecules results in development of ROS within parasites: Oxidative stress is known to occur when there is an imbalance between the production of reactive oxygen species and the cell's ability to detoxify them or to repair the damage caused as a result of the development of oxidative stress. Anti-parasitic drugs often work by disturbing the physiological redox homeostasis of cells, ultimately resulting in toxic modifications of the cell's protein, Lipid and DNA content, gradually killing the cells.

Table 4.2: Nature of inhibition and MKC values (µg/ml) of heterocyclic compounds

Heterocyclic Compound	Nature of inhibition	MKC µg/ml (µM ± SE)
SK-II-52-25	Parasitocidal	1.00 ± 0.002
AP-I-36-22	Parasitocidal	0.21 ± 0.026
SK-II-45-22	Parasitocidal	1.99 ± 0.30
AP-I-6-25	Parasitostatic	NA
AP-I-18-25	Parasitocidal	38.9 ± 3.82
AP-I-12-23	Parasitocidal	3.90 ± 0.59
AP-I-38-23	Parasitocidal	2.39 ± 0.33

Cultures were washed in media, post 36 hr. compound treatment and re-incubated for 72 hrs. in compound-free media. Smears were observed under light microscope to count viable parasites. Compounds were thus classified as parasitocidal/parasitostatic. MKC is defined as the compound concentration in which all parasites are killed during a 36 hr. treatment.

Treatment of *Plasmodium falciparum* with these novel heterocyclic molecules generates peroxides and free radicals, depletes the cellular pool of antioxidants and hinders the parasites redox signaling. Experiments to study the effect of these novel drugs on cellular ROS has been designed such that the parasites treated with a sub-lethal dose of these heterocyclic molecules, accumulate intracellular ROS but do not die, releasing the ROS into the medium. Thus, the effect of oxidative stress and the cell's ability to detoxify it depends upon the concentration of drug used for the treatment.

The measurements of intra-cellular ROS within the parasites upon treatment with these novel heterocyclic molecules were studied using multiple assays (Table 4.3). The DCF-DA assay

employs a cell-permeable fluorogenic dye 2', 7'-Dichlorodihydrofluorescin diacetate (DCFH-DA). DCFH-DA enters treated or non-treated cells where cellular esterases deacetylate it to 2', 7'-Dichlorodihydrofluorescein. This Dichlorodihydrofluorescein is quickly oxidized to a highly fluorescent molecule 2', 7'-Dichlorodihydrofluorescein by cellular ROS. The intensity of fluorescence is proportional to the level of intracellular ROS.

Table 4.3: Measurement of intra-cellular oxidative stress in parasites treated with novel heterocyclic molecules

Heterocyclic Compounds	Change in ROS level (fold ± SD)	Change in lipid peroxidation (fold ± SD)
Untreated	1	1
AP-I-31-21	1.66 ± 0.14	11.03 ± 0.45
AP-I-34-22	1.87 ± 0.21	4.49 ± 0.26
AP-I-36-22	1.20 ± 0.18	9.03 ± 0.37
AP-III-6-25	1.99 ± 0.20	4.88 ± 0.66

DCF-DA was used to monitor ROS generation in treated and untreated parasites. T-bar's assay was employed to estimate the cellular concentration of lipid peroxide, malondialdehyde. All results are expressed as fold increase in ROS or fold increase in lipid peroxidation in treated parasites with respect to untreated.

Lipid peroxidation is a manifestation of the oxidative damage of cellular lipids. The process of treating parasite with drugs generates free radicals which steal electrons from cellular lipids in resulting in cell damage. This is a chain reaction mostly affecting polyunsaturated fatty acids. The generation of oxidative stress in parasites treated with these heterocyclic molecules was cross verified with the standard lipid peroxidation assay (Table 4.3); a well-established protocol to measure oxidative stress in cells. Upon drug treatment, polyunsaturated fatty acid peroxides generate malondialdehyde (MDA) and 4-hydroxyalkenals (HAE) and the quantity of MDA per unit weight of parasites is an indicator of lipid peroxidation.

4.3.4 Parasites treated with heterocyclic molecules exhibit marked morphological distortions: Giemsa stained thin blood smears of treated vs. untreated iRBC shows a huge difference in cellular morphology. The overall general appearance of compound treated parasites reflects the cellular stress due to the influence of PFD0975w specific inhibitors. Visual differences exist between healthy parasites and parasites treated with top 6 heterocyclic PFD0975w interactors, at all stages of the parasites asexual development within human RBCs (Figure 4.5).

The ring form of the parasite derives its name from its ring like appearance under light microscope but we can see that compound treated rings show severe deviation from the native ring like shape. Many of the heterocyclic compounds delayed the development of ring stage parasites. Treated rings are smaller in size, with little or no cytoplasm with visible signs of cell shrinkage.

The morphological distortions seen in compound treated trophozoite varies with the potency of the compound being tested. Trophozoites treated with more potent heterocyclic compounds like AP-I-34-22 and AP-I-36-22 clearly demonstrate developmental arrest at trophozoite stage. The cell volumes of treated trophozoites were lesser than untreated controls with clear indications of cell stress, shrinkage and dehydration. Such morphological distortions imply disruption of key cellular processes operated by the enzymatic activity of PFD0975w. Trophozoites treated with other lesser potent compounds might not necessarily show developmental arrest or cell shrinkage but fragmentation of cytoplasm and dehydration are common to all drug treated trophozoites.

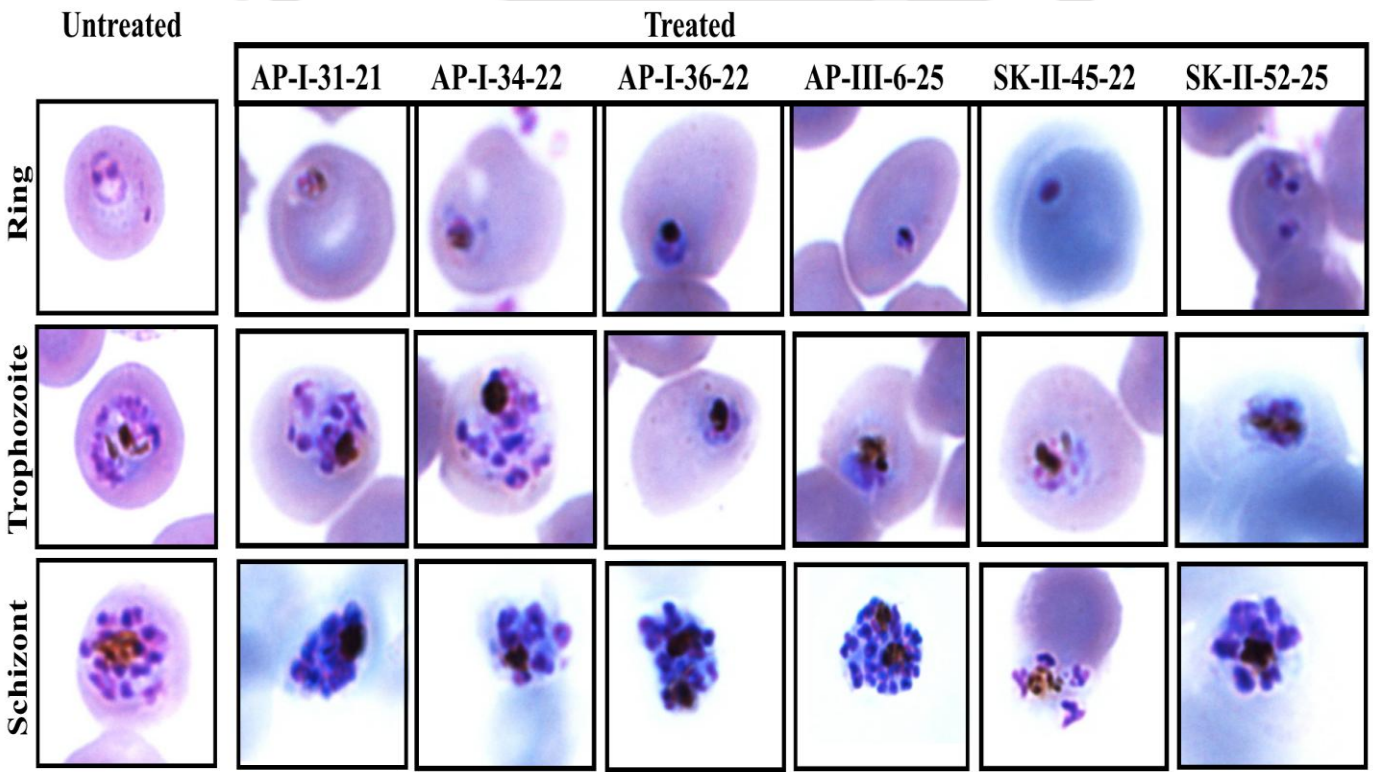

Figure 4.5: Differences in morphology between untreated and heterocyclic compound treated *Plasmodium falciparum*

Schizonts treated with these novel heterocyclic compounds were often smaller in size and contained lesser number of daughter merozoites than their untreated counterparts. Many of the compounds classified under parasitocidal rendered schizonts nonfunctional such that they could not divide into daughter merozoites or infect new RBCs. Above microscopic data supplemented with biochemical and drug screen analyses clearly demonstrate the importance of PFD0975w in the life cycle of the malaria parasite and that the inhibition of such a crucial enzyme results in cell stress and ultimately death.

4.4 Discussion

Cells treated with drugs try to detoxify themselves by metabolizing the drugs. Such metabolism of a drug may produce reactive intermediates which can reduce cellular molecular oxygen into ROS. The work in the current chapter highlights the effects of 11 heterocyclic compounds, which have been designed to specifically inhibit the atypical protein kinase PFD0975w in *Plasmodium falciparum*, whose exact function in the parasite has not been studied previously. These novel heterocyclic molecules borrow the basic skeleton from active antimalarials such as Febrifugine and argentilactone, with known pharmacophoric points unaltered. The characterization of these novel compounds reveals that all of the compounds inhibit parasite growth *in vitro* and most of them are potent enough to be parasitocidal in nature. Since the effect of these inhibitors on the phosphorylation activity of recombinant PfRIO-2 kinase could not be studied, it is possible that these heterocyclic molecules can target other pathways in *Plasmodium falciparum* as well. Since the effect of these inhibitors on the phosphorylation activity of PfRIO-2 kinase could not be studied, it is possible that these heterocyclic molecules can target other pathways in *Plasmodium falciparum* as well, to elicit antimalarial effect.

Thorough study addressing the mechanism of action of these compounds and their efficacy to kill the parasite has been found to be due to the disruption of the redox metabolism of the parasite. Reactive oxygen species are natural byproducts of metabolism and play roles in cell signaling and maintenance of homeostasis. These reactive species include oxygen radicals and reactive non-radicals. Any cell has hardwired mechanisms that modulate the levels of cellular ROS, because an increase in ROS damages key cellular components including DNA, lipid and

proteins. When the cellular antioxidant pool exhausts, oxidative stress results. All cells possess defense mechanisms that scavenge free radicals to prevent intracellular damage and nullify the effects of ROS. These include low molecular weight antioxidants (vitamin E, ascorbic acid and most importantly glutathione) and antioxidant enzymes (such as superoxide dismutase, thioredoxins, glutathione peroxidase, and catalase). As a consequence of their activities, the physiological ROS levels are usually low. However, when cells are treated with drugs such as antimalarials, there is an elevated level of ROS in the system and the defense systems cannot serve to keep the cell alive.

Protein kinases are key players of cellular signaling events and control critical parameters of life such as growth, proliferation, and survival in response external stress such as drugs or inhibitors. It is now known that several kinases are activated upon ROS damage and activation of key kinases are critical in transducing signals in response to ROS. Some of the known key kinases which exert biological effects of ROS are the mitogen-activated protein kinases, p38 and c-Jun N-terminal kinases, apoptosis signal-regulating kinase 1 as well as the phosphatidylinositol 3-kinase and protein kinase C. PFD0975w is hypothesized to be a key kinase regulating the cellular homeostasis in *Plasmodium falciparum* and inhibition of this kinase has shown to have detrimental effects of parasite cells and their ability to fight cellular ROS. Some of the novel compounds characterized above have the potential to be excellent new age antimalarials, if these leads are further optimized and their pharmacokinetics is studied.

4.5 Appendix I

4.5.1 DCF-DA Stock (1mM): 2.4 mg of DCF-DA (Sigma) is dissolved in 5 ml DMSO.

4.5.2 Reagents for lipid peroxidation assay:

4.5.2.*1 Thiobarbituric Acid (TBA):* 67mg of thiobarbituric acid is dissolved in 1mL of DMSO and the volume is made up to 10 ml by adding double distilled water.
4.5.2.*2 10% Trichloroacetic Acid (w/v):* 100 µL of 100% TCA is added to 900 µL double distilled water
4.5.2.*3 1,1,3,3-tetramethoxypropane:* 4.167 µL of 1,1,3,3-tetramethoxypropane is added to 1mL ethanol and the volume is made up to 50 mL using double distilled water.

4.5.3 Reagents for Protein estimation:

4.5.3.1 Solution A (alkaline solution): 0.28 g NaOH and 1.5 g Na_2CO_3 is dissolved in 50 mL ddH_2O
4.5.3.2 Solution B: 0.14 g $CuSO_4.5(H_2O)$ is dissolved in 10 mL of ddH_2O.
4.5.3.3 Solution C: 0.28 g Potassium Sodium Tartrate is dissolved in 10 mL of ddH_2O
4.5.3.4 Lowry Solution (4 ml): 1.96 mL Sol A + 19.6 µL Sol B + 19.6 µL Sol C. This solution is prepared fresh
4.5.3.5 Folin Reagent (1 mL): 454 µL Folin's Reagent is added to 273 µL of ddH_2O.
4.5.3.6 BSA Stock (100 µg/ml): 4 mg BSA is dissolved in 40 ml PBS

4.6 References

- Carmona, D., J. Saez, H. Granados, E. Perez, S. Blair, A. Angulo and B. Figadere (2003). "Antiprotozoal 6-substituted-5,6-dihydro-alpha-pyrones from Raimondia cf. monoica." Nat Prod Res **17**(4): 275-280.

- Chien, P. L. and C. C. Cheng (1970). "Structural modification of febrifugine. Some methylenedioxy analogs." J Med Chem **13**(5): 867-870.

- Jiang, S., Q. Zeng, M. Gettayacamin, A. Tungtaeng, S. Wannaying, A. Lim, P. Hansukjariya, C. O. Okunji, S. Zhu and D. Fang (2005). "Antimalarial activities and therapeutic properties of febrifugine analogs." Antimicrob Agents Chemother **49**(3): 1169-1176.

- Koepfli, J. B., J. F. Mead and J. A. Brockman, Jr. (1947). "An alkaloid with high antimalarial activity from Dichroa febrifuga." J Am Chem Soc **69**(7): 1837.

- Trivedi, V. and S. Nag (2012). "In silico characterization of atypical kinase PFD0975w from Plasmodium kinome: a suitable target for drug discovery." Chem Biol Drug Des **79**(4): 600-609.

- Zhang, Y., J. A. Clark, M. C. Connelly, F. Zhu, J. Min, W. A. Guiguemde, A. Pradhan, L. Iyer, A. Furimsky, J. Gow, T. Parman, F. El Mazouni, M. A. Phillips, D. E. Kyle, J. Mirsalis and R. K. Guy (2012). "Lead optimization of 3-carboxyl-4(1H)-quinolones to deliver orally bioavailable antimalarials." J Med Chem **55**(9): 4205-4219.

Chapter V

Activity profiling of candidate drugs against PFD0975w.

5.1 Introduction.

Protein kinases are key molecules which regulate a wide array of cellular functions such as growth, differentiation, and response to internal and external stimuli. They act as checkpoints, regulating the activity of themselves or their downstream molecules in a signaling cascade. Disturbances in protein phosphorylation, plays a pivotal role in many human disease conditions like cancer and neurodegenerative diseases (Cohen 2002). As more and more protein kinases were targeted, it became evident that their inhibition could revert disease conditions. The search for kinase inhibitors gave way to the commercialization of Gleevec in 2002, as the first kinase inhibitor drug approved by the FDA (Cohen 2002). This success has resulted in a huge number of kinase inhibitors being identified, synthesized and tested in clinical trials for a wide array of disease conditions (Dancey and Sausville 2003, Meijer and Raymond 2003). Many more such developments are expected in coming years. Since parasitic kinases have displayed significant structural and functional differences from vertebrate kinases (Kappes, Doerig et al. 1999, Doerig, Meijer et al. 2002, Doerig 2004), specific inhibition of parasite kinases leaving the host molecules intact, is possible. Hence the inhibition of specific kinases has proved crucial in the development of drugs against a myriad of disease conditions. The malaria parasite has evolved to camouflage from the host immune system in an elegant way. Chemotherapeutic anti-malarial interventions thus aim to selectively target the inhibition of key kinases which are crucial for the parasite's life-cycle.

PFD0975w is a putative ser/thr kinase in the *Plasmodium* genome. Our previous findings (refer chapter II) indicate that this kinase might be an essential gene in *Plasmodium falciparum*, playing a key role in the parasite's ability to deal with stress such as starvation and anti-malarial drug pressure. We hypothesized that the inhibition of this kinase would result in parasite death *in vitro.* Previous work on the modeling of PFD0975w 3D structure, design and synthesis of novel α-pyrone analogs targeting PFD0975w has resulted in a set of molecules with good anti-malarial activity. With this perspective in mind, we wanted to explore the possibility of designing more novel PFD0975w inhibitors, with improved efficiency.

This chapter summarizes the work done to validate PFD0975w as a drug target (Figure 5.1). This includes the scanning of public databases such as ZINC (Irwin and Shoichet 2005), PubChem and ChemBank (Seiler, George et al. 2008) databases to identify novel molecules that bind

within the PFD0975wactive site with a specificity greater than that of its natural substrate ATP. Most of the top hits were structurally similar to ATP and possessed drug-like properties. The structures of the top hits were screened across the set of approved drugs in DrugBank (Law, Knox et al. 2014) to identify drugs which were structurally similar to the top hits and could bind into the proteins active site as well. The most obvious reasons to select the approved drug space for our inhibitor search is that (i) the molecules are already known to be safe in humans and (ii) ease of availability from local markets. The identified drugs were procured from local market and stocks were made in DMSO. These drugs were screened against *Plasmodium falciparum* 3D7 culture to test the efficacy of the compounds on parasite's physiology. Some of the drugs were also shown to bind into the active site pocket of the purified recombinant enzyme, competing with the binding of fluorescent ATP analog. The efficacy of some of these drugs as good anti-malarial candidates were further verified by biochemical assays which aim to quantify the amount of ROS generated within parasites treated with IC_{50} concentration of the active drugs. Efforts were also made to study the localization of PFD0975w in drug treated parasites. Our results indicate Tenofovir, Clindamycin and Methotrexate as good anti-malarial candidates which can disrupt the ATP binding in PFD0975w.

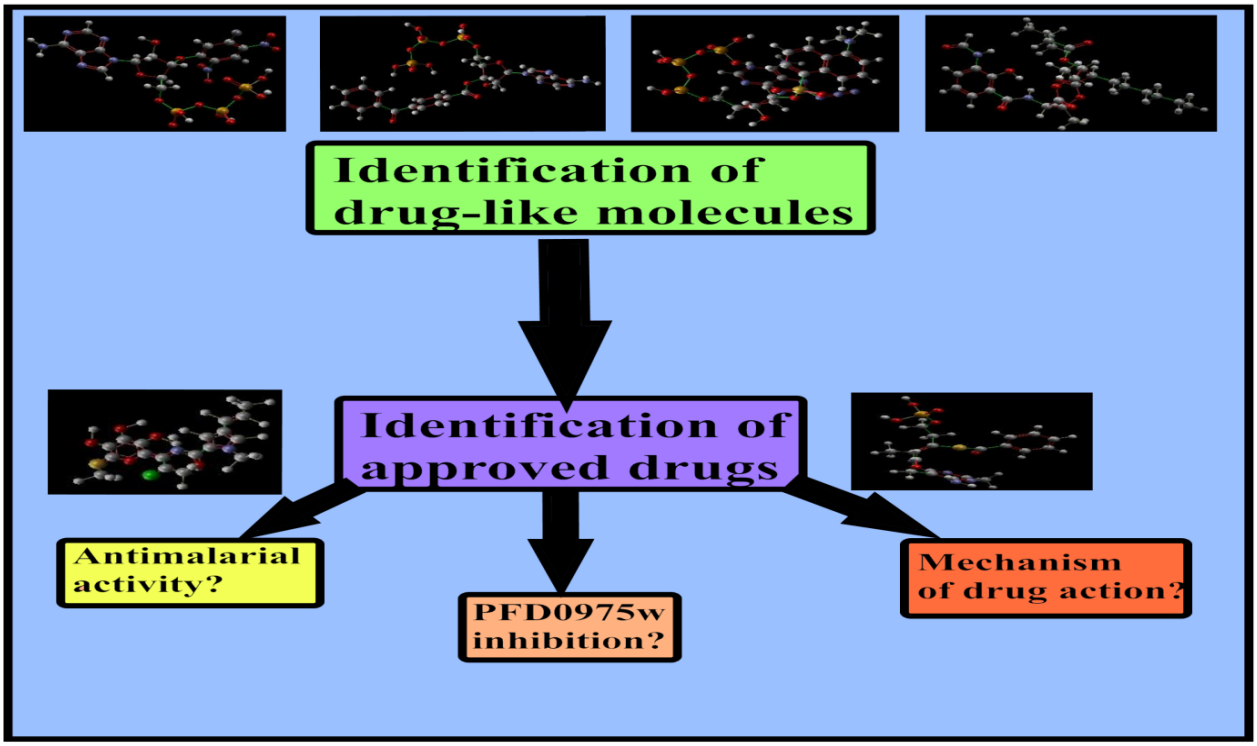

Figure 5.1: Schematic representation of the work discussed in chapter V.

5.2 Experimental procedures.

5.2.2 Heterocyclic databases and collection of compounds: Heterocyclic compounds are collected from ZINC database (http://zinc.docking.org), PubChem (http://pubchem.ncbi.nlm.nih.gov) and ChemBank database (http://chembank.broadinstitute.org). To retrieve the compounds from zinc database (Irwin and Shoichet 2005), adenine triphosphate (ATP) was drawn with the help of chemical editor and converted into alphanumeric code, smiles. It serves as a text to search 70 % similar drug-like molecules in the database and structure file of the corresponding molecules are downloaded in SDF format. The similar searching strategy was used to retrieve the molecules from PubChem (Kaiser 2005) and ChemBank database (Seiler, George et al. 2008). From ZINC database 1701 ATP analogs are collected. From PubChem database 692 analogs are collected and from ChemBank 80 analogs are collected, making a total of 2473 molecules.

5.2.3 Virtual screening of compounds: Docking and virtual screening experiments were performed using MolGro Virtual Docker version 4.0.2. The pdb file of our developed PFD0975wmodel was imported in MVD interface. The ligands / heterocyclic molecules/ drugs to be screened are imported into the MVD console as ligands. All imported files (protein and ligands) are checked for bond length and bond angle errors and corrected as necessary. Automatic cavity detection algorithm was used to detect all possible cavities on the surface of the PFD0975wmodel. From the available cavities, the active site to dock the ligands was selected and a grid of 13$Å^3$ was built around the active site. The number of times one ligand is docked within the cavity is limited to 10 runs and only poses which fits perfectly into the active site were considered for evaluation. Energy minimization of each protein-ligand complex was performed automatically by MVD after the lowest energy pose had been found for that ligand. After the end of the docking run, the results or poses of protein-ligand complexes are arranged on the basis of increasing MolDock score. The best molecule is the one which gives the lowest negative binding score (MolDock Score) within PFD0975w active site pocket. The top poses are saved as individual pdb file containing a snapshot of the protein-ligand complex. The top poses were analyzed in MVD to study the interaction of the top hit inhibitors with the residues of the active site of PFD0975w model.

5.2.4 *In silico* substrate competition assay: Substrate competition assay was performed to study the differences in the mode of binding of ATP and analogs within the active site pocket and to find out whether an inhibitor, specific towards an active form of the PFD0975w kinase, might be sensitive to the presence of substrate (ATP) within the binding pocket.

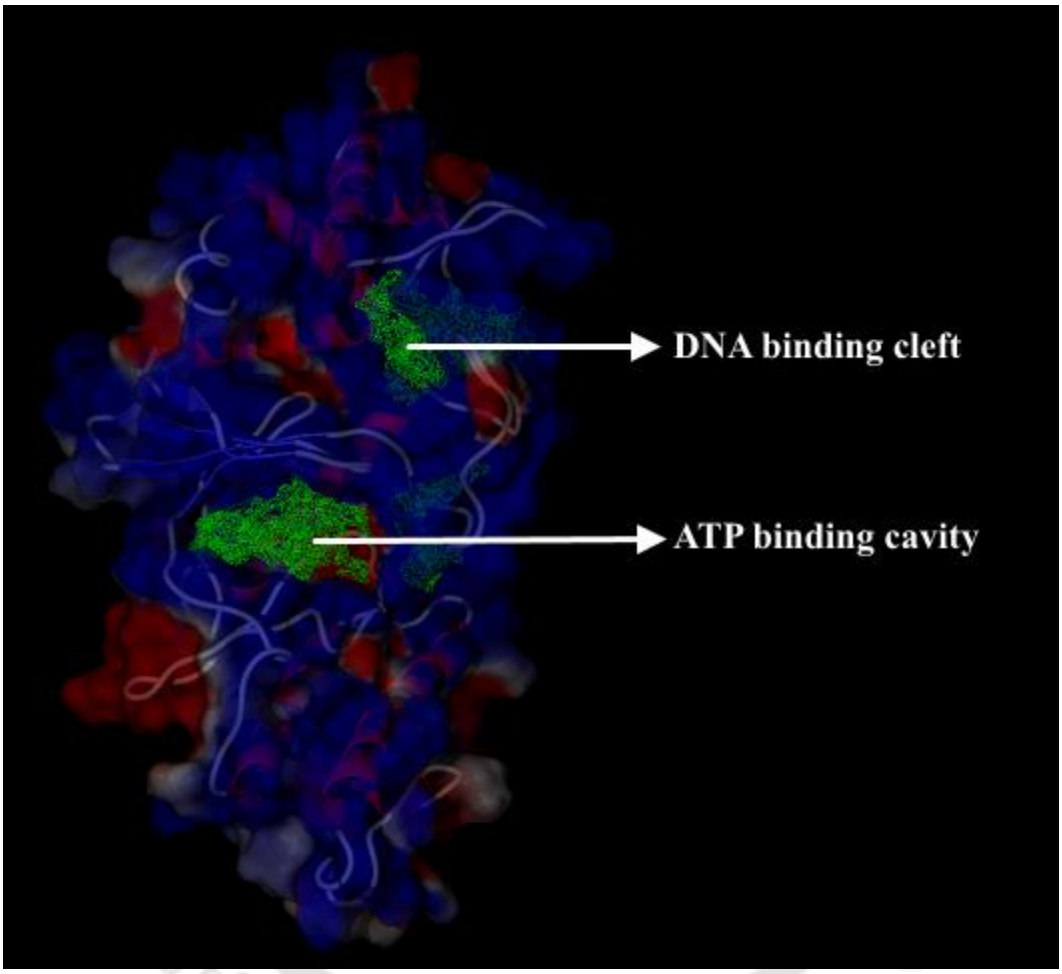

Figure 5.2: The major cavities in PFD0975w 3D model corresponding to the binding of protein substrate, ATP and DNA, as per comparison with known kinase crystal structures.

In substrate competition experiment, PFD0975w-ATP kinase was used as target enzyme instead of PFD0975w native structure. The top hits were allowed to dock at any of the above cavities (Figure 5.2). Docking protocol and parameters remained constant between docking experiments of inhibitors with PFD0975w and PFD0975w-ATP.

5.2.5 Interaction analysis of top hits: The lowest energy poses of top hits from all the databases were loaded on MolGro virtual docker 4.0.2. Electrostatic, hydrophobic, and hydrogen bond

interaction energies were calculated within the active site pocket using respective modules. The interacting residues were labeled using labels option. The 3D models of the ligand bound within the proteins pocket were exported as image files.

5.2.6 Analysis of Drug-likeness: The ADMET properties of compounds were predicted using QikProp utility of Schrodinger's suite 2011 (Schrodinger 2011). QikProp predicts the physicochemical descriptors and pharmaceutically relevant properties which are known to influence absorption, metabolism, and bioavailability. Property or descriptor values that fall outside the 95 % range of similar values for known drugs are indicated with star mark.

5.2.7 Structure based profiling of approved drugs: The structure of the top 5 hits obtained from Zinc, PubChem and ChemBank databases were drawn in the advanced query page of DrugBank website and only FDA approved drugs which are sharing structural similarity (70% or more) with any of the top hits were selected. These newly identified drugs were docked within the active site of PFD0975wfollowing a similar protocol as described above.

5.2.8 Procurement of drugs and preparation of primary and secondary stocks: The final list of 20 drugs was searched in local medicine stores and 7 out of 20 drugs, which were available in Indian markets, were bought. Drugs which came as tablets were crushed and dissolved in 5 ml DMSO. Drugs which came as capsules were taken out of the coating as dissolved in 5 ml DMSO. The solutions were sonicated in ice for 10 minutes (5 sec on and 5 sec off). 1 ml of the solution was taken in fresh micro-centrifuge tubes and spun at 14,000 RPM for 20 minutes to get clear supernatant. Supernatant from primary stock was added to complete RPMI-1640 media to get secondary stocks (100 µg/ml).

5.2.9 *In vitro* cultivation of *Plasmodium falciparum* 3D7: *Plasmodium falciparum* 3D7 was cultured *in vitro* using the standard methods previously described. In brief, Parasite culture was maintained in A^+ human erythrocytes in RPMI-1640 media containing glucose, 10% lipid-rich bovine serum albumin (Albumax II) and hypoxanthine. Cells were incubated at 37°C and 5% CO_2. Media changed after every 24 hrs and parasite growth was monitored by Giemsa staining.

5.2.10 *In-vitro* schizonticidal assay: The *in vitro* antimalarial assay was carried out in 96-well plates as described previously. In brief, test compounds were incubated with ring stage synchronized *P. falciparum* (3D7) parasitized cells at a range of drug concentrations from 0 µg/ml (Control) to 50 µg/ml. After 36 hrs of incubation, blood smears from each well were prepared to record maturation of ring stage parasites into trophozoites and schizonts. MS-Excel Sheet based HN-NonLin program (available from www.malaria.farch.net) was used to calculate IC_{50} of all the compounds based on their schizont inhibition profile using regression analysis.

5.2.11 Determination of the parasitostatic/parasitocidal nature of drugs: Test compounds were incubated with ring stage synchronized *P. falciparum* (3D7) parasitized cells at a range of drug concentrations from 0 µg/ml (Control) to 50 µg/ml. After 36 hrs of incubation, the compounds were removed and the cultures were washed 3 times with albumax-II free RPMI-prepared and number of RBCs containing viable parasite was counted. The active compounds were thus categorized as parasitostatic or parasitocidal depending on the increase in parasitemia or microscopic observation of viable parasites 3 days after drug removal. The minimum concentration of compounds giving no viable parasite was used to calculate minimum killing concentration (MKC) of compounds with parasitocidal activity.

5.2.12 Microscopic imaging of parasite morphology: Giemsa stained thin smears of control as well as drug treated parasitized RBC were visualized under 100X objective in oil emersion and images were captured at using Nikon camera attached to the microscopy system.

5.2.13 Estimation of intra-cellular ROS in drug treated parasites: *Plasmodium falciparum* culture was treated with IC_{50} value of test compound in triplicates and incubated for 48 hrs at 37°C and 5% CO_2. From a 1 µM stock, 10 µL of DCF-DA was added and incubated at above conditions for 1 hr. Parasites were isolated from iRBC using saponin lysis method as follows. Cultures were centrifuged at 3000 RPM for 2 minutes and the media was aspirated. RBC pellet was re-suspended in 1 ml of 0.15% saponin solution and incubated for 5 mins on ice and vortexed at intervals. Parasites were collected by centrifugation at 6000 RPM for 3 mins at 4°C. Parasite pellet was washed 2-3 times with 1 ml of PBS and wash was discarded by spinning at 6000 RPM for 3 minutes. The weight of parasite pellet for control and treated samples (in mg) were noted down. Parasite pellets were re-dissolved in 600 µL of PBS and sonicated on ice for 1

min (5 sec on and 5 sec off). Samples were transferred in triplicates on a 96 well plate. Fluorescence was measured at excitation wavelength of 502 nm and emission wavelength of 523 nm. Results were expressed as fluorescence intensity per milligram of parasite.

5.2.14 Lipid peroxidation assay: Parasites are isolated from drug treated iRBC as described above. Isolated parasites are re-suspended in 300 µL PBS and sonicated for 1 min in ice bath (5 sec on and 5 sec off) followed by centrifugation at 10,000 RPM for 20 mins. A 200 µL aliquot of supernatant is reserved for protein estimation (described below). Remaining 100 µL supernatant is transferred into fresh centrifuge tubes and 200 µL of ice cold 10% TCA is added to precipitate proteins. Mixtures are incubated for 15 minutes in -20°C. TBA (300 µL) is added to samples and standard, which are subsequently heated in a dry bath at 95°C for 15 minutes. Samples and standards are cooled to room temperature and 200 µL sample and standards are transferred to a 96 well dish. Absorbance is read using a plate reader (Molecular devices) at 532 nm in triplicates. Absorbance units per mg of parasite material are calculated and are converted into folds.

5.2.15 Immunolocalization of PFD0975w in drug treated parasites: *Plasmodium falciparum* 3D7 cultures at high parasitemia (~8%) were incubated at IC50 drug concentration in complete RPMI-1640 media for 12 hrs. This culture was used to prepare thin blood smears on glass cover slips. Smears were air dried and fixed in a 1:1 mixture of methanol and acetone at -20°C. Smears were permeabilized with 0.05% Triton-X 100 in PBS for 10 minutes at 37°C and washed three times with PBS. Smears were blocked with 5% BSA for 30 minutes at room temperature with intermittent mixing on a gel rocker. Smears were washed three times with PBS and incubated with anti-PFD0975w antibody (1:500) at 4°C overnight. Smears were washed three times with PBS and incubated with FITC conjugated anti-rabbit IgG (1: 2000) for 4 hrs at 4°C with intermittent mixing on a gel rocker. Finally, smears were washed three times with PBS and mounted on clean glass slides with mounting media containing DAPI. Cells were observed under 100X objective (oil emersion) attached to confocal microscope (Biorad) and images were captured from 5-10 random fields.

5.3 Results.

5.3.1 Identification of novel hits from ZINC and PubChem databases: The main criteria we had in mind while selecting molecules for virtual screening is that the molecules should bear at least 70% structural similarity to the protein's natural substrate ATP. Out of 2473 ATP like compounds, the virtual screening protocol identified 10 hits with a MolDock score (binding energy) greater than that of ATP (~ -195 AU). These hits include ZINC03871614, ZINC85484746, ZINC13434883, CID 129401, CID 195619, CID 49859690, CID 15938961,CID 115205, CID 24916929 (PC),CID 24917010 (PC) (Table 5.1).

Table 5.1: Top hit inhibitors from Zinc and PubChem databases

Molecule ID	Compound Name	MolDock Score (AU)	Re-Rank Score (AU)	Energy from Hydrogen Bonds (AU)	Chemical Structure
ZINC03871614	9-[5-O-(hydroxyl-phosphoryl)pentofuranosyl]-9H-purin-6-amine	**-202.199**	-80.93	-14.33	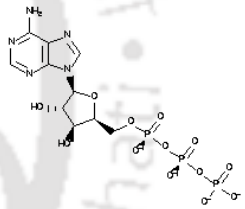
ZINC85484746	Sodium ((2R,3S,4R,5R)-5-(6-amino-9H-purin-9-yl)-3,4-dihydroxytetrahydrofuran-2-yl)methyl dihydrogentriphosphate	**-197.618**	-98.09	-14.48	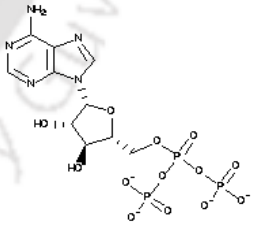
ZINC13434883	2'-Deoxyadenosine 5'-Triphosphate	-196.41	-134.56	-11.02	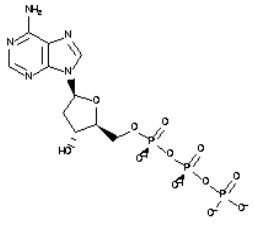

ZINC3725 6281	3'-deoxyATP; 3'-deoxyadenosine 5'-triphosphate	-195.08	-131.24	-9.61	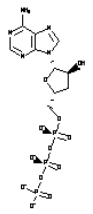
CID 129401	8-azido-2'-O-dansyladenosine triphosphate	**-204.97**	-121.17	-16.09	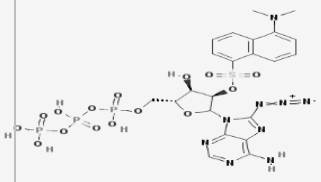
CID 195619	5-azido-2-nitrobenzoyl-8-azido ATP	**-200.49**	-156.45	-16.05	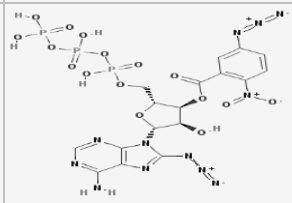
CID 49859690	phosphoribosyl-ATP	**-197.33**	-130.99	-16.37	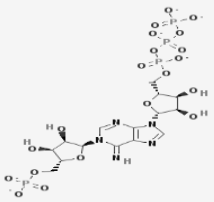
CID 15938961	adenosine thiamine triphosphate	-195.79	-113.69	-5.89	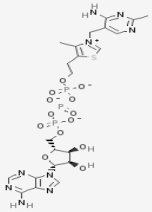
CID 115205	3'-O-(4-benzoyl)benzoyladenosine 5'-triphosphate	-195.73	-101.71	-16.53	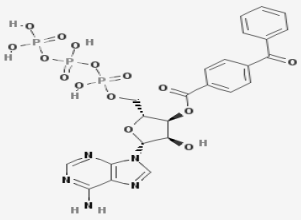
CID 24916929 (PC)	adenosine 5'-tetraphosphate pentaanion	**-219.74**	-153.98	-10.74	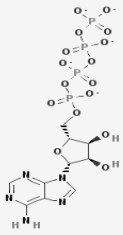

CID 24917010 (PC)	[[[(2R,3S,4R,5R)-5-(2-amino-7-methyl-6-oxo-3H-purin-9-ium-9-yl)-3,4-dihydroxyoxolan-2-yl]methoxy-oxidophosphoryl]oxy-oxidophosphoryl] phosphate	**-209.45**	-148.46	-15.47	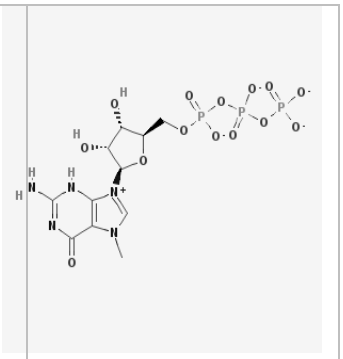
CID 23279499 (PC)	[[[(2R,3S,4R,5R)-5-(6-amino-2-methylsulfanylpurin-9-yl)-3,4-dihydroxyoxolan-2-yl]methoxy-oxidophosphoryl]oxy-oxidophosphoryl] phosphate	-187.09	-128.02	-14.62	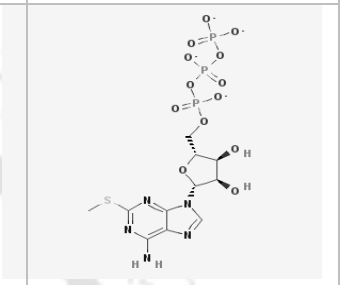
CID 44828494 (PC)	[(2R,4R,5R)-5-(6-amino-2-methylsulfanylpurin-9-yl)-3,4-dihydroxyoxolan-2-yl]methoxy-oxidophosphoryl] phosphate	-171.63	-123.82	-13.48	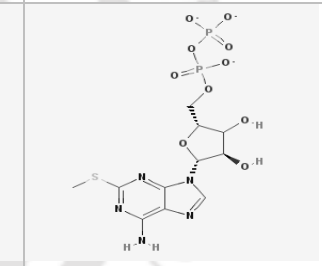
CID 6604891 (PC)	[(2R,3S,4S,5S)-5-(6-amino-2-methylsulfanylpurin-9-yl)-3,4-dihydroxyoxolan-2-yl]methoxy-oxidophosphoryl] phosphate	-170.63	-124.62	-11.39	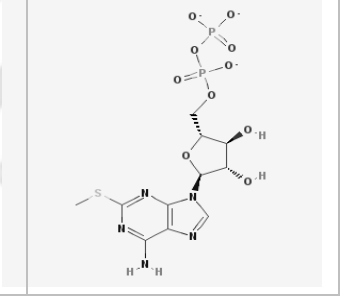

ATP analogs from different databases were collected and docked against the active site pocket of PFD0975w. Top 14 hits are shown in table. The binding score (MolDock score) of molecules which bind with an affinity greater than that of natural substrate ATP (MolDock score = -195.30) have been indicated in bold.

Another important criterion while selecting hits from virtual screening experiment is that the hits should preferably occupy the entire active site cavity, making as much interaction with the

protein atoms as possible. A closer inspection of the binding orientation of the top hits allowed us to further screen down the hits which did not fill the entire cavity, and hence might fail substrate competition. The final five top hits which bound well into the cavity as well as occupied most of the cavity space are CID 195619, CID 49859690, CID 15938961, and CID 129401.

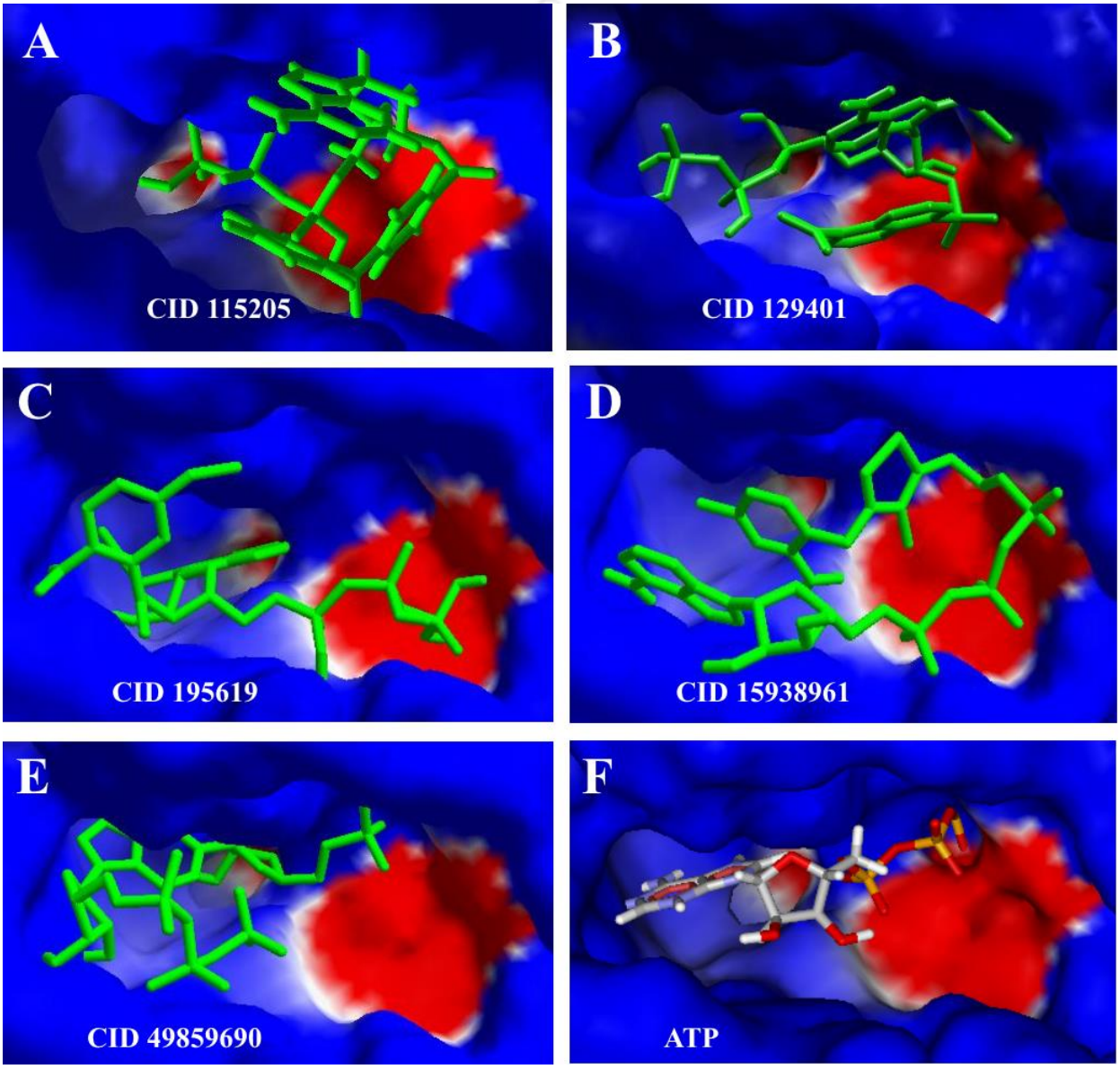

Figure 5.3: The orientation of binding of the top 5 hits, (A) CID 115205, (B) CID 129401, (C) CID 15938961, (D) CID 15938961 and (E) CID 49859690 within PFD0975w active site pocket compared to that of natural substrate (F) ATP.

The binding orientation of the final five best hits within the active site pocket have been carefully studied (Figure 5.3) and their interactions with protein residues of the active site pocket have been charted.

5.3.2 Substrate competition assay: *In silico* substrate completion assay is a tool to predict the strength and selectivity of binding of a particular ligand within a protein's cavity. In case of PFD0975w kinase, the active site is naturally designed to accept ATP, but in the absence of ATP and in the presence of a good inhibitor, the inhibitor occupies the space. Since the catalysis of the inhibitor is not possible, the enzyme would be irreversible non-functional. With this aim in mind, PFD0975w3D model with ATP docked into the active site cavity was chosen to re-dock the top 5 hits obtained above (Table 5.2). The inhibitors were free to bind anywhere within the protein molecule and not just the active site.

Table 5.2: Substrate competition analysis of the top 5 hits from virtual screening.

Compound ID	MolDock Score (Active site) (AU)	MolDock Score (Other sites) (AU)	Energy Difference (AU)
CID 115205	-195.73	32.07	-163.66
CID 129401	-204.97	-14.78	-219.75
CID 15938961	-195.79	-36.54	-232.33
CID 195619	-200.49	-18.36	-218.85
CID 49859690	-197.33	-24.63	-221.96

The binding affinity of the top 5 hits within the PFD0975w active site was tested using an *in vitro* substrate competition assay. ATP was docked into the active site of PFD0975w and the top 5 hits were allowed to bind anywhere within the protein. Table shows that none of the top 5 hits binds well outside the active site. Substrate competition indicates selected ligands bind in an energetically favorable conformation only within the active site.

From Table 5.2 we can clearly see that our chosen inhibitors prefer to bind within the active site cavity rather than anywhere else within the protein. An interesting observation here is that when the active site of the protein is occupied with ATP, none of the top hits could bind within the active site. The top hits rather chose the next best cavity to bind to i.e. the substrate binding cleft. Since the substrate binding cleft of a kinase binds protein, the binding of ATP there is

energetically unfavorable. This is evident from the differences in binding energy at the two locations. A careful visual inspection of the top 4 hits revealed that in the presence of ATP within the active site cavity, the inhibitors bind to the substrate binding cleft (Figure 5.4).

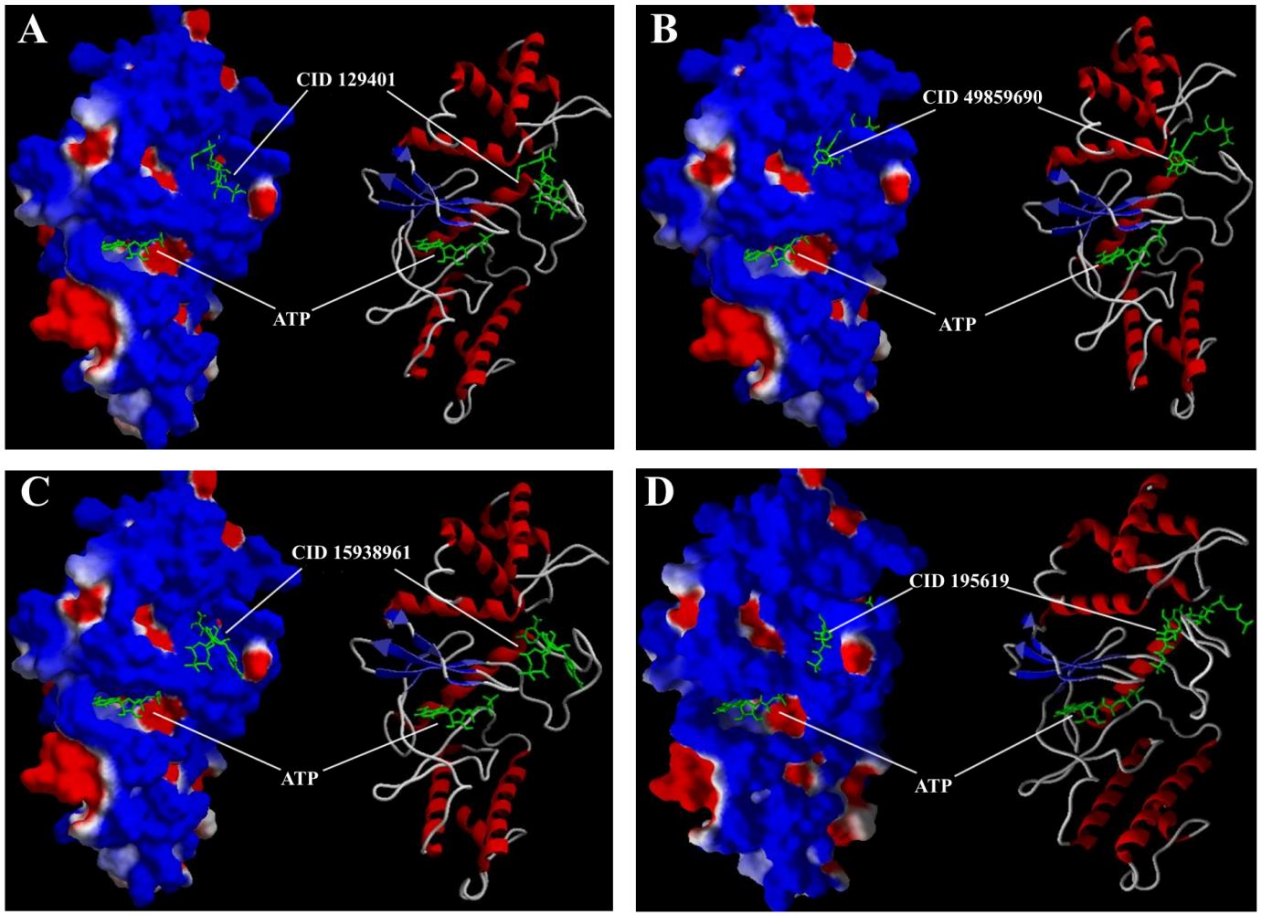

Figure 5.4: Surface charge representation and secondary structure representation of PFD0975w-ATP model and the location of binding of identified top hits during substrate competition with (A) CID 129401, (B) CID 49859690, (C) CID 15938961 and (D) CID 195619

5.3.3 Study of interactions of top hits within PFD0975w active site: The top 4 hits among the 5 hits identified above were studied extensively for the kind of interactions they make within the active site of the protein. CID 115205, CID 129401, CID 195619 and CID 49859690 make extensive interactions within the ATP binding pocket of PFD0975w kinase. The identified hits engage in all the three major types of interactions i.e., electrostatic, hydrophobic and hydrogen

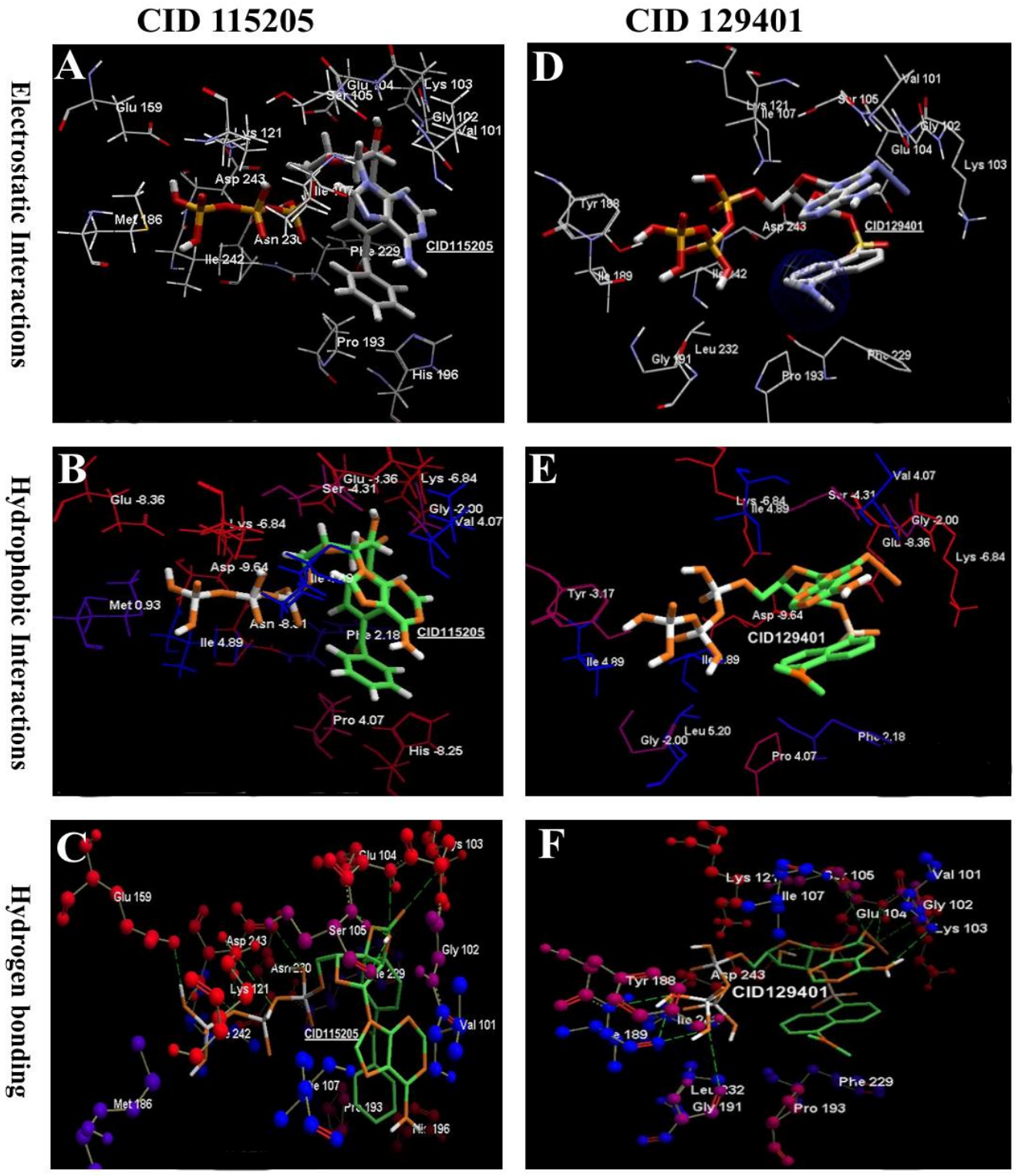

Figure 5.5: 3D map of interactions of inhibitors CID 115205 and CID 129401 within the proteins active site. (A) Electrostatic interaction, (B) Hydrophobic interaction and (C) Hydrogen bonding interactions of CID 115205 within active site. (D) Electrostatic interaction, (E) Hydrophobic interaction and (F) Hydrogen bonding interactions of CID 129401 within active site.

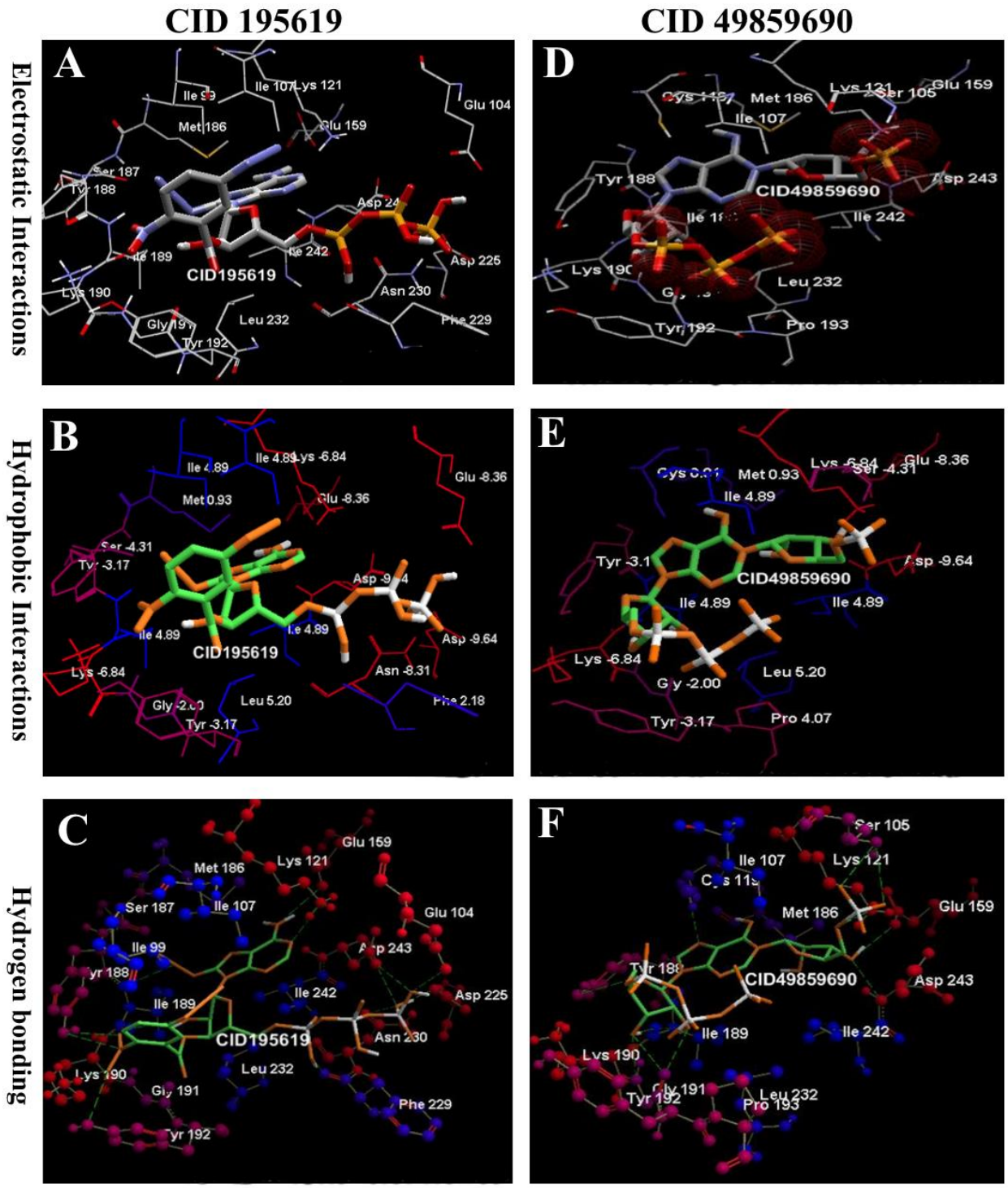

Figure 5.6: 3D map of interactions of inhibitors CID 195619 and CID 49859690 within the proteins active site. (A) Electrostatic interaction, (B) Hydrophobic interaction and (C) Hydrogen bonding interactions of CID 195619 within active site. (D) Electrostatic interaction, (E) Hydrophobic interaction and (F) Hydrogen bonding interactions of CID 49859690 within active site.

bonding, within the pocket. The protein residues which interact with these inhibitors vary depending upon the shape, orientation and charge of these ligand molecules (Figures 5.5 and 5.6). The stronger the interactions within the active site, the greater are the changes of a complete irreversible inhibition of the kinase activity of the enzyme.

5.3.4 Identification of approved drugs from similarity search to top hits: One of the greatest financial risks involved in any drug development project is the failure of a candidate drug at the clinical or pre-clinical trials. Molecules which might exhibit potent anti-malarial activity *in vitro*, might prove to be toxic in animal models. There is no reliable bioinformatics tool to predict whether a given molecule could be toxic in mice or humans, until the real trials are conducted. A novel approach to circumvent this problem is the "re-purposing" of old drugs. In our drug development process targeting PFD0975w, we have looked upon the approved drug-space for molecules which could inhibit PFD0975w by competing with its natural substrate ATP. Our top ten inhibitors against PFD0975w are drug-like molecules with conserved pharmacophoric scaffolds. Our objective is to look for drugs which would be available in Indian pharmacies, and would be similar to our hits with respect to structure and pharmacophoric points. To do this we took help of the inhibitors we had identified so far. The DrugBank is a collection of all therapeutic molecules known, classified into different categories such as approved, experimental, withdrawn and neutraceutical (Law, Knox et al. 2014) . The 'Approved drugs' subset of DrugBank contains 1505 drug molecules and the hits identified previously were used to search for drugs within the approved subset. Only drugs which were greater than 60% similar to the original hit and contained the necessary pharmacophoric attachment points were selected. Table 5.3 lists a collection of 29 approved drugs which are at least 60% structurally similar to any of the previously identified top hits. The process of identification of candidate drugs against PFD0975w have been published (Nag, Chouhan et al. 2013).

The basic advantages behind this "Re-purposing" strategy is to identify drugs which might have unreported anti-malarial activity or drugs whose anti-malarial activity is known but nothing is known regarding the mechanism of its action against *Plasmodium*. These drugs would be safe because they have already undergone the clinical trials and if found to have anti-malarial property could be used instantly. Another advantage is that molecules which are already

contained in marketed drugs are easily available from pharmacy outlets making the process cheap and quick.

Table 5.3: Identification of candidate drugs against PFD0975w from top hits

Top hits	Name of approved drug and percentage similarity to top hits				
ZINC49775260	Dipyridamole 57.47	Idarubicin 52.44	Monoxerutin 51.73	Lymecycline 49.57	Nelfinavir 49.42
Cb-44415375	Benfotiamine 64.55	Adefovir 63.31	Mopidamol 63.24	Tenofovir 61.76	Spirapril 60.44
Cb-44215930	Idarubicin 76.18	Theodrenaline 75.86	Clindamycin 75.83	Reproterol 75.75	Methacycline 72.88
ZINC03871614	Lymecycline 74.22	Valrubicin 56.33	Clarithro-mycin 65.32	Diosmin 69.28	Roxithromycin 67.04
Cb-832054	Mopidamol 58.47	Benfotiamine 55.45	Lisinopril 55.42	Adefovir 54.05	Tenofovir 52.88
CID 49859690	Clomocyclin e 78.32	Methotrexate 78.35	Ramipril 56.28	Quinapril 64.86	Nelfinavir 65.46
Cb-2082655	Miokamycin 40.38	Roxithromycin 38.53	Methotrexate 38.52	Glucametacin 38.21	Aminopterin 38.21
CID 15938961	Ramipril 80.35	Spirapril 74.22	Cilazapril 71.18	Plicamycin 56.66	Lisinopril 67.28
CID 24917010	Demeclo-cycline 66.20	Oxytetra-cycline 46.33	Aminopterin 78.15	Leucovorin 49.93	Methacycline 39.44
CID 115205	Dirithro-mycin 58.92	Methacycline 32.25	Pralatrexate 55.67	Troleando-mycin 43.33	Plicamycin 68.43

Top hits obtained against PFD0975w from virtual screening experiments were used to search for approved drug molecules which were similar to any of the hits and retained the necessary pharmacophores for interaction with active site residues of PFD0975w

5.3.5 Approved drugs which interacts with PFD0975w active site residues: The sdf files for the 29 drug molecules listed above were downloaded from DrugBank and docked into the ATP binding cavity of PFD0975wto identify drug molecules which binds within the active site with favorable binding energies/MolDock score. Table 5.4 lists the top 20 drug molecules selected

from the above 29 molecules which bind into the active site with considerable negative free energy. These drugs are in circulation in markets for a variety of diseased states. Since they bind well into PFD0975w active site, we hypothesize that they would inhibit PFD0975w *in vitro*, and can in principle show anti-malarial activity.

Table 5.4: Drugs which fit well into the active site cavity of PFD0975w

Drug name	MolDock score (AU)	Known use	Reported anti-malaial activity?	Reference	Structure
Aminopterin	-154.39	leukemia	No	-----	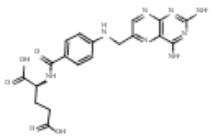
Monoxerutin	-140.68	Hemorrhagic strokes, Internal bleeding	Yes	(Elfawal, Towler et al. 2015)	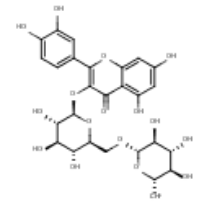
Methotrexate	-137.13	Anti-cancer	Yes	(Dar, Khan et al. 2008)	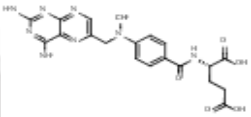
Benphothiamine	-135.48	diabetic retinopathy, neuropathy, and nephropathy	No	---	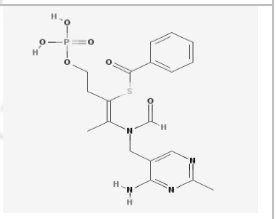
Nelfinavir	-135.25	HIV medication	Yes	(Mishra, Bhattacharya et al. 2010)	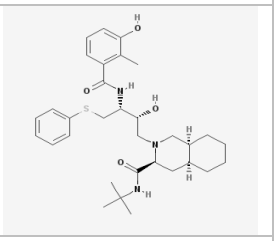
Dipyridamole	-135.12	platelet inhibitor	Yes	(Gero, Scott et al. 1989)	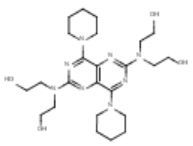

Glucametacin	-132.27	analgesic and antipyretic	No	----	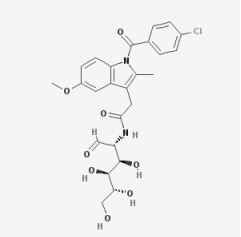
Lisinopril	-130.59	high blood pressure, heart failure and for preventing kidney failure	No	----	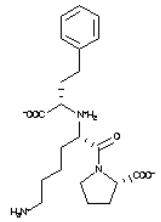
Mopidamol	-125.11	Athero-sclerotic damages, arthritic conditions, inflammatory reactions	No	----	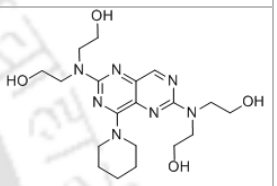
Clindamycin	-124.76	antibiotic	Yes	(Lell and Kremsner 2002)	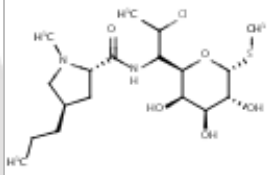
Miocamycin	-124.31	Respiratory tract infections	No	----	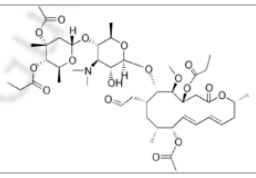
Spirapril	-124.14	Anti-hyper tensive medication	No	----	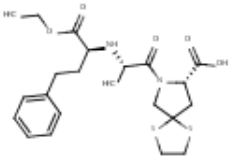
Reproterol/terol	-121.80	Asthma	No	----	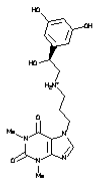

Roxithromycin	-117.97	Antibiotic	Yes	(Min, Khairul et al. 2007)	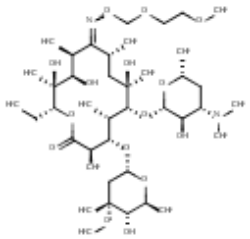
Theodrenaline	-113.70	Cardiac stimulant	No	----	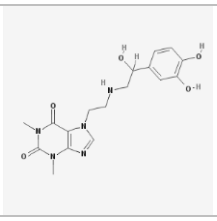
Adefovir	-101.53	Hepatitis-B infection	No	----	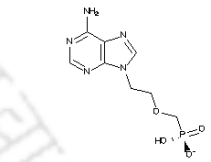
Tenofovir	-99.36	HIV medication	No	----	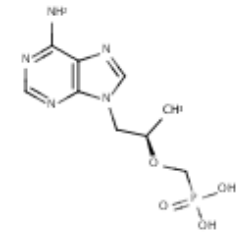
Lymecycline	-90.46	Acne/ Skin infections	No	----	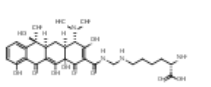
Idarubicin	-65.70	Acute myeloid leukemia	No	----	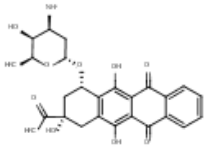
Methacycline hydrochloride	-58.68	Acne/ Skin infections	No	----	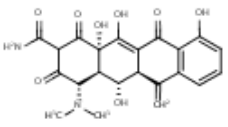

The 3D sdf files of the 29 identified candidate drugs against PFD0975w (Table 5.3) were docked into PFD0975w active site. The result of top 20 drug molecules which binds into the active site have been documented, along with their binding score, known use and reported anti-malarial activity (if any)

5.3.6 *In vitro* antimalarial activity of selected drugs from DrugBank: The above list of 20 drugs was searched in the market but only 7 of them were commercially available. This includes Benfotiamine, Reproterol, Roxithromycin, Metotrexate, Tenofovir, Lisinopril and Clindamycin. Care was taken to select brands which contained mostly the active ingredient with little or no additional compounds, vitamins and stabilizers. A literature survey pointed out that out of the 7 drugs listed above, anti-malarial activity of 3 drugs were already reported i.e., Clindamycin, Methotrexate and Roxithromycin, although there is little idea about the mechanism of anti-malarial action of these drugs. Anti-malarial schizonticidal assay was performed for all the 7 drugs using the procedure described in experimental section. Results show that all the 7 drugs display anti-malarial activity in culture, with some drugs such as Methotrexate, Roxithromycin and Reproterol having considerably low IC_{50}s on *Plasmodium falciparum* 3D7. Table 5.6 summarizes the anti-malarial potentials of the seven selected drugs.

Table 5.6: Anti-malarial activities of seven candidate drugs

Drugs	Polynome	IC_{50}	IC_{90}	IC_{95}	IC_{99}	R^2
Benfotiamine	3	1.476	18.376	34.033	43.505	0.9639
Reproterol	3	0.104	0.242	0.276	0.315	0.7574
Roxithromycin	3	0.462	2.267	22.223	23.587	0.7108
Methotrexate	3	0.098	0.098	0.098	0.101	1.0000
Tenofovir	3	0.521	2.514	10.541	11.815	0.9812
Lisinopril	3	1.293	28.879	37.771	44.041	0.8838
Clindamycin	3	0.585	3.042	19.761	22.642	0.8219

Drug stocks were prepared as described in "experimental procedures". Synchronized ring stage parasites of ~1-2% parasitemia were incubated with above drugs at a concentration between 0 µg/ml (Control) and 50 µg/ml for 36 hrs. Post incubation, smears were made and schizont maturation was monitored with respect to applied drug concentration. IC values, polynome and correlation factors were calculated using regression analysis.

An important aspect of any anti-malarial drug, apart from its IC_{50}, is its capability to elicit a long term protection, even after the withdrawal of the drug. We define this property as the nature of the drug: whether it can kill parasites (parasitocidal) or it can just halt the parasite growth till the drug is present (parasitostatic). Our data (Table 5.7) shows that Reproterol, Roxithromycin,

Metotrexate, Tenofovir and Clindamycin kills the parasites completely such that when the drugs are withdrawn from treated cultures by extensive washing followed by 3 days of incubation without drugs; parasites fail to grow. Such drugs show prolonged effect. Whereas milder drugs like Benfotiamine and Lisinopril are parasitostatic, meaning they do not kill the parasites but arrest the development as long as the drugs are present in the culture. MKC or minimum killing concentration is defined as the concentration of drug beyond which the malaria parasite is killed completely and fails to resume growth even after drug removal. Some of the drugs we tested showed remarkable MKC values such as methotrexate (0.8 µg/ml) and reproterol (1.6 µg/ml).

Table 5.7: Anti-malarial potency and nature of tested candidate drugs against PFD0975w

Drug	IC_{50} Concentration(µg/ml)	Nature of drug	MKC (µg/ml)
Benfotiamine	1.476± 0.04	Parasitostatic	-------
Reproterol	0.104± 0.09	Parasitocidal	1.60
Roxithromycin	0.462± 0.07	Parasitocidal	6.25
Methotrexate	0.098± 0.08	Parasitocidal	0.80
Tenofovir	0.521± 0.03	Parasitocidal	3.20
Lisinopril	1.293± 0.05	Parasitostatic	-------
Clindamycin	0.585± 0.07	Parasitocidal	6.25

Synchronized ring stage parasites of ~1-2% parasitemia were incubated with above drugs at a concentration between 0 µg/ml (Control) and 50 µg/ml for 36 hrs. Post incubation, drugs were removed and cells were washed thrice in media and re-incubated in drug-free media for 72 hrs. After 72 hrs. Smears were made for each drug concentration. Giemsa stained smears were studied to count viable parasites. MKC is defined as the minimum drug concentration at which there is a complete killing of parasites and no revival after drug removal.

5.3.7 Clindamycin, methotrexate and tenofovir disrupts ATP binding within the active site of PFD0975w: Bioinformatics predicts the above seven drug molecules to be active competitors of ATP binding in PFD0975w, but to know for sure whether they actually bind or not, an *in vitro* assay is required. Mant-AMPPNP (described in chapter III) is a fluorescent analog of ATP which has an emission peak at 448 nm. When this analog shifts from free (solution) phase to a bound state (within a protein's cavity), there is an increase in fluorescence emission at 448 nm, upon

excitation with a frequency of 360 nm. Figure 5.7 demonstrates that increase in fluorescence between the unbound (fluorophore only) and bound (fluorophore plus 50 µM protein) state. The interesting thing to observe is that in reaction mixtures containing 1 mM of drugs such as clindamycin, methotrexate and tenofovir, the fluorescence spectra shows a fluorescence depression at 488 nm (Figures 5.7, 5.8 & 5.9). This demonstrates that these three drugs namely, Clindamycin, Methotrexate and Tenofovir clearly compete with the ATP analog for binding into PFD0975w active site. Data suggests that Tenofovir shows 21% disruption in ATP binding, methotrexate shows 15% disruption in ATP binding and clindamycin shows 14% disruption in ATP binding (Figures 5.7, 5.8 & 5.9). Such spectrofluorometric data demonstrates utility and effectiveness of our approach for selecting drugs, which are structurally similar to top hits against PFD0975w and explains well the observed anti-malarial potential of these compounds.

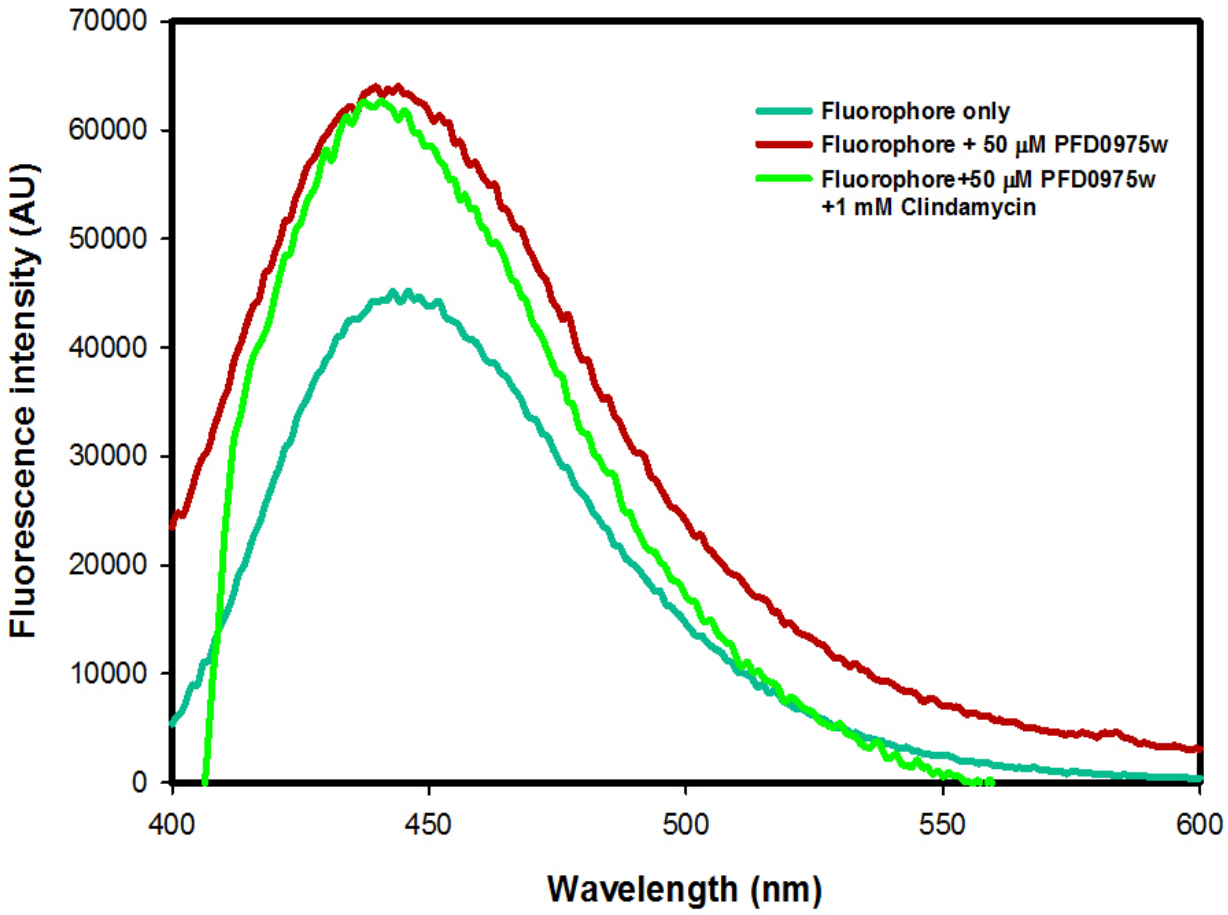

Figure 5.7: Spectrofluorometric data showing the effect of clindamycin on ATP binding. Figure shows the fluorescence emission spectra between 400nm-600nm, of reaction mixtures containing fluorophore only, fluorophore+PFD0975w and fluorophore+PFD0975w+ clindamycin.

Spectrofluorometric data demonstrates that out of the 7 drugs, which have been selected to disrupt substrate binding, through computational studies really competes with ATP for binding into PFD0975w active site. Blocking of ATP binding disrupts substrate phosphorylation by the kinase and is the reason behind the observed anti-malarial action behind these drugs.

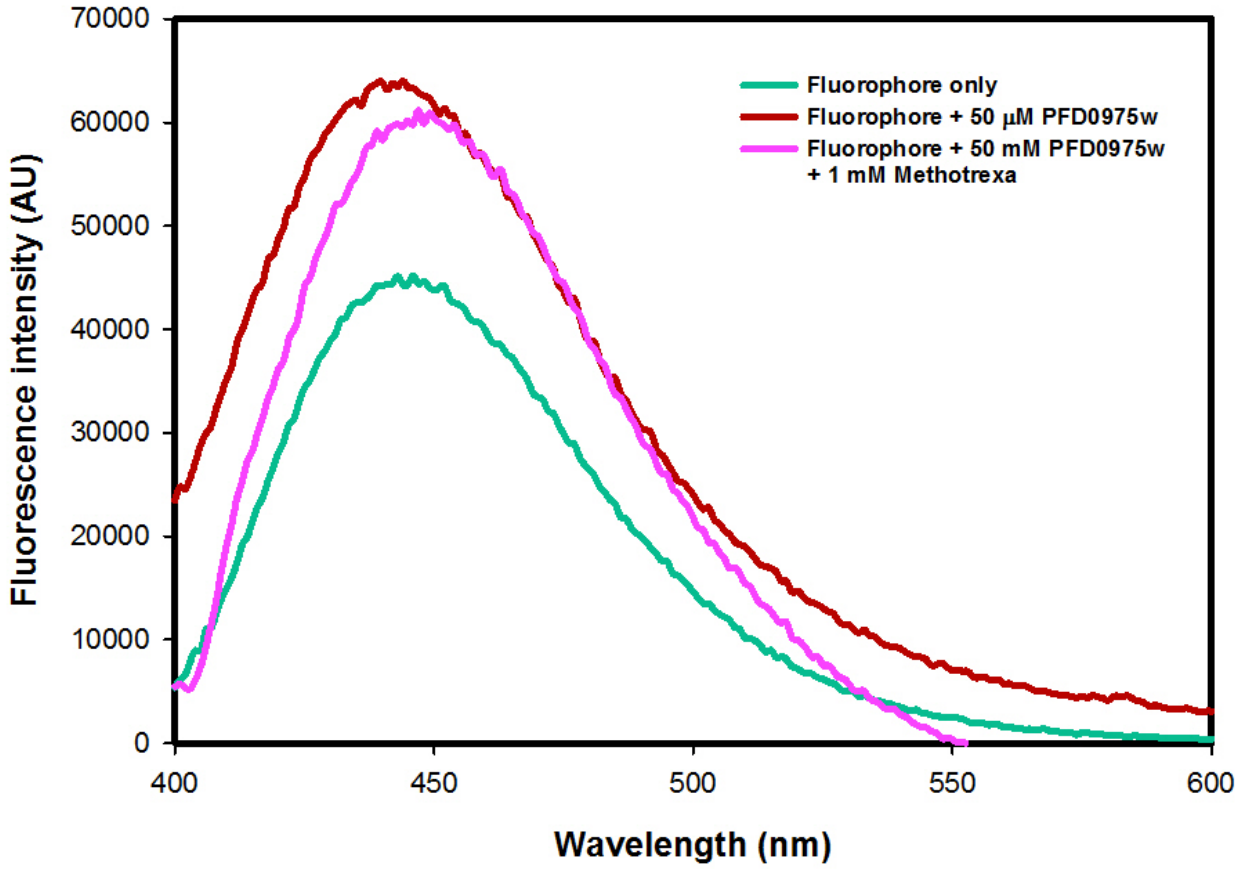

Figure 5.8: Spectrofluorometric data showing the effect of methotrexate on ATP binding. Figure shows the fluorescence emission spectra between 400nm-600nm, of reaction mixtures containing fluorophore only, fluorophore+PFD0975w and fluorophore+PFD0975w+ methotrexate.

5.3.8 Drug treatment generates ROS within parasites: Once certain drugs show response to a disease state, we might ask questions about its mechanism of action. The seven drugs listed above elicit anti-malarial activity *in vitro* and we examined the cause or mechanism of parasite clearance by these drugs. The DCF-DA assay is a simple technique to study the accumulation of ROS within any cell with intact membrane. Parasites were treated with IC_{50} concentration of above drugs for 12 hours before isolating them from RBC. The fluorescence intensity of DCF-DA is directly proportional to the amount of ROS within the cells. Figure 5.7 demonstrates that

almost all of the 7 drugs induce ROS formation within the parasite. Any cell which undergoes stress generates ROS and hence it is evident that at IC_{50} concentration, the drugs induce stress reactions within the parasite, which disturbs the fine balance between

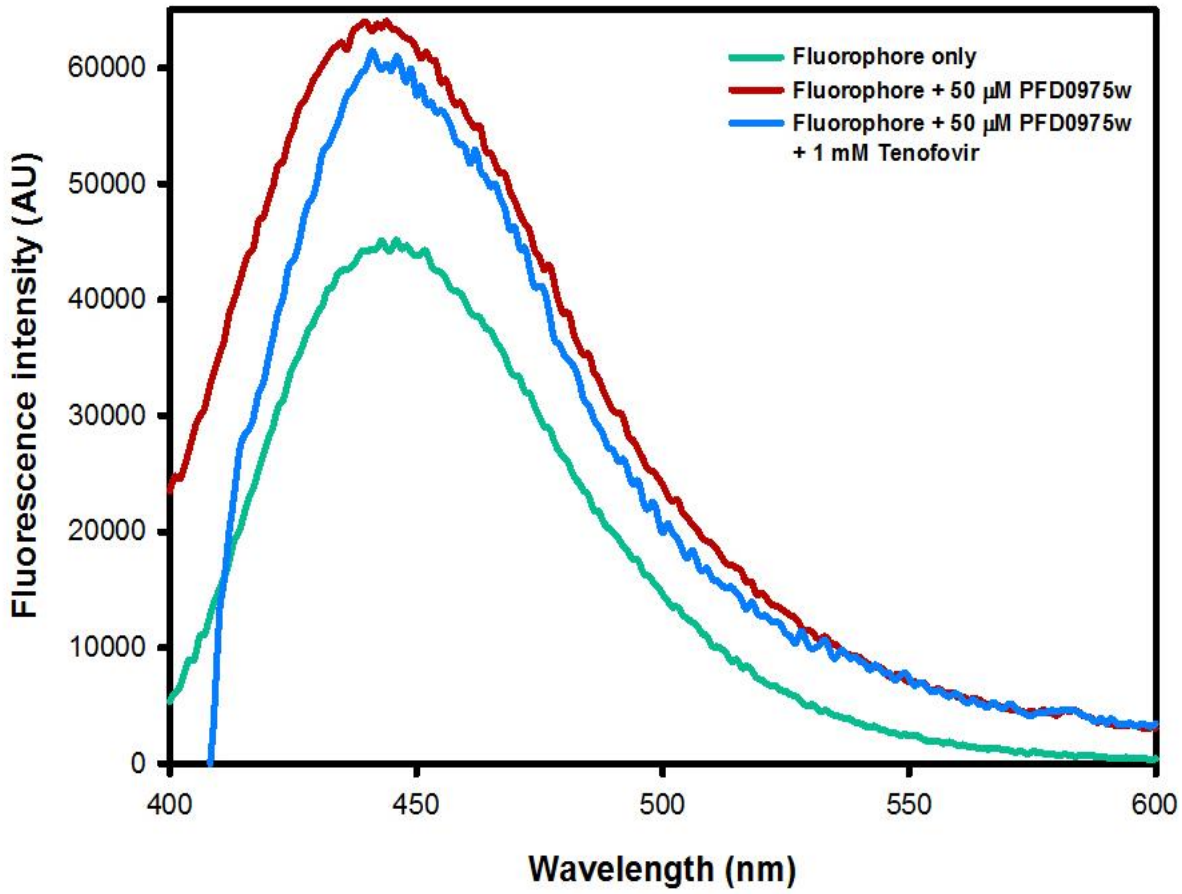

Figure 5.9: Spectrofluorometric data showing the effect of tenofovir on ATP binding. (A) Fluorescence emission spectra between 400nm-600nm, of reaction mixtures containing fluorophore only, fluorophore+PFD0975w and fluorophore+PFD0975w+ tenofovir. (B) Comparison of fluorescence emission intensity of fluorophore, fluorophore+PFD0975w and fluorophore+PFD0975w+ tenofovir.

production and depletion of ROS, resulting in intra-cellular accumulation. Clindamycin followed by Roxithromycin shows the highest ROS, and it well correlates with the fact that these two drugs, although known in the market for different uses, have previously been identified to have anti-malarial property. Through our work we claim that the anti-malarial action of these drugs is due to the inhibition of PFD0975w kinase, which we have shown earlier to be a key protein in parasite stress response.

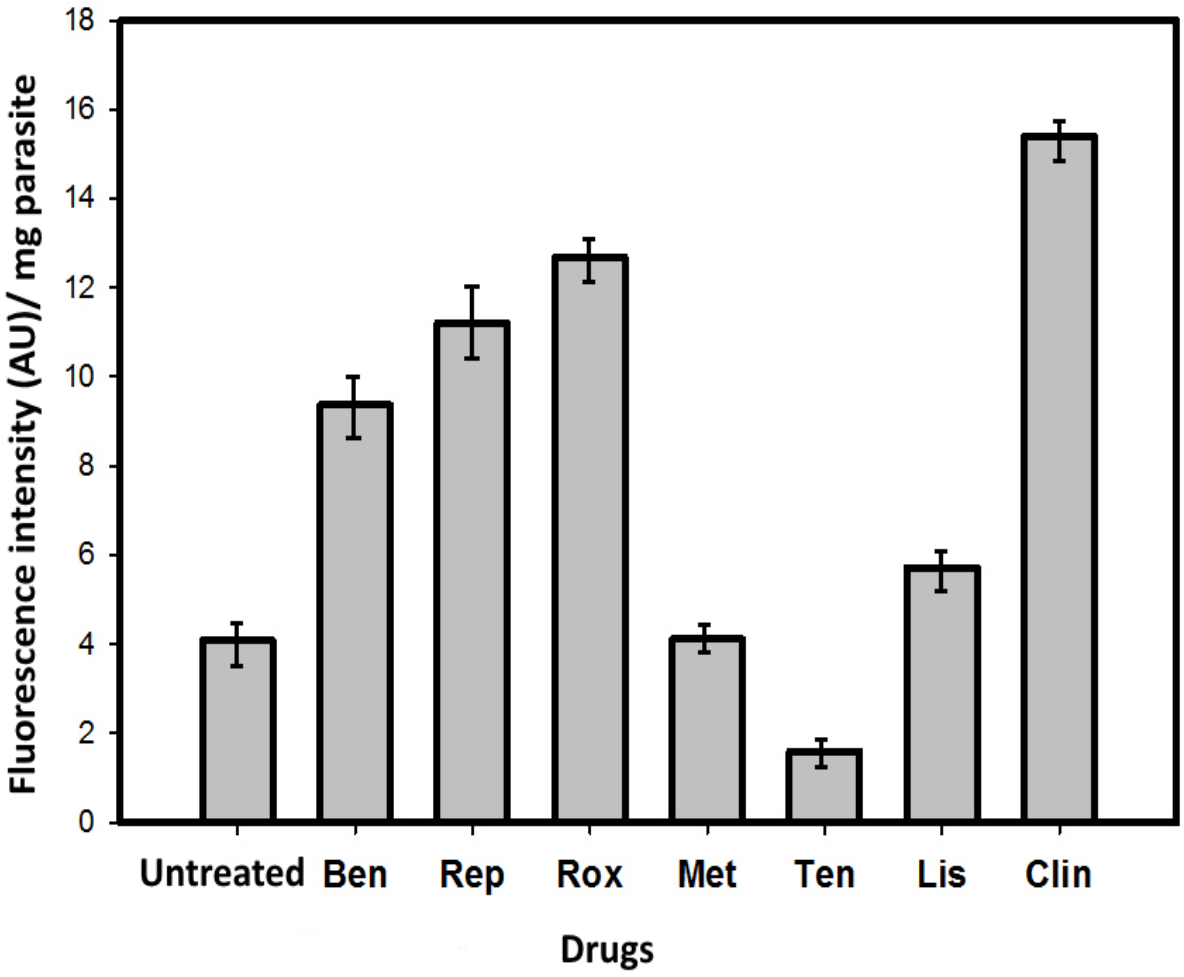

Figure 5.7: The level of Reactive oxygen species within untreated parasites and parasites treated with IC_{50} concentration of different candidate drugs: Benfotiamine (Ben), Reproterol (Rep), Roxithromycin (Rox), Methotrexate (Met), Tenofovir (Ten), Lisinopril (Lis) and Clindamycin (Clin).

5.3.9 Drug treated parasites undergo peroxidation of cellular lipids. Lipid peroxidation is the process of degradation of lipids due to oxidation. A cell under exogenous stress generates free radicals which remove electrons from cellular lipids and membranes, ultimately resulting in cell damage. Lipid peroxidation is a classic symptom of a cell which accumulates ROS and it occurs as a free radical mediated chain reaction. Polyunsaturated fatty acids are mostly affected by free radicals due to the multiple double bonds in and methylene bridges possessing reactive hydrogen. Many anti-microbial and anti-malarial drugs kill their respective pathogens by generating ROS within them. When the balance between the generation and the consumption of ROS goes out of balance, a cell begins to die.

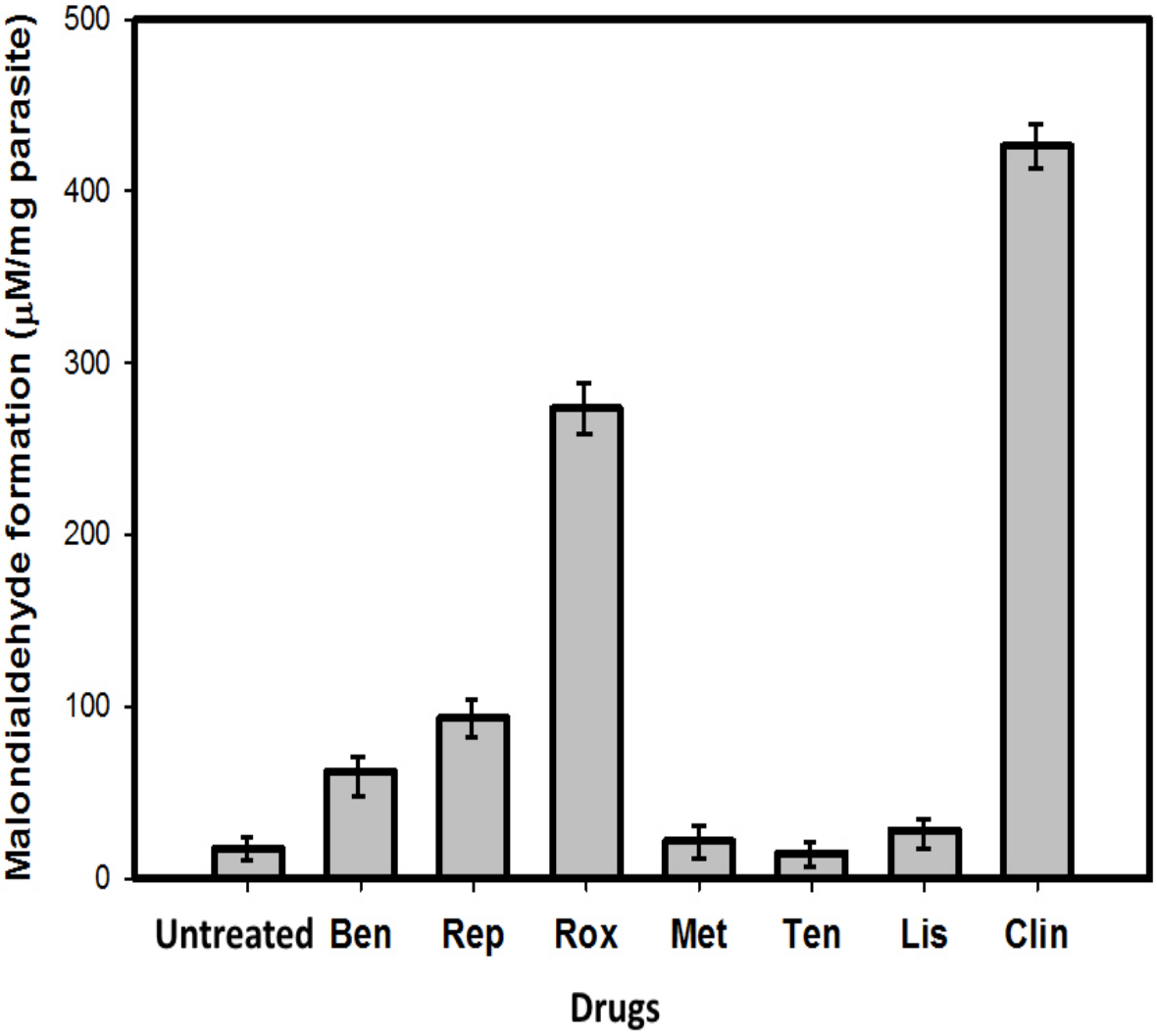

Figure 5.8: The formation of level of lipid peroxide; Malondialdehyde within untreated parasites and parasites treated with IC_{50} concentration of different candidate drugs. Benfotiamine (Ben), Reproterol (Rep), Roxithromycin (Rox), Methotrexate (Met), Tenofovir (Ten), Lisinopril (Lis) and Clindamycin (Clin).

Parasites treated with IC_{50} concentration of Benfotiamine, Reproterol, Roxithromycin and Clindamycin showed an increase in the formation of lipid peroxide; Malondialdehyde (Figure 5.8). The lipid peroxidation data re-confirms that parasites treated with IC_{50} concentrations of Clindamycin generates the maximum intra-cellular ROS as well as lipid peroxides followed by that of Roxithromycin, indicating their immense potential as an antimalarial. The lipid peroxidation and ROS analysis of Clindamycin and Roxithromycin treated parasites sheds light on the previously reported anti-malarial property of these 2 drugs (Lell and Kremsner 2002, Min, Khairul et al. 2007).

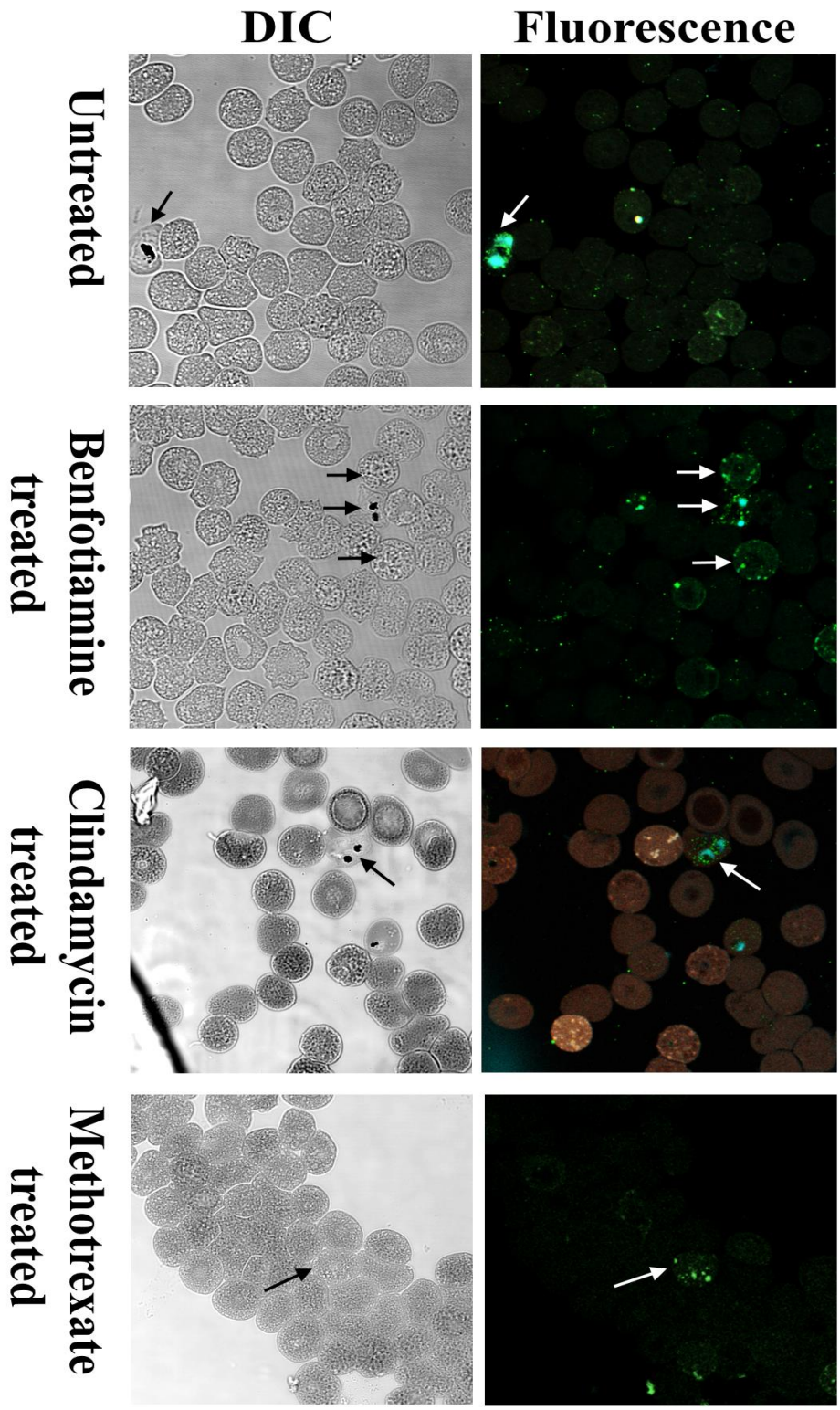

Figure 5.9: Confocal images showing the differences in the localization pattern of PFD0975w in untreated parasites and parasites treated with IC_{50} concentration of Benfotiamine, Clindamycin and Methotrexate.

5.3.10 Drug treatment influences the localization pattern of PFD0975w: Anti-PFD0975w antibody was used to trace the expression pattern of the protein in untreated and drug treated *Plasmodium falciparum*. Figures 5.9 and 5.10 shows the confocal images of the localization pattern of PFD0975w in control vs. treated samples. As previously demonstrated, in untreated parasites, PFD0975w is expressed constitutively throughout parasite cytoplasm (Figure 2.5C). Here also we observed a similar constitutive expression of PFD0975w in untreated parasites, reconfirming our previous finding (Refer Chapter II). In parasites treated with IC_{50} concentration of drugs such as tenofovir, reproterol, methotrexate and benfotiamine shows a clear down regulation of PFD0975w expression. PFD0975w appears to be expressed in a punctuate pattern throughout the cytoplasm of iRBC of treated samples. This pattern of punctuate expression was also previously observed in CQ treated parasites (Figure 2.7), indicating a role of PFD0975w in parasite survival during drug-pressure. PFD0975w localization in parasites treated with clindamycin and lisinopril, however, results in a less scattered expression. Our data suggests a key role of PFD0975w in parasite survival in response to drug treatment.

5.4 Discussion.

The public domain contains thousands of uncharacterized novel molecules which could be potent inhibitors of PFD0975w. Our objective for this section has been to identify good inhibitors against PFD0975w which would block the active site ATP binding. A thorough virtual screening against ATP analogs from different public domains (Irwin and Shoichet 2005) (Seiler, George et al. 2008) identified 14 novel inhibitors. Computational experiments have shown that these 14 inhibitors bind tightly to the protein's active site and an *in silico* substrate competition assay reconfirms the fact that the selected inhibitors are particularly suited to bind exclusively to the proteins active site. One major bottleneck of any drug discovery programme is the in vivo toxicity of final molecules. Many of the above selected inhibitors could prove to be toxic to humans at a later stage of the drug development process. To circumvent this problem we screened for drugs within the approved drug-space, for molecules which were structurally similar (above 50%) to our top hits. This type of a similarity search identified 29 drugs from the approved drug-space of DrugBank (Law, Knox et al. 2014) which were structurally similar to our parent hits.

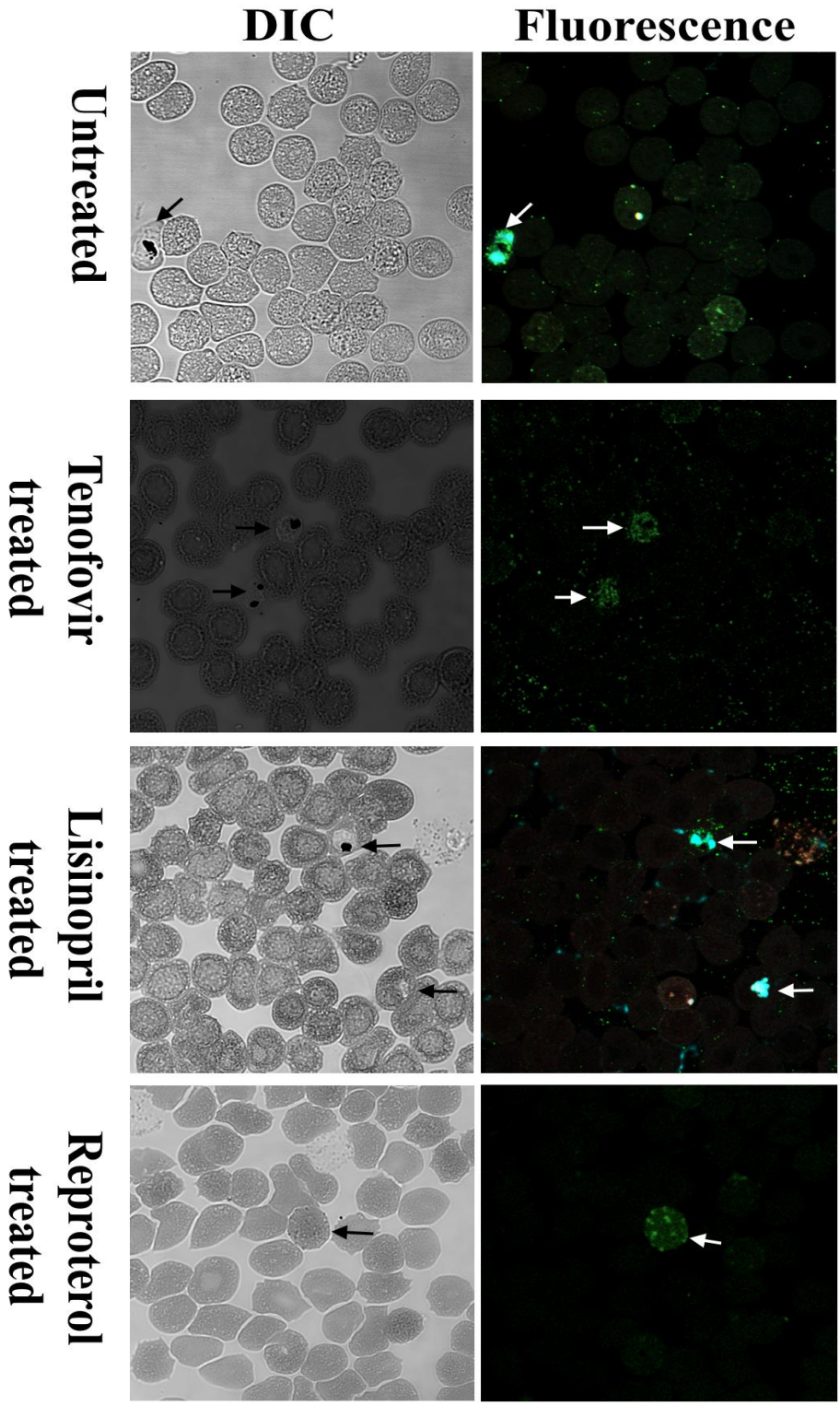

Figure 5.10: Confocal images showing the differences in the localization pattern of PFD0975w in untreated parasites and parasites treated with IC_{50} concentration of Tenofovir, Lisinopril and Reproterol.

These drugs were available in circulation for the treatment of different diseases. Antimalarial activity assay against these drugs identified seven candidate drugs with antimalarial activity. They are Reproterol, Clindamycin, Benfotiamine, Roxithromycin, Tenofovir, Methotrexate and Lisinopril. Antimalarial activity of some of these drugs such as Clindamycin (Lell and Kremsner 2002) and Methotrexate (Dar, Khan et al. 2008) were previously known, either distinctly or in combination with other antimalarials, nevertheless, nothing was known about their targets or mode of action.

Our studies have indicated that the some of the above drugs such as Clindamycin, Methotrexate and Tenofovir exerts their antimalarial influence because they bind into PFD0975w active site, preventing its natural substrate ATP to participate in binding and catalysis. The drugs which exhibit active antimalarial potentials like Reproterol, Roxithromycin and Clindamycin were found to generate ROS imbalance in treated parasites when compared to untreated, indicating stress in treated parasites upon drug treatment. Our results indicate that drugs such as Roxithromycin (Min, Khairul et al. 2007) and Clindamycin (Lell and Kremsner 2002) with previously reported antimalarial activities generate the formation of lipid peroxides in treated parasites, which is a classic outcome of cellular stress. Confocal data reflecting the differences in localization pattern of PFD0975w in untreated and treated samples suggest a vital role of this protein in parasite's response to drug-pressure.

5.5 References.

- Cohen, P. (2002). "Protein kinases--the major drug targets of the twenty-first century?" Nat Rev Drug Discov **1**(4): 309-315.
- Dancey, J. and E. A. Sausville (2003). "Issues and progress with protein kinase inhibitors for cancer treatment." Nat Rev Drug Discov **2**(4): 296-313.
- Dar, O., M. S. Khan and I. Adagu (2008). "The potential use of methotrexate in the treatment of falciparum malaria: in vitro assays against sensitive and multidrug-resistant falciparum strains." Jpn J Infect Dis **61**(3): 210-211.
- Doerig, C. (2004). "Protein kinases as targets for anti-parasitic chemotherapy." Biochim Biophys Acta **1697**(1-2): 155-168.
- Doerig, C., L. Meijer and J. C. Mottram (2002). "Protein kinases as drug targets in parasitic protozoa." Trends Parasitol **18**(8): 366-371.
- Elfawal, M. A., M. J. Towler, N. G. Reich, P. J. Weathers and S. M. Rich (2015). "Dried whole-plant Artemisia annua slows evolution of malaria drug resistance and overcomes resistance to artemisinin." Proc Natl Acad Sci U S A **112**(3): 821-826.
- Gero, A. M., H. V. Scott, W. J. O'Sullivan and R. I. Christopherson (1989). "Antimalarial action of nitrobenzylthioinosine in combination with purine nucleoside antimetabolites." Mol Biochem Parasitol **34**(1): 87-97.
- Irwin, J. J. and B. K. Shoichet (2005). "ZINC--a free database of commercially available compounds for virtual screening." J Chem Inf Model **45**(1): 177-182.
- Kaiser, J. (2005). "Science resources. Chemists want NIH to curtail database." Science **308**(5723): 774.
- Kappes, B., C. D. Doerig and R. Graeser (1999). "An overview of Plasmodium protein kinases." Parasitol Today **15**(11): 449-454.
- Law, V., C. Knox, Y. Djoumbou, T. Jewison, A. C. Guo, Y. Liu, A. Maciejewski, D. Arndt, M. Wilson, V. Neveu, A. Tang, G. Gabriel, C. Ly, S. Adamjee, Z. T. Dame, B. Han, Y. Zhou and D. S. Wishart (2014). "DrugBank 4.0: shedding new light on drug metabolism." Nucleic Acids Res **42**(Database issue): D1091-1097.
- Lell, B. and P. G. Kremsner (2002). "Clindamycin as an antimalarial drug: review of clinical trials." Antimicrob Agents Chemother **46**(8): 2315-2320.
- Meijer, L. and E. Raymond (2003). "Roscovitine and other purines as kinase inhibitors. From starfish oocytes to clinical trials." Acc Chem Res **36**(6): 417-425.
- Min, T. H., M. F. Khairul, J. H. Low, C. H. Che Nasriyyah, N. A'Shikin A, M. N. Norazmi, M. Ravichandran and S. S. Raju (2007). "Roxithromycin potentiates the effects of

chloroquine and mefloquine on multidrug-resistant Plasmodium falciparum in vitro." Exp Parasitol **115**(4): 387-392.

- Mishra, L. C., A. Bhattacharya, M. Sharma and V. K. Bhasin (2010). "HIV protease inhibitors, indinavir or nelfinavir, augment antimalarial action of artemisinin in vitro." Am J Trop Med Hyg **82**(1): 148-150.

- Nag, S., D. Chouhan, S. N. Balaji, A. Chakraborty, K. Lhouvum, C. Bal, A. Sharon and V. Trivedi (2013). "Comprehensive screening of heterocyclic compound libraries to identify novel inhibitors for PfRIO-2 kinase through docking and substrate competition studies." Medicinal Chemistry Research **22**(10): 4737-4744.

- Seiler, K. P., G. A. George, M. P. Happ, N. E. Bodycombe, H. A. Carrinski, S. Norton, S. Brudz, J. P. Sullivan, J. Muhlich, M. Serrano, P. Ferraiolo, N. J. Tolliday, S. L. Schreiber and P. A. Clemons (2008). "ChemBank: a small-molecule screening and cheminformatics resource database." Nucleic Acids Res **36**(Database issue): D351-359.

Published papers

(1) Parveen, A., **Chakraborty, A**., Konreddy, A., Chakravarty, H., Sharon, A., Trivedi, V. and Bal, C. (2013). Skeletal hybridization and PfRIO-2 kinase modeling for synthesis of alpha-pyrone analogs as anti-malarial agent. *European journal of medicinal chemistry*, 70, pp.607--612.

(2) Nag, S., Chouhan, D., Balaji, S., **Chakraborty, A**., Lhouvum, K., Bal, C., Sharon, A. and Trivedi, V. (2013). Comprehensive screening of heterocyclic compound libraries to identify novel inhibitors for PfRIO-2 kinase through docking and substrate competition studies. *Medicinal Chemistry Research*, 22(10), pp.4737--4744.

(3) **Chakraborty, A.** and Trivedi, V. (2015). Streamlining the drug discovery process through repurposing of clinically approved drugs. *Austin Journal of Biotechnology & Bioengineering*, 2(3): 1047.

Communicated manuscripts

(1) **Chakraborty, A.**, Srivastava.K., Sahasrabuddhe, A.A and Trivedi, V* (2015). Methotrexate disturbs parasite life-cycle through targeting PfRIO-2 Kinase.

(2) **Chakraborty, A**., Srivastava.K., Sahasrabuddhe, A.A and Trivedi, V* (2015). Clindamycins antimalarial action depends on PfRIO-2 kinase binding and competition.

(3) **Chakraborty, A.**, Srivastava.K., Sahasrabuddhe, A.A and Trivedi, V* (2015). Antiviral agents are excellent source of antimalarial drugs: PfRIO-2 kinase binding and ATP competition studies.

(4) **Chakraborty, A**., Srivastava.K., Sahasrabuddhe, A.A and Trivedi, V* (2015). PfRIO-2 Kinase is a potential drug target in malaria parasite.

(5) **Chakraborty, A**., Srivastava.K., Sahasrabuddhe, A.A and Trivedi, V* (2015). Screening and identification of potential PfRIO-2 kinase interactors from heterocyclic compound libraries.

Publications in conference proceedings and participation in workshops.

- **Chakraborty, A**. and Trivedi, V. (2012, November). *Exploiting structural features of PfRIO-2 kinase for safe drug discovery against malaria.* Poster presented at the 81st annual meeting of the Society of Biological Chemists, Kolkata, WB.

- Deshmukh, R., **Chakraborty, A.**, Lhouvum,K., Balaji,. S.N., Layek,S. and Trivedi, V. (December 2013). Methemoglobin mediated immune-toxicity modulation of pro-oxidant molecules towards macrophages during malaria. Poster presented at the 82nd annual meeting of the Society of Biological Chemists, School of Life Sciences, University of Hyderabad, Andhra Pradesh, India.

- **Chakraborty, A**. and Trivedi, V. (2014, December). *Biochemical and cellular responses of the malaria parasite towards PFD0975w inhibitors.* Poster presented at the 38th All India Cell Biology Conference "Cellular Response to Drugs.", CDRI-Lucknow, UP.

- Participated in **National conference on- Recent advances in cancer biology & therapeutics 2014,** on December 2014 at IIT Guwahati.

- Participated in **Biotech Hub Symposium-2014** at IIT Guwahati, during December 2014.

- Training on **identification, *in vitro* cultivation and drug sensitivity of malaria parasite** at **National Institute of Malaria Research, New Delhi**, during July 2012**.**

- Participated in **International Symposium on Bioengineering 2012** at IIT Guwahati, during December 2012.

- Participated in a workshop on **'Basic techniques in bioinformatics'** at IIT Guwahati, during October 2011.

Med Chem Res (2013) 22:4737–4744
DOI 10.1007/s00044-013-0483-x

MEDICINAL CHEMISTRY RESEARCH

ORIGINAL RESEARCH

Comprehensive screening of heterocyclic compound libraries to identify novel inhibitors for PfRIO-2 kinase through docking and substrate competition studies

Swagata Nag · Devendra Kumar Chouhan · S. N. Balaji · Arnish Chakraborty · Kimjolly Lhouvum · Chandralata Bal · Ashoke Sharon · Vishal Trivedi

Received: 21 October 2012 / Accepted: 9 January 2013 / Published online: 22 January 2013

Abstract Malaria is most prevalent in tropical climate and causes 1–3 million deaths annually. RIO-2 kinase, an atypical kinase regulates ribosome biogenesis and is necessary for cell cycle progression. Structural characterization of PFD0975w (PfRIO-2 kinase) indicates N-terminal DNA binding winged helix domain (1–84), a linker region (85–147), and C-terminal kinase domain (148–275). Heterocyclic compounds present in different databases represent an enormous reservoir to screen and develop the suitable inhibitor. An extensive screening of heterocyclic compounds present in zinc database, PubChem and ChemBank database was done to identify potent PfRIO-2 kinase specific inhibitors. Initial screening gave 41 compounds with high affinity toward PfRIO-2 kinase than natural substrate ATP. A substrate competition experiment and analysis of binding mode conformation within the ATP binding pocket identifies five compounds; Zc-49775260, Pc-44415375, Pc-44215930, Cb-2082655, and Cb-832054 as potential PfRIO-2 kinase inhibitors. Further analysis of top hits in ADMET parameters, Caco-2 cell permeability profile, human oral absorption, and drug-like properties indicates Pc-44215930 as the best suitable compound among the top hits. Searching top hits candidate heterocyclic compounds in the drug database picked up clindamycin, nelfinavir, methacycline, and other drugs in circulation. Most of these drugs are targeting ribosome maturation and highlights the possibility of PfRIO-2 kinase as a drug target. Hence, screening and substrate competition studies along with ADME analysis of top hit compounds allowed us to identify potential PfRIO-2 kinase inhibitors. We are hopeful that the current study will help to develop effective chemotherapy against malaria utilizing PfRIO-2 kinase as a target.

Keywords Malaria · Docking · ATP · Kinome · RIO kinase · *P. falciparum* · Drug

Introduction

Malaria is most prevalent in tropical climate and causes 1–3 million deaths annually. It is more a serious disease for people living in Asia and Africa where infection is more prevalent (Sachs and Malaney 2002). The disease is in alarming situations due to development of multidrug-resistant strain and requires an urgent need for new chemotherapeutic agents exploiting novel drug targets. The genome sequence of *Plasmodium falciparum* has given the opportunity to identify and validate new drug targets (Gardner et al. 2002). Drug-resistant parasites devise a mechanism to overcome drug induced death and development of oxidative stress (Hastings 2003; Foley and Tilley 1998; Wongsrichanalai et al. 2002). Oxidative stress is in-turn linked to the protein production and co-ordinated regulation of down-stream events (Kumar et al. 2007). The pre-RNA formed after transcription is modified by multiple cleavage and assembly steps to produce mature RNA

Electronic supplementary material The online version of this article (doi:10.1007/s00044-013-0483-x) contains supplementary material, which is available to authorized users.

S. Nag · S. N. Balaji · A. Chakraborty · K. Lhouvum · V. Trivedi (✉)
Malaria Research Group, Department of Biotechnology, Indian Institute of Technology-Guwahati, Guwahati 781039, Assam, India
e-mail: vtrivedi@iitg.ernet.in; vishalash_1999@yahoo.com

D. K. Chouhan · C. Bal · A. Sharon
Department of Applied Chemistry, Birla Institute of Technology, Mesra, Ranchi 835215, India

Table 1 Docked results of selected ATP analogs from different databases

S. no.	Databases/ compound ID	Lowest binding scores of ATP analogs (kcal/mol)		Δ Binding scores (kcal/mol)
		Native PFD0975w	ATP bound PFD0975w	
1.	Cb_831927	−9.05	−4.09	−4.96
2.	Pc_45272815	−7.84	−3.98	−3.86
3.	Pc_5461108	−9.86	−6.56	−3.30
4.	Cb_907530	−9.65	−6.37	−3.28
5.	Cb_907097	−9.22	−6.39	−2.83
6.	Zc_40455206	−10.36	−7.54	−2.82
7.	Pc_44215930	−8.43	−5.70	−2.73
8.	Zc_40688936	−9.33	−6.66	−2.67
9.	Cb_2082655	−4.94	−2.32	−2.62
10.	Pc_23279499	−9.35	−6.73	−2.62
11.	Cb_3644580	−9.92	−7.31	−2.61
12.	Zc_40688973	−8.98	−6.56	−2.42
13.	Zc_12502112	−8.76	−6.39	−2.37
14.	Pc_6604891	−9.00	−6.65	−2.35
15.	Zc_3869450	−8.81	−6.47	−2.34
16.	Cb_832054	−7.82	−5.48	−2.34
17.	Pc_24916929	−10.51	−8.20	−2.31
18.	Zc_49775260	−8.06	−5.83	−2.23
19.	Zc_40685240	−8.83	−6.61	−2.22
20.	Pc_24917010	−9.82	−7.64	−2.18
21.	Pc_24867836	−9.46	−7.30	−2.16
22.	Pc_44828494	−8.87	−6.71	−2.16
23.	Zc_5543746	−8.05	−5.90	−2.15
24.	Pc_45268896	−10.47	−8.33	−2.14
25.	Cb_2086943	−4.31	−2.18	−2.13
26.	Zc_3830180	−8.35	−6.23	−2.12
27.	Zc_3869448	−8.64	−6.56	−2.08
28.	Cb_907395	−9.58	−7.56	−2.02
29.	Cb_1310	−7.28	−5.26	−2.02
30.	Zc_4514079	−7.99	−5.99	−2.00
31.	Zc_36533557	−7.74	−5.80	−1.94
32.	Cb_832083	−8.18	−6.25	−1.93
33.	Cb_2102164	−5.60	−3.70	−1.90
34.	Pc_44415375	−8.46	−6.56	−1.90
35.	Zc_4475067	−7.92	−6.03	−1.89
36.	Pc_24916928	−8.35	−6.47	−1.88

The heterocyclic compounds from zinc (Zc), PubChem (PC), and ChemBank (CB) and docking into the PfRIO-2 kinase or PfRIO-2-ATP kinase was performed as described in Materials and methods

(Jackson et al. 2011). The pre-RNA processing involved endo and exonucleases (cleavage of pre-RNA at conserved sites), methyltransferase (methylation), or small nucleolar ribonucleoproteins (Smith and Steitz 1997). Precise regulation of these components of pre-RNA assembly is required to respond many cellular signals for protein synthesis (Leary and Huang 2001). Disruption of ribosome biogenesis disturbs cellular adaptation to changed environmental condition (oxidative stress, food, temp, etc.), cell growth and proliferation (Bottger 2006). Hence, a number of crucial regulatory steps of ribosome biogenesis can be probed to inhibit growth of an organism and design suitable drug against it.

Bioinformatics and *in silico* analysis has identified ~65 protein kinases in the malaria parasite kinome (Doerig et al. 2008). RIO-2 kinase, an atypical kinase regulates ribosome biogenesis and necessary for cell cycle progression in yeast (Angermayr et al. 2002; Vanrobays et al. 2001). Two RIO like kinase, RIO-1 (PFL1490w) and RIO-2 kinase (PFD0975w) are present in the malaria kinome with uncharacterized function. Structural characterization of PFD0975w (PfRIO-2 kinase) indicates N-terminal DNA binding winged helix domain (1–84), a linker region (85–147), and C-terminal kinase domain (148–275). Kinase domain has well-defined ATP binding pocket with mixed environments to support the different regions of ATP molecules. The difference between ATP binding pocket between PfRIO-2 kinase and human RIO-2 (HuRIO-2 kinase) makes PfRIO-2 kinase an excellent drug target. In comparison to other typical protein kinase present in parasite, PfRIO-2 kinase represent additional advantages as drug target such as the absence of activation loop and difference in other structural features. Recently, we performed an extensive screening of naturally occurring bioactive molecules (phytochemical) to develop potential inhibitors against the PfRIO-2 kinase. An *in silico* screening and substrate competition experiment has identified rutin, bebeerines, isochondrodendrine, nimbin, and punicalagin as a potential PfRIO-2 inhibitor (Nag et al. 2012). Phytochemicals are excellent therapeutic molecule but they represent a number of limitations to be optimized as future drug-like molecule; low abundance, difficulties in chemical modification of side group and chemical synthesis. Hence in the current work, we performed extensive screening of heterocyclic compounds from zinc database (http://zinc.docking.org), PubChem (http://pubchem.ncbi.nlm.nih.gov) and ChemBank database (http://chembank.broadinstitute.org) to identify potent PfRIO-2 kinase specific inhibitors. Substrate ATP was used to search the databases and select potential drug-like molecules. A total of 2,473 heterocyclic compounds with structures similar to ATP are selected and an initial docking screening is performed on PfRIO-2 kinase as a target using AutoDock 4.1. The initial docking screen gave 41 compounds with high affinity toward PfRIO-2 than ATP. A substrate competition experiment and analysis of binding mode conformation within ATP pocket identifies five compounds with zinc ID 49775 260 (Zc-49775260), PubChem ID 44415375 (Pc-4441 5375), PubChem ID 44215930 (Pc-44215930), Chem Bank

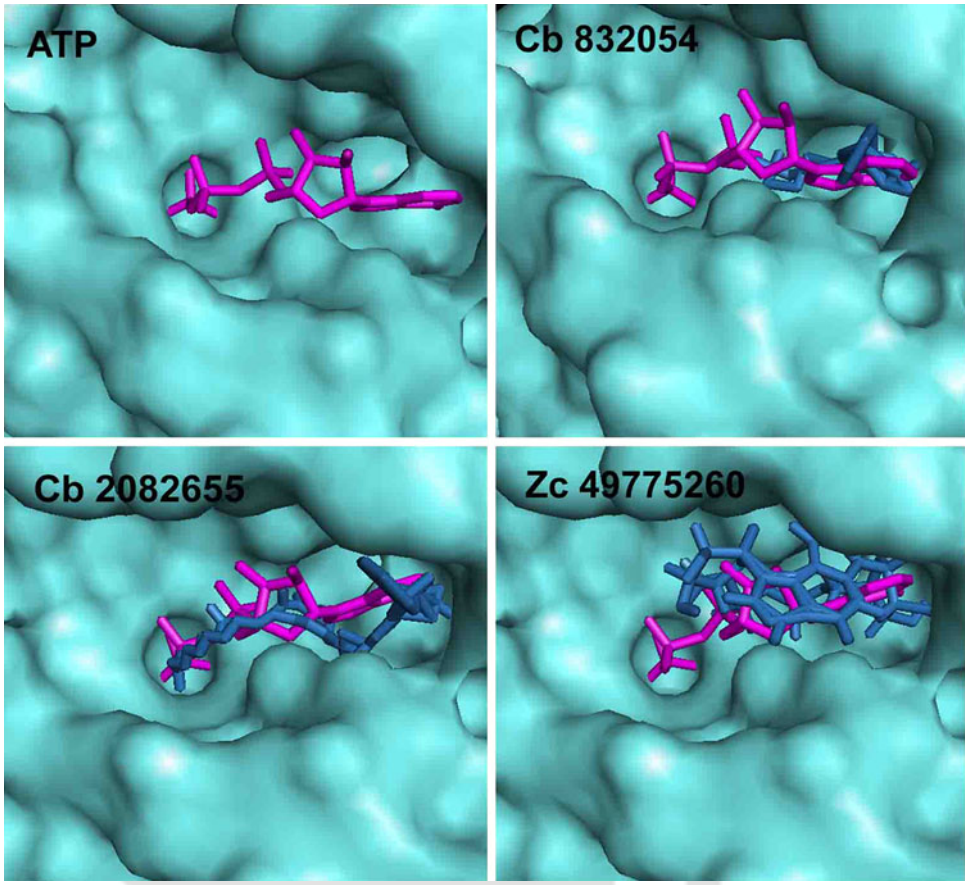

Fig. 1 Heterocyclic compounds from different libraries binds into the ATP binding pocket of the PfRIO-2 kinase. ATP binding pocket in PFRIO-2 is well defined, and heterocyclic compound binds different region with the pocket. A representative of heterocyclic compounds such as Cb-832054, Cb-2082655, and Zc-49775260 binding modes within the binding pocket is shown. ATP and different ligands occupy same conformation within the binding pocket. ATP and ligands were colored as *magenta* and *sky blue colored*, respectively, in different panel (Color figure online)

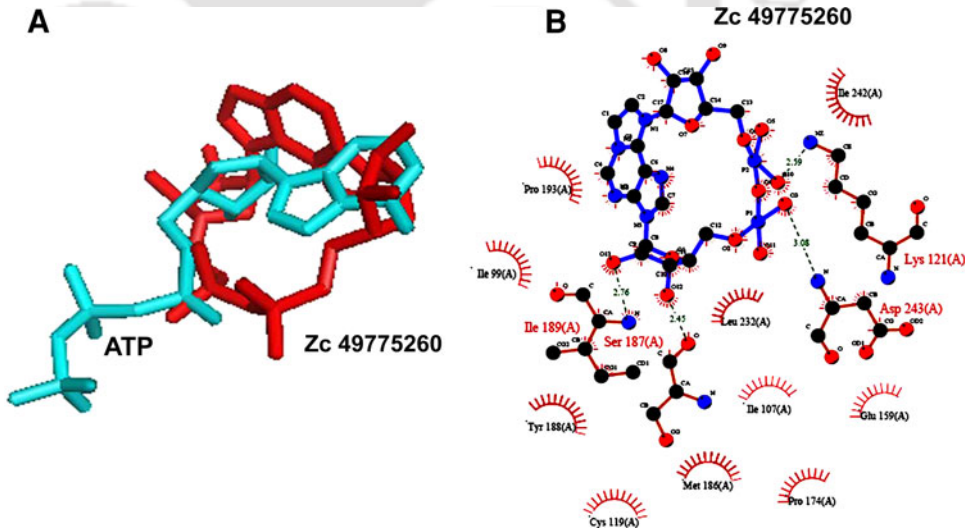

Fig. 2 Heterocyclic compounds adopt a similar 3-D conformation as ATP within binding pocket. Lead heterocyclic compound Zc-49775260 superimpose very nicely to the ATP structure and exhibit extensive interactions with the protein residues. **a** Overlay of ATP and Zc-49775260 and **b** interaction of Zc-49775260 with PfRIO-2 residues was shown, ATP and Zc-49775263 were *magenta* and *sky blue colored*, respectively (Color figure online)

ID 2082655 (Cb-2082655), and Chem Bank ID 832054 (Cb-832054) as potential PfRIO-2 kinase inhibitors. A pharmacological analysis and searching potential heterocyclic compounds in the drug database indicates the suitability of these compounds as potential drug-like molecules. We are hopeful that the current study will help to develop effective chemotherapy against malaria utilizing PfRIO-2 kinase as a target.

Materials and methods

Heterocyclic database and collection of compounds

Heterocyclic compounds are collected from zinc database (http://zinc.docking.org), PubChem (http://pubchem.ncbi.nlm.nih.gov) and ChemBank database (http://chembank.broadinstitute.org). To retrieve the compounds from zinc database

Table 2 Interaction of heterocyclic compounds with PfRIO-2 kinase [present(+)/absent(−)]

S. no.	Protein atom	ATP atom	Zc 49775260	Pc 44415375	Pc 44215930	Cb 2082655	Cb 832054
1.	M186	N6	+	+	+	+	+
2.	I189	N1	+	+	+	+	+
3.	I189	C2	+	+	+	+	+
4.	I99	C1	+	–	+	+	+
5.	I99	O4′	+	–	+	+	+
6.	E104	O2G	–	–	–	–	–
7.	E104	O1B	–	–	–	–	–
8.	E104	O1G	–	–	–	–	–
9.	E104	PG	–	–	–	–	–
10.	E104	O1	–	–	–	–	–
11.	K121	O1A	+	+	+	+	+
12.	K121	O3G	+	+	+	+	+
13.	K121	O3A	+	+	+	+	+
14.	S187	N6	+	+	–	+	–
15.	S105	O3G	–	–	–	–	–
16.	S105	O1G	–	–	–	–	–
17.	S105	O3B	–	–	–	–	–
18.	D243	O1B	+	+	+	+	+
19.	D243	O2G	+	+	+	+	+
20.	R127	O1G	–	–		–	–

(Irwin and Shoichet 2005), adenine triphosphate (ATP) was drawn with the help of chemical editor and converted into alphanumeric code, smiles. It serves as a text to search 70 % similar drug-like molecules in the database and structure file of the corresponding molecules are downloaded in SDF format. The similar searching strategy was used to retrieve the molecules from PubChem (Kaiser 2005) and ChemBank database (Seiler et al. 2008). The number of heterocyclic compounds used for virtual screening from different databases are given in Table S1.

In silico virtual screening of heterocyclic compounds against the PfRIO-2 kinase

The 3-D structure of the PfRIO2 kinase (PFD0975w) was generated as described previously and the virtual docking experiment was performed by AutoDock 4.0 program suite of MGL Tools 1.5.4 software (Rosenfeld et al. 2003). PfRIO-2 (target protein) and candidate molecules were prepared as described (Nag et al. 2012). The complete docking protocol was as follows, first the 3-D co-ordinate of candidate molecules were checked for polar hydrogens, then atomic charges and flexible torsions were defined. The resulting PDBQT file was used as a ligand in docking experiment. For macromolecules PfRIO-2 kinase, polar hydrogen, Kollman charges, and atomic solvation parameters were assigned and a grid of 0.4 Å resolution was centered using an autogrid module of AutoDock 4.1. A number of docking parameters, number of generations, energy evaluation, and the GA run were set as 27000, 2500000, and 10, respectively. Finally, docked conformations were selected based on interaction energy. Initially, the natural substrate ATP was used as a positive control to optimize the docking parameters and the docked conformation was compared with the ATP bound PfRIO-2 kinase generated before (Trivedi and Nag 2012). AutoDock gives several conformation of docked ligand. The affinity of a particular ligand is determined by the interaction energy between a particular ligand conformation and the target protein. It can be used to sort the ligand conformation to choose the best possible ligand conformation. To avoid artifacts and compare binding affinity of different inhibitor molecules, docking protocol and parameters were kept constant.

Substrate competition assay

Intermolecular docking energy of an inhibitor specific toward an active form of the PfRIO-2 kinase might be sensitive to the presence of substrate (ATP) within the binding pocket. ATP was added into the PfRIO-2 kinase and molecular model (PfRIO-2-ATP) was generated as described previously (Trivedi and Nag 2012). In brief, a homology modeling protocol was used to model ATP bound form of the PfRIO-2 kinase using an ATP bound form of AfRIO-2 (PDB code 1ZAO) as a template (LaRonde-LeBlanc and Wlodawer 2004). ATP and Mg^{2+} were taken out from the template structure and added into

Table 3 Docked results of top lead ATP analogs from all databases

S. no.	Databases/ compound ID	Lowest binding scores (kcal/mol) of ATP analogs		Δ Binding scores (kcal/mol)
		PfRIO-2 kinase	HuRIO-2 kinase	
1.	Cb_831927	−9.05	−3.96	5.09
2.	Cb_907530	−9.65	−4.83	4.82
3.	Pc_45272815	−7.84	−3.45	4.39
4.	Cb_2082655	−4.94	−0.80	4.14
5.	Pc_24867836	−9.46	−5.33	4.13
6.	Zc_40688936	−9.33	−5.33	4.00
7.	Zc_40685240	−8.83	−5.11	3.72
8.	Zc_40455206	−10.36	−6.68	3.68
9.	Zc_40688973	−8.98	−5.37	3.61
10.	Zc_3830180	−8.35	−4.85	3.50
11.	Pc_23279499	−9.35	−5.86	3.49
12.	Cb_832054	−7.82	−4.41	3.41
13.	Zc_3869448	−8.64	−5.28	3.36
14.	Cb_3644580	−9.92	−6.67	3.25
15.	Zc_49775260	−8.06	−5.11	2.95
16.	Cb_907097	−9.22	−6.46	2.76
18.	Cb_2086943	−4.31	−1.62	2.69
19.	Pc_5461108	−9.86	−7.23	2.63
20.	Cb_1310	−7.28	−4.76	2.52
21.	Cb_907395	−9.58	−7.07	2.51
22.	Pc_44215930	−8.43	−6.09	2.34
23.	Pc_6604891	−9.00	−6.99	2.01
24.	Zc_4514079	−7.99	−6.09	1.90
25.	Zc_5543746	−8.05	−6.19	1.86
26.	Zc_3869450	−8.81	−7.15	1.66
27.	Pc_45268896	−10.47	−8.92	1.55
28.	Pc_24916929	−10.51	−9.17	1.34
29.	Pc_44828494	−8.87	−7.75	1.12
30.	Pc_24917010	−9.82	−9.53	0.29

The heterocyclic compounds from zinc (Zc), PubChem (Pc), and ChemBank (Cb) and docking into the PfRIO-2 kinase or HuRIO-2 kinase was performed as described in Materials and methods

the modeled structure to generate ATP bound active form of the PfRIO-2 kinase (PfRIO-2-ATP). In substrate competition experiment, PfRIO-2-ATP kinase was used as target enzyme instead of PfRIO-2 native structure. Docking protocol and parameters remained constant between docking experiments of inhibitors with PfRIO-2 and PfRIO-2-ATP.

Drug-like properties estimation

The ADMET properties of compounds were predicted using QikProp utility of Schrodinger's suite 2011 (Schrödinger 2011). QikProp predicts the physicochemical descriptors and pharmaceutically relevant properties which are known to influence absorption, metabolism, and bioavailability. Property or descriptor values that fall outside the 95 % range of similar values for known drugs are indicated with star mark.

Results and discussion

Heterocyclic compound libraries represent a promising source of PfRIO-2 kinase inhibitors

Zinc, PubChem, and ChemBank databases represent a large and enormous collection of heterocyclic compounds with excellent potentials of being leads for drug development. In our previous work, PfRIO-2 Kinase was found to be a suitable drug target as it has a number of structural features which can be exploited. PfRIO-2 kinase has a well-defined binding pocket to harbor substrate ATP (Nunes et al. 2007). Moreover, it exhibits significant differences in an ATP binding pocket from human (HuRIO-2 kinase) homolog (Trivedi and Nag 2012). Substrate ATP was used as an initial molecule to search the database and a total of 2,473 drug-like molecules are selected. The initial docking screen gave 41 molecules with high affinity toward PfRIO-2 than ATP (Table 1). The binding energy of ATP is −2.63 kcal/mol. Under in vivo conditions, an enzyme might have bound substrate or local concentration of substrate might be very high. A substrate competition assay was performed to test relative affinity of heterocyclic compounds toward PfRIO-2 in the presence of substrate ATP. Keeping docking parameters constant, a molecular docking of heterocyclic compounds from first docking screen were again performed with PfRIO-2-ATP as a target. PfRIO-2-ATP contains a bound ATP present within the pocket and serves as substrate bound PfRIO-2 kinase. Docking results of heterocyclic compounds into native enzyme (PfRIO-2 kinase) versus substrate bound form (PfRIO-2-ATP) indicates that heterocyclic compounds exhibit significant differences (Table 1). Docked conformation of all heterocyclic compounds within binding pockets indicates partial, complete, or no overlap between bound ATP and heterocyclic compounds. Five compounds with zinc ID 49775260 (Zc-49775260), PubChem ID 44415375 (Pc-44415375), PubChem ID 44215930 (Pc-44215930), Chem Bank ID 2082655 (Cb-2082655), and Chem Bank ID 832054 (Cb-832054) binds in a similar conformation as ATP within the binding pocket (Fig. 1). All five compounds are structurally very different from ATP but they adopt a similar conformation as ATP to fit into the binding pocket (Fig. 2). The top hits compounds from different libraries interact extensively with the protein residues including several crucial interactions required for

Table 4 Drug-like properties of top hits heterocyclic compounds

S. no.	Property data base no.	Observed values					Range
		Zc-49775260	Pc-44415375	Pc-44215930	Cb-832054	Cb-2082655	
1.	CIQP log S—conformation independent	−2.685	−3.375	−2.844	−2.494	−6.489 M	(−6.5/0.5)
2	QP log BB for brain/blood	−3.477*	−2.899	−1.446	−5.242*	−7.772 M*	(−3.0/1.2)
3.	No. of primary metabolites	7	5	7	3	8	(1.0/8.0)
4.	Apparent Caco-2 permeability (nm/s)	0	1	368	0	0	(<25 poor, >500 great)
5.	Lipinski rule of five violations	3	1	0	3	3	(maximum is four)
6.	Jorgensen rule of three violations	2	1	1	1	2	(maximum is three)
7.	% Human oral absorption in GI (±20%)	0	18	76	0	0 M	(<25 % is poor)

CIQPlogS conformation-independent predicted aqueous solubility, log S. S in mol/dm^3 is the concentration of the solute in a saturated solution that is in equilibrium with the crystalline solid

QPlogBB predicted brain/blood partition coefficient. *Note* predictions are for orally delivered drugs so, for example, dopamine and serotonin are CNS negative because they are too polar to cross the blood–brain barrier

QPPCaco predicted apparent Caco-2 cell permeability in nm/s. Caco-2 cells are a model for the gut blood barrier. QikProp predictions are for non-active transport

Rule of five number of violations of Lipinski's rule of five. The rules are: mol_MW < 500, QPlogPo/w < 5, donorHB ≤ 5, accptHB ≤ 10. Compounds that satisfy these rules are considered drug-like

Rule of three number of violations of Jorgensen's rule of three. The three rules are: QPlogS > −5.7, QPPCaco > 22 nm/s, primary metabolites < 7. Compounds with fewer (and preferably no) violations of these rules are more likely to be orally available

Percent human oral absorption predicted human oral absorption on 0–100 % scale. The prediction is based on a quantitative multiple linear regression model

Asterisks (*) indicates the number of property or descriptor values fall outside the 95 % range of similar values for known drugs

Table 5 Similarity (%) of heterocyclic compounds with existing approved drug molecules

Compound code	Name of drug and % similarity				
Zc-49775260	Dipyridamole 57.47	Idarubicin 52.44	Monoxerutin 51.73	Lymecycline 49.57	Nelfinavir 49.42
Cb-44415375	Benfotiamine 64.55	Adefovir 63.31	Mopidamol 63.24	Tenofovir 61.76	Spirapril 60.44
Cb-44215930	Idarubicin 76.18	Theodrenaline 75.86	Clindamycin 75.83	Reproterol 75.75	Methacycline 72.88
Cb-832054	Mopidamol 58.47	Benfotiamine 55.45	Lisinopril 55.42	Adefovir 54.05	Tenofovir 52.88
Cb-2082655	Miokamycin 40.38	Roxithromycin 38.53	Methotrexate 38.52	Glucametacin 38.21	Aminopterin 38.21

ATP binding (Table 2). As a result, these molecules will be potent to block the ATP binding site as well as will be competent enough to remove bound ATP to inhibit PfRIO-2 kinase catalyzed phosphorylation reactions.

Heterocyclic compounds target PfRIO-2 kinase without affecting HuRIO-2 kinase

The cross reactivity of small molecule heterocyclic with the host enzymes need to be checked before pursuing such molecules for further pharmacological and toxicity characterization. The HuRIO-2 Kinase molecular model was prepared as described previously (Trivedi and Nag 2012). A docking experiment of all top hit heterocyclic compounds with HuRIO-2 kinase was performed under identical parameters as previous docking experiment with PfRIO-2 kinase. The docking results were analyzed to compare the binding energy and binding mode within the ATP binding pocket of HuRIO-2 and PfRIO-2 kinase. Binding energy of top hit heterocyclic compounds with HuRIO-2 kinase and PfRIO-2 kinase indicates a significant difference between human and parasite enzymes (Table 3). Analysis of HuRIO-2 kinase: heterocyclic molecular model further supports the binding energy differences between human and parasite enzymes. Heterocyclic compounds bind very loosely into the HuRIO-2 kinase and interactions within the binding pocket with protein residues is significantly less compared to PfRIO-2-heterocyclic interactions. Although the affinity (binding energy) of most of the compounds is higher than ATP toward HuRIO-2 kinase. But a significant difference in affinity of the same molecule between HuRIO-2 kinase and PfRIO-2 kinase allow us to select a concentration which might exclusively bind to PfRIO-2 kinase.

Top hit candidates have drug-like properties

The predicted ADMET parameters are reported in Table 4. Additional ADMET parameters are given in Table S2. The QikProp analysis was performed using default setting to calculate the ADMET properties with the identification of five most drug-like molecules in relation with the input molecule. The ranges and limits of the properties were analyzed with reference to existing drug properties databases. The selected molecules were also compared with close similarities for the identification of five most drugs like molecules. The Pc-44215930 was considered more interesting as it did not violate the Lipinski's rule of five (Lipinski et al. 2001). Further it is found moderately suitable in terms of Jorgensen's rule. Thus, the present modeling studies support the rational toward the selection of analogs. Overall based on docking, substrate competition studies and *in silico* toxicity analysis found Pc-44215930 as the most promising drug-like molecule with potential to exhibit antimalarial activity utilizing PfRIO-2 kinase as a target. In addition, searching similar drugs to top hits candidate heterocyclic compounds into drug database (QikProp utility of Schrodinger's suite 2011) picked up clindamycin, nelfinavir, methacycline, lymecycline, miokamycin, roxithromycin, and other drugs in circulation for different diseases (Table 5). The antimalarial potential of clindamycin, nelfinavir, and methacycline is documented, and these drugs disturb the ribosome maturation or protein synthesis (Lell and Kremsner 2002; Dar et al. 2008; Holliday and Faulds 1993; Nsanzabana and Rosenthal 2011). RIO-2 kinase has a potential role in ribosome maturation (LaRonde-LeBlanc and Wlodawer 2005) and our current study highlights the possibility of PfRIO-2 kinase as a potential target behind the antimalarial action of these molecules.

Pharmacophore perception

To explore the scope to improve the parent compound Pc-44215930, pharmacophoric sites are identified. The Cb-44215930 was prepared in LigPrep module of Schrodinger's suite 2011 using MMFF'S force field followed by the conformational search utility in MacroModel to find out the best possible conformation for binding. The prepared ligands imported to Phase to develop the Pharmacophoric sites (Fig. 3). The pharmacophoric sites were developed for Pc-44215930 using create a site option in phase pharmacophore model development utility. Hydrogen bond donor, hydrophobic group and ring pharmacophoric sites are present in Pc-44215930 (Fig. 3a). In addition, Pc-44215930 has several hydrogen bond acceptor sites (Fig. 3b). The pharmacophoric site discussed as above may allow the molecule to make interaction with protein residues as evident in the interaction analysis (Table 2). These interactive sites can be modulated to further optimize the inhibitory potentials and identify better antimalarials exploiting PfRIO-2 kinase as a target. In summary, *in silico* docking and substrate competition study is a robust utility to screen heterocyclic compound library and it might assist us to develop a PfRIO-2 kinase targeted antimalarials.

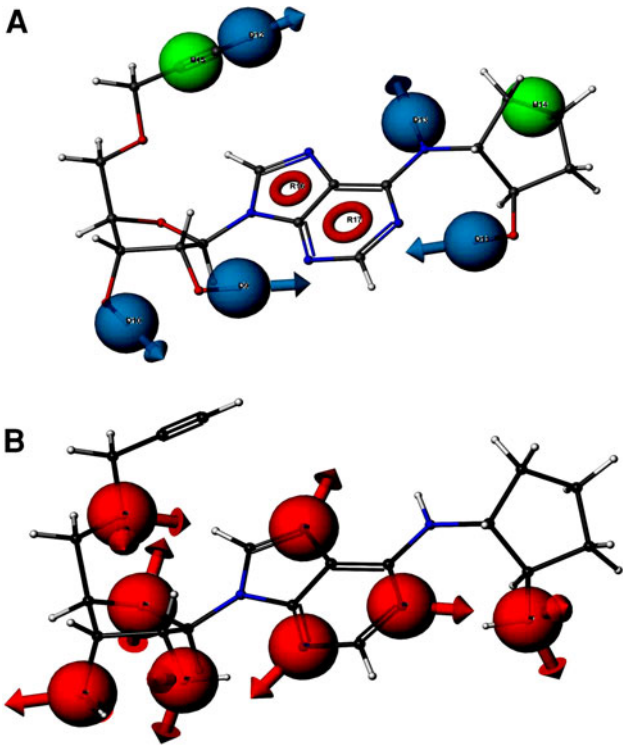

Fig. 3 Pharmacophoric sites of Cb-4215930. **a** Pharmacophoric features showing H-bond donor (*light blue*), hydrophobic (*green sphere*) and ring pharmacophoric sites in Cb-44215930. **b** Phase pharmacophoric features showing H-bond acceptor (*light red*) sites in Cb-44215930 (Color figure online)

Acknowledgments This work was supported by the Department of Biotechnology, Govt of India Grants BT/PR13436/MED/12/450/2009 & BT/41/NE/TBP/2010 to V.T.

Conflict of interest The authors declare that they have no competing interests.

References

Angermayr M, Roidl A, Bandlow W (2002) Yeast Rio1p is the founding member of a novel subfamily of protein serine kinases involved in the control of cell cycle progression. Mol Microbiol 44(2):309–324

Bottger EC (2006) The ribosome as a drug target. Trends Biotechnol 24(4):145–147. doi:S0167-7799(06)00049-7

Dar O, Khan MS, Adagu I (2008) The potential use of methotrexate in the treatment of falciparum malaria: in vitro assays against

sensitive and multidrug-resistant falciparum strains. Jpn J Infect Dis 61(3):210–211

Doerig C, Billker O, Haystead T, Sharma P, Tobin AB, Waters NC (2008) Protein kinases of malaria parasites: an update. Trends Parasitol 24(12):570–577

Foley M, Tilley L (1998) Quinoline antimalarials: mechanisms of action and resistance and prospects for new agents. Pharmacol Ther 79(1):55–87. doi:S0163-7258(98)00012-6

Gardner MJ, Hall N, Fung E, White O, Berriman M, Hyman RW, Carlton JM, Pain A, Nelson KE, Bowman S, Paulsen IT, James K, Eisen JA, Rutherford K, Salzberg SL, Craig A, Kyes S, Chan MS, Nene V, Shallom SJ, Suh B, Peterson J, Angiuoli S, Pertea M, Allen J, Selengut J, Haft D, Mather MW, Vaidya AB, Martin DM, Fairlamb AH, Fraunholz MJ, Roos DS, Ralph SA, McFadden GI, Cummings LM, Subramanian GM, Mungall C, Venter JC, Carucci DJ, Hoffman SL, Newbold C, Davis RW, Fraser CM, Barrell B (2002) Genome sequence of the human malaria parasite *Plasmodium falciparum*. Nature 419(6906): 498–511. doi:10.1038/nature01097

Hastings IM (2003) Malaria control and the evolution of drug resistance: an intriguing link. Trends Parasitol 19(2):70–73. doi:S147149220200017X

Holliday SM, Faulds D (1993) Miocamycin. A review of its antimicrobial activity, pharmacokinetic properties and therapeutic potential. Drugs 46(4):720–745

Irwin JJ, Shoichet BK (2005) ZINC—a free database of commercially available compounds for virtual screening. J Chem Inf Model 45(1):177–182. doi:10.1021/ci049714+

Jackson KE, Habib S, Frugier M, Hoen R, Khan S, Pham JS, Ribas de Pouplana L, Royo M, Santos MA, Sharma A, Ralph SA (2011) Protein translation in *Plasmodium* parasites. Trends Parasitol 27(10):467–476. doi:10.1016/j.pt.2011.05.005

Kaiser J (2005) Science resources. Chemists want NIH to curtail database. Science 308(5723):774. doi:10.1126/science.308.5723.774a

Kumar S, Guha M, Choubey V, Maity P, Bandyopadhyay U (2007) Antimalarial drugs inhibiting hemozoin (beta-hematin) formation: a mechanistic update. Life Sci 80(9):813–828

LaRonde-LeBlanc N, Wlodawer A (2004) Crystal structure of *A. fulgidus* Rio2 defines a new family of serine protein kinases. Structure 12(9):1585–1594. doi:10.1016/j.str.2004.06.016

LaRonde-LeBlanc N, Wlodawer A (2005) A family portrait of the RIO kinases. J Biol Chem 280(45):37297–37300. doi:10.1074/jbc.R500013200

Leary DJ, Huang S (2001) Regulation of ribosome biogenesis within the nucleolus. FEBS Lett 509(2):145–150

Lell B, Kremsner PG (2002) Clindamycin as an antimalarial drug: review of clinical trials. Antimicrob Agents Chemother 46(8): 2315–2320

Lipinski CA, Lombardo F, Dominy BW, Feeney PJ (2001) Experimental and computational approaches to estimate solubility and permeability in drug discovery and development settings. Adv Drug Deliv Rev 46(1–3):3–26

Nag S, Prasad K, Trivedi V (2012) Identification and screening of antimalarial phytochemical reservoir from northeastern Indian plants to develop PfRIO-2 kinase inhibitor. Eur Food Res Technol 234(5):905–911. doi:10.1007/s00217-012-1692-0

Nsanzabana C, Rosenthal PJ (2011) In vitro activity of antiretroviral drugs against *Plasmodium falciparum*. Antimicrob Agents Chemother 55(11):5073–5077. doi:10.1128/AAC.05130-11

Nunes MC, Goldring JP, Doerig C, Scherf A (2007) A novel protein kinase family in *Plasmodium falciparum* is differentially transcribed and secreted to various cellular compartments of the host cell. Mol Microbiol 63(2):391–403

Rosenfeld RJ, Goodsell DS, Musah RA, Morris GM, Goodin DB, Olson AJ (2003) Automated docking of ligands to an artificial active site: augmenting crystallographic analysis with computer modeling. J Comput Aided Mol Des 17(8):525–536

Sachs J, Malaney P (2002) The economic and social burden of malaria. Nature 415(6872):680–685. doi:10.1038/415680a

Schrödinger (2011) Suite 2011. LLC, New York

Seiler KP, George GA, Happ MP, Bodycombe NE, Carrinski HA, Norton S, Brudz S, Sullivan JP, Muhlich J, Serrano M, Ferraiolo P, Tolliday NJ, Schreiber SL, Clemons PA (2008) ChemBank: a small-molecule screening and cheminformatics resource database. Nucleic Acids Res 36:D351–D359. doi:10.1093/nar/gkm843

Smith CM, Steitz JA (1997) Sno storm in the nucleolus: new roles for myriad small RNPs. Cell 89(5):669–672. doi:S0092-8674(00)80247-0

Trivedi V, Nag S (2012) *In silico* characterization of atypical kinase PFD0975w from *Plasmodium* kinome: a suitable target for drug discovery. Chem Biol Drug Des 79(4):600–609. doi:10.1111/j.1747-0285.2012.01321.x

Vanrobays E, Gleizes PE, Bousquet-Antonelli C, Noaillac-Depeyre J, Caizergues-Ferrer M, Gelugne JP (2001) Processing of 20S pre-rRNA to 18S ribosomal RNA in yeast requires Rrp10p, an essential non-ribosomal cytoplasmic protein. EMBO J 20(15): 4204–4213. doi:10.1093/emboj/20.15.4204

Wongsrichanalai C, Pickard AL, Wernsdorfer WH, Meshnick SR (2002) Epidemiology of drug-resistant malaria. Lancet Infect Dis 2(4):209–218. doi:S1473309902002396

European Journal of Medicinal Chemistry 70 (2013) 607–612

Contents lists available at ScienceDirect

European Journal of Medicinal Chemistry

journal homepage: http://www.elsevier.com/locate/ejmech

Preliminary communication

Skeletal hybridization and PfRIO-2 kinase modeling for synthesis of α-pyrone analogs as anti-malarial agent

Afsana Parveen [a], Arnish Chakraborty [b], Ananda Kumar Konreddy [a], Harapriya Chakravarty [a], Ashoke Sharon [a], Vishal Trivedi [b,**], Chandralata Bal [a,*]

[a] Department of Applied Chemistry, Birla Institute of Technology, Mesra, Ranchi 835215, India
[b] Malaria Research Group, Department of Biotechnology, Indian Institute of Technology, Guwahati 781039, Assam, India

ARTICLE INFO

Article history:
Received 13 July 2013
Received in revised form
19 September 2013
Accepted 11 October 2013
Available online 23 October 2013

Keywords:
Anti-malarial
Pyrone analogs
Plasmodium falciparum
RIO2 kinase
Molecular modeling
Induced fit docking

ABSTRACT

The pharmacophoric hybridization and computational design approach were applied to generate a novel series of α-pyrone analogs as plausible anti-malarial lead candidate. A putative active site in flexible loop close to wing-helix domain of PfRIO2 kinase was explored computationally to understand the molecular basis of ligand binding. All the synthesized molecules (**3a**–**g**) exhibited *in vitro* antimalarial activity. Oxidative stress induced by **3a**–**d** were calculated and found to be significantly higher in case of **3b**. Therefore, **3b**, which shown most significant result was identified as promising lead for further SAR study to develop potent anti-malarials.

1. Introduction

Malaria is a protozoal parasitic disease that causes millions of death worldwide every year. In addition, the treatment is becoming more and more difficult because of emergence of drug-resistant malaria. Artemisinin combination therapy (ACT) has been useful over past decades [1], but the recent emergence of ACT resistance [2] provides strong motivation to discover new potential antimalarial drugs. Parasite growth and ability to maintains stress is linked to the down-stream signaling and ribosome biogenesis [3]. RIO like kinase, RIO-1 (PFL1490w) and RIO-2 kinase (PFD0975w) are present in the malaria kinome with uncharacterized function (www.plasmodb.org). Structural characterization of PFD0975w, the RIO-2 kinase of Plasmodium Falciparum (PfRIO-2 kinase) indicates N-terminal DNA binding winged helix domain (1–84), a linker region (85–147) and C-terminal kinase domain (148–275). It has a well defined ATP binding pocket and is significantly different than the human RIO-2 kinase [4]. Further, the absence of activation loop and distinguished structural features of PfRIO-2 kinase provides an opportunity to explore it as a new drug target [4]. Recently, naturally occurring bioactive molecules and selected heterocycles were screened against PfRIO-2 kinase, which allow us to delineate pharmacological points required for inhibitor development against PfRIO-2 kinase [5,6].

Febrifugine (**I**, Fig. 1), a natural product with high anti-malarial activity [7]. was isolated in 1947 from the roots of a Chinese shrub, *Chang Shan*. The 4-quinazolinone moiety, 1′-amino and C-2′ as well as C-3″O-functionalities are crucial for the anti-malarial activity of febrifugine [8]. Argentilactone (**II**, Fig. 1), isolated from the roots and the leaves of *Raimondia cf. monoica* was found to have ED_{50} of 0.1 μg/mL against *Plasmodium falciparum* (*P. falciparum*) [9]. It was the first report of α-pyrone derivative having anti-malarial activity. However, due to toxicity [9,10] both these molecules couldn't develop as a clinical drug. Recently, 4(1*H*)-quinolone ester derivatives (**III**, Fig. 1) with two close keto groups have been considered as promising anti-malarials needing further SAR and optimization [11]. In our ongoing anti-malarial lead identification project, we intended to apply hybridization of the identified pharmacophores (Fig. 1) and generated a novel α-pyrone skeleton (**IV**, Fig. 1). In the current work, we carried out detailed *in-silico*

Abbreviations: RIO2 kinase, right open reading frame 2 kinase; PfRIO2 kinase, *Plasmodium falciparum* RIO2 kinase; ATP, adenosine triphosphate; DNA, deoxyribonucleic acid; w-HTH, wing helix domain.

* Corresponding author. Tel.: +91 651 2276531; fax: +91 651 2275401.
** Corresponding author. Tel.: +91 361 2582217; fax: +91 361 258 2249.
E-mail addresses: vtrivedi@iitg.ernet.in, Vishalash_1999@yahoo.com (V. Trivedi), chandralata.bal@gmail.com, cbal@bitmesra.ac.in (C. Bal).

0223-5234/$ – see front matter © 2013 Elsevier Masson SAS. All rights reserved.
http://dx.doi.org/10.1016/j.ejmech.2013.10.028

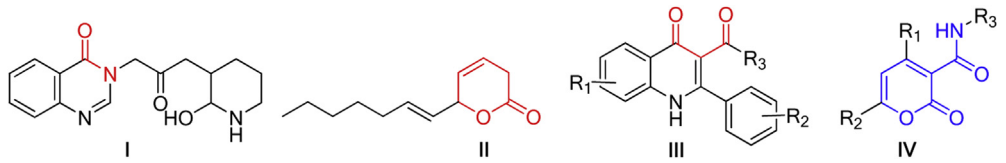

Fig. 1. Structures of reported potent antimalarials (**I**–**III**), identified pharmacophores (red) for hybridization and newly generated hybridized skeleton (blue). (For interpretation of the references to color in this figure legend, the reader is referred to the web version of this article.)

studies (modeling, docking and binding mode analysis) of our newly generated α-pyrone derivatives (**IV**, Fig. 1) to analyze whether they could be potential antimalarials exploiting PfRIO2 kinase. The synthesized molecules were evaluated for their anti-malarial potential. One lead molecule of this novel class was identified for further optimization and mode of action study.

2. Results and discussion

2.1. Molecular modeling

Recently, we developed and explored the 3D structural aspect of PfRIO2 kinase [4,12] as plausible novel anti-malarial drug target to support our anti-malarial drug discovery program. In the present study, the binding sites were identified using SiteMap module of Schrödinger Suite. Four binding sites were identified and named as S1, S2, S3 and S4 (Fig. 2a). The S1 is found within the flexible loop region and close to DNA binding region (wing helix Domain). The S1 site comprised of E104, S105, D106, I107, K121, L125, R127, L163, P174, S187, I189, G191, P193, N227, N230, K232, I242, D243, P245. The S2 subsite is the major groove and known for ATP binding and contains major residues K2, D4, I5, F8, D79, F80, L83, I95, Y108, L120, I122, and M183. The subsite S3 found near to C-terminal was surrounded by S129, F130, R131, I133, N135, Y139, G141, and K142. The amino acid residues L250, R251, H252, V253, A255, K256, P282 formed the S4 subsite. The S3 and S4 are very small and close to surface, which may not be suitable for inhibitor binding. Since the active site is not yet identified, we studied the ligand interactions to S1 and S2 sites of PfRIO2. The protein–ligand interaction study was carried out with two complex models of the protein. The 1st complex comprised both ATP and DNA, while in the 2nd complex only DNA was present. Therefore, in the 2nd complex, ligand can

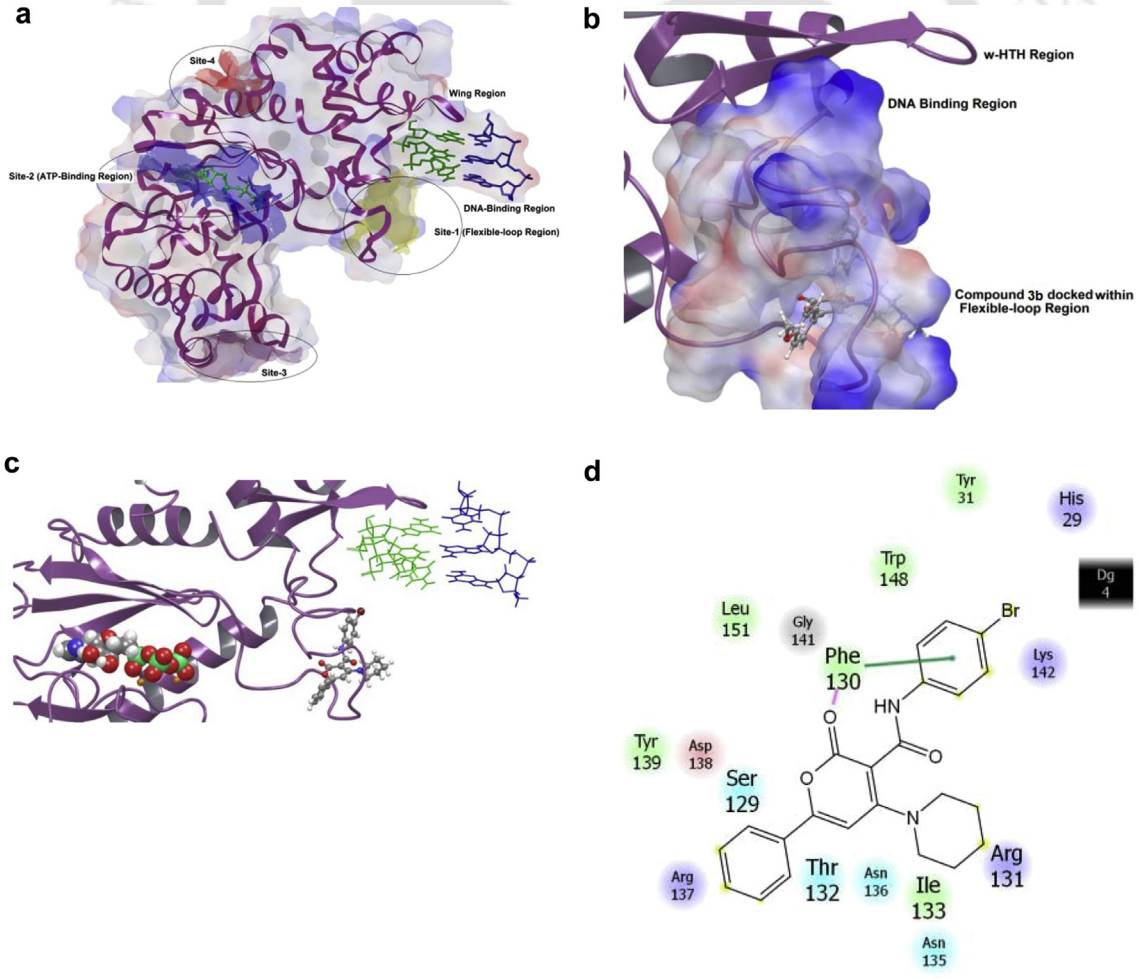

Fig. 2. a) The SiteMap analysis of PfRIO2 kinase showing the four locations as plausible ligand binding site. b) The surface diagram showing the binding of **3b** into S1 site. c) The docked pose of **3b** in the S1 site. d) Ligand–receptor interaction diagram showing the major hot spot residues of flexible loop interacting with **3b**.

utilize the full site including the space of ATP. The ligand structures were built using Maestro interface of and their conformations were optimized by LigPrep. The optimized ligands were docked by default protocols to S1 and S2 sites of the above mentioned two types of PfRIO2 complex using Glide [13]. However the standard docking results didn't show significant interactions and binding energy score. The poor results obtained may be due to the requirement of additional enzyme flexibility within the site. Thus the induced fit docking (IFD) protocols [14] were implemented to conduct the docking experiment followed by side chain refinement using Prime. The prime refinement ensures protein side chain flexibility according to ligand fitting into the active site. This was necessary because the actual conformation of the active site in PfRIO2 is not yet known. When the receptor flexibility was considered, the ligand–protein interactions were found significant in S1 site. It is interesting to note that the molecular docking and interaction profile were found better in the 1st complex model. Therefore, all the docking experiments were conducted on this complex using S1 active site located in the flexible loop region. Fig. 2b is a surface diagram showing binding of **3b** (the most active compound) in the S1 site. Docked pose of **3b** (Fig. 2c) was created to have a more closer look into its binding mode into the flexible loop region near to the DNA binding region. Ligand–receptor interactions were studied in detail and shown in Fig. 2d. This analysis highlighted the major hot spot residues in the flexible loop (hydrophobic: Tyr139, Leu151, Trp148, Tyr31, Ile133, Phe130; acidic: Asp 138; polar/hydrophilic: Ser129, Thr132, Asn136, Asn135; basic: Arg137, Arg131, Lys142, His29) interacting with **3b**. Among them one of the hydrophobic residues Phe130 also forms a $\pi\cdots\pi$ stacking with bromophenyl ring of **3b**. Dg4 (black block in Fig. 2d) indicates the presence of DNA in proximity. The IFD dockings were further scored by extra precision scoring function within the S1 active site to evaluate the energetic preference of compounds and the binding profile results are summarized in Table 1. The negative eMBrAcE (Multi-ligand Bimolecular Association with Energetic) score suggests binding of the ligand with PfRIO2 kinase to lower the energy of PfRIO2–ligand complex. This result also supports the suitability of S1 to be considered as active site. The energetic scores are based on semi-empirical calculation and may not correlate exactly with biological activity, they reveal the possibly of the ligand binding in this novel target enzyme. Ligand binding affinity was also estimated by Glide Emodel score (Table 1). Emodel score is the combination of GlideScore (GScore) and nonbonded interaction energy. The four molecules **3a**–**3d** shown favorable energy score and interestingly the same were found significant in biological screening. In absence of any ligand or inhibitor reported for PfRIO2 kinase, chloroquine, a potent antimalarial was selected for possible comparison. The poor binding score (Table 1) of chloroquine with PfRIO2 limits the possibility of chloroquine–PfRIO2 binding. The significant binding score of some of the synthesized compounds suggest the plausible anti-malarial activity through PfRIO2 kinase inhibition. However more specific biological screening is necessary in future to confirm the mode of action of these class of compounds (Scheme 1).

Table 1
In-silico binding analysis by Glide and eMBrAcE score.

S. No	Compound	Docking[a]	eMBrAcE score[b] (energy difference)		
		Glide Emodel score	*VdW*	Electrostatic	Total (ΔE)
1	**3a**	−72.8	−181.8	−139.0	−140.7
2	**3b**	−78.9	−178.3	−185.3	−319.3
3	**3c**	−74.8	−190.2	−142.9	−222.9
4	**3d**	−76.4	−218.2	−172.3	−172.0
5	**3e**	−62.4	−160.4	−140.1	−107.9
6	**3f**	−69.5	−167.8	−233.4	−282.9
7	**3g**	−67.6	−187.7	−90.4	−207.9
8	Chloroquine	−42.4	−157.5	−81.6	−78.7

[a] Emodel score: the minimized poses are rescored using Schrödinger's proprietary GlideScore scoring function and the binding affinity can be estimated by Glide Emodel score, which is the combination of GlideScore (GScore) and nonbonded interaction energy.

[b] eMBrAcE (Multi-Ligand Bimolecular Association with Energetics): ($\Delta E_{Total} = E_{complex} - E_{ligand} - E_{protein}$); *VdW*: van der Waals interaction. ΔE = energy difference (kcal/mol).

2.2. Chemistry

The required α-pyrone C-3 carboxylic acids (**1a**–**b**) were synthesized in two steps from appropriate acetophenones following synthetic methodology reported by our group [15]. Coupling of respective amines with the carboxyl group of **1a**–**b** was carried out using HATU as a coupling reagent [16]. The coupled products (**2a**–**e**) were obtained in more than 70% yield. The methylthio group in **2a**–**d** were replaced with appropriate secondary amines [17] by heating in dioxane to yield **3a**–**d**. Compounds **3e**–**g** were prepared by heating appropriate intermediates (**2a**, **b**, **e**) with H_2O_2 and catalytic amount of acetic acid in dioxane. All the synthesized compounds were characterized by spectral analysis.

2.3. Anti-malarial activity

Antimalarial potentials of **3a-g** were evaluated in an *in-vitro* schizonticidal inhibition assay. All the compounds were found to block life-cycle stage transitions (Table 2) of *Plasmodium falciparum*. The compound **3d** was parasitostatic while others were parasitocidal. The minimum killing concentration (MKC) was the concentration of compounds required to kill parasite present in the culture. Glutathione (GSH), a non-proteinous thiol plays an important role as a cellular redox buffer [18]. The cell health depends on balance between generation and elimination of reactive oxygen/nitrogen species (ROS/RNS), which maintains the redox balance of the cell and proper function of redox-sensitive signaling proteins. Moderate levels of ROS/RNS may function as signals to promote cell proliferation and survival, whereas severe increase of ROS/RNS can induce cell death [19]. GSH is known to directly bind with some ROS species or assist ROS as a source of reductive power for certain antioxidant systems [20]. Therefore, depletion in GSH will imbalance the level of ROS inside cell leading to oxidative stress. Lipids are most susceptible target of oxidative modification through peroxidation that generates lipid radicals, which can further attack the subsequent lipid molecules and propagate as a chain reaction [21]. The lipid peroxides can form adduct with oxidized proteins which in turn can inactivate 26S and 20S proteasomes leading to accumulation of damaged protein and cell death [22]. The lipid peroxidation related cell death is also associated with formation of malondialdehyde (MDA) and 4-hydroxy-2-nonenal (HNE) [23]. In addition, severe damage to the membrane structure might induce membrane perturbation and compromised cellular integrity. As most of our compounds were parasitocidal, we were curious whether they are able to affect the intracellular ROS level. Therefore, to explore such a possibility, we choose **3a**–**d** for study. Compounds **3a**–**c** are parasitocidal with very good MKC and Schinzoticidal Activity while **3d** was parasitostatic (Table 2). The parasite cultures were treated with the sub-lethal concentration of **3a**–**d** individually and change in intracellular ROS, lipid peroxidation (LP) were measured (Table 3). Untreated parasite culture was used to calculate change in oxidative stress indices (ROS and LP) and expressed as fold ± SD. It was found that cells treated with **3a**–**d** had higher ROS level and consequently higher lipid peroxidation

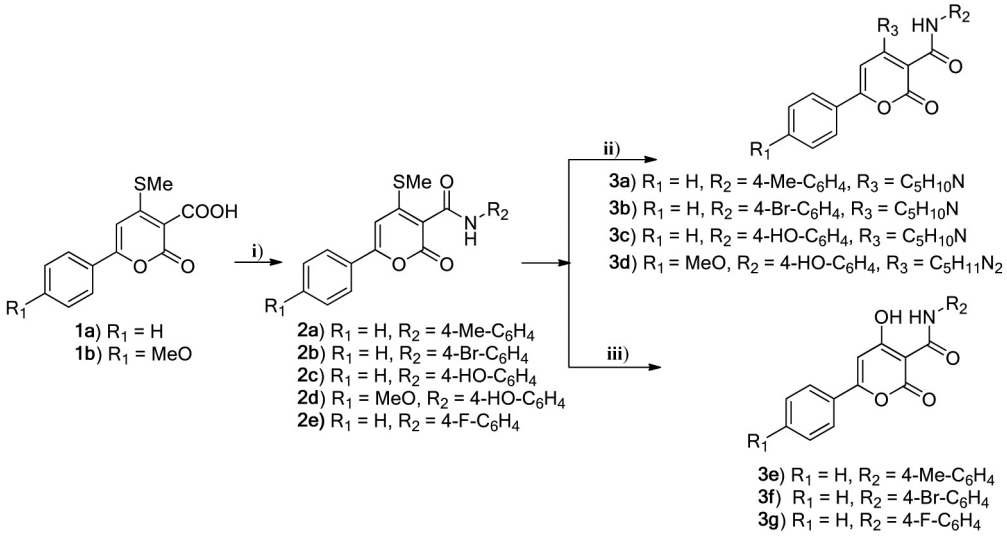

Scheme 1; Reagents and conditions: **i)** R_2NH_2, HATU, DMF, rt, 6h; **ii)** R_3H, Dioxane, 70 °C, 4h; **iii)** H_2O_2, CH_3COOH, Dioxane, 85 °C, 4h.

Scheme 1. Reagents and conditions: i) R_2NH_2, HATU, DMF, rt, 6 h; ii) R_3H, Dioxane, 70 °C, 4 h; iii) H_2O_2, CH_3COOH, dioxane, 85 °C, 4 h.

compared to untreated cells. The results are indicative of several damages to the cellular structure through peroxidation of membrane lipids and may affect proliferation machinery inside the cell. It explains parasiticidal action of most of the α-pyrone derivatives tested in the current study. However, a further detailed study is required to understand the molecular mechanism as well as the cellular machinery involved in the anti-malarial action of these new class of compounds. Also, a PfRIO2 kinase specific assay is needed to understand whether the activity is governed by PfRIO2 kinase.

3. Summary and conclusion

The site identification followed by modeling studies revealed a novel active site within the flexible loop region of PfRIO2 kinase, which can interact with appropriate ligand. The binding mode of designed compounds with target protein was analyzed by IFD molecular docking. Overall, the pharmacophoric hybridization and modeling approach were explored to generate a novel series of α-pyrone molecules for synthesis. All the synthesized molecules showed *in vitro* antimalarial activity. One of the synthesized compounds, **3b**, with most significant result was identified as promising lead for further SAR study. The detailed molecular modeling and chemical modifications are in process to convert this preliminary lead into antimalarial drug candidate.

Table 2
Anti-malarial activities of different α-pyrone analogs (**3a**–**g**).

Comp Code	Schinzoticidal Activity IC_{50} (μM ± SE)	Nature of inhibition	MKC (μM ± SE)
3a	0.859 ± 0.59	Parasitocidal	1.00 ± 0.002
3b	0.337 ± 0.19	Parasitocidal	0.21 ± 0.026
3c	0.765 ± 0.28	Parasitocidal	1.99 ± 0.30
3d	1.568 ± 0.48	Parasitostatic	NA
3e	1.42 ± 0.37	Parasitocidal	38.9 ± 3.82
3f	0.75 ± 0.33	Parasitocidal	3.90 ± 0.59
3g	0.90 ± 0.23	Parasitocidal	2.39 ± 0.33
Chloroquine	0.078 ± 0.012	ND	ND

ND = Not determined.

4. Experimental section/materials and methods

4.1. Computational studies

In absence of PfRIO2 co-crystal structure, our previously described model of PfRIO2 kinase complex with short chain of DNA including ATP was used for current modeling studies [12]. The modeling was carried out using the latest modeling suite from Schrödinger [24]. The Protein Preparation Wizard (PPW) was utilized iteratively to check for any errors related to bond-order, metal charges (+2 for Mn ion), proton assignment, or H-bonding to ensure the chemical correctness of model. The SiteMap program [25,26] can successfully suggest possible binding sites [27]. Therefore, this method was used and "four site points" were disclosed as possible ligand binding site in PfRIO2 kinase (Fig. 2a). The S1 active site was found optimum for ligand binding and used for docking studies. The 3D structure of compounds is treated in LigPrep module of Schrödinger using OPLS2005 force field followed by conformational search analysis through MacroModel [28] using MMFFs force field to obtain the low energy conformer. SiteMap analysis followed by molecular docking [14] of conformationally optimized molecules in S1 active site was used to identify the binding mode of compounds (Fig. 2d). Several docked poses were generated and the best docked poses with lowest Emodel Score were selected for comparative analysis (Table 1). The Emodel energy score has been further verified by the eMBrAcE module of Schrödinger [28]. This module has been used to determine the binding energy differences through minimization using OPLS2005

Table 3
Effect of **3a**–**d** on antioxidant system of malaria parasite.

Compounds	Change in ROS level (fold ± SD[a])	Change in lipid peroxidation (fold ± SD)
Untreated	1	1
3a	1.66 ± 0.14	11.03 ± 0.45
3b	1.87 ± 0.21	4.49 ± 0.26
3c	1.20 ± 0.18	9.03 ± 0.37
3d	1.99 ± 0.20	4.88 ± 0.66

[a] Standard deviation.

force field. The calculations were performed with GB/SA continuum water solvation model. The eMBrAcE minimization was performed for 5000 steps or until the energy difference between subsequent conformations was 0.05 kJ mol^{-1}. The energetic calculations provided energy difference in terms of *VdW*, electrostatic and total ($\Delta E = E_{complex} - E_{ligand} - E_{protein}$). The implicit-water model was used during minimization, conformational search, molecular docking, SiteMap analysis, and energetic calculation.

4.2. Chemistry

4.2.1. General

All reactions were carried out in oven-dried glassware under nitrogen atmosphere. The chemicals and solvents were purchased from Spectrochem, Across, Rankem or Sigma–Aldrich. Melting points were recorded on Veego melting point apparatus. Analytical thin layer chromatography (TLC) was performed on precoated plates (silica gel 60 F-254) purchased from Merck Inc. Purification by gravity column chromatography was carried out on silica gel (100–200 mesh). Electro UV/Vis spectrophotometer was used for recording the UV spectra. $^{1}H/^{13}C$ NMR were obtained from a Varian (400 MHz) spectrometer or Bruker spectrometer using $CDCl_3$ or DMSO-d_6, as solvents. Peaks are recorded with the following abbreviations: s, singlet; bs, broad singlet; d, doublet; t, triplet; q, quartet; m, multiplet; *J*, coupling constant (hertz).

4.2.2. General procedure for the synthesis of **3a–d**

To a solution of an appropriate 2*H*-pyran-4-methylthio-3-carboxamide (**2a–d**, 3.3 mmol) in dioxane, appropriate secondary amine (6.7 mmol) was added and stirred for 4 h at 70 °C. The reaction was monitored by TLC for completion. The solvent was removed under reduced pressure. The ice cold water was added and stirred for 2 h at 0–5 °C. The resulting precipitate was filtered and purified by column chromatography to obtain pure compound.

*4.2.2.1. 2-Oxo-6-phenyl-4-(piperidin-1-yl)-N-(p-tolyl)-2H-pyran-3-carboxamide (**3a**).* Yield: 55%; mp: 133–135 °C; MS-ESI (*m*/*z*): [M^+] 388.6; UV (MeOH) λ_{max} 256.8 nm, 316 nm; IR: (KBr) cm^{-1} 1635, 1674, 2856, 2937, 3275; ^{1}H NMR (400 MHz, DMSO-d_6): δ 1.70 (bs, 6H, $3CH_2$) 2.42 (s, 3H, $ArCH_3$), 3.75 (bs, 4H, $2NCH_2$), 7.50 (s, 1H, CH), 7.55–7.59 (m, 2H, ArH), 8.0–8.05 (m, 5H, ArH), 8.45–8.52 (m, 2H, ArH), 10.82 (s, 1H, NH).

*4.2.2.2. N-(4-Bromophenyl)-2-oxo-6-phenyl-4-(piperidin-1-yl)-2H-pyran-3-carboxamide (**3b**).* Yield: 78%; mp: 210–211 °C; MS-ESI (*m*/*z*): [$M^+ + 2$] 455.0, [M^+] 453.3; UV (MeOH) λ_{max} 259 nm, 324 nm; IR: (KBr) cm^{-1} 1639, 1692, 2843, 2939, 3105, 3325; ^{1}H NMR (400 MHz, $CDCl_3$): δ 1.75 (bs, 6H), 3.56 (bs, 4H), 6.67 (s, 1H), 7.41–7.43 (m, 2H), 7.47–7.50 (m, 3H), 7.57–7.59 (m, 2H), 7.83–7.85 (m, 2H), 10.68 (s, 1H).

*4.2.2.3. N-(4-Hydroxyphenyl)-2-oxo-6-phenyl-4-(piperidin-1-yl)-2H-pyran-3-carboxamide (**3c**).* Yield: 67%; mp: 134–135 °C; MS-ESI (*m*/*z*): [$M^+ + 1$] 391.20; UV (MeOH) λ_{max} 254 nm, 307 nm; IR: (KBr) cm^{-1} 1633, 1666, 2895, 2937, 3184 (broad); ^{1}H NMR (400 MHz, DMSO-d_6): δ 1.75 (bs, 6H, $3CH_2$), 3.55 (bs, 4H, $2NCH_2$), 5.40 (s, 1H, ArOH), 6.65 (s, 1H, CH), 6.79–6.81 (m, 2H, ArH), 7.48–7.50 (m, 5H, ArH), 7.82–7.84 (m, 2H, ArH), 10.36 (s, 1H, NH).

*4.2.2.4. N-(4-Hydroxyphenyl)-6-(4-methoxyphenyl)-4-(4-methylpiperazin-1-yl)-2-oxo-2H-pyran-3-carboxamide (**3d**).* Yield: 31%; mp: >245 °C; MS-ESI (*m*/*z*): [$M^+ + 1$] 436.36; UV (MeOH) λ_{max} 239 nm, 313 nm; IR: (KBr) cm^{-1} 1560, 1612, 1726, 2949, 3066, 3294 (broad); ^{1}H NMR (400 MHz, DMSO-d_6): δ 2.82 (bs, 3H, NCH_3), 3.35–3.42 (m, 8H, $4CH_2$), 4.12 (s, 3H, OCH_3), 7.17–7.19 (d, J = 8 Hz, 1H, ArH), 7.55 (s, 1H, CH), 7.58–7.62 (m, 2H, ArH), 7.76–7.78 (d, J = 8 Hz, 1H, ArH), 7.92–7.94 (d, J = 8 Hz, 1H, ArH), 8.30–8.32 (d, J = 8 Hz, 1H, ArH), 8.50–8.54 (m, 2H, ArH), 9.88 (s, 1H, NH), 11.22 (s, 1H, ArOH).

4.2.3. General procedure for the synthesis of **3e–g**

To a solution 2*H*-pyran-4-methylthio-3-carboxamide (**2a–b**, **e**, 3.3 mmol) in dioxane, 30% (w/w in H_2O) Hydrogen Peroxide solution (6.6 mmol), acetic acid 2–3 drops was added at room temperature. The resulting reaction mixture was stirred at 85 °C for 4 h. The reaction was monitored by TLC for completion. The reaction mixture was diluted with cold water (25 ml) and extracted with DCM, concentrated under reduced pressure. The crude was column purified to get **3e–g**.

*4.2.3.1. 4-Hydroxy-2-oxo-6-phenyl-N-(p-tolyl)-2H-pyran-3-carboxamide (**3e**).* Yield: 35%; mp: 198–199 °C; MS-ESI (*m*/*z*): [$M^+ + 1$] 322.1; UV (MeOH) λ_{max} 247 nm, 340 nm; IR: (KBr) cm^{-1} 1545, 1699, 2906, 3041, 3234; ^{1}H NMR (400 MHz, $CDCl_3$): δ 2.35 (s, 3H, CH_3), 6.65 (s, 1H, CH), 7.17–7.19 (d, J = 8.0 Hz, 2H, ArH), 7.50–7.55 (m, 5H, ArH), 7.87–7.89 (d, J = 6.8 Hz, 2H, ArH), 10.91 (s, 1H, NH).

*4.2.3.2. N-(4-Bromophenyl)-4-hydroxy-2-oxo-6-phenyl-2H-pyran-3-carboxamide (**3f**).* Yield: 40%; mp: 220–222 °C; MS-ESI (*m*/*z*): [M^+] 386.1, [$M^+ + 2$]: 388.2; UV (MeOH) λ_{max} 253 nm, 342 nm; IR: (KBr) cm^{-1} 1597, 1628, 1697, 3101, 3238; ^{1}H NMR (400 MHz, $CDCl_3$): δ 6.67 (s, 1H, CH), 7.48–7.57 (m, 7H, ArH), 7.88–7.90 (d, J = 6.8 Hz, 2H, ArH), 11.02 (s, 1H, NH).

*4.2.3.3. N-(4-Fluorophenyl)-4-hydroxy-2-oxo-6-phenyl-2H-pyran-3-carboxamide (**3g**).* Yield: 30%; mp > 260 °C; MS-ESI (*m*/*z*): [$M^+ - 1$] 323.9; UV (MeOH) λ_{max} 236 nm, 340 nm; IR: (KBr) cm^{-1} 1547, 1637, 1697, 3066, 3236; ^{1}H NMR : (400 MHz, DMSO-d_6): δ 7.02 (s, 1H, CH), 7.14–7.19 (m, 2H, ArH), 7.50–7.55 (m, 3H, ArH), 7.61–7.64 (m, 2H, ArH), 7.86–7.88 (d, J = 6.8 Hz, 2H, ArH), 10.40 (s, 1H, NH).

4.3. Anti-malarial activity

4.3.1. In-vitro schizonticidal inhibition assay

The *in vitro* antimalarial assay was carried out in 96-well microtitre plates as described previously [29,30]. In brief, test compound was incubated with ring stage synchronized *P. falciparum* (3D7) parasitised cell. After 42 h incubation, the blood smears from each well was prepared to record maturation of ring stage parasites into trophozoites and schizonts. MS-Excel Sheet based HN-NonLin program (www.malaria.farch.net) was used to calculate IC_{50} of **3a–g** compounds based on their schizont inhibition profile using regression analysis. To determine the nature of parasite growth inhibition (parasitostatic/parasitocidal), the compounds were removed and the cultures were washed 3 times with albumax II free RPMI-1640 and incubated in complete media with fresh hematocrit for another 72 h. A thin smear was prepared and number of RBCs containing viable parasite was counted. The minimum concentration of compounds giving no viable parasite was used to calculate minimum killing concentration (MKC) of compounds with parasitocidal activity.

4.3.2. Measurements of oxidative stress indices

Parasite cultures were treated with 3**a**-**d** separately. The intracellular ROS was measured by a fluorescent probe (2′,7′-dichlorofluorescein diacetate) and lipid peroxidation was measured as described previously [29,31].

Acknowledgments

This research received funding from Department of Biotechnology (DBT), New Delhi, India through grant no. BT/PR13436/

MED/12/450/2009 & BT/41/NE/TBP/2010. AP is thankful to UGC, India for MANF Junior Research Fellowship. AK and HC acknowledges BIT Mesra for Institute Research Fellowship. AC acknowledges the financial support in the form of a fellowship from IIT-Guwahati. Authors acknowledge Dr. Reddy's Institute of Life Sciences, Hyderabad for NMR-Mass Facility and Central Instrument Facility, BIT Mesra for analytical support.

Appendix A. Supplementary data

Supplementary data related to this article can be found at http://dx.doi.org/10.1016/j.ejmech.2013.10.028.

References

[1] I. Hastings, How artemisinin-containing combination therapies slow the spread of antimalarial drug resistance, Trends Parasitol. 27 (2011) 67–72.
[2] A.P. Phyo, S. Nkhoma, K. Stepniewska, E.A. Ashley, S. Nair, R. McGready, S. Al-Saai, A.M. Dondorp, K.M. Lwin, P. Singhasivanon, Emergence of artemisinin-resistant malaria on the western border of Thailand: a longitudinal study, The Lancet. 379 (2012) 1960–1966.
[3] S. Kumar, U. Bandyopadhyay, Free heme toxicity and its detoxification systems in human, Toxicol. Lett. 157 (2005) 175–188.
[4] V. Trivedi, S. Nag, In silico characterization of atypical kinase PFD0975w from plasmodium kinome: a suitable target for drug discovery, Chem. Biol. Drug Des. 79 (2012) 600–609.
[5] S. Nag, D. Chouhan, S.N. Balaji, A. Chakraborty, K. Lhouvum, C. Bal, A. Sharon, V. Trivedi, Comprehensive screening of heterocyclic compound libraries to identify novel inhibitors for PfRIO-2 kinase through docking and substrate competition studies, Med. Chem. Res. (2013) 1–8.
[6] S. Nag, K. Prasad, V. Trivedi, Identification and screening of antimalarial phytochemical reservoir from northeastern Indian plants to develop PfRIO-2 kinase inhibitor, Eur. Food Res. Technol. 234 (2012) 905–911.
[7] J.B. Koepfli, J.F. Mead, J.A. Brockman, An alkaloid with high antimalarial activity from *Dichroa Febrifuga*1, J. Am. Chem. Soc. 69 (1947), 1837–1837.
[8] S. Jiang, Q. Zeng, M. Gettayacamin, A. Tungtaeng, S. Wannaying, A. Lim, P. Hansukjariya, C.O. Okunji, S. Zhu, D. Fang, Antimalarial activities and therapeutic properties of febrifugine analogs, Antimicrob. Agents Chemother. 49 (2005) 1169–1176.
[9] D. Carmona, J. Saez, H. Granados, E. Perez, S. Blair, A. Angulo, B. Figadere, Antiprotozoal 6-substituted-5,6-dihydro-alpha-pyrones from *Raimondia cf. monoica*, Nat. Prod. Res. 17 (2003) 275–280.
[10] P.L. Chien, C.C. Cheng, Structural modification of febrifugine. Some methylenedioxy analogs, J. Med. Chem. 13 (1970) 867–870.
[11] Y. Zhang, J.A. Clark, M.C. Connelly, F. Zhu, J. Min, W.A. Guiguemde, A. Pradhan, L. Iyer, A. Furimsky, J. Gow, T. Parman, F. El Mazouni, M.A. Phillips, D.E. Kyle, J. Mirsalis, R.K. Guy, Lead optimization of 3-carboxyl-4(1*H*)-quinolones to deliver orally bioavailable antimalarials, J. Med. Chem. 55 (2012) 4205–4219.
[12] D. Chouhan, A. Sharon, C. Bal, Molecular and structural insight into *Plasmodium falciparum* RIO2 kinase, J. Mol. Model. 19 (2013) 485–496.
[13] R.A. Friesner, R.B. Murphy, M.P. Repasky, L.L. Frye, J.R. Greenwood, T.A. Halgren, P.C. Sanschagrin, D.T. Mainz, Extra precision glide: docking and scoring incorporating a model of hydrophobic enclosure for protein–ligand complexes, J. Med. Chem. 49 (2006) 6177–6196.
[14] W. Sherman, T. Day, M.P. Jacobson, R.A. Friesner, R. Farid, Novel procedure for modeling ligand/receptor induced fit effects, J. Med. Chem. 49 (2006) 534–553.
[15] S. Karampuri, P. Bag, S. Yasmin, D.K. Chouhan, C. Bal, D. Mitra, D. Chattopadhyay, A. Sharon, Structure based molecular design, synthesis and biological evaluation of alpha-pyrone analogs as anti-HSV agent, Bioorg. Med. Chem. Lett. 22 (2012) 6261–6266.
[16] L.A. Carpino, 1-Hydroxy-7-azabenzotriazole. An efficient peptide coupling additive, J. Am. Chem. Soc. 115 (1993) 4397–4398.
[17] A. Sharon, P.R. Maulik, C. Vithana, Y. Ohashi, V.J. Ram, Synthesis of biphenanthrenyls and role of C–H···X noncovalent interactions in conformational control, Eur. J. Org. Chem. 2004 (2004) 886–893.
[18] M. Marí, A. Morales, A. Colell, C. García-Ruiz, J.C. Fernández-Checa, Mitochondrial glutathione, a key survival antioxidant, Antioxid. Redox Signal. 11 (2009) 2685–2700.
[19] D. Trachootham, W. Lu, M.A. Ogasawara, N.R.-D. Valle, P. Huang, Redox regulation of cell survival, Antioxid. Redox Signal. 10 (2008) 1343–1374.
[20] V.I. Lushchak, Glutathione homeostasis and functions: potential targets for medical interventions, J. Amino Acids 2012 (2012) 736837.
[21] A.W. Girotti, Lipid hydroperoxide generation, turnover, and effector action in biological systems, J. Lipid Res. 39 (1998) 1529–1542.
[22] D. Poppek, T. Grune, Proteasomal defense of oxidative protein modifications, Antioxid. Redox Signal. 8 (2006) 173–184.
[23] I. Pinchuk, E. Schnitzer, D. Lichtenberg, Kinetic analysis of copper-induced peroxidation of LDL, Biochim. Biophys. Acta 1389 (1998) 155–172.
[24] Schrödinger Suite, LLC, New York, NY, 2012.
[25] SiteMap-V-2.5, V 2.5, Schrödinger, LLC, New York, NY, 2011.
[26] T.A. Halgren, Identifying and characterizing binding sites and assessing druggability, J. Chem. Inf. Model. 49 (2009) 377–389.
[27] M. Nayal, B. Honig, On the nature of cavities on protein surfaces: application to the identification of drug-binding sites, Proteins 63 (2006) 892–906.
[28] MacroModel-V-9.9, Schrödinger, LLC, New York, NY, 2011.
[29] V. Trivedi, P. Chand, K. Srivastava, S.K. Puri, P.R. Maulik, U. Bandyopadhyay, Clotrimazole inhibits hemoperoxidase of *Plasmodium falciparum* and induces oxidative stress. Proposed antimalarial mechanism of clotrimazole, J. Biol. Chem. 280 (2005) 41129–41136.
[30] K.V. Sashidhara, S.R. Avula, G.R. Palnati, S.V. Singh, K. Srivastava, S.K. Puri, J.K. Saxena, Synthesis and in vitro evaluation of new chloroquine–chalcone hybrids against chloroquine-resistant strain of *Plasmodium falciparum*, Bioorg. Med. Chem. Lett. 22 (2012) 5455–5459.
[31] S.N. Balaji, V. Trivedi, Methemoglobin incites primaquine toxicity through single-electron oxidation and modification, J. Basic Clin. Physiol. Pharmacol. 24 (2013) 105–114.

Austin Journal of Biotechnology & Bioengineering

Open Access

Austin Publishing Group

Editorial

Streamlining the Drug Discovery Process through Repurposing of Clinically Approved Drugs

Arnish Chakraborty and Vishal Trivedi*
Department of Biosciences & Bioengineering, Indian Institute of Technology-Guwahati, India

***Corresponding author:** Vishal Trivedi, Malaria Research Group, Department of Biosciences and Bioengineering, Indian Institute of Technology-Guwahati, Guwahati-781039, Assam, India, Tel: +91-361-2582217; Fax: +91-361-258-2249; Email: vtrivedi@iitg.ernet.in

Received: July 20, 2015; **Accepted:** July 22, 2015; **Published:** July 24, 2015

Editorial

Drug repurposing (also known as Drug repositioning) is an approach to drug design and development where known compounds are assigned to new indications. In this process one starts from already existing clinical drugs and assigns a new therapeutic target to the molecule. This approach is quickly gaining popularity both in industry as well as in academia as it banks upon the initial knowledge and investment which brought the drug to the market at the first instance. The major bottleneck of de novo drug development is that almost 90% of the identified novel molecules fail the clinical trials, resulting in the rise of the overall pharmaceutical R&D cost. The repurposing strategy helps to overcome such barriers. There are notable advantages of this approach over the traditional drug discovery process (Figure 1). Firstly, the repurposed drugs have already undergone clinical trials in the past and as a result their safety is ensured. Secondly, the repurposing strategy is cheap and takes much lesser time to develop a drug. Several pharmaceutical companies therefore endorse this low-risk repositioning strategy to improve their profits.

The Drug Repurposing Work Flow

The starting materials for a repurposing process are drug molecules which (a) have been approved for clinical use (b) have passed safety trial (Phase I) but failed to demonstrate efficacy (Phase II) for a disease (c) have been replaced by better therapeutics and (d) have become generic due to patent expiry [1]. The drug repurposing process can be broadly classified into the following two strategies: (i) Existing compound-novel target approach: It is based on the observation that many drugs bind to multiple targets. These secondary targets could be related to a different disease or physiological condition and (ii) Known mechanism-new disease: It is based on the observation that several biological processes and signaling pathways are relevant for more than one disease and hence the same drug which inhibits a biological process can exert effect on two different disease states [1]. Once a secondary target has been assigned to a drug, proof-of-concept experimentation has to be performed to study the effect of the drug on the newly identified target. Computational biology, chemical biology, in vitro/cell-based assays and in vivo analysis are frequently used to validate the repositioning. Upon validation of the hypothesis, the drug can leap directly into the phase II and III clinical trials. Moreover the availability of previous clinical and pharmacokinetic data along with the knowledge of the range of viable dose for that particular drug substantially reduces the risks associated with the further development of the molecule.

Case Studies

One of the most promising instances of a repurposed drug is Zidovudine, which was originally designed for cancer in 1964 [2]. The drug was later found to be potent against HIV in 1985. Released in 1987 by Glaxo Smithkline as AZT, it became the first drug to be approved for HIV treatment. Mifepristone, a glucocorticoid receptor antagonist, is another example of a repurposed drug which was initially synthesized in 1980 in France by Danco laboratories as an oral abortifacient and was licensed for use in France in 1988 and in the USA in 2000 [3]. The Drug has been repositioned for psychotic major depression and bipolar disorder under the trade name of Corlux by Corcept therapeutics [4]. Aspirin is the most frequently used analgesic and antipyretic drug in the world. It was licensed by the German company Bayer pharmaceuticals in 1897. The drug was later found to possess anti-cancer properties (Table 1). Clinical trials held in 2011 studied the risk of cancer death among patients who regularly took aspirin for 4 years and patients who did not take the drug. It was found out that, aspirin use lowered the overall risk of cancer by 20%. Another example of repositioning is that of the acetyl cholinesterase inhibitor Galantamine which was licensed as Nivalin by Sopharma in 1960 as a treatment for paralysis due to Polio. With the licensing of the polio vaccine in 1962 and the gradual eradication of polio, Galantamine remained abandoned for years until 2000 when it was repurposed for Alzheimer's disease by Johnson & Johnson under the trade name Reminyl.

Conclusion and Future Directions

The Drug repositioning strategy is widely used as an alternative

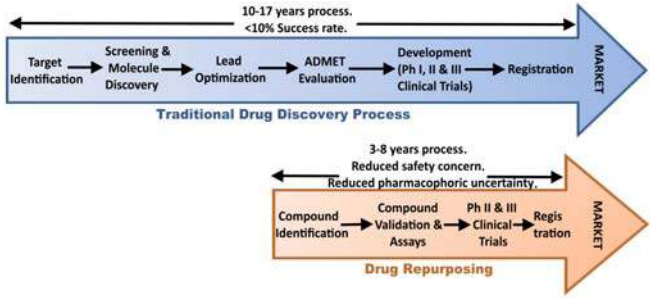

Figure 1: Schematic representation of the steps involved in Traditional drug discovery process *vs.* Drug repurposing with the salient features of both the processes.

Citation: Chakraborty A and Trivedi V. Streamlining the Drug Discovery Process through Repurposing of Clinically Approved Drugs. Austin J Biotechnol Bioeng. 2015;2(3): 1047.

Table 1: List of repurposed clinical drugs for the treatment of various diseases.

	Original Indication		Repurposed Indication	
Drug	**Disease**	**Target/s**	**Disease**	**Target/s**
(a) Drugs repurposed for Infectious diseases				
Zidovudine	Cancer	Telomerase [2]	HIV/AIDS	HIV reverse transcriptase [4]
Amphotericin	Fungal infections	Cell membrane sterols [5]	Leishmaniasis	Signaling pathways for IFN-γ, IL-12 and TNF- α activation in host [6]
Cycloserine	Urinary tract infections	Peptidoglycan synthesis in *E.Coli* [7]	Tuberculosis	Peptidoglycan synthesis in *M. tuberculosis* [8]
Clindamycin	Skin infections/acne	Ribosomal peptidyl transferase [9]	Malaria	*Plasmodium* apicoplast [10]
Paromomycin	Amoebiasis	16S Ribosomal rRNA [11]	Leishmaniasis	Mitochondrion function [12]
(b) Drugs repurposed for Neurological diseases				
Milnacipran	Depression	Serotonin–Norepinephrine re-uptake [13]	Fibromyalgia	Serotonin–Norepinephrine re-uptake [14]
Atomoxetine	Parkinson's disease	Noradrenaline re-uptake [15]	Attention deficit hyperactivity disorder	Noradrenaline re-uptake [16]
Galantamine	Polio, paralysis	Acetylcholinesterase [17]	Alzheimer's disease	Acetylcholinesterase [18]
Ropinirole	Hypertension	Dopamine D2 receptor [19]	Parkinson's disease/ restless leg syndrome	Dopamine D2 receptor [20]
Mifepristone	Pregnancy termination	Progesterone receptor [3]	Psychotic major depression	Glucocorticoid receptors [3]
(c) Drugs repurposed for Cancer				
Aspirin	Analgesic and antipyretic	COX-1 and COX-2 [21]	Colorectal cancer	COX-2 inhibition and down-regulation of NF-κB and AP-1 signaling [22]
Rapamycin	Immunosuppressant	mTOR signaling [23]	Lymphoma and leukemia	mTOR pathway/VEGF signaling [24]
Methotrexate	Acute leukemia	Dihydrofolate reductase [25]	Osteosarcoma, breast cancer and Hodgkin lymphoma	NF-κBandTNF-α signaling [26]
Nitroxoline	Urinary tract infections *(P. aeruginosa)*	Bacterial biofilm formation [27]	Bladder and breast cancer	Cathepsin B [28]
Minocycline	Acne vulgaris	Bacterial protein synthesis [29]	Ovarian cancer	NF-κB and TGF-β1 signaling [30]

approach to drug development since it lowers the risk of safety and toxicity and at the same time saves millions of dollars worth of pharmaceutical R&D. Over the decades many drugs have been repositioned and licensed for use in alternate indications and many more repurposed drugs are currently at the phase II and III clinical trials. The Drug repositioning approach is thus a simple yet powerful strategy to fuel pharmaceutical research and streamline the drug discovery process.

References

1. Sleigh SH, Barton CL. Repurposing strategies for therapeutics. Pharmaceutical Medicine. 2010; 24: 151-159.
2. Gomez DE, Armando RG, Alonso DF. AZT as a telomerase inhibitor. Front Oncol. 2012; 2: 113.
3. Fiala C, Gemzel-Danielsson K. Review of medical abortion using mifepristone in combination with a prostaglandin analogue. Contraception. 2006; 74: 66-86.
4. Ashburn TT, Thor KB. Drug repositioning: identifying and developing new uses for existing drugs. Nat Rev Drug Discov. 2004; 3: 673-683.
5. Foglia F, Rogers SE, Webster JR, Akeroyd F, Gascoyne K, Lawrence MJ, et al. Neutron scattering studies of the effects of formulating amphotericin B with cholesteryl sulfate on the drug's interactions with phospholipid and phospholipid-sterol membranes. Langmuir: the ACS journal of surfaces and colloids. 2015.
6. Mondal S, Bhattacharya P, Rahaman M, Ali N, Goswami RP. A curative immune profile one week after treatment of Indian kala-azar patients predicts success with a short-course liposomal amphotericin B therapy. PLoS Negl Trop Dis. 2010; 4: e764.
7. Lambert MP, Neuhaus FC. Mechanism of D-cycloserine action: alanine racemase from Escherichia coli W. J Bacteriol. 1972; 110: 978-987.
8. Prosser GA, de Carvalho LP. Kinetic mechanism and inhibition of Mycobacterium tuberculosis D-alanine:D-alanine ligase by the antibiotic D-cycloserine. FEBS J. 2013; 280: 1150-1166.
9. Schlünzen F, Zarivach R, Harms J, Bashan A, Tocilj A, Albrecht R, et al. Structural basis for the interaction of antibiotics with the peptidyl transferase centre in eubacteria. Nature. 2001; 413: 814-821.
10. Lell B, Kremsner PG. Clindamycin as an antimalarial drug: review of clinical trials. Antimicrob Agents Chemother. 2002; 46: 2315-2320.
11. Vicens Q, Westhof E. Crystal structure of paromomycin docked into the eubacterial ribosomal decoding A site. Structure. 2001; 9: 647-658.
12. Croft SL, Coombs GH. Leishmaniasis--current chemotherapy and recent advances in the search for novel drugs. Trends Parasitol. 2003; 19: 502-508.
13. Lopez-Ibor J, Guelfi JD, Pletan Y, Tournoux A, Prost JF. Milnacipran and selective serotonin reuptake inhibitors in major depression. Int Clin Psychopharmacol. 1996; 11 Suppl 4: 41-46.
14. Staud R, Lucas YE, Price DD, Robinson ME. Effects of Milnacipran on Clinical Pain and Hyperalgesia of Fibromyalgia Patients: Results of a 6 Week Randomized Controlled Trial. J Pain. 2015.
15. Kehagia AA, Housden CR, Regenthal R, Barker RA, Müller U, Rowe J, et al. Targeting impulsivity in Parkinson's disease using atomoxetine. Brain. 2014; 137: 1986-1997.
16. Haynes V, Lopez-Romero P, Anand E. Attention-deficit/hyperactivity disorder Under Treatment Outcomes Research (AUTOR): a European observational study in pediatric subjects. Atten Defic Hyperact Disord. 2015.
17. Xin L, Yamujala R, Wang Y, Wang H, Wu WH, Lawton MA, et al. Acetylcholineestarase-inhibiting alkaloids from Lycoris radiata delay paralysis of amyloid beta-expressing transgenic C. elegans CL4176. PLoS One. 2013; 8: e63874.
18. Buendia I, Parada E, Navarro E, León R. Subthreshold Concentrations of Melatonin and Galantamine Improves Pathological AD-Hallmarks in

Hippocampal Organotypic Cultures. Mol Neurobiol. 2015.

19. Parker SG, Raval P, Yeulet S, Eden RJ. Tolerance to peripheral, but not central, effects of ropinirole, a selective dopamine D2-like receptor agonist. Eur J Pharmacol. 1994; 265: 17-26.

20. Wijemanne S, Jankovic J. Restless legs syndrome: clinical presentation diagnosis and treatment. Sleep Med. 2015; 16: 678-690.

21. Bartfai T, Conti B. Fever. ScientificWorldJournal. 2010; 10: 490-503.

22. Li H, Zhu F, Boardman LA, Wang L, Oi N, Liu K, et al. Aspirin Prevents Colorectal Cancer by Normalizing EGFR Expression. EBioMedicine. 2015; 2: 447-455.

23. Xie X, Jiang Y, Lai X, Xiang S, Shou Z, Chen J. mTOR inhibitor versus mycophenolic acid as the primary immunosuppression regime combined with calcineurin inhibitor for kidney transplant recipients: a meta-analysis. BMC Nephrol. 2015; 16: 91.

24. Cella CA, Minucci S, Spada F, Galdy S, Elgendy M, Ravenda PS, et al. Dual inhibition of mTOR pathway and VEGF signalling in neuroendocrine neoplasms: From bench to bedside. Cancer Treat Rev. 2015.

25. Rajagopalan PT, Zhang Z, McCourt L, Dwyer M, Benkovic SJ, Hammes GG. Interaction of dihydrofolate reductase with methotrexate: ensemble and single-molecule kinetics. Proc Natl Acad Sci U S A. 2002; 99: 13481-13486.

26. Spurlock CF, Tossberg JT, Matlock BK, Olsen NJ, Aune TM. Methotrexate inhibits NF-κB activity via long intergenic (noncoding) RNA-p21 induction. Arthritis Rheumatol. 2014; 66: 2947-2957.

27. Sobke A, Klinger M, Hermann B, Sachse S, Nietzsche S, Makarewicz O, et al. The urinary antibiotic 5-nitro-8-hydroxyquinoline (Nitroxoline) reduces the formation and induces the dispersal of Pseudomonas aeruginosa biofilms by chelation of iron and zinc. Antimicrob Agents Chemother. 2012; 56: 6021-6025.

28. Mirkovič B, Renko M, Turk S, Sosič I, Jevnikar Z, Obermajer N, et al. Novel mechanism of cathepsin B inhibition by antibiotic nitroxoline and related compounds. ChemMedChem. 2011; 6: 1351-1356.

29. Laux B. [Treatment of acne vulgaris. A comparison of doxycycline versus minocycline]. Hautarzt. 1989; 40: 577-581.

30. Ataie-Kachoie P, Badar S, Morris DL, Pourgholami MH. Minocycline targets the NF-κB Nexus through suppression of TGF-β1-TAK1-IκB signaling in ovarian cancer. Mol Cancer Res. 2013; 11: 1279-1291.

Citation: Chakraborty A and Trivedi V. Streamlining the Drug Discovery Process through Repurposing of Clinically Approved Drugs. Austin J Biotechnol Bioeng. 2015;2(3): 1047.